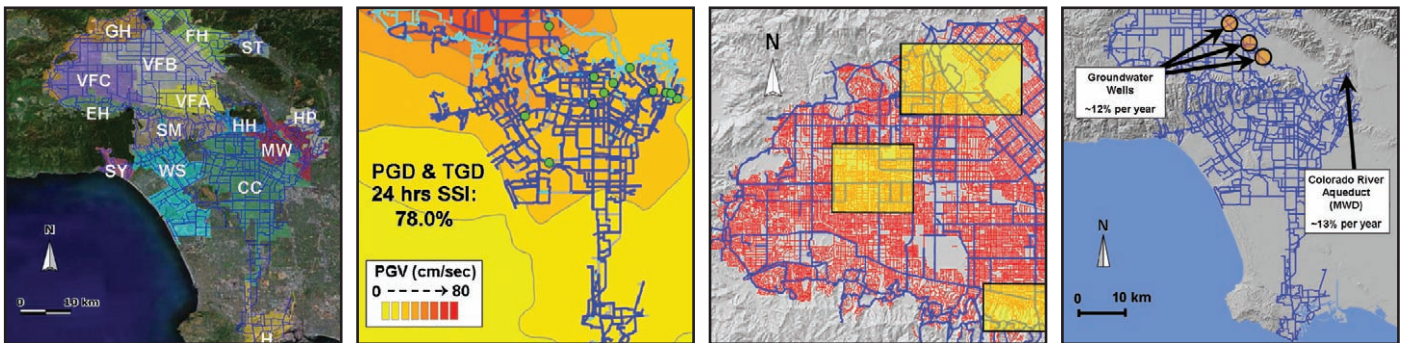


Water Supply Performance During Earthquakes and Extreme Events

by
Amanda L. Bonneau and Thomas D. O'Rourke



Technical Report MCEER-09-0003

February 16, 2009

NOTICE

This report was prepared by the University at Buffalo, State University of New York as a result of research sponsored by MCEER through a grant from the Earthquake Engineering Research Centers Program of the National Science Foundation under NSF award number EEC-9701471 and other sponsors. Neither MCEER, associates of MCEER, its sponsors, the University at Buffalo, State University of New York, nor any person acting on their behalf:

- a. makes any warranty, express or implied, with respect to the use of any information, apparatus, method, or process disclosed in this report or that such use may not infringe upon privately owned rights; or
- b. assumes any liabilities of whatsoever kind with respect to the use of, or the damage resulting from the use of, any information, apparatus, method, or process disclosed in this report.

Any opinions, findings, and conclusions or recommendations expressed in this publication are those of the author(s) and do not necessarily reflect the views of MCEER, the National Science Foundation, or other sponsors.

Water Supply Performance During Earthquakes and Extreme Events

by

Amanda L. Bonneau¹ and Thomas D. O'Rourke²

Publication Date: February 16, 2009

Submittal Date: January 16, 2009

Technical Report MCEER-09-0003

Task Number 10.1.2

NSF Master Contract Number EEC 9701471

- 1 Former Ph.D. Candidate, School of Civil and Environmental Engineering, Cornell University
- 2 Thomas R. Briggs Professor of Engineering, School of Civil and Environmental Engineering, Cornell University

MCEER

University at Buffalo, State University of New York

Red Jacket Quadrangle, Buffalo, NY 14261

Phone: (716) 645-3391; Fax (716) 645-3399

E-mail: mceer@buffalo.edu; WWW Site: <http://mceer.buffalo.edu>

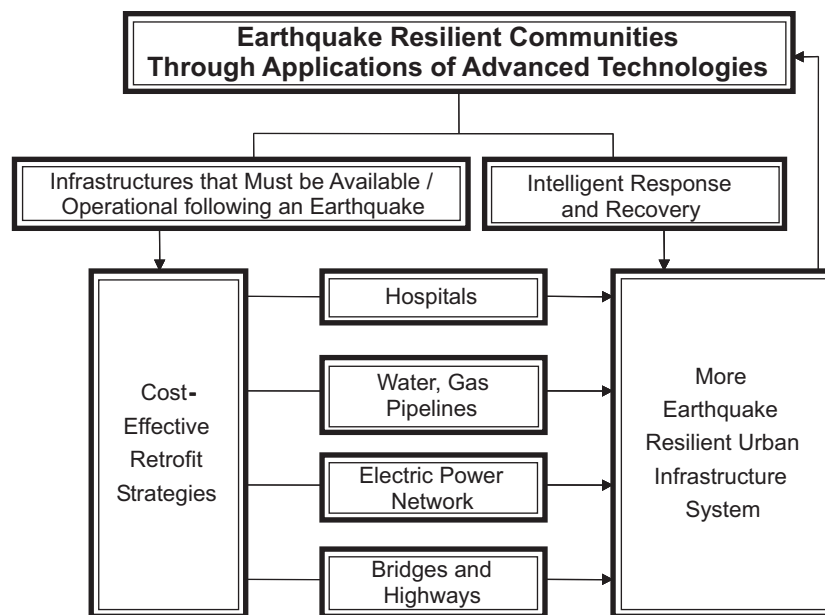
Preface

The Multidisciplinary Center for Earthquake Engineering Research (MCEER) is a national center of excellence in advanced technology applications that is dedicated to the reduction of earthquake losses nationwide. Headquartered at the University at Buffalo, State University of New York, the Center was originally established by the National Science Foundation in 1986, as the National Center for Earthquake Engineering Research (NCEER).

Comprising a consortium of researchers from numerous disciplines and institutions throughout the United States, the Center's mission is to reduce earthquake losses through research and the application of advanced technologies that improve engineering, pre-earthquake planning and post-earthquake recovery strategies. Toward this end, the Center coordinates a nationwide program of multidisciplinary team research, education and outreach activities.

MCEER's research is conducted under the sponsorship of two major federal agencies: the National Science Foundation (NSF) and the Federal Highway Administration (FHWA), and the State of New York. Significant support is derived from the Federal Emergency Management Agency (FEMA), other state governments, academic institutions, foreign governments and private industry.

MCEER's NSF-sponsored research objectives are twofold: to increase resilience by developing seismic evaluation and rehabilitation strategies for the post-disaster facilities and systems (hospitals, electrical and water lifelines, and bridges and highways) that society expects to be operational following an earthquake; and to further enhance resilience by developing improved emergency management capabilities to ensure an effective response and recovery following the earthquake (see the figure below).



A cross-program activity focuses on the establishment of an effective experimental and analytical network to facilitate the exchange of information between researchers located in various institutions across the country. These are complemented by, and integrated with, other MCEER activities in education, outreach, technology transfer, and industry partnerships.

This report presents the development of a functional Decision Support System for the seismic and multi-hazard performance of water supplies. An improved hydraulic network model of the full 2007 Los Angeles Department of Water and Power (LADWP) water distribution system is presented. The improved model includes an enhanced simulation of the time-dependent response, all sources of earthquake damage (loss of aqueducts, electric power outage, effects of permanent and transient ground deformations on pipelines), and fragility curves to characterize probabilistically the seismic damage to facilities such as tanks, reservoirs, regulation stations and pumps. The network model is validated through comparison of model results for the effects of the 1994 Northridge earthquake with actual areas of lost water service as well as pre- and post-earthquake flow measurements documented by LADWP. Parametric studies show that the most important factor affecting the post-earthquake system performance is the demand, followed by transient ground displacements. System serviceability is not influenced significantly by moderate changes in negative pressure tolerance, moderate variations in leakage rates, or changes in the percentages of breaks and leaks that cover the range of previous observations. An actual decision support problem faced by LADWP system management is used to demonstrate the application of the proposed methodology. The LADWP is modeled with and without several key reservoirs, which have been removed from service to meet water quality standards, to assess their influence on supplying water after an earthquake. It is demonstrated that opening the disconnected reservoirs immediately after a severe earthquake improves serviceability, with the most substantial impact in areas with the highest population densities.

ABSTRACT

This report investigates water supply performance during earthquakes and extreme events. The effects of the World Trade Center (WTC) disaster on the New York City water supply is investigated in detail and hydraulic network analyses are performed for fireboat hose and pumper truck relays that responded to land-based fires. Previous research by Shi (2006) and Wang (2006) is expanded to develop a functional decision support system (DSS) for the seismic and multihazard performance of water supplies, using the Los Angeles Department of Water and Power (LADWP) system as a test bed. This work also involves a parametric study of seismic water supply performance, de-aggregation of results according to sources of earthquake damage and geographic subsets of the LADWP system, and application of the methodology to an actual decision support problem faced by LADWP management.

Field investigations and analyses for the WTC disaster show that fireboats provided approximately 150% of the water initially available in underground pipelines and that the principal bottleneck in the conveyance of water from fireboats is hose size. There are substantial benefits from deploying 127 mm (5 in.) and 178 mm (7 in.) diameter hoses, and in using two pumper trucks per hose relay, as opposed to three.

Improvements in modeling include full representation of the 2007 LADWP system, simulation of time-dependent response in a robust and reliable manner, and inclusion of all sources of earthquake damage including loss of the Los Angeles Aqueducts (LAAs), electric power outage, permanent and transient ground deformation (PGD and TGD) effects in trunk and distribution pipelines, and fragility curves to probabilistically represent damage to facilities such as tanks, reservoirs, regulation stations, and pumps.

The hydraulic network model is validated through comparison of model results for the effects of the 1994 Northridge earthquake with actual areas of lost water service as well as pre-and post-earthquake measurements of flow documented by LADWP. Parametric studies for seismic water supply performance show that the most important factor affecting post-earthquake system performance is demand. Simulations show that TGD effects had substantially greater impact on

water supply performance than PGD effects. System serviceability is shown to not be significantly influenced (less than 5% change in serviceability) by moderate changes in negative pressure tolerance, large changes in leakage rates, or variations in the percentages of breaks and leaks.

The LADWP system is modeled with and without several key reservoirs, which have been removed from service to meet water quality standards, to assess their influence on supplying water after an earthquake. These results indicate that post-earthquake system performance can degrade significantly with increased demand, and that opening the disconnected reservoirs immediately after a serious earthquake improves serviceability, with the most substantial improvements experienced by water service areas with the highest population densities.

ACKNOWLEDGMENTS

This research was funded by the Earthquake Engineering Research Centers Program of the National Science Foundation (NSF) through the Multidisciplinary Center for Earthquake Engineering Research (MCEER). The financial support from the NSF and MCEER is gratefully acknowledged.

Thanks and acknowledgements are given to Craig Davis, Jianping Hu, and Victor Vargas, Los Angeles Department of Water and Power (LADWP), for their time and contribution to this work. Special thanks also go to Lt. Peter Farrenkopf and the firefighters of Marine Company 6, who welcomed us to the Brooklyn Naval Yard, provided first-person accounts of fireboat activities on 9/11, and compiled fireboat operating characteristics for use in this research.

TABLE OF CONTENTS

Chapter	Title	Page
1	INTRODUCTION	1
1.1	Background	1
1.2	Objectives	7
1.2.1	Water Supply Performance During the WTC Disaster	7
1.2.2	Model Improvements and Validation	8
1.2.3	Parametric Study of Seismic System Performance.....	9
1.2.4	De-Aggregation of System Simulation Results	9
1.2.5	Application of Decision Support System	10
1.3	Scope	10
2	WATER SUPPLY AND FIRE PROTECTION SYSTEM PERFORMANCE DURING THE WORLD TRADE CENTER DISASTER	13
2.1	Introduction	13
2.2	Fire Department of New York	14
2.3	New York City Water Supply	16
2.4	Fire Department Response	18
2.4.1	Land-based Response	18
2.4.2	Marine Response	19
2.4.2.1	McKean	22
2.4.2.2	Firefighter	23
2.4.2.3	Kane	24
2.4.2.4	Smoke II	24
2.5	Water Supply Performance	25
2.5.1	Collateral Damage	28
2.6	Hydraulic Network Analysis	29
2.7	Parametric Analysis	35
2.8	Fire Protection During 1989 Loma Prieta Earthquake	38
2.9	Discussion	41
2.10	Conclusions	43
3	EARTHQUAKE DECISION SUPPORT SYSTEM FOR WATER SUPPLIES	45
3.1	Decision Support System	45
3.2	System Definition	50
3.3	Earthquake/System Interaction	51
3.3.1	Scenario Earthquakes	51
3.3.2	Transient Ground Deformation	52
3.3.3	Permanent Ground Deformation	56
3.4	System Damage	56
3.4.1	Pipeline Damage	56
3.4.2	Pipeline Break Simulation	59
3.4.3	Pipeline Leak Simulation	60

TABLE OF CONTENTS (CONT'D)

Chapter	Title	Page
3.4.4	Post-earthquake Flows at Demand Nodes	63
3.4.5	Facility Damage	66
3.5	Hydraulic Network Analysis	68
3.6	Compilation of Results	69
3.7	Economic and Social Consequences	70
3.8	Model Validation with Respect to the Northridge Earthquake	71
3.8.1	LADWP System Performance during Northridge Earthquake	71
3.8.2	LADWP Hydraulic Network Model for the Northridge Earthquake	73
3.8.3	Damage Simulation	73
3.8.3.1	Trunk Line Damage	73
3.8.3.2	Distribution System Damage	75
3.8.3.3	Tank Damage	75
3.8.3.4	Water-Power Interaction/Pump Station Damage	77
3.8.4	Comparison of Simulated and Observed Earthquake Performance	78
3.8.4.1	System-wide Functionality	79
3.8.4.2	Geographic Distribution of Lost Service	80
3.8.4.3	Flow Measurements at Key Locations in the LADWP System	82
3.9	Conclusions	86
4	PARAMETRIC STUDY OF WATER SUPPLY RESPONSE TO EARTHQUAKES	89
4.1	Introduction	89
4.2	Scale and Time in System Modeling	90
4.2.1	Time Dependent Effects	91
4.2.2	Number and Size of Pipelines	93
4.3	PGD vs. TGD Effects	96
4.3.1	Actual Northridge Earthquake Damage	98
4.3.2	M _w 6.5 Scenario	101
4.3.3	M _w 7.0 Scenario	107
4.4	Parametric Studies	111
4.4.1	Negative Pressure Tolerance	112
4.4.2	Percentage of Breaks vs. Leaks	113
4.4.3	Leakage Rate	114
4.4.4	Leak Type Probability	117
4.5	Conclusions	118
5	DE-AGGREGATION OF EARTHQUAKE EFFECTS ON WATER SUPPLY PERFORMANCE	121
5.1	Introduction	121
5.2	System Modeling	122
5.3	De-Aggregation of Earthquake Effects	125
5.3.1	System Performance Due to Los Angeles Aqueduct Outage	125

TABLE OF CONTENTS (CONT'D)

Chapter	Title	Page
5.3.2	System Performance Due to Electric Power Outage	128
5.3.3	System Performance with Northridge Trunk Line Damage	129
5.3.4	System Performance Due to Tank Damage	131
5.3.5	Combined Effects of Electric Power Loss and Northridge Trunk Line Damage on System Performance	133
5.3.6	Combined Effects of Los Angeles Aqueduct Outage, Electric Power Loss, Northridge Trunk Line Damage, and Distribution System Damage on System Performance	135
5.4	Conclusions	137
6	APPLICATION OF DECISION SUPPORT SYSTEM	141
6.1	Introduction	141
6.2	LADWP Reservoirs	142
6.3	Repeat M_w 7.0 Northridge Scenario Earthquake	144
6.4	Simulation Results for M_w 7.0 Earthquake	144
6.4.1	System-wide Serviceability Results	145
6.4.2	Dense Population Area Serviceability Results	149
6.4.3	Serviceability Results for the 15 Water Service Areas	153
6.5	Conclusions	156
7	SUMMARY AND CONCLUSIONS	159
7.1	Introduction	159
7.2	Water Supply Performance During the WTC Disaster	160
7.3	Model Improvements and Validation	162
7.4	Parametric Study of Seismic System Performance	164
7.5	De-Aggregation of System Simulation Results	165
7.6	Application of Decision Support System	167
7.7	Future Research Directions	168
8	REFERENCES	173
APPENDIX A: ADJUSTMENTS FOR VARIABLE DEMAND IN FRAGILITY RELATIONS FOR LOCAL WATER DISTRIBUTION NETWORKS ..		183
APPENDIX B: LADWP TRUNK LINE DAMAGE FROM 1994 NORTHRIDGE EARTHQUAKE		189
APPENDIX C: MODELING PROCEDURES FOR PUMPS AND TANKS AT HIGH ELEVATIONS		203
APPENDIX D: SIZE DISTRIBUTION OF PIPELINES IN LOS ANGELES AND NEW YORK CITY WATER SUPPLIES		207

LIST OF FIGURES

Figure	Title	Page
1.1	LADWP Water Distribution System	3
2.1	Structure of the FDNY Command System	15
2.2	NYC Water Supply System with Water Tunnels 1, 2 and 3	17
2.3	Aerial View of the WTC Site Before the Collapse of WTC1 and WTC2	20
2.4	FDNY Fireboat Travel Routes on September 11, 2001	21
2.5	Schematic of Fireboat Deployments near the WTC Comple	22
2.6	Schematic of Operational Status of Water Mains near WTC Area on September 12, 2001	26
2.7	Water Flow vs. Time for the Water Supply to Lower Manhattan on September 11, 2001	28
2.8	Schematic of Hose and Pumper System for Hydraulic Network Modeling of Fireboat Firefighter Flows to WTC Site	31
2.9	Schematic of Hose and Pumper System for Hydraulic Network Modeling of Fireboat McKean Flows to WTC Site	34
2.10	Schematic of Hose and Pumper System for Hydraulic Network Modeling of Fireboat Kane/Smoke II Flows to WTC Site	34
2.11	Schematic of Hose and Pumper Trucks for Parametric Study – 1 Hose Relay with 3 Pumper Trucks	36
2.12	Schematic of Hose and Pumper Trucks for Parametric Study – 2 Hose Relays with 4 Pumper Trucks	36
2.13	Travel Route and Tie-Up Location for Fireboat Phoenix and Hose 40 Line Deployments after the Loma Prieta Earthquake	40
3.1	Generic Framework for the Effects of Hazards on Lifeline System Performance	47
3.2	Flow Chart for Hydraulic Network Analysis of Water Supplies Damaged by Earthquakes	48
3.3	PGV Contour Surface for Mean + $\sigma_{\text{inter-event}}$ PGV for Verdugo Scenario Earthquake at Rock Site Conditions	54
3.4	PGV Contour Surface for Mean + $\sigma_{\text{inter-event}}$ PGV for Verdugo Scenario Earthquake after Site Condition Corrections	55
3.5	Regressions for RR vs. PGV for Steel (WSJ Steel Distr.), Cast Iron (CI), Ductile Iron (DI), and Asbestos Cement (AC) Distribution Pipelines	58
3.6	Regressions for RR vs. PGV for (a) Cast Iron and Ductile Iron Trunk Lines, and (b) Concrete, Riveted Steel, and Steel Trunk Lines	58
3.7	Simulation Models for a Pipeline Break and Leak	60
3.8	Comparison Between Model Predictions and Sprinkler Data	62
3.9	Locations of LADWP Local Distribution Systems Used to Develop Fragility Curves for Demand Nodes	65
3.10	Fragility Curves Comparing Simulated and Observed Results for 66 Repair Rate vs. Normalized Demand	66

LIST OF FIGURES (CONT'D)

Figure	Title	Page
3.11	Fragility Curves for Water Tanks	67
3.12	LADWP Damaged Tanks, Trunk and Distribution Line Repairs, and Water Outage Areas after the Northridge Earthquake	72
3.13	Location of Breaks, Leaks and Damaged Tanks used in Repeat Northridge Earthquake Simulation	74
3.14	Zones of PGD in the LADWP Water Supply System	76
3.15	Pump Station Operational Status 2 Hours after the Northridge Earthquake	78
3.16	Comparison of Simulated Flows 24 Hours after the Earthquake with Zones of Documented Lost Service	81
3.17	SCADA Flow Stations and Key Locations of Flow	83
3.18	Comparisons Between Simulation Results and Measured SCADA Flows Before and After the Northridge Earthquake	84
4.1	Simplified Schematic for Interaction Between Los Angeles Filtration Plant and Clearwell Tank	93
4.2	System Serviceability vs. Relative Demand for System Response 24 Hours after the Northridge Earthquake	96
4.3	Locations of Northridge Earthquake Damage and Zones of PGD	99
4.4	PGD Only Simulation Results at 24 Hours for the Actual Northridge Earthquake Damage	100
4.5	TGD Pipeline Damage Locations and Pipeline Flow at 24 Hours for the Actual Northridge Earthquake Damage	102
4.6	PGD and TGD Pipeline Damage Locations and Pipeline Flow at 24 Hours for the Actual Northridge Earthquake Damage	103
4.7	TGD Pipeline Damage Locations and Pipeline Flow at 24 Hours for the TGD Only $M_w6.5$ Repeat Northridge Earthquake Scenario	105
4.8	PGD and TGD Pipeline Damage Locations and Pipeline Flow at 24 Hours for the Combined PGD & TGD $M_w6.5$ Repeat Northridge Earthquake Scenario	106
4.9	Histogram for TGD only and Combined PGD and TGD System Serviceability 24 Hours after a $M_w6.5$ Repeat Northridge Earthquake Scenario	107
4.10	TGD Pipeline Damage Locations and Pipeline Flow at 24 Hours for the TGD Only $M_w7.0$ Repeat Northridge Earthquake Scenario	109
4.11	PGD and TGD Pipeline Damage Locations and Pipeline Flow at 24 Hours for the Combined PGD and TGD $M_w7.0$ Repeat Northridge Earthquake Scenario	110
4.12	Histogram for TGD Only and Combined PGD and TGD System Serviceability 24 Hours after a $M_w7.0$ Repeat Northridge Earthquake Scenario	111
4.13	Mean and Median SSI values at 0 and 24 Hours for 0 MPa, -0.034 MPa (-5 psi), and -0.069 (-10 psi) Minimum Negative Pressure Tolerance	113

LIST OF FIGURES (CONT'D)

Figure	Title	Page
4.14	Mean and Median SSI values at 0 and 24 Hours after the Earthquake for Various Breaks/Leaks Scenarios	114
4.15	Leakage Rate Curves for the 5 Leak Types	116
4.16	Mean and Median SSI values at 0 and 24 Hours after the Earthquake for 50% Increase and Decrease in Leakage Rate	116
4.17	Mean and Median SSI values at 0 and 24 Hours after the Earthquake for Various Leak Type Probabilities	118
5.1	Modifications to 2002 LADWP Hydraulic Network to Produce 2007 Hydraulic Network	124
5.2	Water Service Areas in the LADWP System	126
5.3	Serviceability Index after 24 Hours for 15 Water Service Areas with Loss of Los Angeles Aqueducts and No Other Damage	127
5.4	Serviceability Index after 24 Hours for 15 Water Service Areas with Electric Power Loss and No Other Damage	129
5.5	Northridge Trunk Line Damage	130
5.6	Serviceability Index after 24 Hours for 15 Water Service Areas with Northridge Trunk Line Damage and No Other Damage	131
5.7	Serviceability Index after 24 Hours for 15 Water Service Areas with LAAs Off and Northridge Trunk Tank Damage	133
5.8	Serviceability Index after 24 Hours for 15 Water Service Areas with Northridge Trunk Line Damage and Electric Power Loss for Los Angeles Aqueducts On	134
5.9	Serviceability Index after 24 Hours for 15 Water Service Areas with Northridge Trunk Line Damage, Electric Power Loss, and Los Angeles Aqueducts Off	135
5.10	Serviceability Index after 24 Hours for 15 Water Service Areas with Northridge Trunk Line Damage, Electric Power Loss and Distribution System Damage for Los Angeles Aqueducts Off	136
6.1	Locations and Storage Capacities of Los Angeles, Encino, Lower Stone Canyon, and Hollywood Reservoirs	143
6.2	Median Trunk Line at 24 Hours for Summer and Winter Demands with Out-of-Service Reservoirs Open and Closed	146
6.3	SSI at 24 Hours for Repeat Northridge Earthquake Scenario, Winter Demand with Out-of-Service Reservoirs Open and Closed	147
6.4	SSI at 24 Hours for Repeat Northridge Earthquake Scenario, Summer Demand, with Out-of-Service Reservoirs Open and Closed	147
6.5	LADWP Pipelines and Water Service Areas Superimposed on 2000 Census Block Group Image	150
6.6	Dense Population Area SSI at 24 Hours for Repeat Northridge Earthquake Scenario, Winter Demand with Out-of-Service Reservoirs Open and Closed ...	152

LIST OF FIGURES (CONT'D)

Figure	Title	Page
6.7	Dense Population Area SSI at 24 Hours for Repeat Northridge Earthquake Scenario, Summer Demand with Out-of-Service Reservoirs Open and Closed	152
6.8	Serviceability Index at 24 Hours for 15 Water Service Areas for Winter Demand with Out-of-Service Reservoirs Open and Closed	154
6.9	Serviceability Index at 24 Hours for 15 Water Service Areas for Summer Demand with Out-of-Service Reservoirs Open and Closed	154
6.10	Comparison of 24 Hour SSI for the 15 Water Service Areas for a Repeat Northridge Earthquake Scenario, Out-of-Service Reservoirs Open and Closed for Winter and Summer Demand Scenarios	155
A.1	Map Showing the Distribution System 1000 Hydraulic Network Model	186
A.2	Simulated vs. Linearly Approximated ND_w Values for Distribution Zone 1000	187
B.1	Granada Trunk Line Repairs	190
B.2	Rinaldi Trunk Line Repairs	194
B.3	Roscoe Trunk Line Repairs	196
B.4	Other Trunk Line Damage Locations	199
B.5	Other Trunk Line Repairs outside Van Norman Complex	201
C.1	Simulation Results for Mount Washington Pump Premise Logic Controls Off and On	205
D.1	Pipeline Diameters in the NYC and LADWP Water Systems	207

LIST OF TABLES

Table	Title	Page
2.1	Summary of Hydraulic Network Components of Fireboat/Pumper Truck Relay	33
2.2	Summary of Parametric Study for WTC Fireboat Pumping Scenarios	38
3.1	Probability of Leak Types for Different Pipe Materials	62
B.1	Granada Trunk Line Damage Information Summary	191
B.2	Rinaldi Trunk Line Damage Information Summary	195
B.3	Roscoe Trunk Line Damage Information Summary	197
B.4	Other Trunk Line Damage Information Summary 1	200
B.5	Other Trunk Line Damage Information Summary 2	202

CHAPTER 1

INTRODUCTION

1.1 Background

The concept of a “lifeline” system was developed to evaluate the performance of large, geographically distributed networks during earthquakes (Duke and Moran, 1972). There are six principal lifeline systems: electric power, gas and liquid fuels, telecommunications, transportation, waste disposal, and water supply. Taken individually, or in aggregate, these systems are intimately linked with the economic well-being, security, and social fabric of the communities they serve (O’Rourke, 2007).

A water supply is one of the most important lifeline systems. It protects virtually all buildings and facilities from fire, underpins basic residential services and household functionality, and supports most commercial and industrial operations. Concomitantly, water supply damage can physically undermine and disrupt neighboring lifeline systems. Water supply damage, in particular, has been used to illustrate the concept of cascading damage, whereby damage and loss of function propagate through several lifeline networks. For example, failure of a single water main in the Garment District of New York City (NYC) flooded an electric power substation, causing serious fires, cutting off electricity in mid-town Manhattan, interrupting telecommunication services, shutting down a large part of the subway system, and generating millions of dollars of indirect economic losses due to business disruption (O’Rourke, 1993). In such cases, the initial damage propagates through

loss of operability in large parts of interdependent systems until there is a pervasive loss of critical infrastructure service with serious, regional economic consequences.

It is well known that water supplies are vulnerable to earthquakes. There has been extreme damage to water supplies during previous earthquakes, such as the 1906 San Francisco (e.g., Schussler, 1906; Manson, 1908; Lawson, 1908; Scawthorn, et al., 2006), 1971 San Fernando (e.g., Steinbrugge, et al., 1971; Subcommittee on Water and Sewerage Systems, 1973; Eguchi, 1982), and 1994 Northridge (e.g., Lund and Cooper, 1995; Hall, 1995; Eguchi and Chung, 1995; O'Rourke, et al., 2001) earthquakes. Moreover, there has been extensive research focused on the seismic modeling of water supply systems (e.g., Eguchi, et al., 1983; Ballantyne, et al., 1990; Khater and Grigoriu, 1989; Markov et al., 1994; Shinozuka, et al., 1981, 1992, 1998; Hwang, et al., 1998; Chang, et al., 2000a; Wang, 2006; Shi, 2006; Shi, et al., 2006; and Wang and O'Rourke, 2007).

Most recently, research by Shi (2006) and Wang (2006) has resulted in a comprehensive modeling process for the seismic performance of water supply systems, using the Los Angeles Department of Water and Power (LADWP) system as a test bed. As illustrated in Figure 1.1, the LADWP system contains nearly 12,000 km (7,456 mi.) of trunk and distribution pipelines, making it the second largest U.S. water distribution network. It serves about 4 million people, and is highly vulnerable to risks that threaten its sustainability. Los Angeles is experiencing fast growth in a relatively arid climate, with high water use per capita. It depends on imported water for 87% of its supplies from areas that are increasingly susceptible to drought, and by way of a small number of transmission and aqueduct systems that are vulnerable to earthquakes, landslides, and human threats. As shown in the figure, approximately

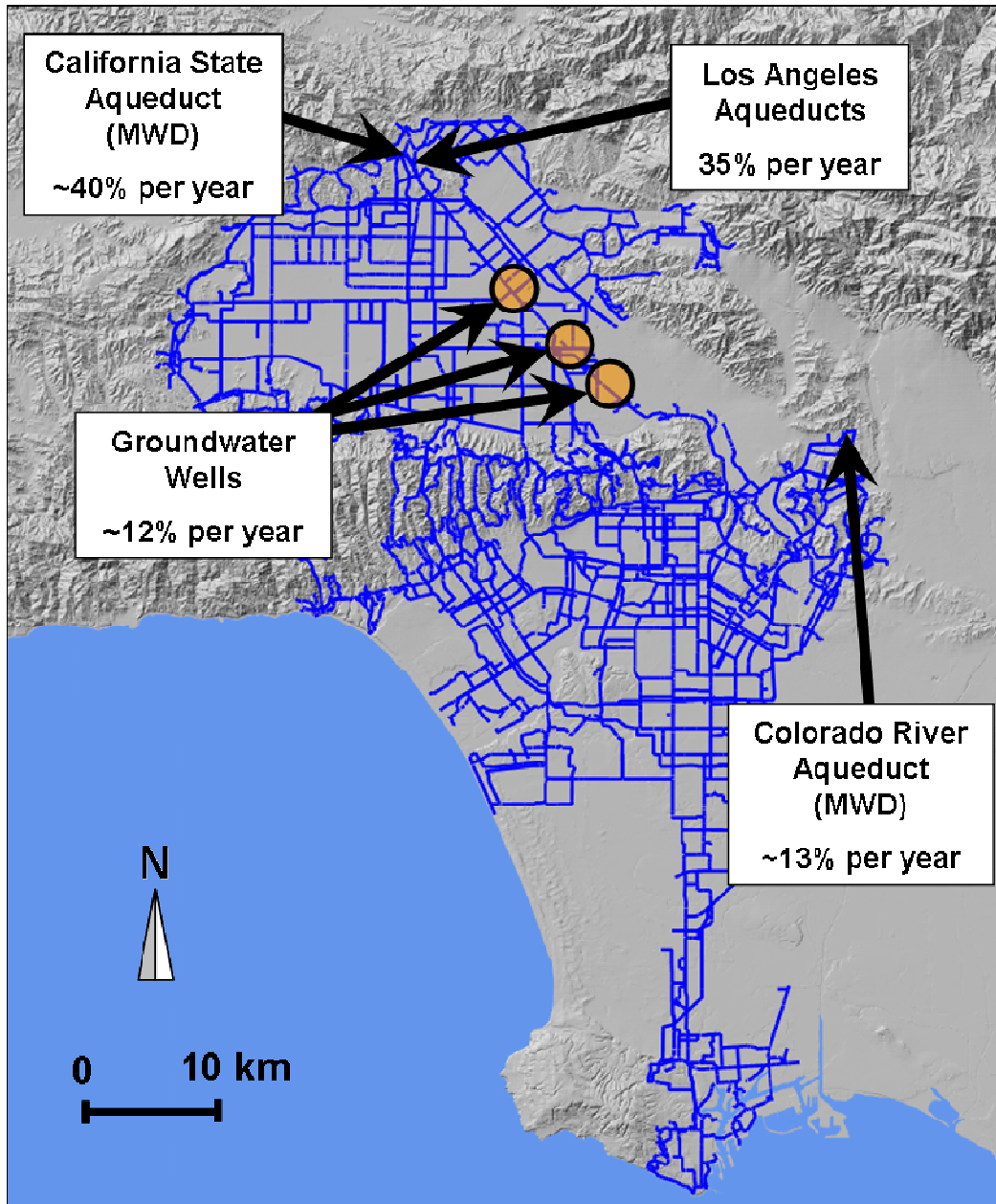


Figure 1.1 LADWP Water Distribution System

40% of the LADWP water comes from the California State Aqueduct, 35% from the Los Angeles Aqueducts, 13% from the Colorado River Aqueduct, and 12% from groundwater wells.

The modeling methodology developed by Shi (2006) and Wang (2006) is generic, and the architecture of its computer programs is adaptable to any water supply or simulation of extreme event. The methodology works in conjunction with an easily accessible hydraulic network model, EPANET, which is available on-line from the U.S. Environmental Protection Agency (EPA, 2008), as well as a special program for damaged network flow modeling, known as Graphical Iterative Response Analysis for Flow Following Earthquakes (GIRAFFE). Details on the development and evaluation of GIRAFFE are provided by Wang (2006), Shi (2006), Shi, et al., (2006), and Wang and O'Rourke (2007).

The model developed for the LADWP water supply simulates all 11,633 km (7,228 mi.) of water trunk and distribution pipelines and related facilities (e.g., tanks, reservoirs, pressure regulation stations, pump stations, etc.) in the LADWP system. The decision support system accounts for the aggregated seismic hazard in Los Angeles through an ensemble of 59 scenario earthquakes. The 59 scenario earthquakes also provide a library of seismic scenarios, from which engineers can select specific scenarios or combinations of scenarios to assess system performance. The decision support system works with risk and reliability assessment tools to provide metrics of system performance. The computer simulations account for the interaction of the water and electric power supplies, and model output can be used to evaluate the regional economic and community impacts of water losses. All system

input and output can be visualized through GIS with advanced query logic and web-based features. The simulations are dynamic in time, and can account for loss of service as tanks and local reservoirs lose water over time through leaks and breaks in pipelines.

The adaptation of water supply system simulation to replicate the effects of extreme events other than earthquakes represents the next step in model development. Broadening simulation capabilities to address multiple hazards requires additional data from actual case histories. Such information helps to understand and quantify the interdependencies among water supplies and other critical infrastructure systems. O'Rourke, et al., (2003, 2005a, 2005b, 2005c) describe the interdependent performance of the NYC water supply, fire protection, electric power, telecommunications, natural gas, and steam systems during the World Trade Center (WTC) disaster. The information presented in these publications and the databases collected during the associated investigations provide an excellent basis for a more comprehensive assessment of water supply performance during extreme events.

A decision support system (DSS) is a computer-based information and modeling system that works interactively with users to address unstructured problems for strategic planning, management, and operations (Turban, 1995). The DSS benefits from an iterative, or evolutionary, process whereby users provide feedback that influences the DSS development (Sprague and Watson, 1989; Keen, 1980). By providing a framework for quantifying the effects of water losses on emergency responders, regional businesses, and service area neighborhoods, the DSS is able to expand the scope of decision making beyond the engineering and operational applications that have been the traditional focus of water supply modeling.

Although Shi (2006) and Wang (2006) developed a comprehensive modeling process for the seismic performance of water supplies, additional modeling refinements are needed for successful integration into a functional DSS. Refinements include improved time-dependent modeling, updates in system characterization, and the inclusion of all potential sources of earthquake disruption, including damaged tanks and reservoirs. The final stage of DSS development requires the use of post-earthquake water supply simulations to make real decisions about unbounded management problems.

Recently, researchers have created models that link system reliability and serviceability assessments to regional economic impacts (Bruneau, et al., 2003; Chang, et al., 1996, 2000a, 2002; Rose and Liao, 2003; Shinozuka, et al., 1998). For example, Chang, et al., (1996, 2000a, 2002) has shown through system simulations how water distribution damage is tied to regional economic impact through a methodology that correlates water losses with areas of economic activity, adjusts for business resiliency, and accounts for direct and indirect economic losses. Indirect economic losses were initially estimated with Input-Output analysis (Rose, et al., 1997). More recently, Rose and Liao (2005) have evaluated the regional economic consequences of earthquakes, regulatory failures, and terrorist attacks utilizing information on water supply disruption in conjunction with a Computable General Equilibrium (CGE) model of Los Angeles County.

Although Shi (2006) and Wang (2006) developed a comprehensive modeling process for the seismic performance of water supplies, additional modeling refinements are needed for successful integration into a functional DSS. Refinements include improved time-dependent modeling, updates in system characterization, and

the inclusion of all potential sources of earthquake disruption, including damaged tanks and reservoirs. The final stage of DSS development requires the use of post-earthquake water supply simulations to make real decisions about unbounded management problems.

1.2 Objectives

The goals of this work are to investigate comprehensively and report on the effects of the WTC disaster on the NYC water supply, and to expand on the research of Shi (2006) and Wang (2006) to develop a functional DSS for the seismic and multihazard performance of water supplies, using the LADWP system as a test bed. Research described in this work on the seismic performance of water supplies has resulted in the implementation of several important model improvements, as well as upgrading the model developed by Shi (2006) and Wang (2006) to represent the LADWP system as of 2007. It also involves a parametric study of seismic water supply performance, de-aggregation of system simulation results according to individual sources of earthquake damage and geographic subsets of the system, and application of the methodology to an actual decision support problem faced by LADWP management. The goals of the report are addressed by focusing on five objectives as briefly described under the subheadings that follow.

1.2.1 Water Supply Performance During the WTC Disaster

The performance of the NYC water supply and fire protection systems during the WTC disaster was investigated in detail. The water losses sustained by distribution pipelines are described herein and their influence on fire fighting as well

as telecommunication and transportation lifelines are evaluated. Hydraulic network analyses are performed to quantify the performance of hose and pumper truck relays from fireboats to the WTC site, and the results of the analyses are used to recommend tactical improvements in firefighting with marine sources of water. The performance of the fire protection system during the WTC disaster is compared with fire protection system performance during the 1989 Loma Prieta earthquake.

1.2.2 Model Improvements and Validation

Models have been developed by Shi (2006) and Wang (2006) for the 2002 LADWP water system. Those models are able to represent time dependent changes in system performance in only an approximate way. Hence, model improvements are required to represent time-dependent system response in a more robust manner. Additional improvements are required to update previous models to conditions that better reflect the current system and to integrate all sources of earthquake damage into modeling and DSS capabilities. Finally, the LADWP hydraulic network model needs to be validated by comparison with system performance during an actual earthquake. Improvements in the hydraulic network model have been made as part of this work, including incorporation of an accurate time-dependent simulation of reservoirs and tanks, upgrade to 2007 LADWP system conditions, and integration of stochastic and deterministic modeling techniques for all sources of potential earthquake damage. The resulting hydraulic network model and DSS are described, and the model is validated by comparing system simulation results with detailed observations and measurements of LADWP system performance during and after the 1994 Northridge earthquake.

1.2.3 Parametric Study of Seismic System Performance

A hydraulic network model is sensitive to various decisions about the time increment and size of the model. Some of the most fundamental questions involve minimum time increment for reliable modeling and the number and type of pipelines that need to be modeled. Additional variables affecting system performance include the effects of permanent ground deformation (PGD) and transient ground deformation (TGD) on post-earthquake operability, as well as the effects of certain modeling characteristics, such as minimum negative pressure tolerance, the percentages of pipeline breaks and leaks associated with earthquake damage, and the characterization of leakage in damage underground pipelines. This study presents a series of parametric studies to explore the sensitivity of system response to these aforementioned parameters.

1.2.4 De-Aggregation of System Simulation Results

The hydraulic network model embodied in the DSS for the LADWP water supply accounts comprehensively for various sources of earthquake damage and disruption. Earthquake effects can also be de-aggregated such that the water supply response is simulated for one source of disruption at a time, or for any combination of sources. System simulations are performed in this work for de-aggregated single sources of damage associated with the Northridge earthquake, the combined effect of multiple damage sources, and all sources of Northridge earthquake damage. By de-aggregating the damage, the most important sources of disruption with respect to lost system service are evaluated and system vulnerabilities are identified.

1.2.5 Application of Decision Support System

One of the primary functions of a DSS is to provide solutions for an unbounded problem in a way that allows managers to evaluate different potential outcomes and select the most appropriate measures to improve system performance. This study applies the DSS to an unbounded problem of LADWP water supply management involving the removal of three large reservoirs from service because of water quality requirements, and assesses the impact of removal on the potential response of the water supply to a future earthquake. Simulation results are presented for conditions in which the reservoirs removed from service are 1) disconnected from the system, and 2) reconnected on an emergency basis, and their significance with respect to storage capacity is discussed.

1.3 Scope

The work is divided into seven chapters, the first of which provides background and objectives of the study. Chapter 2 focuses on the performance of the NYC water supply and fire protection system during the WTC disaster, and assesses water losses sustained by damaged water distribution pipelines. The impact of water system disruption on emergency response and the performance of telecommunications and transportation infrastructure are also explained. Hydraulic network analyses are performed to quantify the performance of hose and pumper truck relay systems from fireboats to the WTC site, and to provide guidance on the most effective selection of hose size, number of hose lines and pumper trucks for future use of fireboats for landside fire protection. The performance of the fire protection system in NYC is

compared with fire protection system performance during the 1989 Loma Prieta earthquake.

Chapter 3 describes in detail a decision support system (DSS) developed for the seismic performance of water supplies, and implemented by LADWP. This chapter also presents the results of the LADWP hydraulic network model calibration and validation with respect to the 1994 Northridge earthquake.

Chapter 4 discusses the importance of time and scale in hydraulic network modeling, and presents the results of parametric studies to evaluate the sensitivity of the system simulation results to key variables. The parameters investigated include the choice of time interval for time-dependent system modeling, nodal demands from distribution pipelines, the effects of permanent ground deformation (PGD) and transient ground deformation (TGD) on post-earthquake operability, minimum negative pressure tolerance, the percentages of pipeline breaks and leaks associated with earthquake damage, and the characterization of leakage in damaged underground pipelines.

Chapter 5 provides a description of the LADWP system model updated for 2007 conditions, and presents simulation results for de-aggregated sources of actual damage and disruption of service associated with 1994 Northridge earthquake. The de-aggregated scenarios performed include the loss of the Los Angeles Aqueducts (LAAs), electric power outage, Northridge earthquake trunk line damage, and Northridge earthquake tank damage. Simulation results for the combined effects of these damage sources are also presented, as well as a simulations including all sources of damage from the Northridge earthquake.

Chapter 6 provides an application of the DSS to an unbounded problem of water supply management involving the removal of reservoirs from LADWP service, and evaluates the effects of reservoir removal on system performance during a repeat Northridge earthquake. Simulation results are presented for conditions in which the reservoirs removed from service are 1) disconnected from the system, and 2) reconnected on an emergency basis. The geographic distribution of system performance is assessed, and the implications of the results are discussed with respect to emergency planning.

The final chapter summarizes the research findings and presents conclusions pertaining to the work. It also provides recommendations for future research.

CHAPTER 2

WATER SUPPLY AND FIRE PROTECTION SYSTEM PERFORMANCE DURING THE WORLD TRADE CENTER DISASTER

2.1 Introduction

Although much has been written about the structural collapse and building fire damage associated with the World Trade Center (WTC) disaster (FEMA, 2002; NIST 2005) there has been comparatively little written about the effects on other parts of the infrastructure. O'Rourke, et al. (2005a, 2005b, 2005c, 2006), for example, summarized the consequences of the WTC disaster on critical infrastructure systems, such as electric power, telecommunications, and water distribution. Zimmerman (2003) described the response and recovery of various infrastructure systems after September 11, 2001 (9/11), and drew attention to the need for flexibility in both physical and social systems as an important aspect of community resilience.

This paper focuses on the performance of the NYC water supply and fire protection system during the WTC disaster. It describes the NYC fire department and water supply system, and provides an account of the fire department response to the disaster. The water losses sustained by damaged water distribution pipelines are discussed and their impact on emergency response and the performance of telecommunications and transportation infrastructure are explained. The results of hydraulic network analysis are presented to quantify the performance of hose and pumper truck relay systems from fireboats to the WTC site. The results of a

parametric study of fire fighting relay systems are summarized to provide guidance on the most effective selection of hose size, number of hose lines and pumper trucks for future use of fireboats for landside fire protection. The performance of the fire protection system in NYC is compared with fire protection system performance during the 1989 Loma Prieta earthquake, and recommendations are made for improved emergency response from both a tactical and strategic perspective.

2.2 Fire Department of New York

The Fire Department of New York (FDNY) protects more than 8 million residents in an area of 830 km² (320 mi²) (FDNY, 2005). The uniformed force consists of more than 11,400 fire officers and firefighters. In addition, the FDNY includes 2,800 emergency medical technicians, paramedics and supervisors assigned to the Bureau of Emergency Medical Service (EMS), as well as 1,200 civilian employees (FDNY, 2005). Figure 2.1 depicts the structure of the FDNY Command System, which is organized into 9 divisions, each of which is subdivided into battalions. On average, a battalion will have 3 to 4 engine companies and 2 to 4 ladder companies (9/11 Commission, 2005).

Engine companies operate what are commonly referred to as fires engines, each of which is equipped with a water tank, pump, and hoses. The standard FDNY engine is equipped with a 3,785 lpm (1,000 gpm) pump and a 1,893 liter (500 gal.) tank of water (PBS, 2005). An on-duty engine company usually consists of an officer and 4 to 5 firefighters (Smith, 2002).

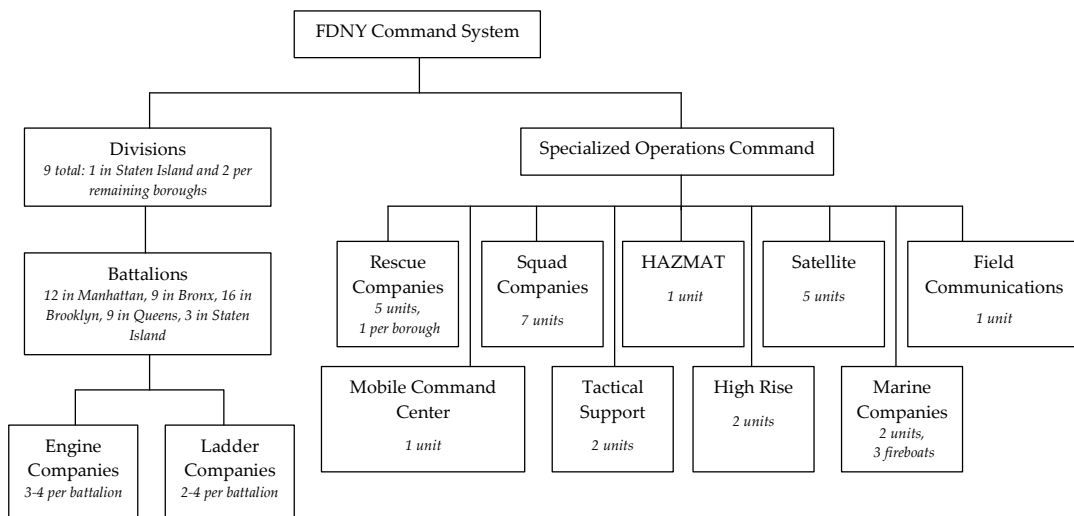


Figure 2.1 Structure of the FDNY Command System (Smith, 2002)

Ladder companies operate larger trucks (sometimes called hook and ladders) with equipment that supports rescue operations and forcible entry. Ladder companies are also responsible for the ventilation and overhaul of a fire area to ensure there is no heat or fire in the walls. An on-duty ladder company typically consists of an officer and 5 firefighters (Smith, 2002).

The FDNY also has a number of Specialized Operations Command Units that have had specific training in specialized tools and techniques for emergency situations. These include rescue companies, squad companies, marine companies, a hazardous materials unit, satellite units, a field communication unit, a mobile command center, tactical support, and high rise units.

On 9/11, there were 205 engine, 133 ladder, and 3 marine companies on call throughout the city. The marine companies of the FDNY maintain a fleet of 3

operational fireboats that can be used to fight open water fires, supplement land-based fire fighting, and perform rescue and transport operations.

2.3 New York City Water Supply

The City of New York, through its Department of Environmental Protection (NYC DEP), delivers as much as 4.9 billion liters (1.3 billion gal.) of water during the summer to roughly 9 million people per day (8 million NYC residents, 1 million consumers in 4 upstate counties and nearly 100,000 commuters and tourists) (NYC DEP, 2005). The water system is composed of 19 reservoirs and 3 controlled lakes which provide for 2,196 billion liters (580 billion gal.) of total storage capacity. Water flows from 3 main reservoir systems: the Croton, Catskill and Delaware Systems. Nearly 97% of water distribution is driven by gravity, with pumping required for the remaining 3% (NYC DEP, 2005).

Figure 2.2 shows the water supply system south of the Kensico Reservoir. When water reaches the Hillview Reservoir, at an elevation of 90 meters above sea level, it has sufficient pressure to reach the 6th floor of most NYC buildings without pumping. From the Hillview Reservoir, water enters one of 3 main city water distribution tunnels as shown in Figure 2.2b. City Tunnel 1, commissioned in 1917, carries water from the Hillview Reservoir to trunk lines in the Bronx and Manhattan. City Tunnel 2, commissioned in 1938, carries water from the Hillview Reservoir to trunk lines in the Bronx, Queens, and Brooklyn. City Tunnel 3, which has been under construction since 1970, will involve nearly 96 km (60 mi.) to service areas in the Bronx, Manhattan, Queens, and Brooklyn. Figure 2b indicates the completed phases of Tunnel 3, as well as those currently under construction and planned for future

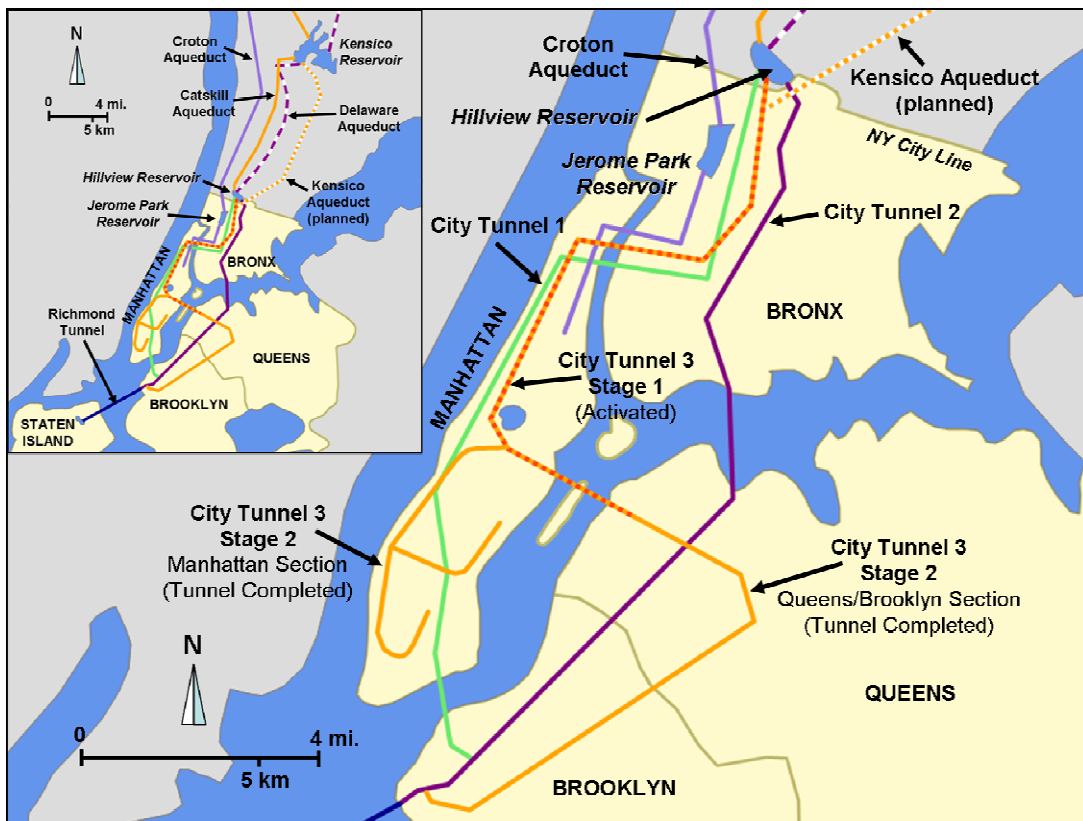


Figure 2.2 New York City Water Supply System with Water Tunnels 1, 2 and 3
(NYC DEP, 2005)

construction. City Tunnel 3, which is scheduled for completion in 2020, will allow for complete dewatering and repair of either City Tunnels 1 or 2.

City Tunnel 1 is the backbone of supply for 90% of the water consumed in Manhattan. The tunnel is about 183-213 m (600-700 ft.) below street surface and transmits water to the distribution pipeline system through riser shafts. The shafts are equipped with regulators to decrease pressure to a level compatible with the capacity of the distribution pipelines.

The water distribution system within NYC is composed of approximately 10,934 km (6,800 mi.) of pipelines, 75% of which are cast iron mains mostly installed before 1950. The remaining 25% of the system are ductile iron pipelines installed after 1970 (Chapin, 2001).

2.4 Fire Department Response

The FDNY response to the WTC disaster involved 3 principal operations: 1) rescue activities based at the WTC towers, 2) firefighting with water from hydrants, mainly, but not exclusively, on the eastern side of the WTC site, and 3) fireboats pumping water from the Hudson River to deliver water to the western side of the disaster area.

2.4.1 Land-based Response

Figure 2.3 is an aerial view of the WTC site before the collapse of the twin towers, which shows the locations of key buildings involved in the land-based response of the FDNY. The FDNY response to the 9/11 attack began shortly after the first plane crashed into WTC 1 at 8:46 am. By 9:00 am, 21 engine companies, 9 ladder companies, 4 elite rescue teams, 2 squad companies, and the hazmat team and its support staff had been dispatched to the scene. When the second plane hit WTC 2 at 9:03 am, further units were dispatched and by 9:54 am nearly one third of all FDNY units had been dispatched to the WTC site (9/11 Commission, 2005). This was the largest emergency response event in FDNY history involving over 1,000 firefighters (NIST, 2005).

FDNY command posts were set up in the lobbies of WTC 1, WTC 2 and the Marriott Hotel (WTC 3), and in the first floor of buildings at the corner of Vesey and West Sts. and West and Liberty Sts. Although the primary objective of the response was rescue, there was substantial effort focused on fire suppression and containment.

The majority of fires occurred on the eastern side of the WTC Complex, primarily in WTC 4, 5 and 7. Firefighters ran hoses from trucks and hydrants on the eastern side of the site to combat these fires. Water pressures at hydrants adjacent to the WTC complex declined throughout the day due to losses from water mains ruptured by the collapse of the towers. In the afternoon of 9/11, the decision was made to abandon WTC 7, which collapsed about 5 pm.

2.4.2 Marine Response

Fires on the western side of the WTC area were fought primarily with water pumped from the Hudson River, which is two to three blocks from the WTC Complex. The FDNY dispatched all 3 in-service fireboats, as well as one that was in the process of being dry-docked for maintenance. The accounts of the activities of each boat on 9/11 and the days following were obtained through interviews with Marine Company firefighters who were involved in the response. Figure 2.4 illustrates the travel routes of the fireboats on the morning of 9/11. Figure 2.5 depicts the tie-up locations of each fireboat and the hose and pumper systems extending towards the WTC area.



Figure 2.3 Aerial View of the WTC Site Before the Collapse of WTC1 and WTC2
(FEMA, 2002)

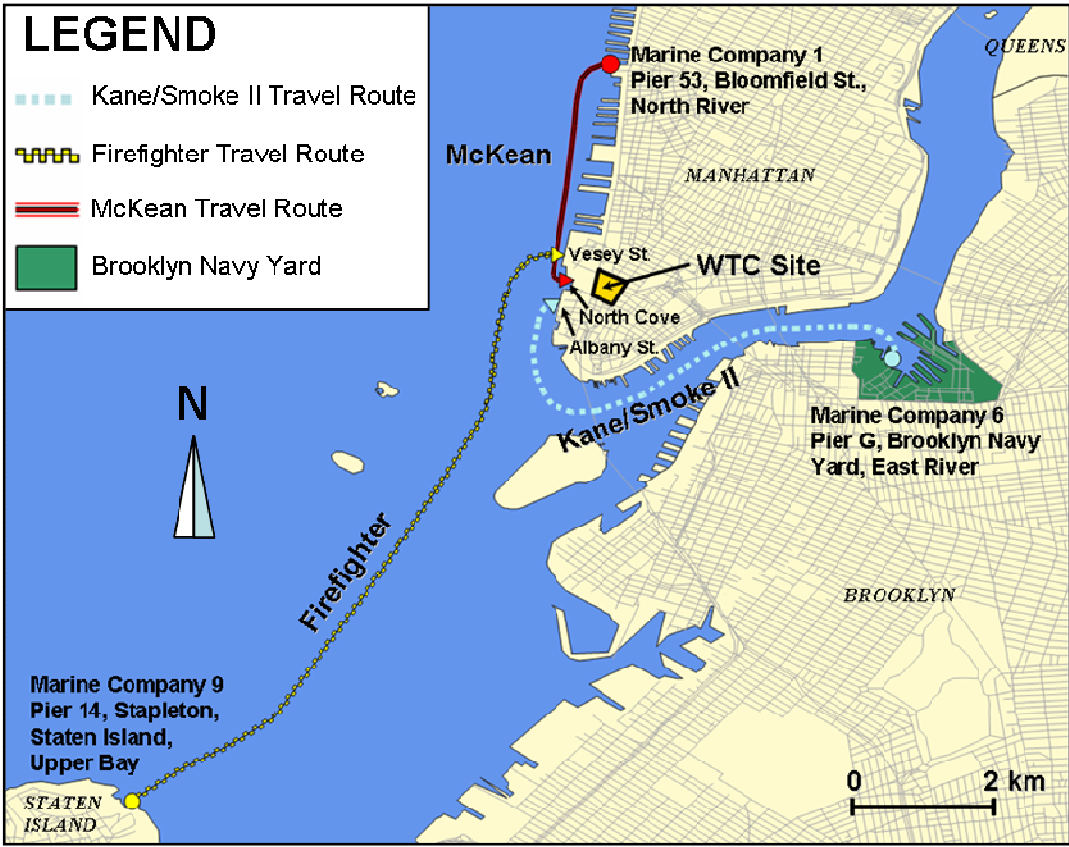


Figure 2.4 FDNY Fireboat Travel Routes on September 11, 2001

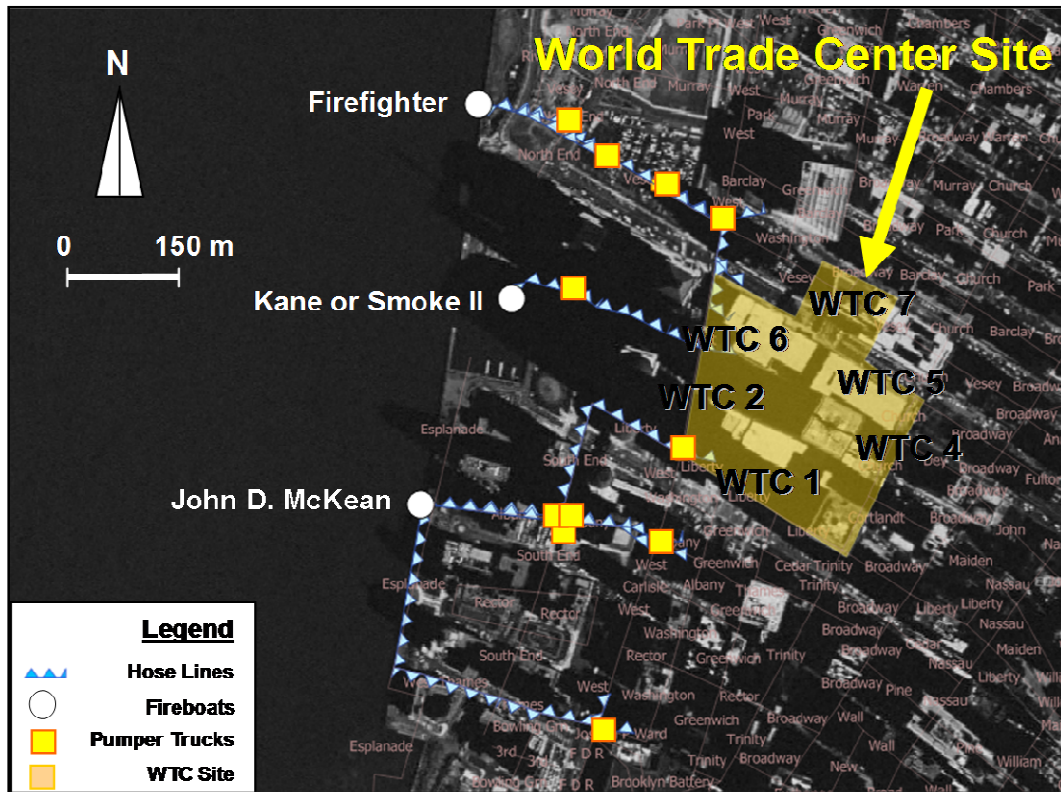


Figure 2.5 Schematic of Fireboat Deployments near the WTC Complex

2.4.2.1 McKean

As shown in Figure 2.4, the John D. McKean, maintained by Marine Company 1, left its berth at Bloomfield St. when it received information about the first plane crash at approximately 8:48 am. The McKean arrived at Albany St. within 12 minutes of the first plane crash and before the second plane hit WTC 2. The McKean made two trips across the Hudson to Jersey City to deliver people to safety. Approximately 200 people were transported to New Jersey on one of these trips.

As shown in Figure 2.5, the McKean returned to tie up at Albany St. at roughly 10 am. Firefighters ran eight 89 mm (3.5 in.) hose lines and one 127 mm (5 in.) hose

line through the streets towards the WTC area. These lines pumped continually for the first 1.5 days. For the next 2 to 3 days, five 89 mm (3.5 in.) supply lines were used, and only three lines were used as needed in subsequent days. Most lines were directed down Liberty St. to an engine pumper at the corner of Liberty and South End Avenue, and then on to the WTC site. Another line was deployed for firefighting near the corner of West Side Highway and West Thames St. (Farrenkopf, 2005). The McKean crew estimates that pumps operated for 386 hours from September 11 to 28. In the first 3 days following the disaster, the fireboat pumped continuously, and then pumped as needed for the remaining 15 days.

2.4.2.2 Firefighter

The largest fireboat in the fleet, the Firefighter, maintained by Marine Company 9, left Staten Island and arrived at Vesey St. approximately 1 hour after the first plane crash (see Figure 2.4). The Firefighter did not transport victims to New Jersey. As shown in Figure 2.5, it tied up near Vesey St., and ran lines from the boat towards the WTC area. The Firefighter did not use full pumping capacity, and only operated 2 of its 4 pumps, for a pumping capacity of 37,854 lpm (10,000 gpm). Records show that 3 hose lines were used to convey water from the Firefighter, including two 127 mm (5 in.) and one 89 mm (3.5 in.) diameter hoses. Initially, one engine pumper was deployed at the corner of Vesey and West Sts. to run water into the Verizon Building. In the 24 hours following the disaster, 3 additional pumper trucks were deployed between the Firefighter and the pumper at West and Vesey St. to convey additional water to the Verizon Building. It is estimated that the Firefighter pumps operated for 255 hours.

2.4.2.3 *Kane*

The fireboat of Marine Company 6, the Kevin C. Kane, was undergoing repairs at the time of the 9/11 attack, but by 10 am that day, the Kane was put back in service and dispatched from Pier G at the Brooklyn Navy Yard, as shown in Figure 2.4. Like the McKean, the Kane made two trips between the lower west side of Manhattan and Jersey City to transport civilians to safety. As shown in Figure 2.5, the Kane tied up at North Cove at approximately 10:45 am and ran hose lines through Winter Garden towards the burning WTC area. The Kane and Smoke II alternated pumping duties while the other boat returned to the Brooklyn Navy Yard to be ready to respond should an attack in another area arise. The FDNY Marine Division estimates that the Kane pumps operated for 244 hours.

2.4.2.4 *Smoke II*

The Smoke II was within 15 minutes of having its main shaft disconnected for maintenance work at the Brooklyn Navy Yard when the WTC attack occurred. The Smoke II was brought back into service and arrived at North Cove within 15 minutes of the first plane crash. Its travel route is shown in Figure 2.4. The Smoke II made one trip to Jersey City transporting victims, and then alternated pumping duty and in-service duty with the fireboat Kane. It is estimated that the Smoke II operated its pumps for a total of 156 hours.

2.5 Water Supply Performance

Figure 2.6 presents a plan view of the area of lower Manhattan surrounding the WTC complex in which the locations of damaged water mains are shown. There were about 10 locations of ruptured water mains within the disaster area. Damage was caused primarily by direct impact from collapsing structures and falling debris. All locations of damage in Figure 2.6 were at mains of 300 (12 in.) and 500 mm (20 in.) nominal diameter, with the exception of a 400 mm (16 in.) diameter main that was abandoned within the WTC site.

As discussed previously, water pressures declined due to losses through the ruptured mains, hampering the activities of firefighters. Measurements at 6 pm disclosed that water pressure two to three blocks from the WTC site had declined to a level approximately one third of that under normal flow conditions. From about 6 pm to 2 am, NYC DEP personnel shut gate valves in the pipeline network surrounding the site to isolate damaged pipelines from the rest of the system. Isolating the broken mains restored pressure in the intact system outside the perimeter of closed gate valves.

The gate valves and isolated pipelines are identified in Figure 2.6. The area of the isolated water distribution system was approximately 0.8 km^2 (0.3 mi^2). As pointed out by O'Rourke, et al. (2003), large areas of the gas and steam systems, 1.2 km^2 (0.5 mi^2) and 3.4 km^2 (1.3 mi^2), respectively, were likewise isolated after the WTC disaster. Although physical damage to water, gas, and steam pipelines was confined principally to the area of debris impact surrounding the WTC complex, the extent of damage at the time of the disaster was unknown. Consequently, conservative

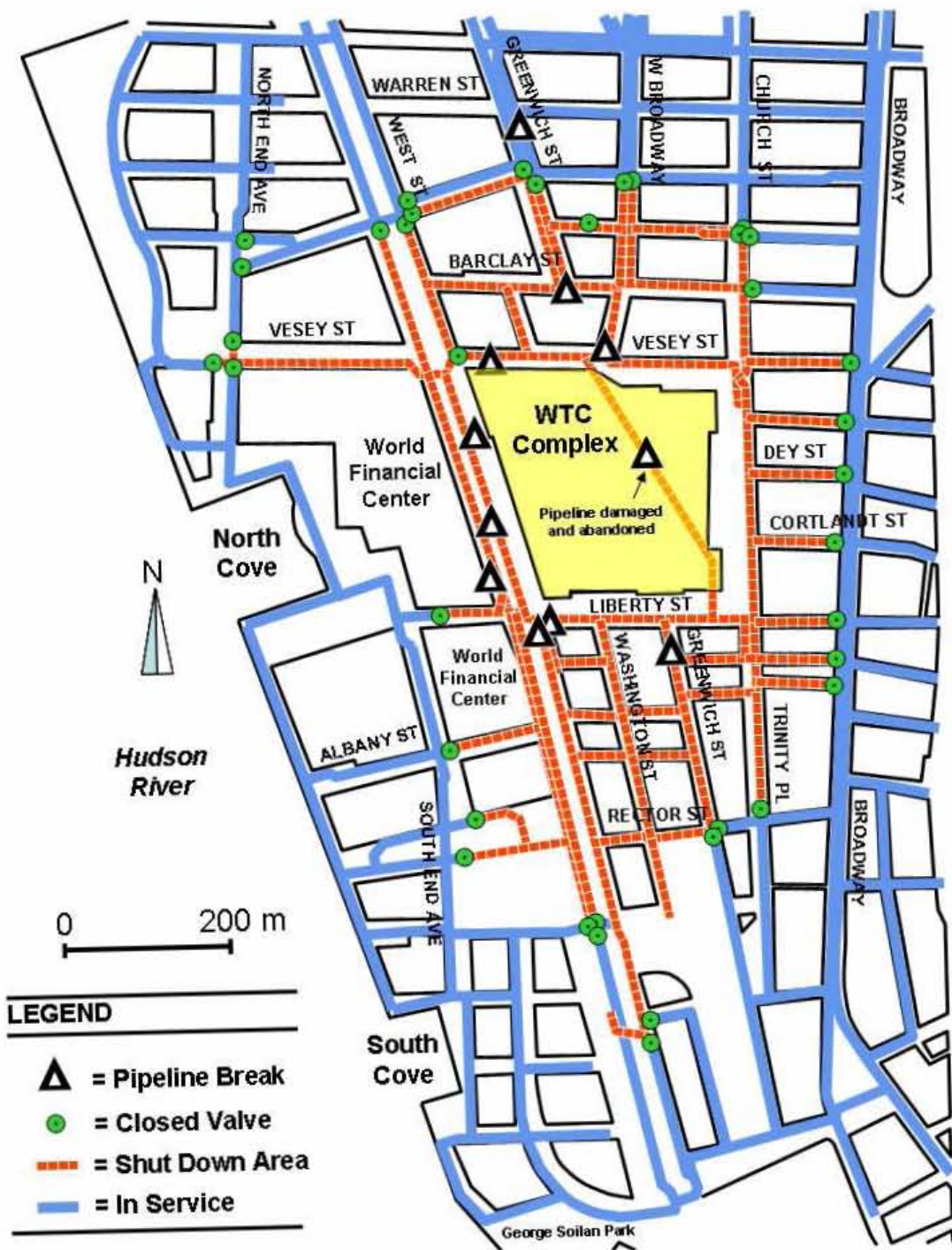


Figure 2.6 Schematic of Operational Status of Water Mains near WTC Area on September 12, 2001

decisions were made about the size of the isolation zones. One to two weeks were required for restoration of most or all of the isolated zones.

Four riser shafts for Water Tunnel 1 in lower Manhattan provide water for the distribution system that serves the WTC area and nearby neighborhoods. Flow measurement records at each shaft were combined to plot the hydrograph in Figure 2.7. As discussed previously, the shafts are equipped with regulators so that the hydrograph represents a relatively accurate assessment of flow at constant pressure. Various times are labeled on the hydrograph to mark local highs and lows of the flow record.

The normal flow cycle for lower Manhattan is similar to that of other urban centers. Minimum daily flow occurs typically between 3 and 4 am, with peak daily flow at about 9 am. As depicted in the figure, the flow was rising to its daily peak when the WTC1 and WTC2 were struck at approximately 8:46 and 9:03 am, respectively. Water usage declined to 100 Mgd/379 Mld (70,000 gpm/264,979 lpm) as daily patterns of use were interrupted until 9:59 am when the WTC2 was struck. Losses from ruptured water mains associated with the collapse of the WTC2 led to a rapid increase in flow of about 55 Mgd/208 Mld (38,000 gpm/143,846 lpm) for a total 155 Mgd/587 Mld (108,000 gpm/408,825 lpm). The flow increased gradually by an additional 1.4 Mgd/5.3 Mld (5,000 gpm/18,927 lpm) after 10:20 am as fire fighters drew water from hydrants surrounding the site.

An independent assessment of water drawn from the distribution system was made by interviewing deputy fire chiefs, who were in command on the eastern and western sides of the WTC complex. The chiefs were able to identify hydrants, hoses,

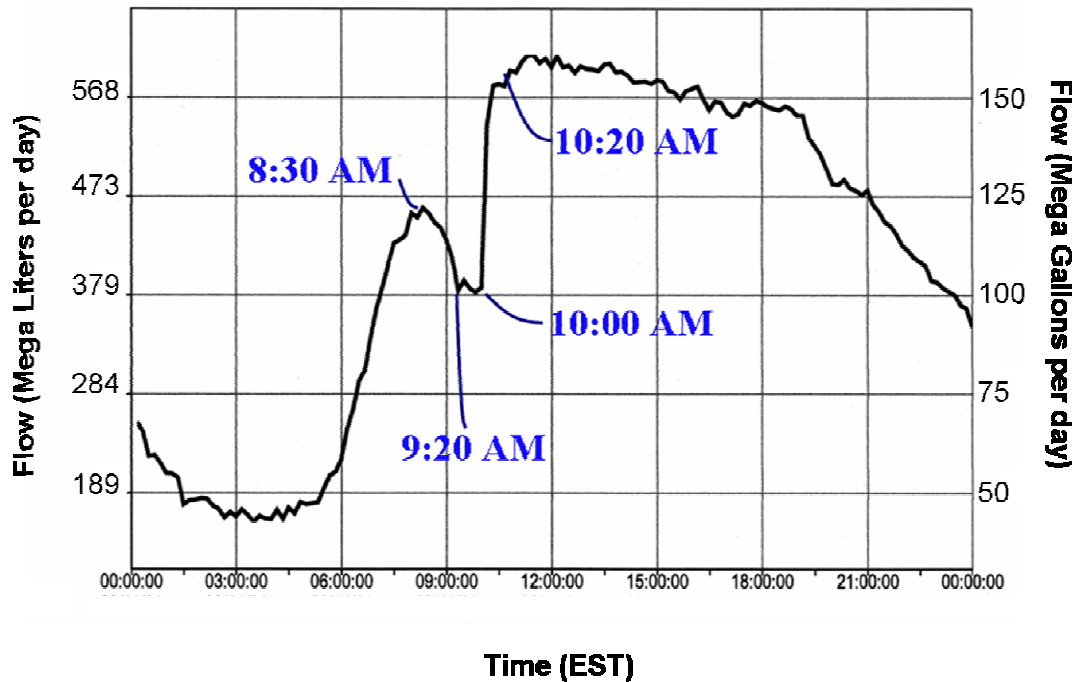


Figure 2.7 Water Flow vs. Time for the Water Supply to Lower Manhattan on September 11, 2001

and fire engines used at the site from which it was estimated that approximately 4,500 gpm/17,034 lpm were being drawn from the water distribution system. Hence, the estimate obtained from fire department commanders and the rate shown by the flow measurements are in reasonably good agreement.

2.5.1 Collateral Damage

Water from the ruptured pipelines flowed into the underground sections of the WTC complex and flooded the Port Authority and Trans-Hudson (PATH) tunnels beneath the Hudson River. Before 9/11, PATH trains had transported commuters from Exchange Place Station on the New Jersey side of the Hudson to the WTC

Station in the WTC underground complex. Exchange Place Station, which is lower in elevation than the WTC Station, was also flooded.

Water flooded the cable vault of the Verizon Building at 140 West St., where 70,000 copper pairs and additional fiber optic lines had been severed by falling debris. Nearly 41,600,000 liters (10,990,000 gal.) of water had to be pumped from the vault during recovery. The seventh and ninth floors of the telecommunications building also sustained water damage.

The capacity of the telecommunications office at 140 West St. had been one of the largest in the world. The building housed four digital switches, 500 optical-transport systems, 1,500 channel banks, 17,000 optical fiber lines, 4.4 million data circuits, and 90,000 message trunks. As a result of the damage and flooding, Verizon lost 200,000 voice lines, 100,000 private branch exchange lines, 4.4 million data circuits, and 11 cell sites. More than 14,000 business and 20,000 residential customers were affected.

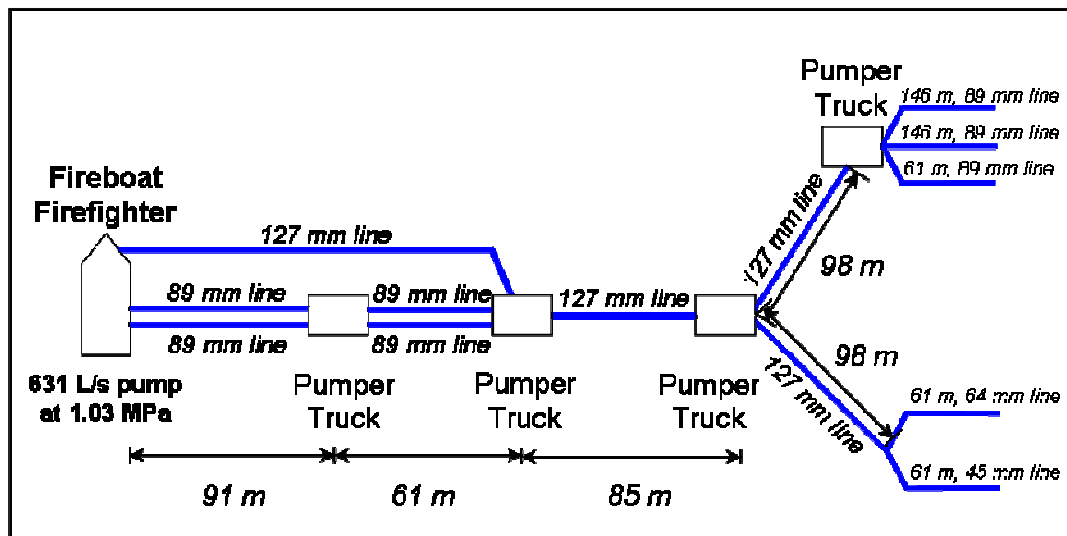
2.6 Hydraulic Network Analysis

Hydraulic network analyses were performed to help evaluate the actual water flow from fireboats to the WTC site and to perform a parametric study of the important variables influencing water relay systems during an emergency. The first of these analyses involved the collection of information about the actual deployment of fireboats and firefighting equipment. Reports prepared by FDNY personnel and interviews with Marine Division firefighters on duty during 9/11 were used to determine the number of hose connections per fireboat manifold, sizes and

deployment of hoses, number and location of pumper trucks, truck characteristics, pumping duration at each boat, and approximate number and type of hand lines to spray water at the WTC site. Where possible, this information was supplemented by aerial photographs that were used to identify and count the number of hose lines originating at the fireboats.

Interviews with firefighters disclosed that there were difficulties experienced with access to fittings for connecting the fireboat manifold with hose lines as well as connections between hose lines of variable diameter and various engines deployed to the site. Fireboats were equipped with a variety of hose sizes and hose couplings, but in some cases firefighters ran short on hose couplings needed to extend larger diameter 89 mm (5 in.) hose relays. This caused a delay in setting up the hose relays as firefighters searched other fireboats and fire trucks for necessary couplings. A greater number of larger diameter hose lines might have been deployed from the fireboats had an adequate number of hose sizes and corresponding couplings been on board.

The basic deployment of hose lines and relay system, using the fireboat Firefighter as an example, is shown schematically in Figure 2.8. The fireboat drew water from the Hudson River via two, 37,854 lpm (10,000 gpm) pumps. Water was pumped to a manifold on the deck of the boat that is equipped with multiple outlets for hose line connections. Hoses were connected to the manifold, and the hose lines were run towards the WTC site. Fire engines equipped with 3,785 lpm (1,000 gpm) pumps, called pumper trucks, were integrated into the hose relay to provide a boost in pressure. At the end of the relay system, smaller diameter hoses with nozzles, called hand lines, were used by firefighters to spray water. To model the hydraulic flow in this system, the computer program EPANET was used. EPANET is a Windows-based



$1 \text{ mm} = 0.04 \text{ in.}$, $1 \text{ m} = 3.28 \text{ ft.}$, $1 \text{ MPa} = 145.04 \text{ psi}$, $1 \text{ L/s} = 15.85 \text{ gpm}$

Figure 2.8 Schematic of Hose and Pumper System for Hydraulic Network Modeling of Fireboat Firefighter Flows to WTC Site

software program distributed by the Environmental Protection Agency (EPA) for the simulation and analysis of flow and pressures in hydraulic distribution networks. In essence, the program solves a series of nonlinear equations for the continuity of incompressible flow and conservation of in pressurized pipeline networks. Various parameters are required to model the flow, including hose diameter, length and coefficient of friction, changes in elevation within the system, and pump characteristics. Table 2.1 lists the fire protection system components and characteristics necessary to model a fireboat hose and pumper system. The pumping characteristics of both the fireboat pumps and pumper trucks were modeled by one point pump curves. This modeling method is commonly used for water distribution systems and uses the flow and pressure at a known point to estimate the head versus flow characteristics of the pump (Armando, 1987; EPA, 2005). The rated flow and pressure associated with the fireboats and pumper trucks were obtained from FDNY

Marine Company Officers (Farrenkopf, 2005). The operating flows and pressures for each fireboat and the pumper trucks are listed in Table 2.1.

The manifold that enables the distribution of water from the fireboat into multiple hose lines was included as a 1.5 m long (5 ft.) pipe with 208 mm (8 in.) ID, and frictional coefficient of 130. The elevation of the manifold was determined based on the tie-up location of the fireboat. Relay hoses were 89 mm (3.5 in.), 127 mm (5 in.) or 178 mm (7 in.) ID, and lengths varied between 60 and 300 m (200 and 1000 ft.). Elevations were determined from a GIS by overlaying hose paths with a digital elevation map of Lower Manhattan. The lines used were smooth, rubber-lined hoses, so a frictional coefficient of 150 was used. Hand lines are smaller diameter hoses that can be equipped with nozzles. Standard 64 mm (2.5 in.) ID hand lines, 30.5 m (100 ft.) in length with a frictional coefficient of 150 were used in the EPANET model. Nozzles were modeled as virtually frictionless, short hoses, 305 mm (12 in.) in length and 35 mm (1.2 in.) ID, with a loss coefficient of 1, to simulate water freely spraying from the nozzle. The elevations of the originating and terminating nodes of the nozzle were assumed to be constant.

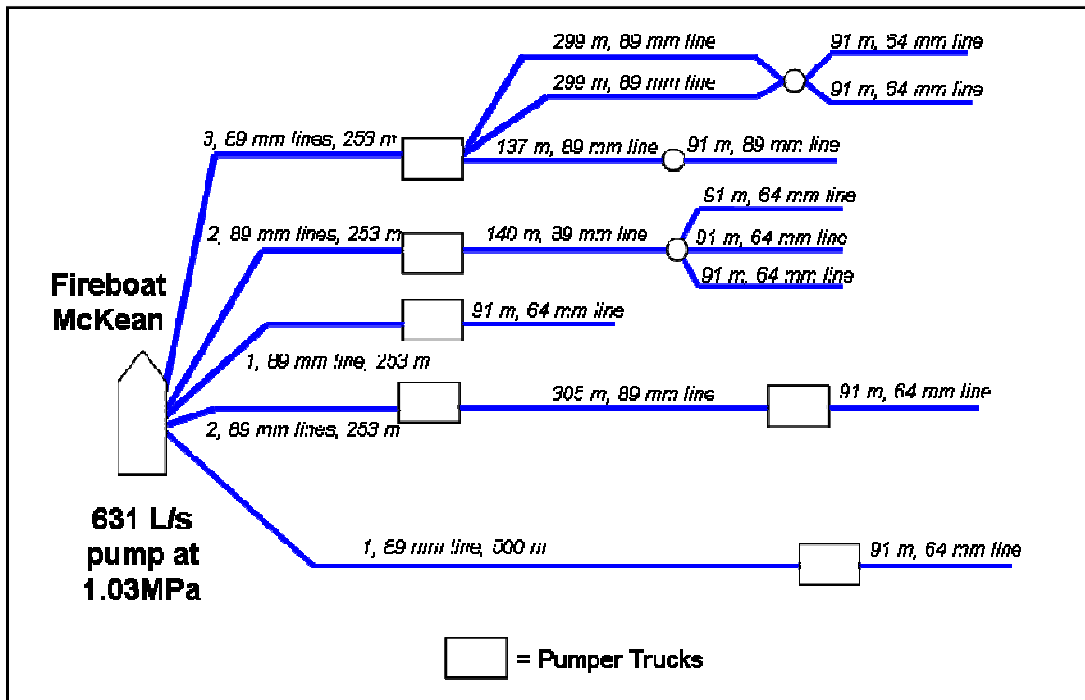
Analyses were performed for the Firefighter using the actual hose diameters and distances, number of pumper trucks, and hand lines depicted in Figure 2.8. The Firefighter docked at Vesey St. and ran three hose lines from its manifold, delivering water nearly 340 m (1,115 ft.) inland. The results showed that the Firefighter supplied about 9,500 lpm (2,500 gpm). Similar analyses were performed for the McKean, Kane and Smoke II. Figures 2.9 and 2.10 show the hose relay systems for the McKean and Kane/Smoke II, respectively. The McKean pumped water through nine hoses from its manifold, and supplied the greatest amount of water of the three

Table 2.1 Summary of Hydraulic Network Components of
Fireboat/Pumper Truck Relay

Hydraulic Component	Modeling Characteristic
Fireboat Pump	One point pump curve with rating of 631 l/s at 1.03 MPa for the Firefighter and McKean; and 316 l/s at 1.03 MPa for the Kane; and 126 l/s at 1.03 MPa for the SmokeII
Fireboat Manifold	ID = 203 mm, length = 1.5 m, and friction coefficient = 130
Pumper Truck	One point pump curve with rating of 63 l/s at 1.03 MPa
Hoses	ID = 89, 127, or 178 mm, and friction coefficient = 150
Hand Lines	ID = 64 mm, and friction coefficient = 150
Hose Nozzle	ID = 35 mm, length = 305 mm, and loss coefficient = 1

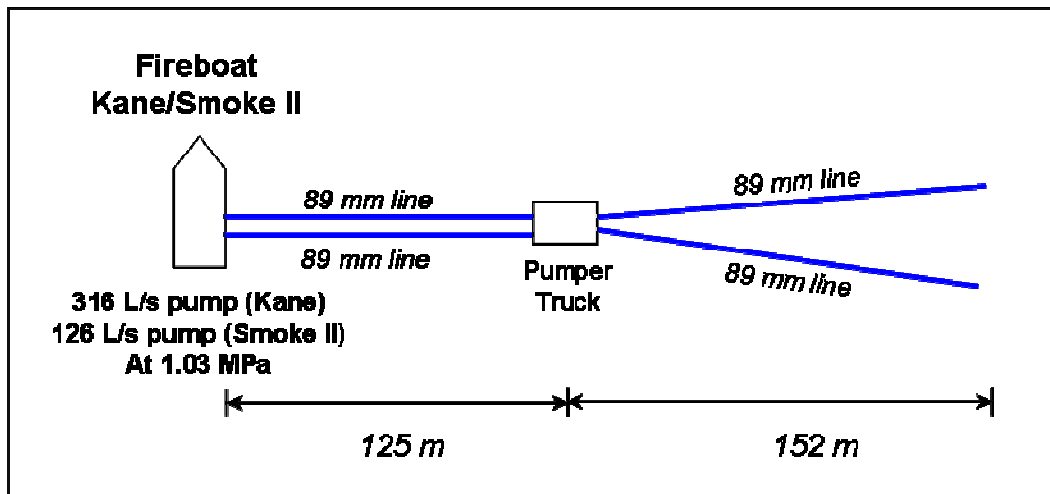
$$1 \text{ mm} = 0.04 \text{ in.}, 1 \text{ m} = 3.28 \text{ ft.}, 1 \text{ l/s} = 15.85 \text{ gpm}$$

fireboat operations, roughly 13,250 lpm (3,500 gpm). The McKean was able to deliver water as far as 640 m (2,100 ft.) inland. The Kane and Smoke II alternated pumping duties, and together supplied about 4,550 lpm (1,200 gpm) via two hose lines reaching approximately 275 m (900 ft.) inland. Excess water unable to flow through hoses and land-based equipment was discharged back into the Hudson River without specific measurement. Hence, the fireboat pumping records do not provide an accurate measure of water actually delivered to the WTC site. The FDNY did, however, make estimates for how much water each fireboat supplied. The results of the hydraulic network analyses show 27,300 lpm (7,200 gpm) of simultaneous flow



1 mm = 0.04 in., 1m = 3.28 ft., 1 MPa = 145.04 psi, 1 L/s = 15.85 gpm

Figure 2.9 Schematic of Hose and Pumper System for Hydraulic Network Modeling of Fireboat McKean Flows to WTC Site



1 mm = 0.04 in., 1m = 3.28 ft., 1 MPa = 145.04 psi, 1 L/s = 15.85 gpm

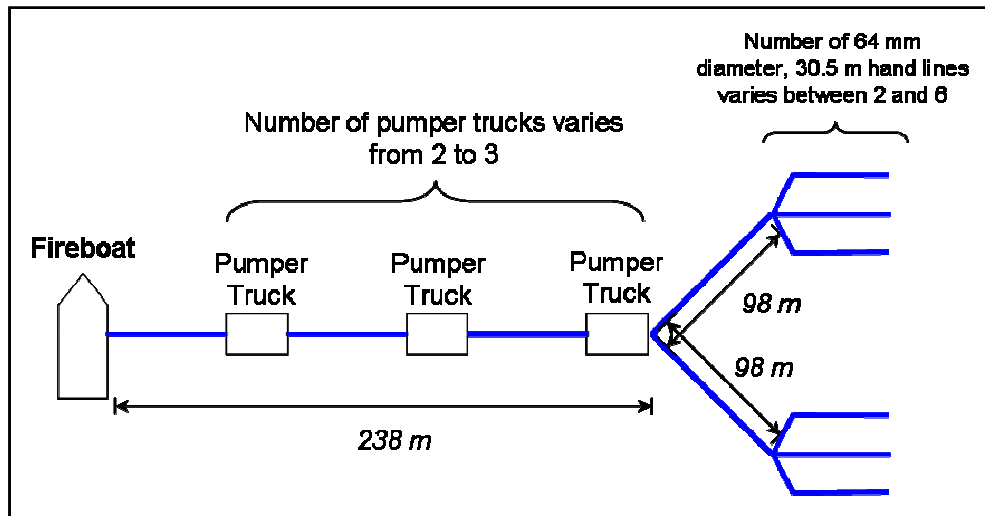
Figure 2.10 Schematic of Hose and Pumper System for Hydraulic Network Modeling of Fireboat Kane/Smoke II Flows to WTC Site

for the three fireboat operations, which is about 25% less than FDNY's estimate of 34,100 lpm (9,000 gpm), based on pumping at an assumed 30% of maximum capacity.

The fireboats were able to provide about 27,300 lpm (7,200 gpm) compared to the 17,000 to 19,000 lpm (4,500 to 5,000 gpm) of water available from hydrants surrounding the site for several hours after the towers collapsed. Marine-side water to the disaster site was approximately 44 to 60% greater than land-side water.

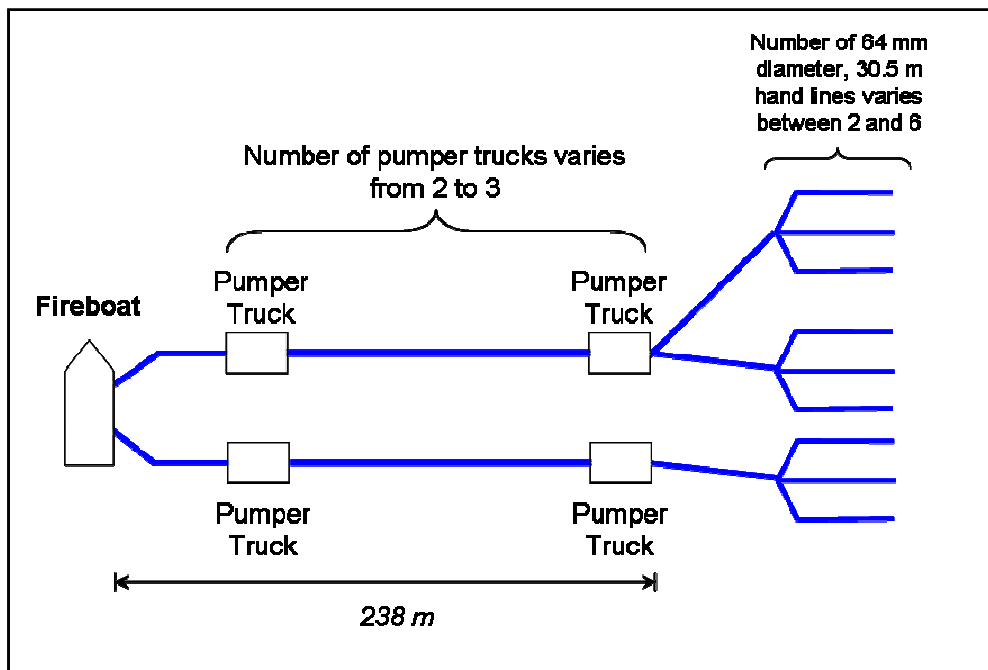
2.7 Parametric Analysis

A parametric study was conducted on a simplified hose network connected to the Firefighter to evaluate the effects of hose diameter, number of pumper trucks, and configuration of truck and hose line on the quantity of water that can be conveyed to a conflagration site. Figure 2.11 shows a schematic of this streamlined hose and pumper system. Scenarios involving 89 mm (3.5 in.), 127 mm (5 in.) and 178 mm (7 in.) ID supply hoses were considered with both two pumper and three pumper trucks. The number of 64 mm diameter (2.5 in.), 30 m long (100 ft.) hand lines was altered to find the optimal configuration for each scenario that permitted the largest flow of water while maintaining adequate nozzle pressures of 517 to 690 kPa (75 to 100 psi). When feasible, an additional relay of hoses and pumper trucks was added and the number of hand lines was manipulated to achieve the optimal scenario. Figure 2.11 depicts one hose relay with three pumper trucks, and Figure 2.12 illustrates an example of two hose relays with four pumper trucks.



$1 \text{ mm} = 0.04 \text{ in.}, 1 \text{ m} = 3.28 \text{ ft}$

Figure 2.11 Schematic of Hose and Pumper Trucks for Parametric Study – 1 Hose Relay with 3 Pumper Trucks



$1 \text{ mm} = 0.04 \text{ in.}, 1 \text{ m} = 3.28 \text{ ft}$

Figure 2.12 Schematic of Hose and Pumper Trucks for Parametric Study – 2 Hose Relays with 4 Pumper Trucks

The results of the parametric study, summarized in Table 2.2, show that hose size has a major impact on the ability to supply water inland from marine-side sources. The total flow at a relay distance equivalent to that at the WTC site is approximately 4,200 lpm (1,100 gpm), 15,150 lpm (4,000 gpm) and 20,800 lpm (5,500 gpm) for the 89 mm (3.5 in.), 127 mm (5 in.) and 178 mm (7 in.) ID hoses, respectively. In addition, the parametric study indicates that two pumper trucks, rather than three, represents the best deployment of resources. With three trucks there is only an approximate 5 to 9% increase in the flow relative to that supplied with two trucks. With a 5-in.-diameter hose, for example, it is possible to set up two relays in parallel, each using two pumper trucks to move 7,900 lpm (2,000 gpm) for a total of 15,800 lpm (4,000 gpm). Supplying an additional pumper truck in each relay actually decreases the total flow to 14,550 lpm (3,800 gpm), as adequate nozzle pressure cannot be maintained to support enough hand lines to generate increased flow. Similarly, a 178 mm (7 in.) diameter hose in tandem with two pumper trucks can supply 10,225 lpm (2,700 gpm) for a combined 20,450 lpm (5,400 gpm) from two parallel relays. The addition of a third pumper in each 178 mm (7 in.) hose relay only increases total flow to 20,960 lpm (5,540 gpm), a gain of less than 3%. The analytical results show that none of the hose sizes are able to supply water at an appropriate nozzle pressure with three parallel relays.

The results of these analyses are helpful for strategic thinking about the deployment of fire boats to fight land-based fires. As the results show, the principal bottleneck in the distribution of marine-side water to inland fire sites is the hose size. As the hose size doubles from 89 to 178 mm (3.5 to 7 in.) in the parametric study, the maximum flow at acceptable nozzle pressure increases by five-fold. Moreover, for relay distances of approximately 366 to 396 m (1,200 to 1,300 ft.), two pumper trucks

Table 2.2 Summary of Parametric Study for WTC Fireboat Pumping Scenarios

Hose Size	1 Hose Relay		2 Hose Relays	
	No. Pumper Trucks	Flow	No. Pumper Trucks	Flow
3.5	2	3,899 lpm (1,030 gpm)	<i>not feasible</i>	<i>not feasible</i>
	3	4,500 lpm (1,189 gpm)	<i>not feasible</i>	<i>not feasible</i>
5	2	7,934 lpm (2,096 gpm)	4	15,861 lpm (4,190 gpm)
	3	8,506 lpm (2,247 gpm)	6	14,551 lpm (3,844 gpm)
7	2	10,232 lpm (2,703 gpm)	4	20,453 lpm (5,403 gpm)
	3	10,486 lpm (2,770 gpm)	6	20,964 lpm (5,538 gpm)

per relay represents the best use of scarce resources for water delivery.

2.8 Fire Protection During 1989 Loma Prieta Earthquake

The most serious fire caused by the 1989 Loma Prieta earthquake was extinguished with the assistance of the San Francisco Fire Department (SFFD) fireboat and special firefighting equipment, referred to as the Portable Water Supply System

(PWSS). Because of similarities with the WTC firefighting operation, it is worth reviewing the fire and fire suppression activities associated with the Loma Prieta earthquake.

Descriptions of fire following the 1989 Loma Prieta earthquake have been provided in several publications (e.g., Scawthorn, et al., 1992; O'Rourke and Pease, 1992; and Scawthorn, et al., 2006), and only the salient details are given here. The most serious fire after the Loma Prieta earthquake broke out at the corner of Divisadero and Beach Sts. in the Marina District, as illustrated in Figure 2.13. Because of damage in underground pipelines, inadequate water was available from nearby hydrants to fight the fire. The fireboat Phoenix, operated by SFFD, was dispatched from its berth at Pier 22½ as shown in Figure 2.13 and arrived at the Marina about an hour and 45 minutes after the main shock. The fireboat Phoenix has the ability to pump 36,300 lpm (9,600 gpm) at a pressure of 1.03MPa (150 psi) and was the only fireboat operated by SFFD at the time. The fireboat tied up in the Marina harbor (see Figure 2.13) and hooked up with special hose tenders belonging to SFFD. The hose tenders are part of the PWWS, which was implemented for fire protection only two years before. Each hose tender consists of a truck with 1,525 m (5,000 ft.) of 127 mm (5 in.) diameter hoses, portable hydrants, and special valves, which can connect with fireboats, underground cisterns, and the underground pipeline network to provide an additional measure of flexibility under emergency circumstances. The PWSS is now equipped with a portable, diesel-driven pump that can draft water directly from the bay with a pumping capacity of 4,550 lpm (1,200 gpm) (Scawthorn, et al., 2006).

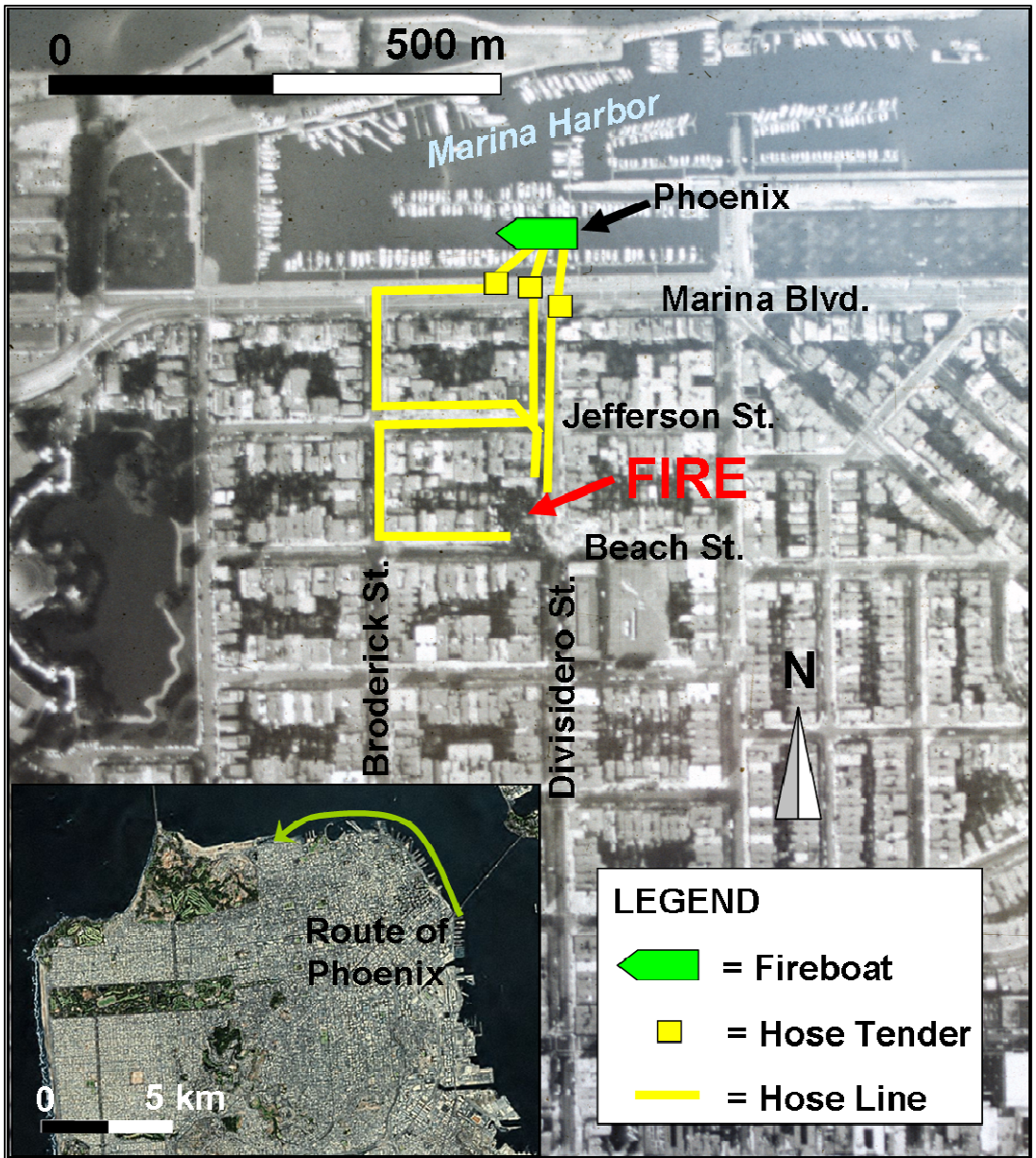


Figure 2.13 Travel Route and Tie-Up Location for Fireboat Phoenix and Hose Line Deployments after the Loma Prieta Earthquake

Approximately 2 hours after the main shock, the first PWSS water was directed to the fire by hose lines from Marina Blvd down Divisadero St. Two more hose tenders arrived to convey water by the routes shown in Figure 2.13. The maximum combined water flow to the fire was reported as 23,000 lpm (6,100 gpm) (O'Rourke and Pease, 1992), and the fire was brought under control about 4 hours after the earthquake.

2.9 Discussion

The WTC disaster provides a graphic illustration of the interdependencies of critical infrastructure systems. The building collapses triggered water main breaks that flooded rail tunnels, a commuter station, and the vault containing all the cables for one of the largest telecommunication nodes in the world. These included the Security Industry Data Network and the Security Industry Automation Corporation circuits used to execute and confirm block trades on the stock exchange. Before trading resumed on the New York Stock Exchange on Monday, September 17, 2001, the telecommunications network had to be reconfigured. Hence, ruptured water mains were linked directly with the interruption of securities trading and the restoration of international financial stability.

Water main performance frequently affects the operation of neighboring infrastructure in crowded urban environments. For example, a systematic review of major infrastructure accidents in New York shows 50 major incidents involving cast iron water main rupture and flooding from 1980-1990. Several of these accidents resulted in multi-million dollar damage and disruption (O'Rourke, 1993). Cast iron

pipelines comprise 70 to 80% of the pipelines in many U.S. water distribution systems, such as those in New York City and Los Angeles.

Damage to water distribution pipelines surrounding the WTC site was sufficiently severe that pressure losses from leaking water mains interfered with firefighting. Similar disruption of the water supply was experienced after the Loma Prieta earthquake when seismic damage of underground pipelines deprived firefighters of water needed to extinguish the Marina fire. In both cases, the loss of pipeline water was compensated by water pumped from fireboats dispatched to the area of conflagration.

Of particular interest is the use of special hose tenders after the Loma Prieta earthquake that were able to convey water rapidly from the bay. Since the Loma Prieta earthquake, a number of cities vulnerable to earthquakes have adopted PWSS concepts in fire protection systems. San Francisco has acquired a second fireboat, Guardian, capable of pumping 1,600 L/s (24,000 gpm). Fireboat and PWSS equipment have been acquired by Vancouver, British Columbia and the cities of Oakland, Berkeley, and Vallejo, CA.

September 11 experience supports a similar strategy for extreme events of non-earthquake origin. Fireboat deployment and implementation of PWSS concepts provide options for supplying water under emergency conditions. Water supply from fireboats to land-based locations is especially important where significant damage to the distribution pipeline system has occurred or where the capacity of the existing pipeline system is limited.

2.10 Conclusions

Water supply performance during the WTC disaster underscores the importance of water supply systems in crowded urban environments. Not only is the water distribution infrastructure critical for fire protection and the support of household and commercial activities, water main damage can rapidly cascade into damage of nearby gas, electric, telecommunications, and transportation facilities with substantial direct and indirect economic losses. Water from ruptured water mains during the WTC disaster flooded one of the commuter rail PATH tunnels, eventually threatening Exchange Place Station in New Jersey, and flooded a vault with telecommunication cables that carried financial data needed for securities trading on the New York Stock Exchange.

The analytical studies and results described in this chapter have important tactical ramifications for fire protection during extreme events. Fireboats are frequently equipped with high capacity pumps, well suited for spraying water on burning waterfront properties. When fireboats are used to pump water to shore, the principal bottleneck in the conveyance system is the hose size. Hydraulic network models with standard 89 mm (3 in.) hose lines and pumper trucks show that the maximum flow that can be delivered is only 10% of the pumping capacity of a large fireboat. The sensitivity analyses presented herein show considerable benefits from deploying 127 mm (5 in.) and 178 mm (7 in.) diameter hoses. Moreover, the analyses also show that two pumper trucks per relay, as opposed to three, is a better use of critical equipment when relay distances are in the range of 365 m (1,200 ft.) to 400 m (1,300 ft.).

From a strategic perspective, fireboat deployment during the WTC disaster and the Loma Prieta earthquake were essential for controlling fires. Estimated flows from fireboat pumping records and hydraulic network analyses indicate that water supplied from fireboats during the WTC disaster was approximately 150% of the water initially available in underground pipelines. Moreover, flow and pressure in underground pipelines network declined steadily during 9/11 until all flow was shut off by isolating the area of suspected damage from the rest of the distribution pipeline network. Experience in the San Francisco Bay Area during and after the Loma Prieta earthquake reinforces the WTC experience, and demonstrates that water can be conveyed rapidly from marine locations for distances as great as 1 km (0.6 miles), provided that appropriate planning and equipment acquisition have been undertaken.

CHAPTER 3

EARTHQUAKE DECISION SUPPORT SYSTEM FOR WATER SUPPLIES

3.1 Decision Support System

This chapter describes a decision support system (DSS) developed for the seismic performance of water supplies, and implemented by the Los Angeles Department of Water and Power (LADWP). It conforms to the definition of a DSS as a computer-based information and modeling system that works interactively with users to address unstructured problems for strategic planning, management and operations (Turban, 1995). The DSS is adaptive; it benefits from an iterative or evolutionary process whereby users provide feedback that influences the DSS development (Sprague and Watson, 1989; Keen, 1980). The conceptual and organizational basis of the DSS follows the multihazard framework for lifeline system performance depicted in Figure 3.1, which is generalized from the framework proposed by O'Rourke, et al. (2004) for the seismic performance of lifelines.

The framework includes five major components: hazards, system characteristics, hazard/system interaction, system response, and consequences. Hazards, such as earthquakes, floods, accidents, human threats, and hurricanes can be applied to a lifeline system. The effects of one hazard can be evaluated, or the hazards can be combined for an integrated hazard assessment. As shown in Figure 3.1, a system is defined by both physical and operational characteristics. The interaction between the hazard and water supply system is assessed for both above ground

facilities (e.g., tanks, electric power substations, pump stations) and underground facilities (e.g. pipelines). Fragility assessments are performed for system components to determine their post-event functionality, thus producing information about system response and the changes in that response resulting from alterations of the system. Such information is used by system managers for increasing pre-event resilience through strategic planning, system improvements, and adjustments in daily operating procedures. System response also has post-event consequences, including emergency operations, system restoration, community impact, and regional economic effects.

It is the post-event consequences that involve the greatest amount of interaction among system operators, external organizations, and the community receiving service. By providing a framework for quantifying the effects of water losses on emergency responders, regional businesses, and service area neighborhoods, the DSS is able to expand the scope of decision making beyond the engineering and operational applications that have been the focus of conventional water supply modeling. A distinguishing characteristic of the DSS, therefore, is its ability to address multi-institutional, economic, and social factors.

A special hydraulic network analysis software program, Graphical Iterative Response Analysis for Flow Following Earthquakes (GIRAFFE) was developed and implemented in the DSS for the purpose of analyzing water systems damaged by earthquakes. GIRAFFE is built on the freely available, open source hydraulic analysis program, EPANET, developed by the Environmental Protection Agency (EPA, 2007). Details of the development, capabilities and validation of GIRAFFE can be found in Shi (2006).

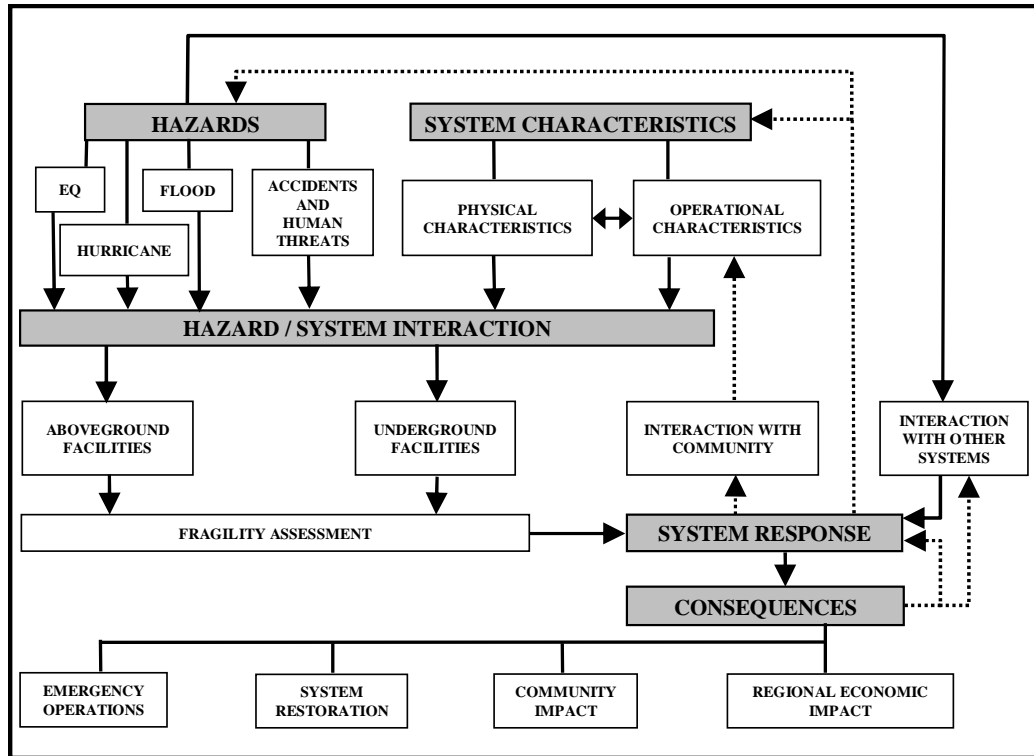


Figure 3.1 Generic Framework for the Effects of Hazards on Lifeline System Performance

Figure 3.2 shows a flow chart for GIRAFFE simulation, highlighting the preprocessing, analysis and post processing steps. GIRAFFE simulation involves five major modules: system definition, earthquake/system interaction, system damage, hydraulic network analysis, and compilation of results. In the system definition module, a user defines the physical and operational characteristics, topology, and pre-earthquake water demands of the hydraulic network being analyzed. The earthquake/system interaction module links permanent ground deformation (PGD) and

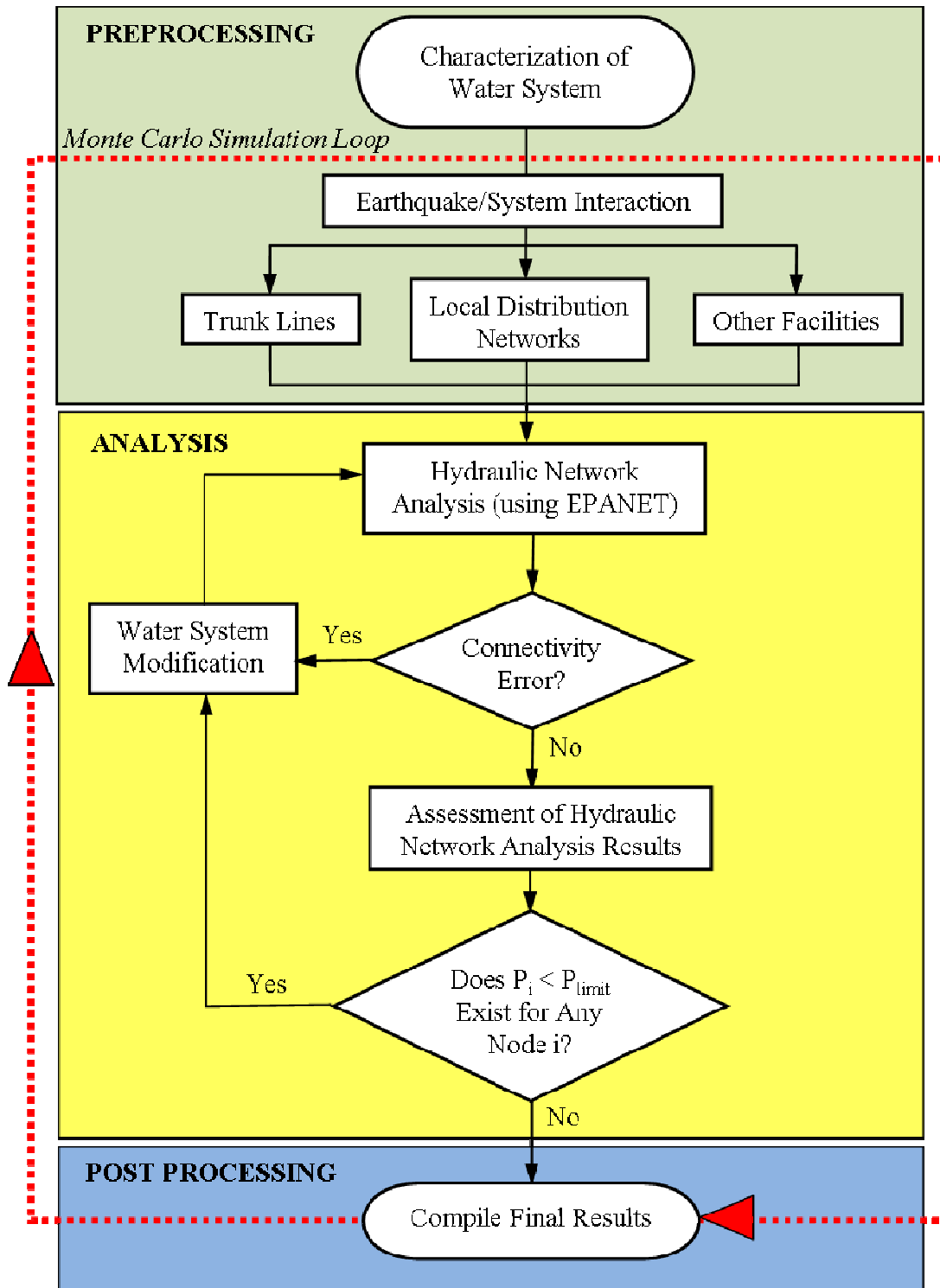


Figure 3.2 Flow Chart for Hydraulic Network Analysis of Water Supplies Damaged by Earthquakes

transient ground deformation (TGD), or seismic wave effects, with the locations and severity of damage to pipelines and water distribution facilities (e.g., tanks, reservoirs, regulation stations, etc.). Two types of pipeline are distinguished: 1) trunk lines with predominantly nominal diameter, $D_p, \geq 600$ mm that convey large quantities of water from reservoirs to local distribution networks, and 2) distribution lines with $D_p < 600$ mm that convey water mainly to residences and businesses.

The earthquake/system interaction module adds damage to pipelines and other facilities, and characterizes the damage for hydraulic network analysis. GIRAFFE provides two simulation options for system damage: deterministic and probabilistic. In a deterministic simulation, the user explicitly defines all damage that will be imposed on the system, and GIRAFFE performs hydraulic network analyses on that damaged system. In a probabilistic simulation, GIRAFFE uses a Poisson process to simulate the occurrence of pipeline damage based on seismic demands and pipe characteristics. As indicated in Figure 3.2, the damaged system is reconfigured to remove portions of the system that have been 1) physically disconnected, and 2) rendered hydraulically unreliable by the presence of unsustainable negative pressures identified by the hydraulic network analyses.

For the probabilistic simulation, GIRAFFE performs multiple Monte Carlo simulations, each generating different damage scenarios. The user can specify the number of Monte Carlo simulations to be performed, or can allow GIRAFFE to determine the number of simulations based on a self-termination algorithm that automatically stops when convergence criteria have been met. The compilation of results is performed, and the results displayed with the aid of a geographic information system (GIS) that shows the spatial distribution of damage and system functionality.

Results quantified and visualized by GIS provide the input for further simulations and DSS treatment of emergency response, system restoration, regional economic effects, and community impact.

3.2 System Definition

The characteristics of the water supply are incorporated in the hydraulic network model that accounts for water sources, tanks, reservoirs, pipelines, valves, pumps, pre-earthquake water demands, and topographic effects on water pressure and flow. As described above, GIRAFFE uses EPANET (EPA, 2007), which is readily available online and used in hydraulic network analysis by many U.S. water supply operators.

The LADWP hydraulic network model simulates 2,200 km of trunk and distribution pipelines, of which 1020 km have $600 \text{ mm} \leq D_p \leq 3800 \text{ mm}$, and the rest have $300 \text{ mm} \leq D_p < 600 \text{ mm}$ system. The remaining 9,800 km of small diameter distribution pipelines are not modeled explicitly, but are instead represented by 1,052 demand nodes. The majority of demands are less than 63 l/s, indicating residential consumption. Approximately 10% of the nodal demands are greater than 63 l/sec, reflecting industry usage. Remaining model components include 103 tanks, 180 reservoirs, 436 valves, and 282 pumps. Reservoirs are modeled as having fixed head, and the level does not change with time. Tank levels, however, vary dynamically and are adjusted after each simulation time step based on either the initial water level and tank diameter, or an associated curve that relates water elevation to the volume of water available in the tank.

3.3 Earthquake/System Interaction

Earthquake/system interaction involves characterizing the strong motion, or TGD, for various scenario earthquakes that can affect the water supply system, and predicting the locations and characteristics of PGD triggered by liquefaction, landslides, and surface fault rupture. Various empirical and analytical soil-structure interaction models are used to link water supply damage with TGD and PGD.

3.3.1 Scenario Earthquakes

An ensemble of 59 scenario earthquakes was developed to characterize the seismic hazards affecting the LADWP system (Lee, et al., 2005). The ensemble can be used to evaluate the aggregated seismic hazard for the system, or individual scenario earthquakes can be used to evaluate system performance for seismic events selected by the water supply operator.

The selection of scenario earthquakes follows the approach proposed by Chang, et al. (2000b) and Shinozuka, et al., (2003) in which a select number of scenario earthquakes are chosen to approximate the aggregated seismic hazard for a lifeline network. The 59 scenario earthquakes were chosen from the USGS 2002 dataset (USGS, 2005) as explained by Lee, et al. (2005) and Wang (2006) to include earthquakes that generate ground motion that may significantly affect water supply performance. Each scenario earthquake is associated with a moment magnitude, M_w , and specific fault segments or background earthquake source areas identified by USGS (2005), and is assigned an annual frequency of occurrence. The cumulative frequency of occurrence at a particular location is calculated for all 59 scenario

earthquakes by summing the annual frequencies of occurrence, starting with the highest or most severe seismic hazard, and plotting the cumulative annual frequency versus the seismic hazard.

An annual frequency of occurrence, or seismic hazard, curve for spectral acceleration with 5% damping at $T = 1$ sec, S_{A1} , was developed from the 59 scenario earthquakes for bedrock motion at 56 sites throughout the LADWP system (Wang, 2006), and adjusted to match that of the USGS 2002 dataset at each of the 56 sites by a multivariate, nonlinear optimization process. The 59 annual occurrence frequencies for the 59 scenario earthquakes are the optimized variables in this matching process. Following the procedure proposed by Chang, et al. (2000b), the annual frequencies for the 59 scenarios are adjusted to match better those of the full earthquake event set compiled by USGS through the optimization process. The hazard curve for representing the entire LADWP system is selected by minimizing an error function for the sum of the differences between the system hazard curve and USGS 2002 dataset at each of the 56 control points. The error function is measured at 50 points with equal weights, and 6 control points at critical reservoirs and pump stations for which there is a six-fold increase in the weighting to underscore the importance of these facilities.

3.3.2 Transient Ground Deformation

For each of the 59 scenario earthquakes, the peak ground acceleration (PGA), PGV, and spectral acceleration with 5% damping at $T = 0.2$ sec ($S_{A0.2}$), and $T = 1$ sec (S_{A1}) at equivalent rock sites, respectively, are generated at 572 points in a grid with uniform separation of points and interval of 0.03° longitude and latitude covering the LADWP water supply system. Four attenuation relationships (i.e., Abrahamson and

Silva, 1997; Boore et al., 1997; Sadigh et al., 1997; and Campbell and Bozorgnia, 2003) with equal weights are used to calculate the ground motion parameters, and those parameters corresponding to the mean plus inter-event standard deviation are used in the analyses. The inter-event standard deviation helps to account for uncertainty in the earthquake source and magnitude. Mean values are used from the attenuation relationships because seismic wave motion throughout the entire LADWP system should reflect average values associated with seismic path and rock site conditions. In all cases, PGV is estimated from S_{A1} using the conversion equation in HAZUS (FEMA, 1999) as:

$$V_p = \frac{386.4S_{A1}}{3.30\pi} \quad (3.1)$$

in which, V_p is PGV in units of m/sec, and S_{A1} is in units of g.

Site response is accounted for by using the GIS site-condition map for the Los Angeles region (Wills et al., 2000) to determine the NEHRP site condition coefficients (FEMA, 2003), which are multiplied with the strong motion parameters for equivalent rock sites to obtain the surface strong motion parameters at the 572 grid points throughout the LADWP system. Ground motion contour surfaces are generated from the grid values using local polynomial interpolation procedures in the GIS (Wang, 2006). As an example, Figure 3.3 shows PGV contour surfaces developed for a M_w 6.9 Verdugo scenario earthquake, and Figure 3.4 shows the PGV contours corrected for site conditions. Comparison of the two figures shows site amplification effects, especially southwest of the Verdugo Fault.

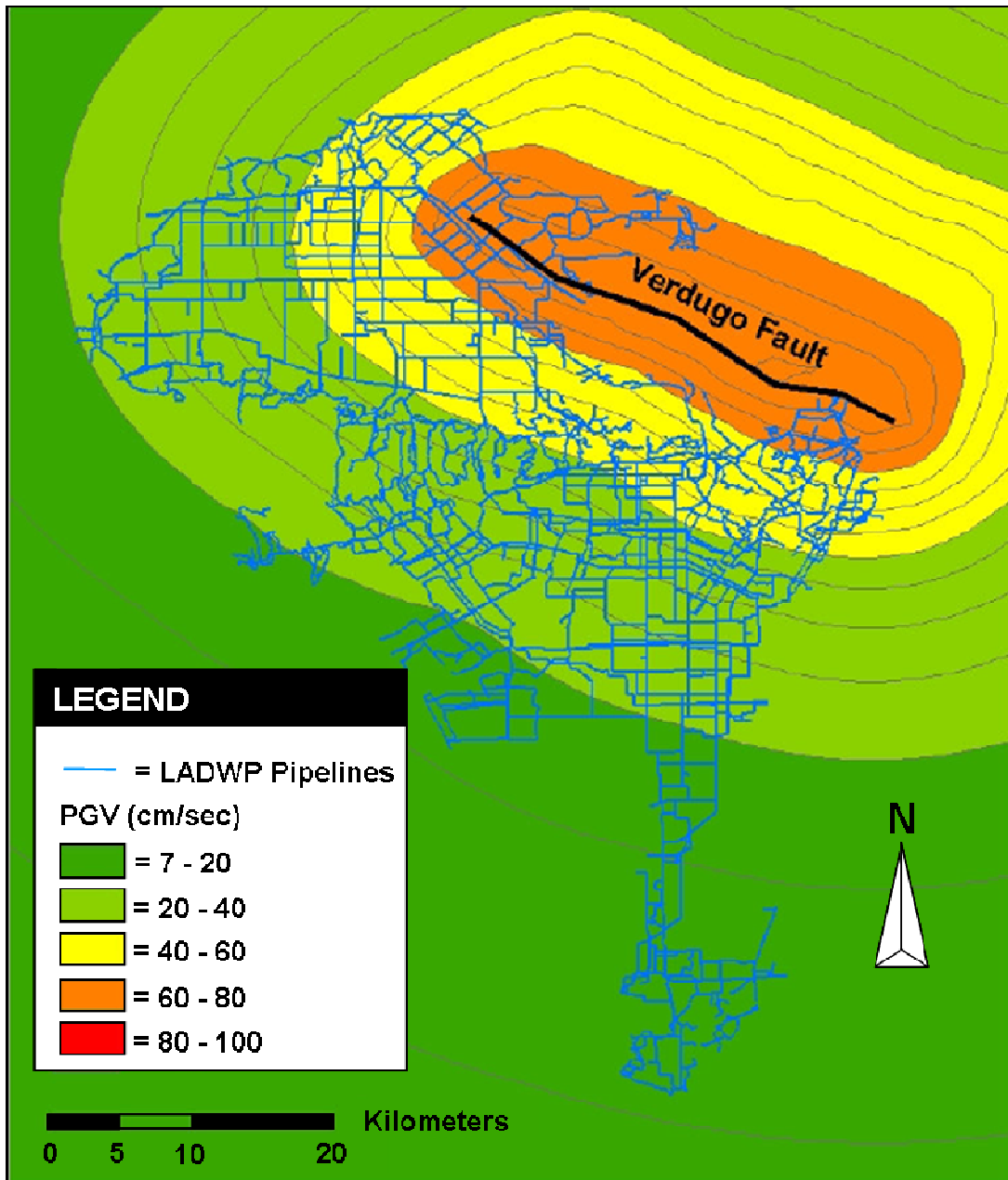


Figure 3.3 PGV Contour Surface for Mean + $\sigma_{\text{inter-event}}$ PGV for Verdugo Scenario Earthquake at Rock Site Conditions (Wang, 2006)

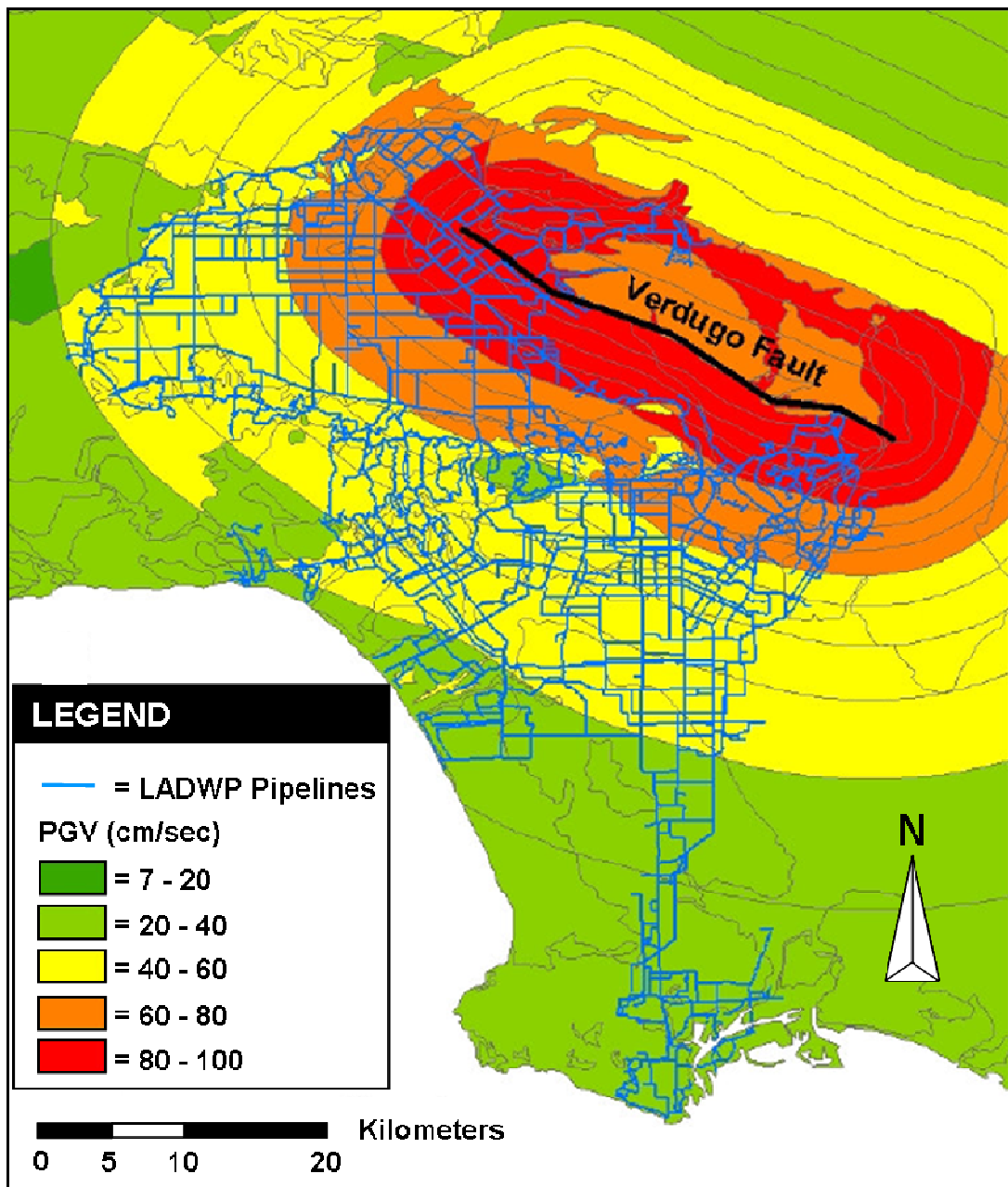


Figure 3.4 PGV Contour Surface for Mean + $\sigma_{\text{inter-event}}$ PGV for Verdugo Scenario Earthquake after Site Condition Corrections (Wang, 2006)

3.3.3 Permanent Ground Deformation

The approach currently adopted for the LADWP system is to evaluate PGD hazards and their effects on pipeline and facility performance on a scenario-by-scenario basis, utilizing local expertise and the most appropriate geotechnical characterization and soil-structure interaction analytical procedures. Methods for estimating PGD triggered by earthquakes and their effects on underground pipelines have been proposed (ASCE, 1984; O'Rourke, 1998; O'Rourke and Liu, 1999; Honegger and Nyman, 2004; Bardet, et al., 1999a, 1999b) and applied on a variety of lifeline projects to evaluate the seismic performance of oil, gas, and water supply systems. Many of these methods are directly applicable for evaluating the seismic performance of water supplies. Some, like the models proposed by Bardet, et al. (1999a, 1999b), are especially attractive because they can be readily adapted to large, geographically distributed systems through GIS.

3.4 System Damage

The system damage module determines the locations and flow loss characteristics of pipeline damage, post-earthquake flows at demand nodes, and the hydraulic functionality of damaged facilities other than pipelines. Each of these processes is described in the subheadings that follow.

3.4.1 Pipeline Damage

Pipeline damage is estimated with the aid of regressions developed from previous earthquake records that correlate pipeline repair rate, RR , defined as the

number of repairs per km, with PGV. Investigations have shown that the most statistically significant regressions for seismic damage to underground pipelines are those involving PGV (Toprak, 1999; Jeon, 2002). Figures 3.5 and 3.6 show the regressions developed from post-earthquake repair records and strong motion recordings for water distribution pipelines developed by Jeon and O'Rourke (2005) and for water trunk pipelines developed by O'Rourke, et al. (2004) and Wang (2006), respectively.

To generate the locations of seismic pipeline damage probabilistically, it is assumed damage follows a Poisson process with each pipe segment having a probability of failure given by:

$$P(F)_n = 1 - e^{-(RR)L_n} \quad (3.2)$$

in which $P(F)_n$ is the probability of failure of pipe n , and L_n is the length of pipe n .

Let L_k be the pipeline distance between the $(k-1)^{th}$ and k^{th} locations of damage. The $\{L_1, L_2, \dots, L_k, \dots\}$ set consists of independent, exponential random variables with a mean equal to $1/RR$ (Sheldon, 2000) and is generated using a Monte Carlo simulation algorithm given by:

$$L_k = -\frac{1}{RR} \ln(1 - u_1) \quad (3.3)$$

where u_1 is a random variable which is uniformly distributed between 0 and 1. By generating the interarrival distance L_k repeatedly until the cumulative length exceeds the total pipe length, one is able to simulate the locations of earthquake damage. Since

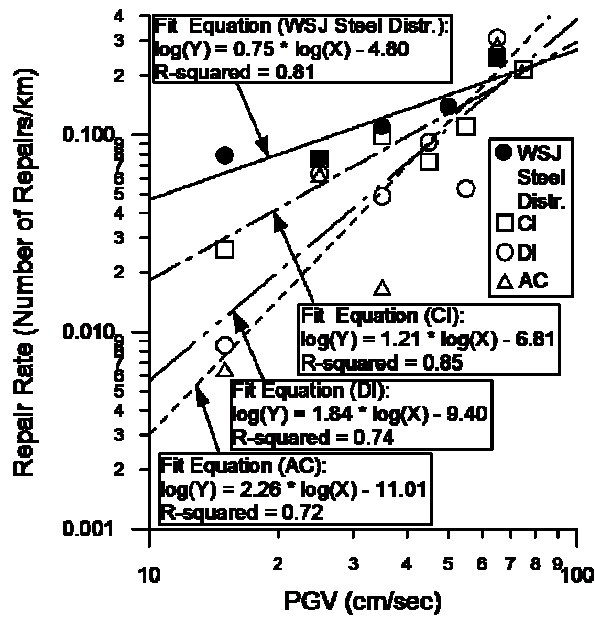


Figure 3.5 Regressions for RR vs. PGV for Steel (WSJ Steel Distr.), Cast Iron (CI), Ductile Iron (DI), and Asbestos Cement (AC) Distribution Pipelines (Jeon, 2002)

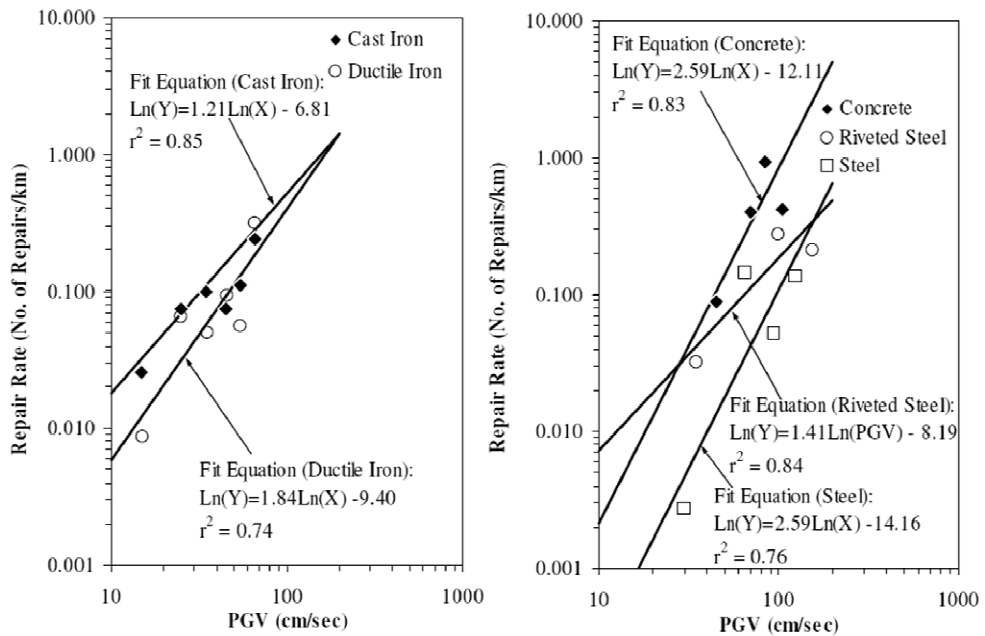


Figure 3.6 Regressions for RR vs. PGV for (a) Cast Iron and Ductile Iron Trunk Lines, and (b) Concrete, Riveted Steel, and Steel Trunk Lines (Wang, 2006)

the spatial distribution of simulated damage is one of many possible outcomes, a Monte Carlo simulation is run to evaluate a number of damage scenarios sufficient to acquire reliable statistics about the mean system performance and its variability. A minimum of 15 Monte Carlo simulations are performed and the mean and coefficient of variation (COV) of the system serviceability index (SSI) of the first 10 simulations is compared with that of 15 simulations. If the variation is insignificant, i.e., the mean and COV of the SSI with the additional five simulations are both within ± 0.02 difference when compared with those without the additional five simulations, GIRAFFE concludes a sufficient number of Monte Carlo simulations has been performed such that representative simulation results are generated. If the convergence criteria are not satisfied, GIRAFFE will perform an additional five simulations and re-evaluate the mean and COV results. Users have the ability to set the mean and COV convergence criteria to values other than the default 0.02 setting.

Pipeline damage is classified as either a break or leak. In HAZUS (NIBS, 1997) it is recommended that 80% and 20% of earthquake damage occurs as leaks and breaks, respectively, under seismic wave effects. These percentages are close to those used by Ballantyne et al. (1990) and Hwang et al. (1998), who assumed 85% and 15% leaks and breaks, respectively, for PGV-related damage to cast iron pipelines. With GIRAFFE, users have the ability to set the percentages of leaks and breaks to values other than the default settings of 80% and 20%, respectively.

3.4.2 Pipeline Break Simulation

Figure 3.7a illustrates how pipeline breaks are modeled in GIRAFFE simulations. The broken pipe is completely disconnected and divided into two

segments. A fictitious pipe and reservoir are attached at each broken end of the pipe, simulating water flowing into the surrounding soil. Check valves ensure that water only flows from the broken pipe into the reservoirs which are fixed at atmospheric pressure to simulate the broken pipe being open to the atmosphere.

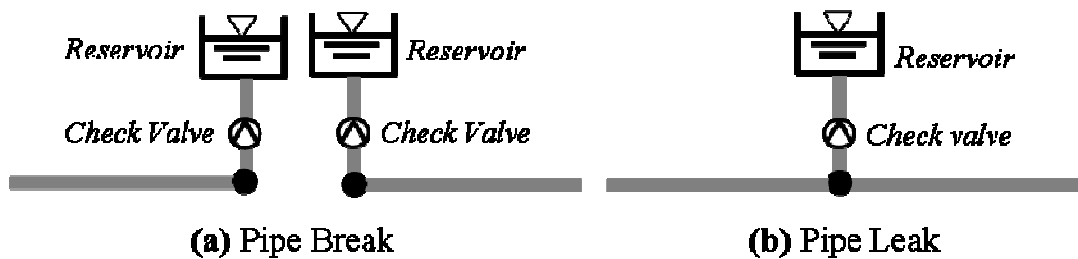


Figure 3.7 Simulation Models for a (a) Pipeline Break and (b) Leak

3.4.3 Pipeline Leak Simulation

Figure 3.7b shows the pipe leak model, with which leakage is simulated by a fictitious pipe open to the atmosphere, simulated as an empty reservoir with the same elevation as the leak location. A check valve constrains flow from the leaking pipe in one direction. The roughness and minor loss coefficients of the fictitious pipe are taken as infinite and 1, respectively, such that all energy loss from the leak is related to the minor loss.

Using Borda's formulations for a sudden expansion in flow cross-sectional area (e.g., Jeppson, 1976), Shi (2006) shows that the hydraulic head loss, p_l/γ_w , associated with leakage can be approximated by

$$\frac{p_l}{\gamma_w} = \frac{1}{2gA_l} Q^2 \quad (3.4)$$

in which p_l is the internal pressure in the pipe, γ_w is the unit weight of water, g is gravitational acceleration, A_l is the leak orifice area, and Q is the water flow rate. Equation 3.1 requires a ratio of leak to pipe cross-sectional area less than 0.05 to be accurate within 10% of the valid theoretical head loss. Re-arranging Equation 3.4 results in

$$Q = \left(\frac{2g}{\gamma_w} \right)^{0.5} A_l p_l^{0.5} \quad (3.5)$$

in which the flow discharge coefficient, C_D , is defined as,

$$C_D = \left(\frac{2g}{\gamma_w} \right)^{0.5} A_l \quad (3.6)$$

To validate the above relationship, data from fire protection sprinkler tests (Puchovsky, 1999), covering a typical range of orifice areas, are plotted in Figure 3.8 with respect to the theoretical discharge coefficients in Equation 3.8. The theoretical and measured discharge coefficients compare favorably, and show that the measured values are on average about 10% lower than the theoretical predictions.

The pipe leakage area, A_l , is specified for each leak occurrence, and this is used to determine the diameter of the fictitious pipe and thus the amount of water leaking from the pipe. Shi (2006) categorized leaks into five major types pertaining to joint pullout, round crack, longitudinal crack, local loss of pipe wall, and local tear of pipe wall, and developed a set of empirical equations to estimate the leakage area based on leak type, pipe material and joint properties. Table 3.1 shows Shi's (2006)

estimated probability of occurrence for the five leak types in pipes of different materials. GIRAFFE allows users the option of altering these values for simulation runs.

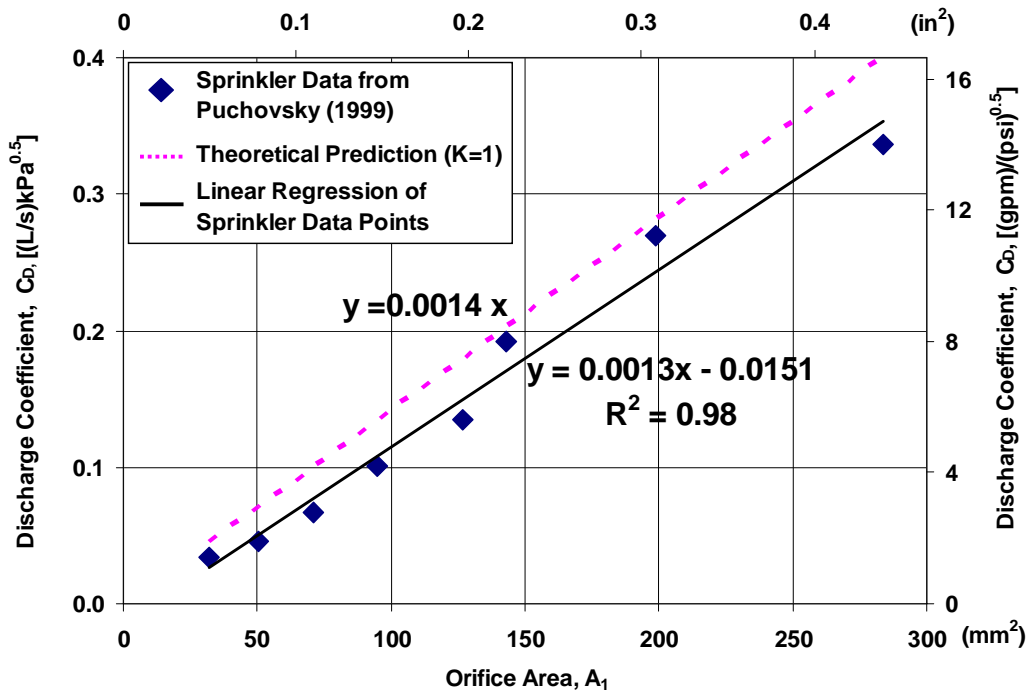


Figure 3.8 Comparison Between Model Predictions and Sprinkler Data (Shi, 2006)

Table 3.1 Probability of Leak Types for Different Pipe Materials

Pipe Material	Type 1 Joint Pullout	Type 2 Round Crack	Type 3 Longitudinal Crack	Type 4 Local Loss of Pipe Wall	Type 5 Local Tear of Pipe Wall
Cast Iron	0.3	0.5	0.1	0.1	N/A ¹
Ductile Iron	0.8	N/A ¹	0.1	0.1	N/A ¹
Riveted Steel	0.6	N/A ¹	0.3	0.1	N/A ¹
Welded Steel	N/A ¹	N/A ¹	N/A ¹	N/A ¹	1.0
Jointed Concrete	1.0	N/A ¹	N/A ¹	N/A ¹	N/A ¹

1: Not Applicable

3.4.4 Post-earthquake Flows at Demand Nodes

Most distribution pipelines ($D_p < 600$ mm) are not explicitly modeled in a GIRAFFE hydraulic network, but are accounted for by aggregating them into demand nodes in the system. Each demand node represents a part of a local distribution system. To simulate damage to the distribution network, Shi (2006) developed demand fragility curves that relate local distribution line damage (measured in repair rate, i.e. number of repairs per kilometer) and the increase in nodal demand.

The fragility curves were developed on the basis of Monte Carlo simulations of flow in damaged local distribution networks in the LADWP system. The local distribution networks are shown in Figure 3.9 and were selected as representative of different network topologies, pressure levels, and geographic areas. Each local distribution network contains both trunk and distribution pipelines. In the Monte Carlo simulations, trunk lines were kept undamaged and their flows were monitored before and after distribution line damage occurred. Several locations in the trunk lines were sampled for each system, and the ratios of flow before and after damage were calculated to obtain the ratio of demand after to demand before damage, which is referred to as normalized demand, ND . Linear regression analyses were performed on the results of the Monte Carlo simulations to develop fragility curves relating ND with RR .

As explained by Shi (2006), the mean slopes and intercepts for these linear regressions at 26 trunk line locations in 5 distribution systems were evaluated by linear regressions against the mean pressure, p , of the distribution system with an error term modeled as a Gaussian random variable. The confidence intervals of the linear

regression parameters were determined using conventional statistical methods (e.g., Ronald, et al., 1998). The resulting linear regressions follow the following formulation:

$$ND = c(p) + m(p)RR \quad (3.7)$$

in which $c(p)$ and $m(p)$ are the intercept and slope of the regression. Since RR is correlated with PGV , ND can be assessed from simulated strong motions generated for the scenario earthquakes.

Shi (2006) compared the confidence intervals predicting ND derived from analysis of 5 local distribution systems (labeled in Figure 3.7 as 1449, 1000, 579, 448 & 462, and 426) with linear regressions of ND vs. RR for a sixth local distribution system (labeled 205 in Figure 3.9) and showed that all the new regression were within the 90% confidence level. As an example, Figure 3.10 shows the linear regressions for local distribution network 426 relative to the mean, 68%, and 90% confidence intervals of the predictive model. The local distribution network regressions for system 426 fall mostly between the mean and 68% confidence limits. The 90% confidence limit sets an upper bound on the regressed data from all six distribution systems, and is used in system simulations for predicting local distribution performance.

The fragility relationships between ND and RR were developed for winter demand conditions, which must be adjusted for summer demand. Appendix A provides a simplified method for adjusting the fragility relationships to reflect alternative demand states.

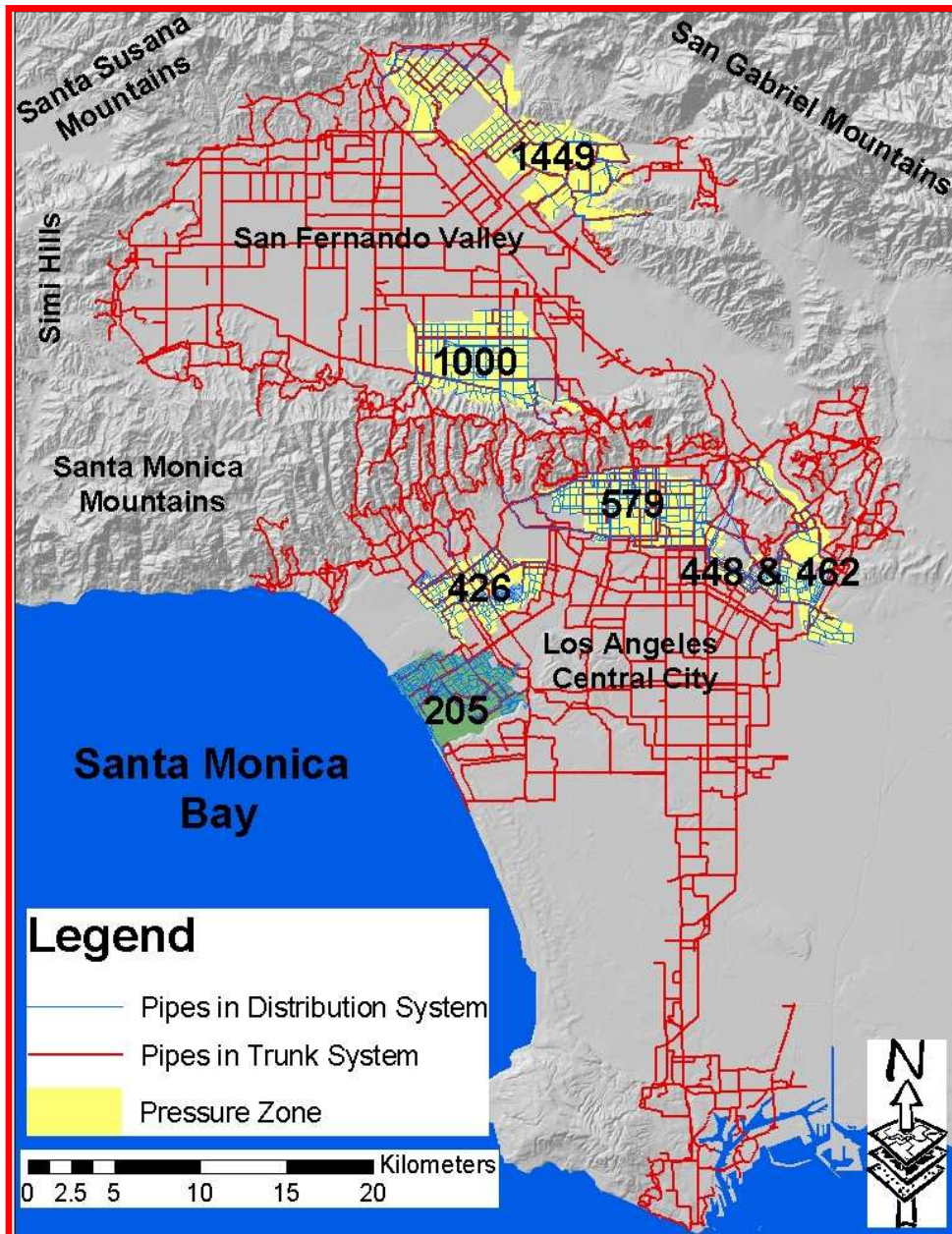


Figure 3.9 Locations of LADWP Local Distribution Systems Used to Develop Fragility Curves for Demand Nodes (Shi, 2006)

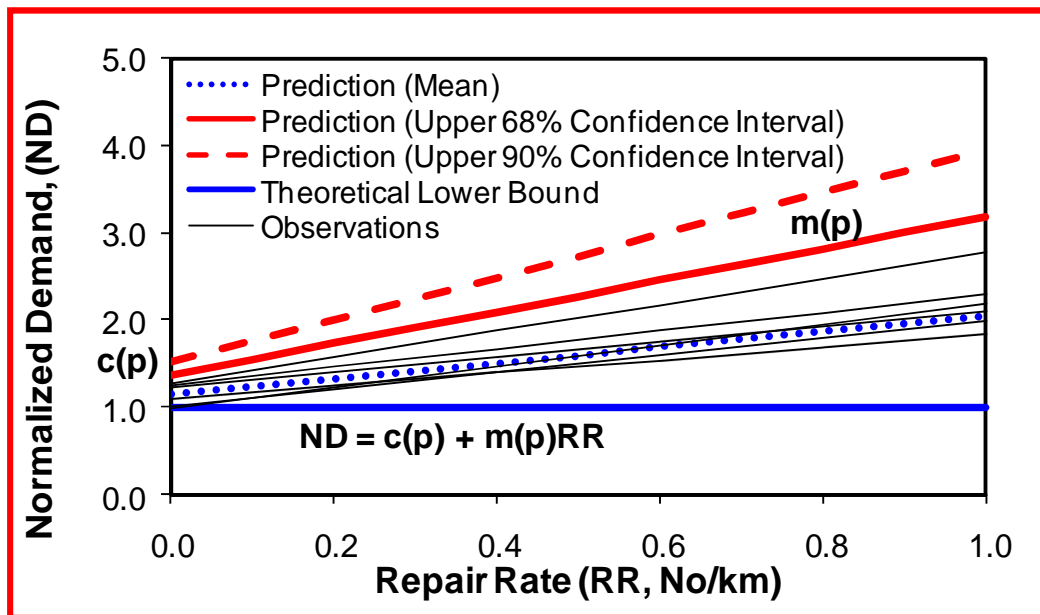


Figure 3.10 Fragility Curves Comparing Simulated and Observed Results for Repair Rate vs. Normalized Demand (Shi, 2006)

3.4.5 Facility Damage

Fragility curves are developed from the observed earthquake performance of facilities such as tanks, reservoirs, regulation stations, chlorination stations, special valves, and fittings. The fragility curves for tanks, for example, were developed for the different types of aboveground tanks used by LADWP: steel, unanchored concrete, and anchored concrete. Two damage states are defined pertaining to 1) relatively minor to moderate damage for which the tank remains functional for at least 24 hours after an earthquake, and 2) severe damage for which the tank is non-functional for 24 hours after an earthquake. The functional damage state corresponds to damage states 1, 2 and 3 as defined in HAZUS (FEMA, 2006), and the non-functional damage state corresponds to HAZUS damage states 4 and 5.

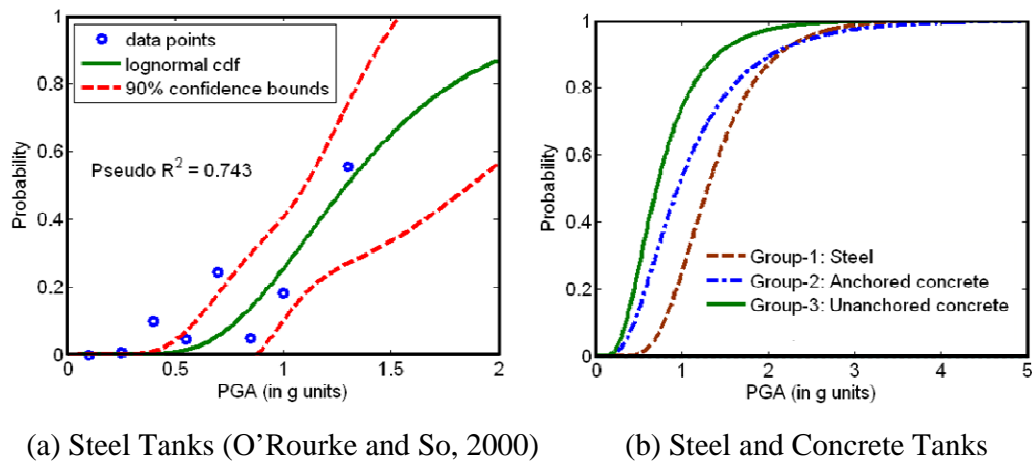


Figure 3.11 Fragility Curves for Water Tanks

For steel tanks, the fragility curve proposed by O'Rourke and So (2000) is used. This curve was developed by reviewing the records of seismic performance for 400 tanks in 9 separate earthquake events, and classifying them according to HAZUS damage states. Figure 3.11a shows the probability of tank damage as a function of PGA, which was developed by a lognormal fit to the data for all tanks with damage equal to or exceeding HAZUS damage state 4. Also, shown in the plot are the 90% confidence bounds and pseudo r^2 of the data.

HAZUS fragility curves for unanchored and anchored concrete tanks are used, corresponding approximately to pre- and post-1950 constructions. Figure 3.11b shows the fragility curves used in GIRAFFE for steel and concrete tanks. HAZUS fragility curves for unanchored and anchored tanks are plotted with the curve proposed by O'Rourke and So (2000) for steel tanks.

During a GIRAFFE simulation, a random number is generated between 0 and 1 and compared with the probability of tank failure. If the random number is less than

the probability of tank failure, the tank is considered damaged and non-functional for the first 24 hours after the seismic event.

3.5 Hydraulic Network Analysis

As shown in the GIRAFFE simulation flow chart in Figure 3.2, once a system is damaged, it is passed to the EPANET hydraulic engine for analysis. EPANET will send error messages back to GIRAFFE if there are components that are disconnected from the main system (due to pipe breaks) preventing EPANET from running a successful analysis. GIRAFFE will remove components isolated by damage and no longer connected hydraulically, and send the modified system back to EPANET for analysis. Once the isolated components are removed, GIRAFFE will parse the EPANET results and identify the lowest nodal pressure in the system. If the lowest pressure is below the user defined minimum pressure tolerance, GIRAFFE eliminates the node as well as the links and operational parameters associated with that node. EPANET runs another hydraulic analysis on this newly modified system, and GIRAFFE performs another check on the lowest pressure. This process continues until there is no pressure lower than the minimum pressure limit defined for the simulation, and hydraulic analysis is complete.

The GIRAFFE modeling approach transforms a damage state into an operational state by removing all pipelines that do not satisfy a minimum pressure tolerance, thus removing unreliable portions of the system to display the remaining part of the network that meets threshold serviceability requirements for minimum pressure tolerance. The resulting operational network provides valuable information

to operators and decision makers regarding what portions of the network are operational, vulnerable areas of the network, and mitigation strategies.

3.6 Compilation of Results

The final module compiles the results of the hydraulic analysis in a tabular format that can be imported into a Geographic Information System (GIS) for visualization and manipulation. Hydraulic analysis results are given for the five system components: pipelines, pumps, valves, nodes, and tanks (reservoirs are treated as tanks with fixed grade). Flows and pressures are reported for pipes, valves and pumps. Demands, pressures, and grades are reported for tanks and nodes. For a deterministic simulation, the results for the five components are reported for each time step of the analysis. For a probabilistic simulation, the results for the five system components are reported for each time step for all Monte Carlo simulation runs performed.

An index for measuring the seismic serviceability of the damaged water supply system is also reported at the end of a simulation. The system serviceability index (SSI) is the ratio of all post-earthquake demands to pre-earthquake demands in the system, and is defined as:

$$SSI = \frac{\sum_{i=1}^{n_i} \overline{Q}_i}{\sum_{i=1}^{n_{i0}} \overline{Q}_i} \quad (3.8)$$

where Q_i is the customer demand at node i , n_{i0} and n_i are the number of satisfied customer demands before and after imposing system damage. The serviceability can be calculated for each demand node, for the entire system, or for any subset of the

system. In a probabilistic simulation, the serviceability is reported for each Monte Carlo simulation run.

3.7 Economic and Social Consequences

As previously discussed, it is the post-event consequences that involve the greatest amount of interaction among system operators, external organizations, and the community receiving service. An area of great opportunity therefore is the use of the DSS to address the economic and social consequences of water supply performance. Output from water system simulations in terms of serviceability over time provide input for further simulations and decision making in relation to emergency response, system restoration, regional economic effects, and community impact. Quantification and visualization of the spatial variability of water supply serviceability through GIS provides the link between water supply performance and the geographic distribution of businesses, demographic characteristics, and interaction with other lifelines systems.

Researchers have been investigating the economic and social consequences of water supply disruption, and have been developing models for time dependent restoration. For example, Rose has evaluated the regional economic consequences of earthquakes, regulatory failures, and terrorist attacks utilizing information on water supply disruption in conjunction with computable general equilibrium (CGE) model of Los Angeles County (Rose 2006, Rose and Liao 2005). Davidson has evaluated the time and spatial distribution of post-earthquake electric power and water supply restoration using discrete event modeling (Cagnan et al. 2006, Cagnan and Davidson 2007). Chang, et al. (2008) have developed models linking lifeline system performance and community disaster resilience. They explore methods for

considering socio-economic impacts in decision making and the appropriate seismic performance goals for utilities.

3.8 Model Validation with Respect to the Northridge Earthquake

The 1994 Northridge earthquake (M_w 6.7) was selected for model calibration and validation. The Northridge earthquake is familiar to current LADWP personnel. In addition to data recorded during the Northridge earthquake, many employees have personal knowledge and experience with system damage and operations following the event. Damage caused by this earthquake has been assessed as over \$40 billion (Eguchi, and Chung, 1995). The earthquake is historically significant for the City of Los Angeles, and an appropriate scenario to benchmark decision support model simulation results with actual seismic performance.

3.8.1 LADWP System Performance during Northridge Earthquake

Data from LADWP and the Metropolitan Water District (MWD) shows 79 locations of damage in trunk lines and 1,013 locations of damage in distribution lines (Shi, 2006). Among the 79 trunk line damage locations, 67 occurred in LADWP trunk lines and 12 occurred in trunk lines owned and operated by the Metropolitan Water District (MWD). MWD pipelines are embedded in the LADWP system and interconnections between the two systems are not normally open. Under emergency situations, or times when LADWP needs to purchase supplemental water, these connections can be opened. Five LADWP water storage tanks were also damaged (Brown, et al., 1995). Figure 3.12 shows the LADWP water service area with the locations of trunk line and distribution line repairs, damaged tanks, and water

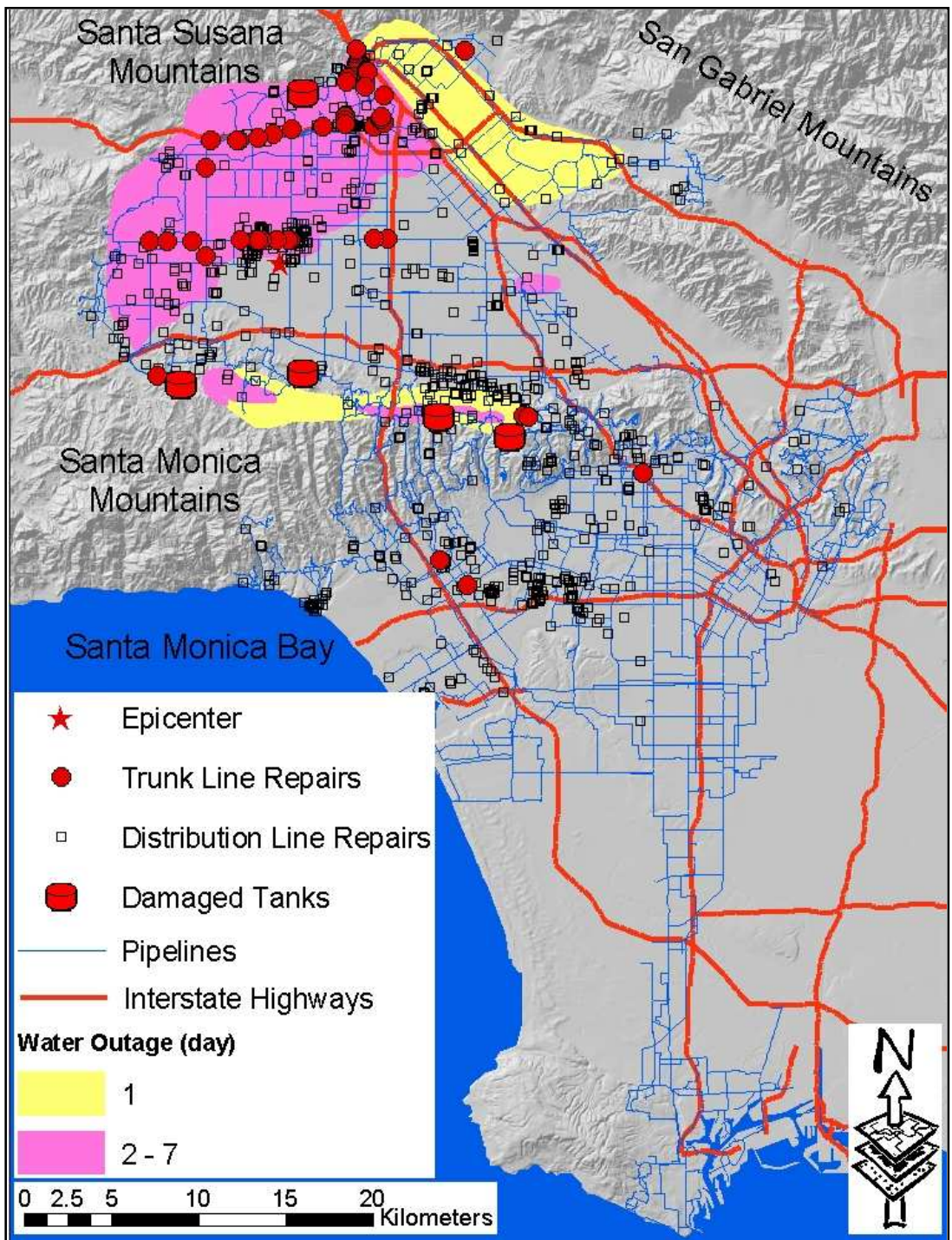


Figure 3.12 LADWP Damaged Tanks, Trunk and Distribution Line Repairs, and Water Outage Areas after the Northridge Earthquake (Shi, 2006)

outage areas (Lund, et al., 2005) following the earthquake.

3.8.2 LADWP Hydraulic Model for the Northridge Earthquake

The GIRAFFE simulation model was built from a 2002 hydraulic network model used at LADWP. Connections to the Upper and Lower Hollywood Reservoirs (5.4 M m³, 1.4 B gal), Encino Reservoir (14.8 M m³, 3.9 B gal) and Lower Stone Canyon Reservoir (13.6 M m³, 3.6 B gal) have since been closed, but were open at the time of the Northridge earthquake. To simulate conditions in 1994, these reservoirs were included in the GIRAFFE hydraulic simulation model. Moreover, pipelines and valve settings were changed in consultation with LADWP planning and operations personnel to replicate the 1994 system.

3.8.3 Damage Simulation

To simulate the response of the hydraulic network model, damage was added to system components and GIRAFFE was then used to perform hydraulic network analysis of the damaged system. The damage simulation of the trunk lines, distribution system, tanks, and pump stations are described in the following sections.

3.8.3.1 Trunk Line Damage

Detailed descriptions of the LADWP trunk line damage are provided by Shi (2006). For system analysis, breaks in the Granada and Rinaldi Trunk Lines, and multiple leaks in the northern half of the system were simulated. Leaks occurring in

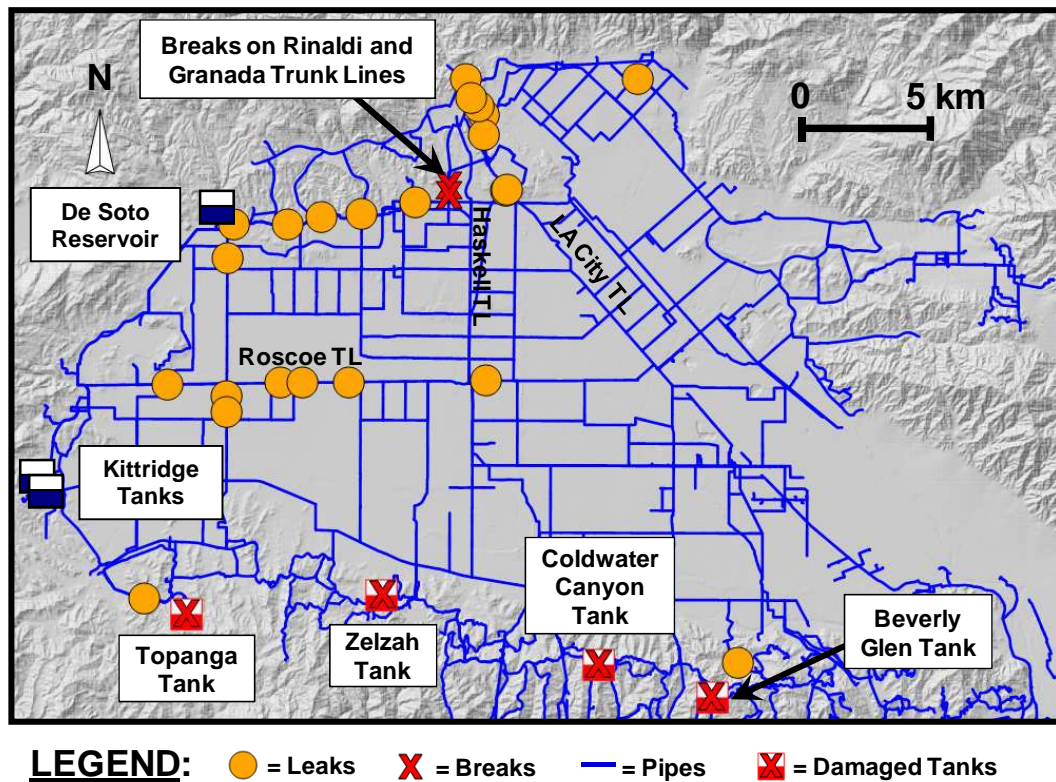


Figure 3.13 Location of Breaks, Leaks and Damaged Tanks used in Repeat Northridge Earthquake Simulation

close proximity along the same pipeline were modeled as one leak with an appropriately increased leak orifice area. Leaks or breaks situated immediately downstream of a pipe break had no effect on system flow and were not modeled. Leak and break locations for the simulations are shown in Figure 3.13.

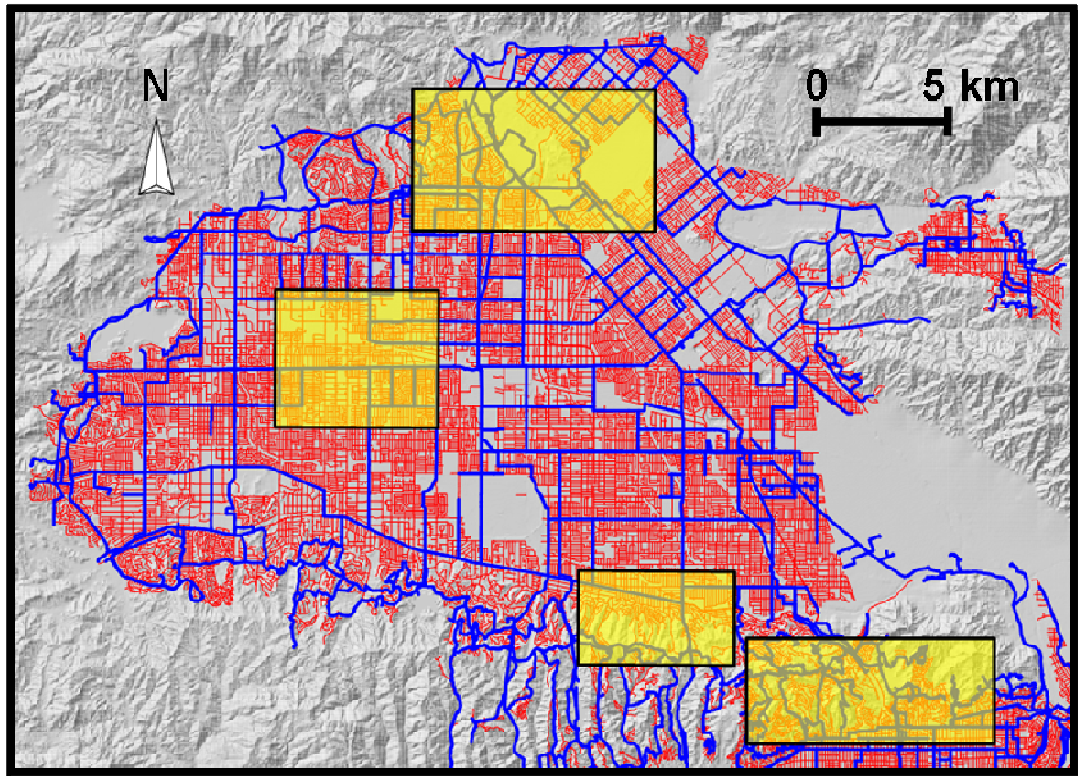
A summary of all damage to the LADWP and MWD trunk lines in the LADWP service area is presented in Appendix B. Damage locations attributed to TGD and PGD are identified.

3.8.3.2 Distribution System Damage

As described previously, damage to the distribution system is not modeled as explicit breaks and leaks, but is simulated as an increase in nodal demands. PGV recorded by 164 strong ground motion stations during the Northridge earthquake were used to generate pipeline *RR*, which were then applied to the fragility curves developed by Shi (2006) to determine increased nodal demands. Previous research by Jeon and O'Rourke (2005) and discussions with LADWP personnel show that four regions in the northern half of the LADWP water system were subject to significant PGD-induced damage. The actual *RRs* in these zones were determined from GIS data on distribution pipeline damage compiled by Jeon and O'Rourke (2005) and used with the distribution system fragility curves to find the nodal demands in the PGD zones. Figure 3.14 shows the four zones of PGD.

3.8.3.3 Tank Damage

Brown et al. (1995) summarize the performance of the 65 LADWP tanks (48 welded or riveted steel and 17 reinforced concrete or prestressed concrete tanks) in service at the time of the Northridge earthquake. Overall, tank performance was good, and only 5 tanks were damaged. Modern tanks performed well, while all of the damaged tanks were constructed before 1950. The damaged tanks are highlighted in pink in Figure 3.13. The Coldwater and Beverly Glen Tanks were both riveted steel tanks with 9 million liter (2.3 million gal.) capacities. Both suffered partial roof collapse and damage to the inlet/outlet lines. The Topanga and Zelzah Tanks were both welded steel tanks with 0.9 million liter (230,000 gal.) and 3.8 million liter



LEGEND

— = Trunk Lines — = Distribution Pipelines = Zones of PGD

Figure 3.14 Zones of PGD in the LADWP Water Supply System

(1 million gal.) capacities, respectively. Both tanks experienced damage to the tank inlet/outlet lines, and Zelzah also suffered a collapsed roof. The 2.3 million liter (608,000 gal.) capacity, riveted steel Granada High Tank had extensive damage and was taken out of service following the earthquake and is not represented in the simulation model. Since all tanks had pipe connection failures, the inlet and outlet lines for the 4 damaged tanks in the hydraulic model were disconnected in the simulation of post-earthquake performance.

3.8.3.4 Water-Power Interaction/Pump Station Damage

The Northridge earthquake caused an immediate system-wide blackout for the LADWP electric power system, after which electricity was restored incrementally beginning 1 hour after the earthquake, and fully restored within 27 hours (Cağnan, 2005). To account for interaction between the water and electric power systems, pump stations that lost power during the Northridge earthquake were identified and reconfigured to emergency power loss status. In the event of power loss, pump stations with secondary sources of power or back-up generators will continue to operate with a modified number of pumps. Electric power outage data from the actual 1994 Northridge earthquake were used to simulate the configuration of pumps for various time increments following the earthquake event. It was found that using the configuration of pumps operating 2 hours following the earthquake for the entire 24 hour simulation produced nearly identical results (differing by less than 1%) to an analysis where power was incrementally restored to pump stations at 2, 6, 12, 18 and 24 hours. Thus, the 2 hour configuration of operational pumps, shown in Figure 3.15, was used as an equivalent power state for the 24 hour simulation. It should be noted that nearly 56% of the pump stations without power 2 hours after the earthquake had back up generators or internal combustion (IC) units that in some cases pumped more water than during normal operating conditions. Van Norman Pump Station No. 2, one of the largest and most important pump stations in the LADWP water system, is located in the Van Norman Complex, where power was not restored until more than 18 hours after the earthquake. This pump station does not have back up generators, and was not in operation for nearly 24 hours after the earthquake.

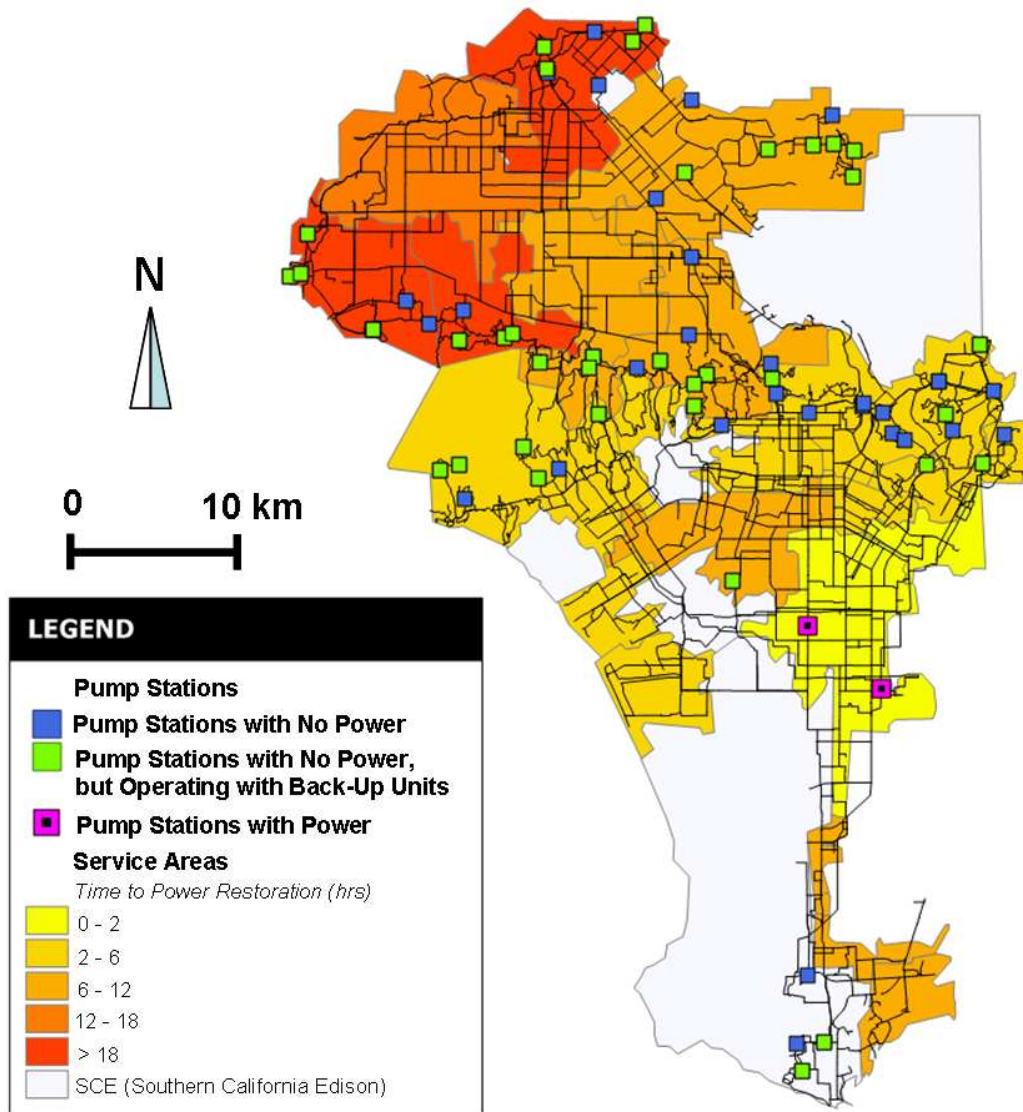


Figure 3.15 Pump Station Operational Status 2 Hours after the Northridge Earthquake

3.8.4 Comparison of Simulated and Observed Earthquake Performance

A simulation of the 1994 Northridge earthquake effects on the LADWP system was conducted by representing trunk line breaks, distribution system damage through increased nodal demands, tank damage, and pump station interruptions from electric

power losses, as previously described. In addition, the loss of flow from the LAAs was accounted for. Although damaged, the Los Angeles Aqueduct 1 (LAA1) was able to operate at very low flow for approximately 1 week after the earthquake to allow for repairs to Los Angeles Aqueduct 2 (LAA2). LAA2 was out of service for repairs in the first week following the earthquake, and then placed in service while LAA1 was shut down for repairs. Both LAA1 and LAA2 were shutdown for 3 weeks, beginning in the last week of February, to allow for repairs to be made to the open channel (Lund and Cooper, 1995). The effects of the lost aqueduct flows were modeled by closing the flow of water from the Los Angeles Filtration Plant, where the LAA1 and LAA2 provide water to the LADWP hydraulic network model. The simulation was run for 24 hours.

Comparisons between simulated and observed performance are made on the basis of 1) system-wide functionality, 2) geographic distribution of lost service, and 3) flow measurements at key locations in the system. Each basis for comparison is discussed under the subheadings that follow.

3.8.4.1 System - wide Functionality

The system serviceability index, SSI, is defined as the percentage of total flow available at all demand locations (nodes) at some time after the earthquake to the total flow before the earthquake. The model simulations show $SSI = 71.6\%$ at 24 hours after the earthquake, which means that 28.4% of the system was without significant water service. This measure of system serviceability agrees well with the LADWP estimates.

3.8.4.2 Geographic Distribution of Lost Service

Figure 3.16 compares the simulation results for 24 hours after the earthquake with the areas of water outage, or lost service, during the first day and for 2 to 7 days after the earthquake. The area in Figure 3.16a is the San Fernando Valley, which is the epicentral area for the earthquake and the region in which the great majority of lost service was documented. The turquoise colored pipelines are those with flow insufficient for reliable service. The areas of recorded outage compare favorably with the geographic coverage of pipelines that have flows insufficient for reliable service, thereby showing that the model accounts well for the geographic dispersion of lost water service. The median SSI 24 hours after the earthquake is 71.8%, which falls within LADWP estimates of 70-75% serviceability 24 hours after the actual Northridge earthquake (Adams, 2008). The LADWP water outage zones contain 70-80% of the unsatisfied demand nodes for the simulation.

In the map of the LADWP system in Figure 3.16b there is a zone of turquoise pipelines near the center of the system in the Santa Monica Mountains. These pipelines are located at high elevations where automatic controls in the local pump stations are not modeled in sufficient detail to replicate the actual pressure levels in the pipes. Under these conditions, the hydraulic network model defaults to a conservative estimate of low pressure and corresponding loss in local serviceability. These zones represent less than 2% of the demand nodes in the system. Hence, the model is biased to conservative results at high elevations that has only a small effect on system serviceability. The modeling procedures for pumps and storage tank performance at higher elevations are discussed in Appendix C.

It should be noted that the Kittridge Tanks and DeSoto Reservoir were depleted shortly after the earthquake. The broken portion of the Granada Trunk Line prevented the replenishing of the Kittridge Tanks in the western San Fernando Valley. The breaks in the Rinaldi Trunk Line cut off the water supply to the De Soto Reservoir in the northern San Fernando Valley. The GIRAFFE simulation appropriately captured this behavior, showing the Kittridge Tanks and De Soto Reservoir were depleted within 2 hours after the earthquake.

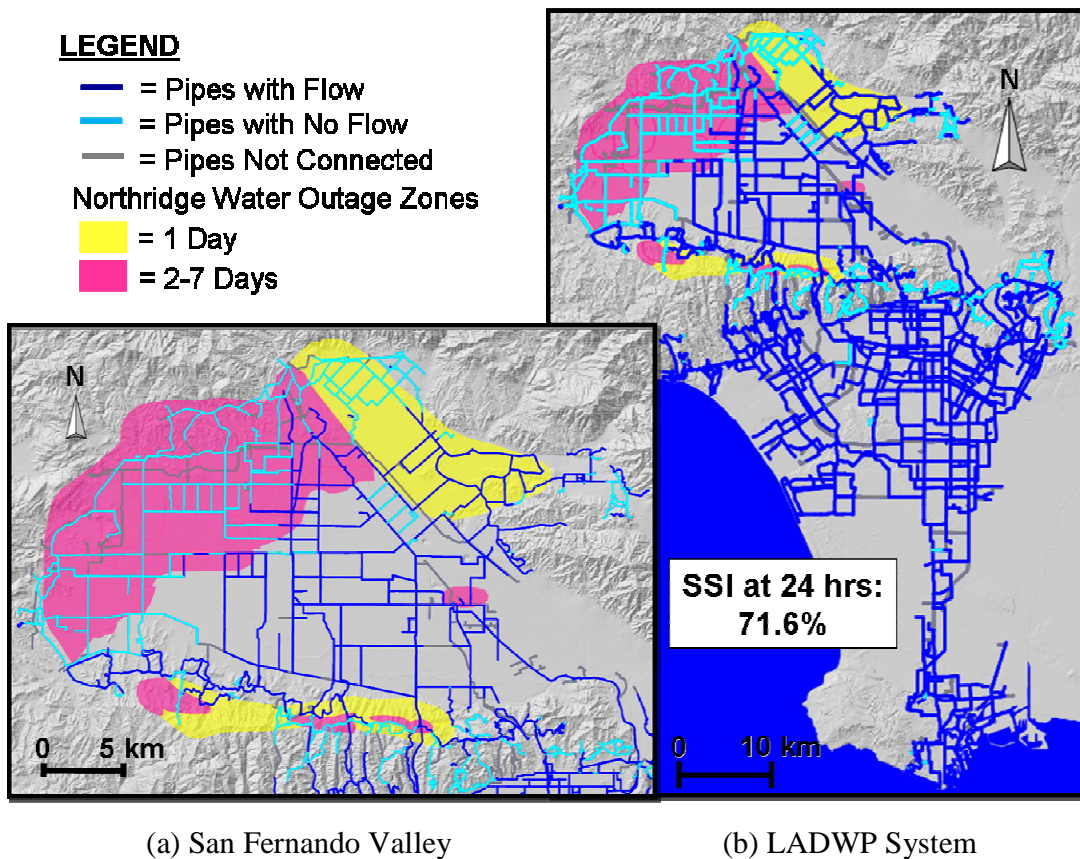


Figure 3.16 Comparison of Simulated Flows 24 Hours after the Earthquake with Zones of Documented Lost Service

3.8.4.3 Flow Measurements at Key Locations in the LADWP System

To confirm that pre-earthquake flows simulated in the model are consistent with actual flows in the system, pre-earthquake simulated flows were determined at four key locations shown in Figure 3.17: Stone Canyon Inlet, Franklin Reservoir, Hollywood Inlet, and River Supply Conduit. These flows were compared with typical ranges of flow provided by LADWP engineering staff. At each location the simulated flow fell within the typical flow ranges for January, thus confirming the appropriate levels of flow from north to south in the system.

LADWP monitors system performance at various locations using a Supervisory Control and Data Acquisition (SCADA) system. Flow monitor records showing data before, during, and after the Northridge earthquake were obtained and reviewed by Shi (2006). Some of the data were not reliable due to earthquake damage and the loss of electric power at the SCADA stations. Using the screening process described by Shi (2006) to remove unreliable data, five SCADA flow meter records were selected for comparison with the simulated flows: the LA Reservoir Outlet, Encino Reservoir outflow, Granada Trunk Line, Morella & Van Owen Regulator Station, and Astoria Pump Station, all of which are shown in Figure 3.17.

Figure 3.18 compares the simulation and the recorded SCADA flows. In general, the simulated flows compare favorably with the monitored flows at each location. The pre-earthquake simulation closely follows measured flow variations before the earthquake. Following the earthquake, flow from the LA Reservoir increased to nearly 20,000 l/s (317,000 gpm) due to water losses associated with damage to major trunk lines downstream. Leaking sections of two large trunk lines

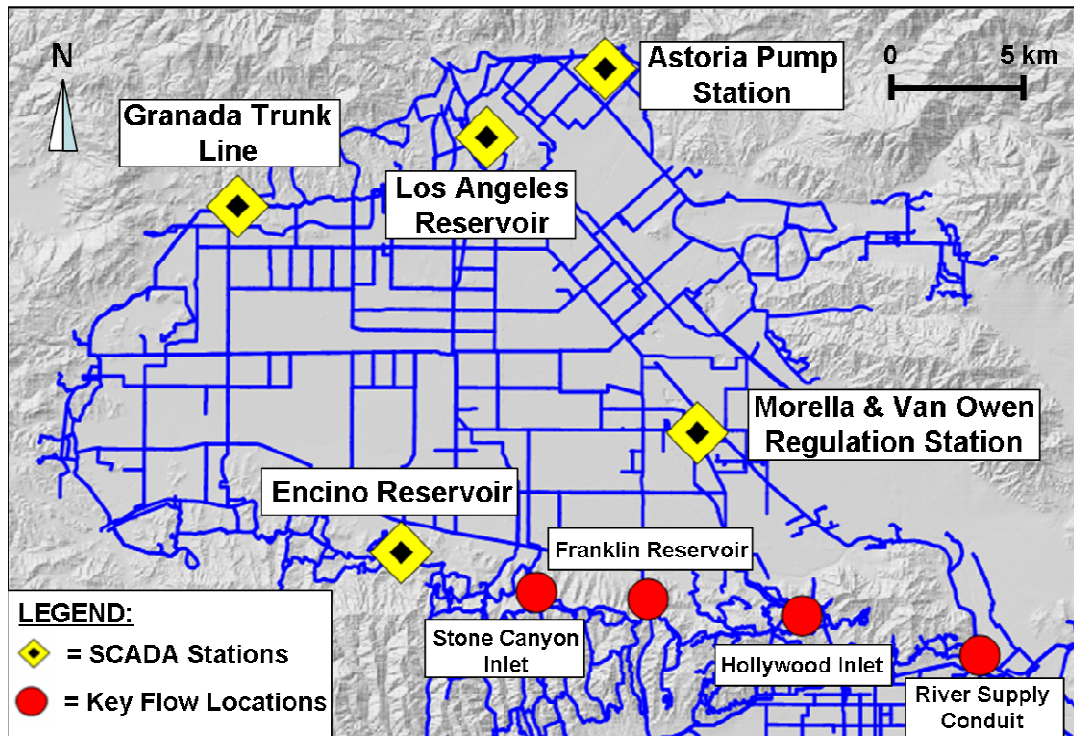
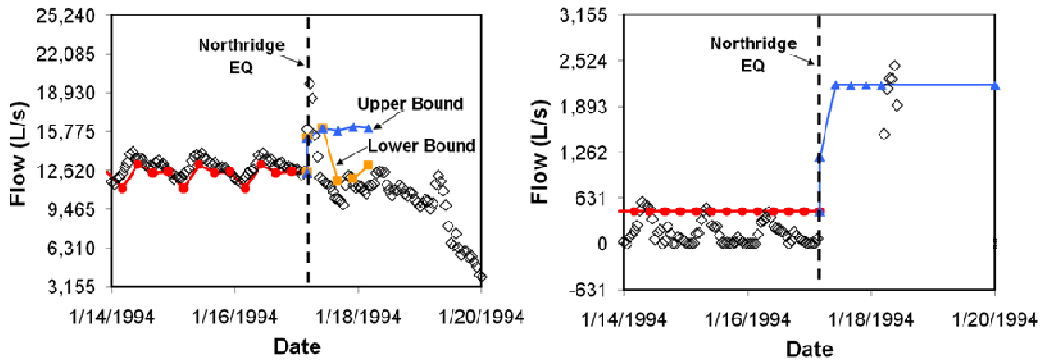


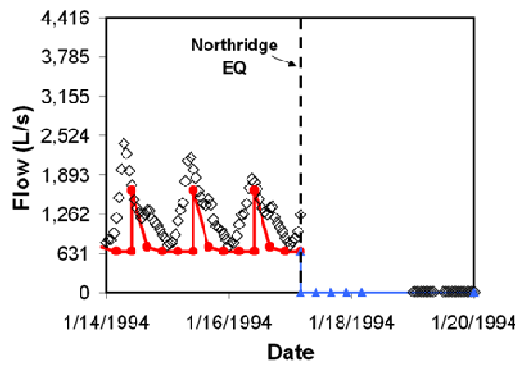
Figure 3.17 SCADA Flow Stations and Key Locations of Flow

were isolated in the lower Van Norman Complex within 6 hours after the earthquake to curtail water losses (Adams, 2008), after which the monitored flow in the LA Reservoir Outlet dropped to a range of 10,000 to 12,500 l/s (158,500 to 198,000 gpm). Two post-earthquake simulations were performed with one and two trunk lines isolated within 6 hours to set upper and lower limits on flow from the reservoir. The flow associated with the isolation of two trunk lines compares favorably with the measurements.

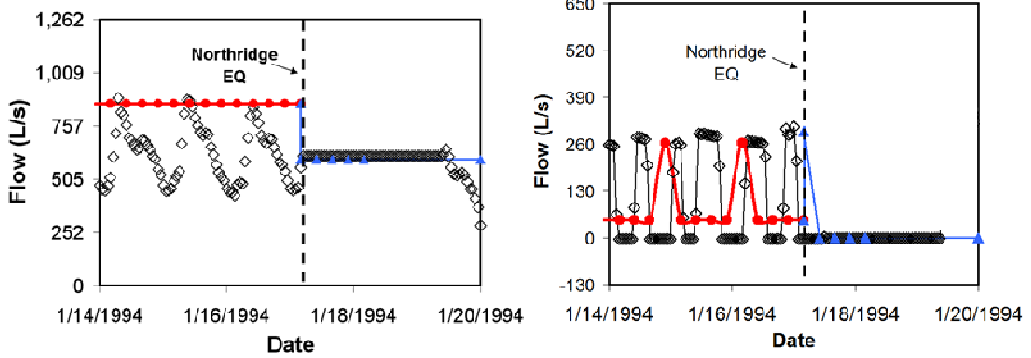


(a) Los Angeles Reservoir Outlet

(b) Encino Reservoir



(c) Granada Trunk Line



(d) Morella & Van Owen Regulation Station

(e) Astoria Pump Station

LEGEND: \diamond = Monitored Data
 —●— = Pre-Earthquake Simulation
 —▲— = Post-Earthquake Simulation

Figure 3.18 Comparisons Between Simulation Results and Measured SCADA Flows Before and After the Northridge Earthquake

Simulated pre-earthquake flows from the Encino Reservoir fall within the range of measured flows. Flow from the Encino Reservoir increased dramatically following the earthquake because it had to provide more water to the southern part of San Fernando Valley to compensate for the loss of water sources normally feeding the Valley from the north.

The simulated pre-earthquake flows in the Granada Trunk Line (GTL) follow the daily fluctuations experienced in this part of the system. The earthquake-induced rupture of the GTL results in zero simulated flow, which is identical with the actual loss of water in this pipeline.

The simulated flow rate through the Morella & Van Owen Regulator Station prior to earthquake is 862 l/s (13,100 gpm), which is near the peak values of measured daily flows. This automated regulation station is controlled by a series of operating rules based on nearby tank levels and node pressures that causes daily fluctuations in flow. The hydraulic network model cannot account for this operating logic, explicitly, but instead makes an approximation of system behavior over the simulation time period. Also shown in Figure 3.18 are the simulated flow rates at the Astoria Pump Station, which vary between 50 and 265 l/s (790 to 4,200 gpm), before the earthquake. Again, hydraulic network modeling limitations do not allow simulation of all cycles of daily flow, but the model is able to capture about half of them. Both the simulated and measured flows drop to zero after the earthquake.

In general, the GIRAFFE simulation compares favorably with the major features of the observed response of the LADWP system during the 1994 Northridge earthquake.

3.9 Conclusions

A DSS has been developed for LADWP to plan operations, emergency response, and new system facilities and configurations to optimize water supply performance during and after earthquakes. The system is generic, and the architecture of its computer programs is adaptable to any water supply. The system works with a special program for damaged network flow modeling, known as Graphical Iterative Response Analysis for Flow Following Earthquakes (GIRAFFE). It simulates all 11,633 km (7,228 mi.) of water trunk and distribution pipelines and related facilities (e.g., tanks, reservoirs, pressure regulation stations, pump stations, etc.) in the LADWP system, and accounts for the aggregated seismic hazard in Los Angeles through an ensemble of 59 scenario earthquakes. The simulations are dynamic in time, and can account for loss of service as tanks and local reservoirs lose water over time through leaks and breaks in pipelines.

Specific model improvements were accomplished as part of this work. The model was upgraded to represent the LADWP system in 2007. The DSS now contains models for the LADWP system in 2002 and 2007. Modifications to the 2002 model can be implemented to represent system performance in 1994, thereby providing an appropriate basis for simulations of water supply response to the 1994 Northridge earthquake.

Additional model improvements include the ability to model the time dependent response of the system in a more robust manner, by enabling the levels of tanks and reservoirs to vary during a simulation. These refinements in the dynamic capability of the simulations require the appropriate selection of simulation time

increment. To select properly, it is necessary to consider the smallest operational time increment for system functionality, which generally depends on the capacity of key storage facilities. The model was also updated with the ability to include all sources of earthquake damage and disruption including the loss of the Los Angeles Aqueducts, loss of electric power, PGD and TGD effects in trunk and distribution pipelines, and fragility curves to probabilistically represent damage to facilities such as tanks, reservoirs, regulation stations, and pumps.

The hydraulic network model was validated through comparison of model results for the effects of the 1994 Northridge earthquake with the actual areas of lost water service and pre- and post-earthquake measurements of flow documented by LADWP. There is very good agreement between model results and LADWP records with respect to system-wide serviceability (28% water outage over the entire system), geographic distribution of lost service, and pre- and post-earthquake flows over time at key locations.

CHAPTER 4

PARAMETRIC STUDY OF WATER SUPPLY RESPONSE TO EARTHQUAKES

4.1 Introduction

A decision support system (DSS) for the seismic performance of water supplies has been developed, as described in Chapter 3. Details about the development and evaluation of the hydraulic network model embodied in the DSS GIRAFFE are provided by Wang (2006), Shi (2006), Shi et al. (2006), and Wang and O'Rourke (2007).

The purpose of this chapter is to use the LADWP hydraulic network model to study the sensitivity of system response to various parameters. Foremost among these parameters are time and size of the model. Other important parameters include the effects of permanent ground deformation (PGD) and seismic wave interaction, referred to herein as transient ground deformation (TGD), as well as minimum negative pressure tolerance, the percentages of pipeline breaks and leak associated with earthquake damage, and the characterization of leakage in damage underground pipelines.

4.2 Scale and Time in System Modeling

The post-earthquake performance of a water supply system is time-dependent. Losses from ruptured and leaking pipelines will reduce water levels in the tanks and reservoirs, thereby reducing pressure and flow within the system. Tanks and reservoirs with limited storage capacity will run dry if measures are not taken to isolate broken and leaking pipelines by closing off areas of severe damage from other portions of the network. It is not possible to isolate damaged pipelines after an earthquake until crews have inspected the system, identified areas of serious water losses, and undertaken measures to close off leaking and ruptured lines. During the time required for isolating damage, the serviceability of the system degrades.

Of additional importance is the scale and level of detail incorporated in the model. All models involve tradeoffs between system simplifications that reduce accuracy and the provision for system complexity that increases the cost and time of modeling. Some of the most fundamental decisions include the size and number of pipelines that need to be modeled. Previous hydraulic network models for simulating earthquake performance have focused on the larger, more important pipelines in the network, which are the trunk lines, and have represented the smaller distribution pipelines as demands for flow at various locations in the trunk line network (Khater and Waisman, 1999). Damage to the trunk lines is modeled explicitly. Because distribution demands remain constant, neither damage to the distribution lines nor post-earthquake changes in water usage are represented by this type of simulation.

4.2.1 Time Dependent Effects

Post-earthquake water supply performance changes with time because water losses through leaking pipelines reduce storage levels in tanks and local reservoirs, thereby reducing hydraulic head and availability of water that drives flow and pressure throughout the system. A time increment is selected for analysis, and the hydraulic heads and flows are calculated at the end of each time increment and used as input for the next.

The effects of time increment can be illustrated by the interaction between the Los Angeles Filtration Plant, which receives and distributes water from the LAAs, and the Clearwell Tank (3.9 million gal., 14.8 million liter capacity). A simplified schematic of the Filtration Plant and Clearwell Tank interaction is shown in Figure 4.1. A check valve between the two water storage facilities restricts flow in one direction, from the Filtration Plant to the Clearwell Tank. In the first time step of a simulation (at 0 hours), the hydraulic head at Clearwell Tank is higher than that of the Filtration Plant, so no flow occurs between the two. The analysis is performed assuming constant demands over the selected time step period, and tank volumes are updated at the end of each time step using the following equation,

$$v = v_i - Dt \quad (4.1)$$

where v is the tank volume after the time step, v_i is the initial tank volume at the beginning of the time step, D is the demand rate on the tank (gpm), and t is the time step unit in hours.

For the example in Figure 4.1, if a six-hour simulation time step is selected, the Clearwell Tank goes dry after the second hour, but tank levels, pressures and hydraulic heads are not re-calculated until hour six. The empty Clearwell Tank causes negative pressures that result in the removal of the tank and connecting pipelines. This is not a realistic result because the Los Angeles Filtration Plant would supply water to the Clearwell Tank to keep it in service. If a one-hour time step is selected for the same simulation, the Filtration Plant supplies water to the Clearwell Tank in the second hour of the analysis and many time steps thereafter, thereby preserving an important water source and modeling realistic system functionality.

This example highlights the importance of selecting a time step that is less than or equal to the smallest operational time increment for system functionality. The selection of this time interval will generally depend on the capacity of key storage facilities. For the LADWP system, the storage capacities under earthquake flow conditions of the Clearwell, as well as several other tanks in the network, were less than two hours, and a one-hour time step was used to account appropriately for system behavior.

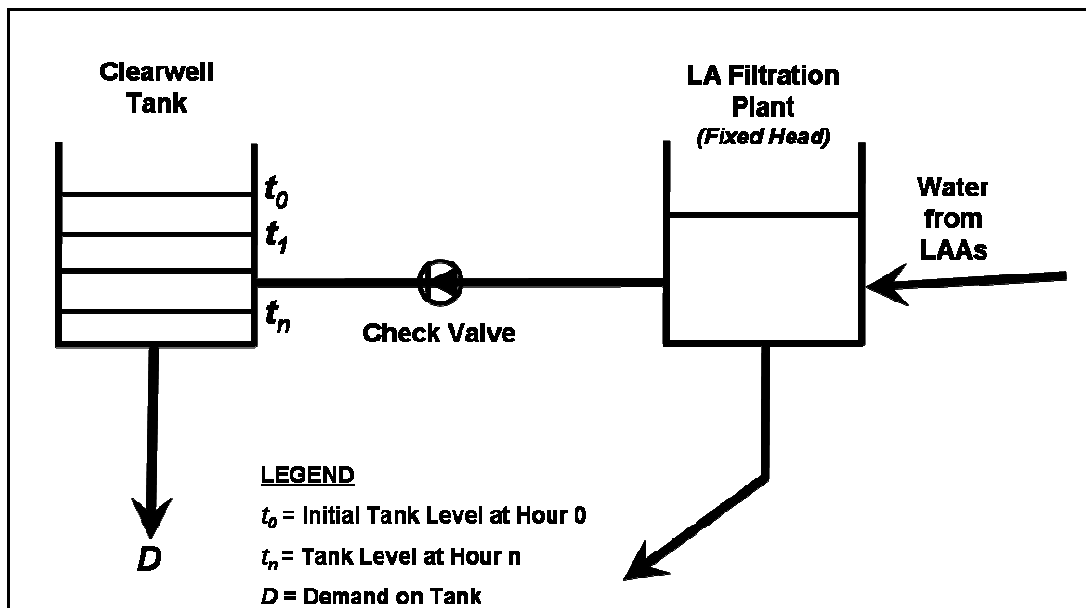


Figure 4.1 Simplified Schematic for Interaction Between Los Angeles Filtration Plant and Clearwell Tank

4.2.2 Number and Size of Pipelines

As the size of pipelines in the model decreases, the number of pipelines that need to be simulated increases, thereby increasing the time and cost of modeling. Relatively small diameter pipelines comprise the largest percentage of pipelines in a water supply. According to statistics compiled in 2000, 88% of the pipelines in the LADWP water supply system (Jeon, 2002) and 82% of pipelines in the NYC water system (Chapin, 2001) have diameters less than 400 mm (16 in.). (Figure D.1 in Appendix D shows the composition of pipeline diameters for the NYC and LADWP water systems.) Expertly modeling pipelines with diameters less than 400 mm (16 in.), which populate the distribution systems, would involve the construction of hydraulic network models for 82-88% of the pipelines, or on average 8,000 km (4,971 mi.) of pipelines for each of the Los Angeles and NYC systems.

The approach followed in this work is to represent the local distribution networks as demand nodes and to adjust the demand at these nodes using fragility curves to reflect the level of earthquake damage within the local distribution networks. Not accounting for distribution pipeline damage results in a static or constant demand at each node, whereas damage increases the demand thereby placing greater stress on the overall system.

A hydraulic network model was created to represent the LADWP system during the 1994 Northridge earthquake. As explained in Chapter 3, the model included the effects of the electric power loss to pump stations, the closing of the Haskell Trunk Line approximately 6 hours after the earthquake, and severe damage to 5 tanks in the southern San Fernando Valley. The model accounts implicitly for earthquake damage to distribution pipelines through fragility curves that relate local distribution line damage, measured in repair rate, (i.e. the number of repairs per kilometer of pipeline, correlated with PGV and PGD), and the increase in nodal demand. The importance of modeling distribution system response can be assessed by changing the distribution system demand and determining how the system serviceability changes as a function of demand, both immediately after the earthquake and 24 hours later.

To determine the importance of distribution system demand, simulations were performed with the LADWP hydraulic network model, including all sources of Northridge earthquake damage, and the only variable changed was the pre-earthquake demand scenario. Five cases were simulated using a baseline winter demand, 50% of winter demand, typical summer demand, and 150% and 200% of summer demand. The results in Figure 4.2 show SSI versus relative demand (the ratio of the demand

used in the simulation to the baseline winter demand) for 24 hours after the earthquake, and are shown as red triangles fit with a 3rd degree polynomial regression line. The typical summer demand is 233% of the winter demand. The results indicate that relative demand has a significant effect on system serviceability. The effect is relatively small at relative demands of 0.5 to 1, but increases as relative demand increases from approximately 1.5 to 4.7.

To evaluate the importance of modeling damage to distribution pipelines, an additional five simulations were performed for the same demand scenarios for all sources of Northridge earthquake damage, except distribution system damage. As explained in Chapter 3, distribution system damage will increase demands. Instead of increasing demands, the demands remained static, thus representing a case of no change and no damage in the distribution system. The results of these simulations are shown as blue diamonds in Figure 4.2 and fit with a 3rd degree polynomial regression line. There is a significant difference between the two plots with the simulation of earthquake damage producing a reduction in SSI of 15 to 30%. The loss of serviceability becomes more intense as relative demand increases. These results emphasize that modeling a system without increasing nodal demands (i.e. modeling damage to distribution pipelines) would be neglecting a parameter that has a significant influence on the system serviceability.

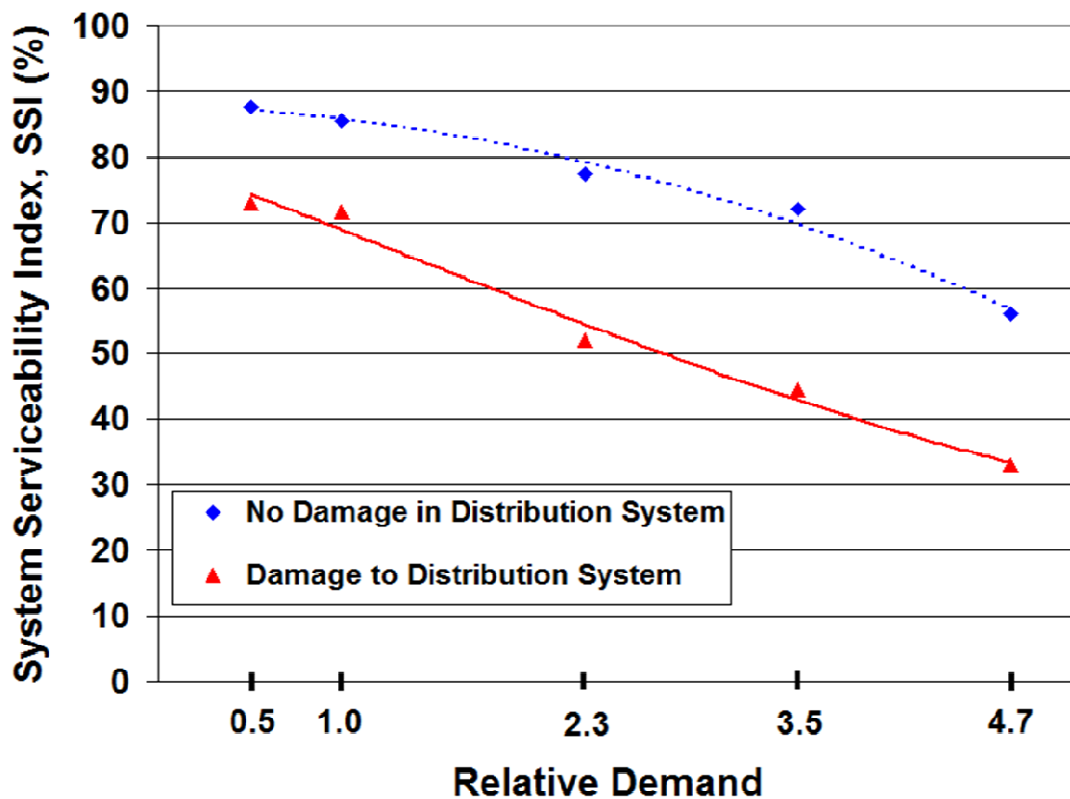


Figure 4.2 System Serviceability vs. Relative Demand for System Response 24 Hours after the Northridge Earthquake

4.3 PGD vs. TGD Effects

It is well recognized that PGD is one of the most pervasive causes of lifeline damage during earthquakes (O'Rourke, 1998). Damage to buried pipelines caused by liquefaction-induced PGD was responsible for loss of water to the central business district of San Francisco after the 1906 earthquake (O'Rourke, et al., 2006; Scawthorn, et al., 2006) and contributed to the loss of water in all 86 reservoirs supplying Kobe City after the 1995 Kobe earthquake (O'Rourke, 1996). Given the severity of lifeline damage caused by PGD and its well-documented consequences after major earthquakes, significant emphasis has been placed on PGD effects in guidelines for the

seismic design of lifeline facilities (e.g., ASCE, 1984; O'Rourke and Liu, 1999; Honegger and Nyman, 2004).

Seismic wave, or TGD effects, can also have serious consequences on lifeline system performance. Although not as severe locally as PGD, TGD/wave propagation can disturb an entire network, damaging lifelines weak from corrosion or vulnerable to malfunction at joints. Recent investigations focused on the 1994 Northridge earthquake effects on the Los Angeles water supply (Davis, et al., 2007) have shown that TGD was the source of serious system-wide effects.

The hydraulic network model for the LADWP system provides an opportunity to evaluate in considerable detail how the Los Angeles water supply was affected by PGD and TGD during the 1994 Northridge earthquake. As explained in Chapter 3 and Appendix B, earthquake damage to the LADWP trunk lines has been carefully documented with respect to PGD and TGD effects. Moreover, zones of PGD effects triggered by the Northridge earthquake have been identified and records of distribution pipeline damage have been used to quantify the hydraulic effects of PGD on LADWP local distribution networks (Jeon and O'Rourke, 2005). Hence, it is possible using the LADWP hydraulic network model to simulate system response to PGD and TGD effects independently of each other and to combine their effects to determine system serviceability.

The contributions of PGD, TGD, and combined PGD and TGD damage on post-earthquake system performance were evaluated using the actual records of Northridge earthquake damage in the LADWP system as well as simulations of repeat Northridge earthquake scenarios of $M_w6.5$ and $M_w7.0$. The actual earthquake damage

involves a deterministic analysis because the damage is known explicitly, according to type and location. The scenario earthquake damage involves a stochastic analysis wherein trunk line damage is generated through Monte Carlo simulations.

4.3.1 Actual Northridge Earthquake Damage

Figure 4.3 shows the locations of Northridge earthquake trunk line repairs that were explained in Chapter 3, and identifies each location as PGD- or TGD-induced damage. In total, 5 PGD-induced leaks, 2 PGD-induced breaks, 17 TGD-induced leaks, and 4 TGD-damaged tanks were included in the simulation. Figure 4.3 also indicates the 4 zones of PGD where nodal demands are increased, as described in Chapter 3, to account for the likelihood of significant amounts of PGD-induced damage to distribution pipelines in these areas.

Three simulations were performed for the LADWP hydraulic model for a winter demand scenario: PGD only, TGD only and combined PGD and TGD. Because damage to the trunk lines was applied explicitly, an earthquake scenario was only necessary for simulating damage to the distribution system via demand node increases. The PGV data recorded by 164 strong ground motion stations during the 1994 Northridge earthquake were used to estimate PGV values in all parts of the distribution system, and these PGVs were used with the fragility relationships described in Chapter 3 to determine the nodal demand increases for the hydraulic simulation.

Figure 4.4 shows the results for the simulation performed with only the PGD-

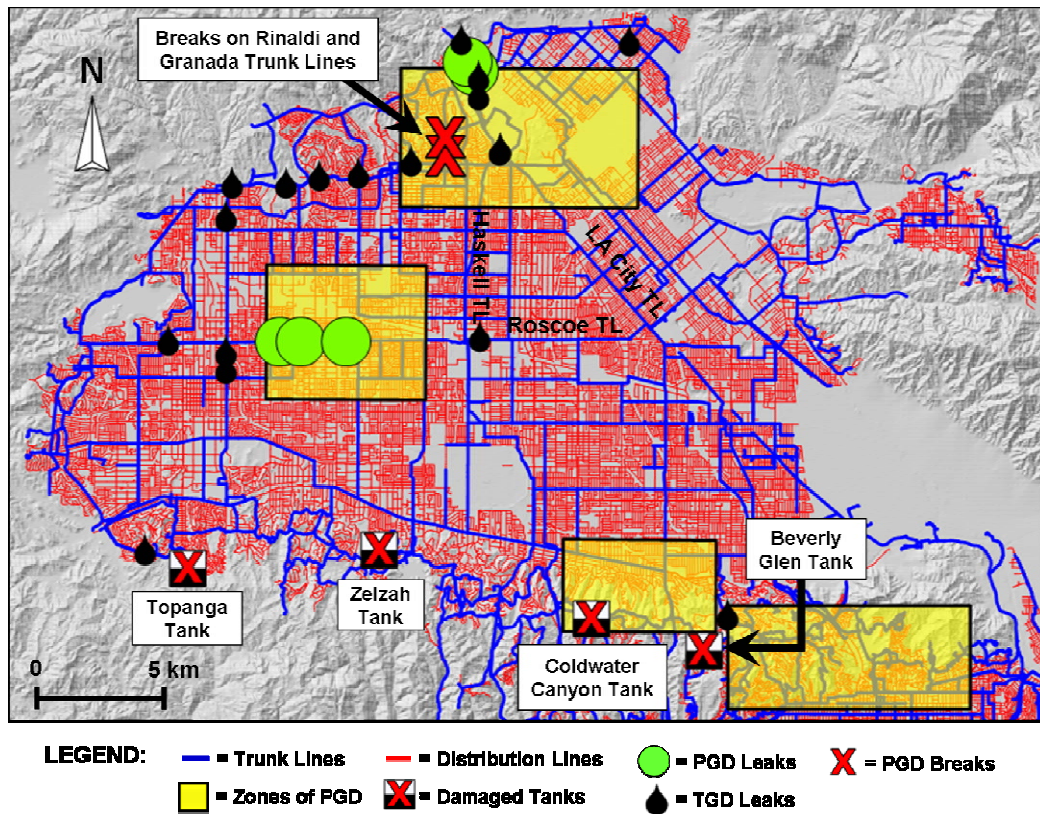


Figure 4.3 Locations of Northridge Earthquake Damage and Zones of PGD

induced damage 24 hours after the repeat Northridge earthquake scenario. The PGD-induced damage locations are shown as purple dots, pipelines with flow are dark blue, pipelines with no flow are turquoise, and pipelines that are not connected with the LADWP system (MWD pipelines or well lines, as explained in the previous chapter) are gray. The SSI immediately after the earthquake was 97.6%, and 89.4% 24 hours after the earthquake. The majority of loss of flow at 24 hours occurs in the western San Fernando Valley, due to pipeline breaks on the Rinaldi and Granada Trunk Lines.

Figure 4.5 shows the results 24 hours after the Northridge earthquake for only the TGD-induced pipeline damage. The TGD-induced damage locations are shown as green dots. The PGV contours created from the data recorded by the 164

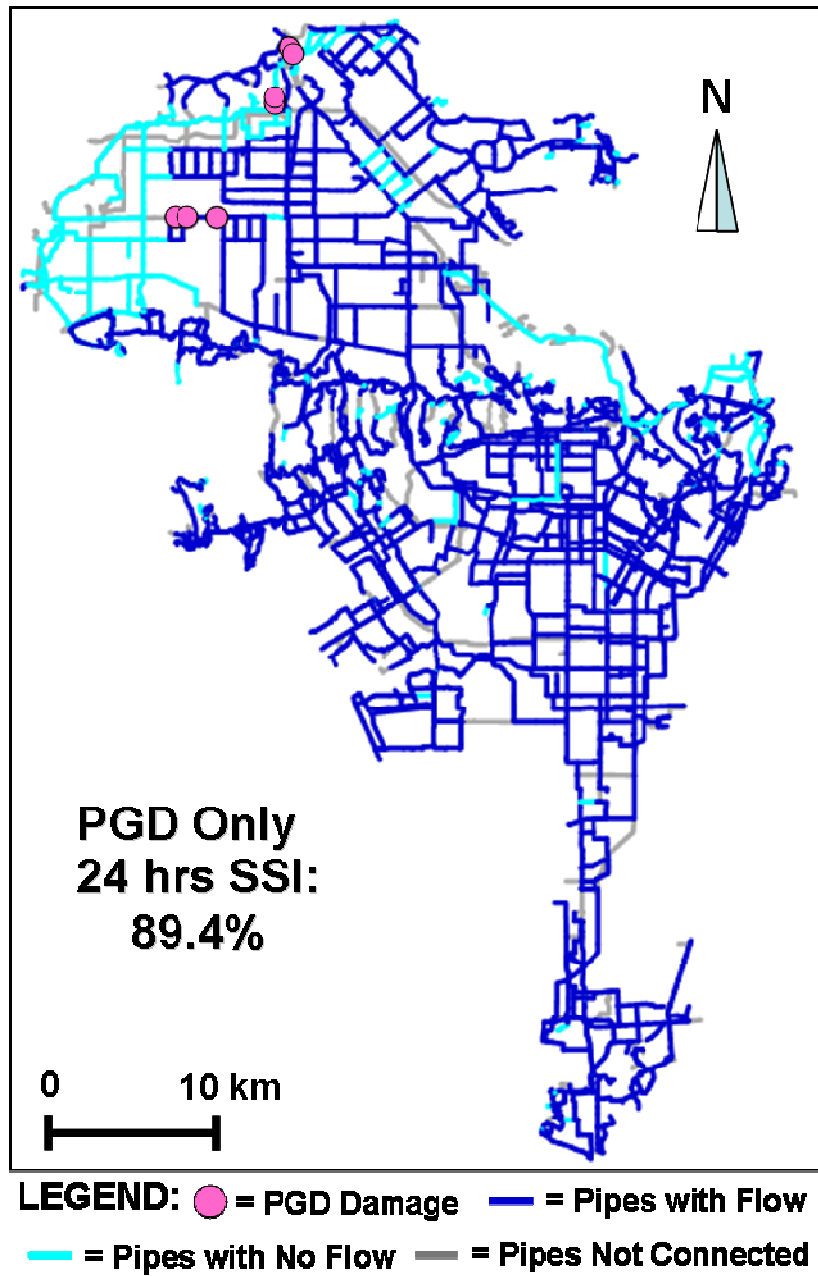


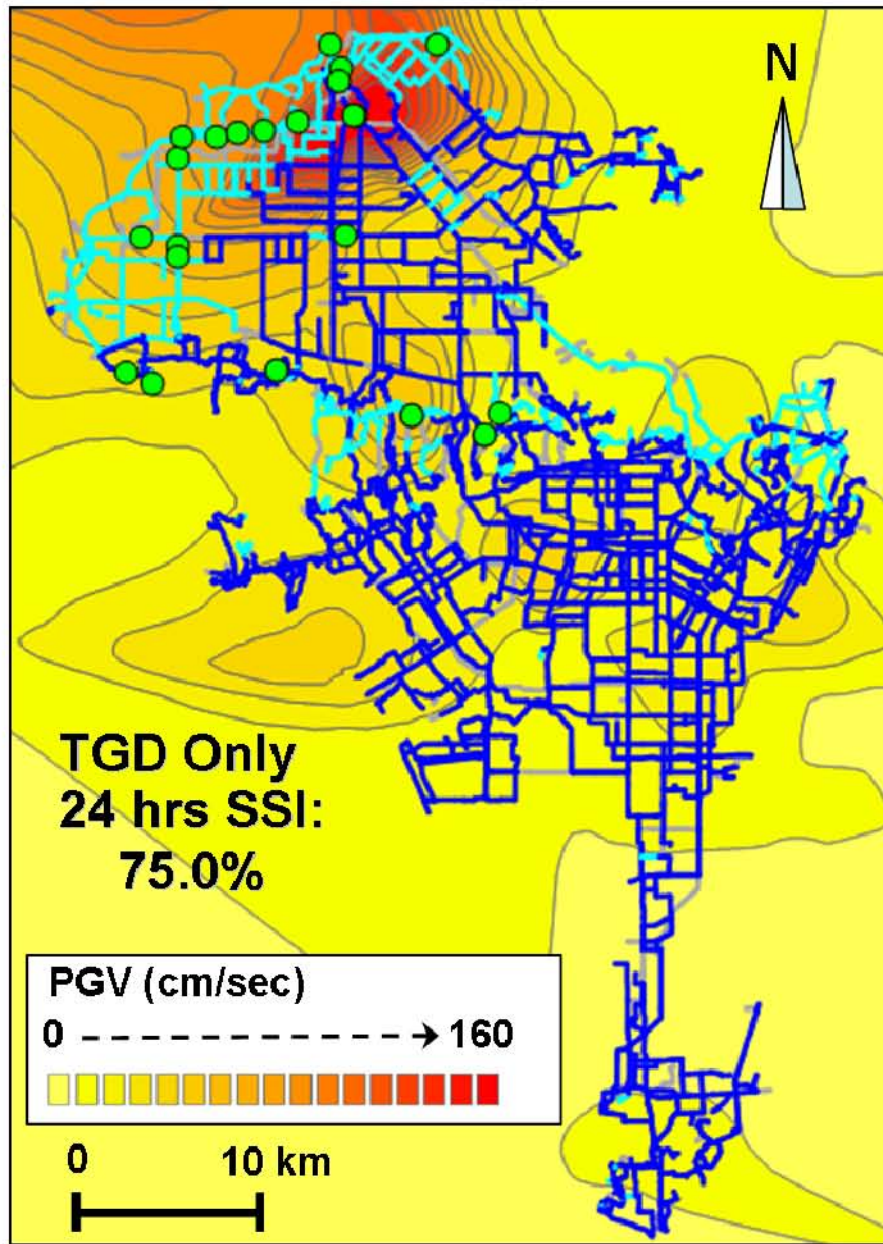
Figure 4.4 PGD Only Simulation Results at 24 Hours for the Actual Northridge Earthquake Damage

strong ground motion stations are also shown in the figure. The SSI immediately after the earthquake was 100%, and 24 hours later the SSI decreased to 75.0%. A similar loss of flow is seen in Figure 4.4 and 4.5, but the TGD-induced damage shows more loss of flow in the northern and southern parts of the San Fernando Valley.

Figure 4.6 shows the system performance 24 hours after the repeat Northridge earthquake simulation for the combined PGD- and TGD-induced pipeline damage. The median SSI immediately after the earthquake was 92.8%, and 24 hours after the earthquake the SSI was 74.6%. Combining the PGD and TGD damage produces a 24 hour SSI that is only 0.4% lower than that of the TGD damage only scenario. In this deterministic scenario, PGD-induced damage does not have as significant of an effect on system performance as damage induced by TGD.

4.3.2 M_w 6.5 Scenario

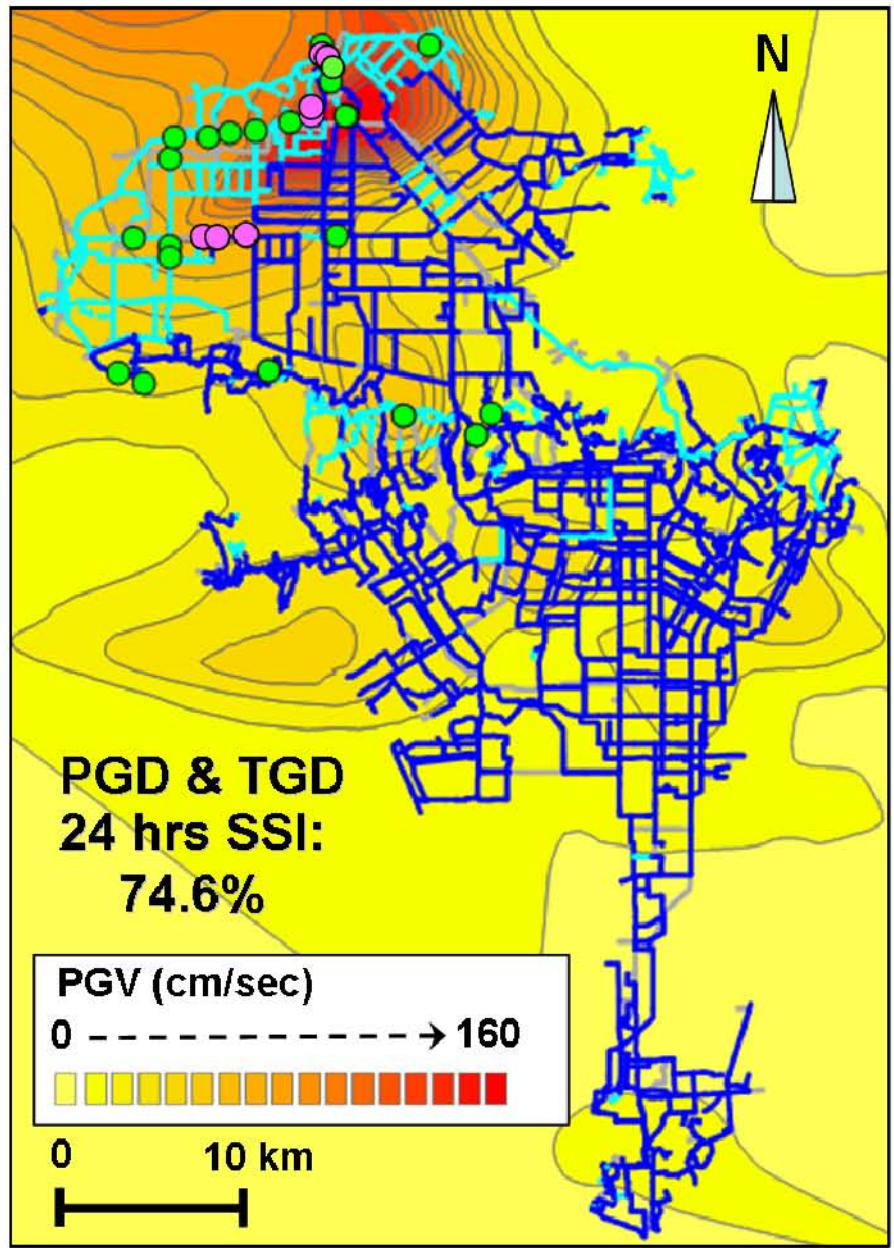
The individual contribution of PGD- and TGD-induced damage to system performance was also explored for the LADWP (2002) hydraulic model as subject to a M_w 6.5 repeat Northridge earthquake scenario. The results for the PGD only simulation are deterministic and the same as presented in Section 4.3.1.



LEGEND:

- = TGD Damage
- = Pipes with No Flow
- = Pipes with Flow
- = Pipes Not Connected

Figure 4.5 TGD Pipeline Damage Locations and Pipeline Flow at 24 Hours for the Actual Northridge Earthquake Damage



LEGEND:

- = Pipes with Flow
- = TGD Damage
- = PGD Damage
- = Pipes with No Flow
- = Pipes not Connected

Figure 4.6 PGD and TGD Pipeline Damage Locations and Pipeline Flow at 24 Hours for the Actual Northridge Earthquake Damage

To simulate a scenario with only TGD-induced damage, a Monte Carlo simulation was performed on the LADWP hydraulic network for winter demand and a $M_w6.5$ repeat Northridge earthquake. In this scenario, the additional nodal demand increases for the 4 zones of PGD are also applied, as discussed in the previous section. GIRAFFE stochastically generates a different pattern of breaks and leaks for each of the 15 simulation runs, and the median case results are presented in Figure 4.7. The TGD damage locations in pipes with diameters greater than 610 mm (24 in.) are shown as green dots. The PGV contours associated with the $M_w6.5$ repeat Northridge earthquake scenario are also shown. The median SSI immediately after the earthquake was 99.2%, and 24 hours later the median SSI was 79.4%. Figure 4.8 shows the median system performance for the combined PGD and TGD Monte Carlo simulation, where the PGD- and TGD-induced damage locations (in pipelines with diameters larger than 610 mm) are indicated. The median SSI immediately after the earthquake is 96.0%, and falls to 78.0% 24 hours later.

Figure 4.9 shows a histogram of the SSIs for the TGD only and for the combined PGD and TGD simulations. The Monte Carlo simulation convergence algorithm (explained in Chapter 3) resulted in 15 simulations for each case. The SI statistics for 24 hours after the earthquake are summarized in this histogram by showing the number of Monte Carlo simulations resulting in a particular SI divided by the total number of simulations to provide an approximate probability index. This histogram of “probability” allows comparison of performance outcomes for the TGD only and the combined PGD and TGD scenarios. Again, there is only a very small difference in system serviceability 24 hours after the earthquake between the TGD only and combined PGD and TGD scenarios, indicating PGD-induced damage does not have as serious an effect on system performance as damage induced by TGD.

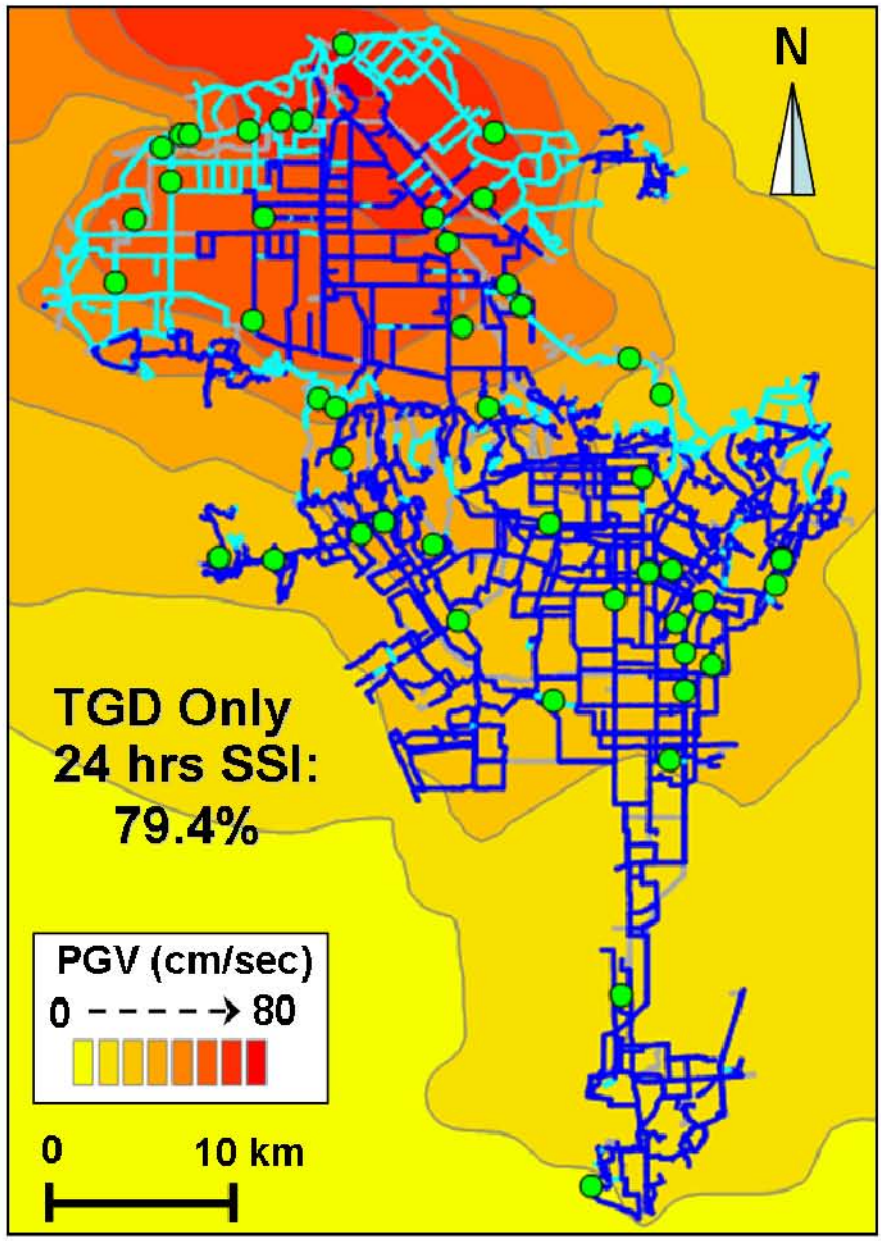


Figure 4.7 TGD Pipeline Damage Locations and Pipeline Flow at 24 Hours for the TGD Only M_w 6.5 Repeat Northridge Earthquake Scenario

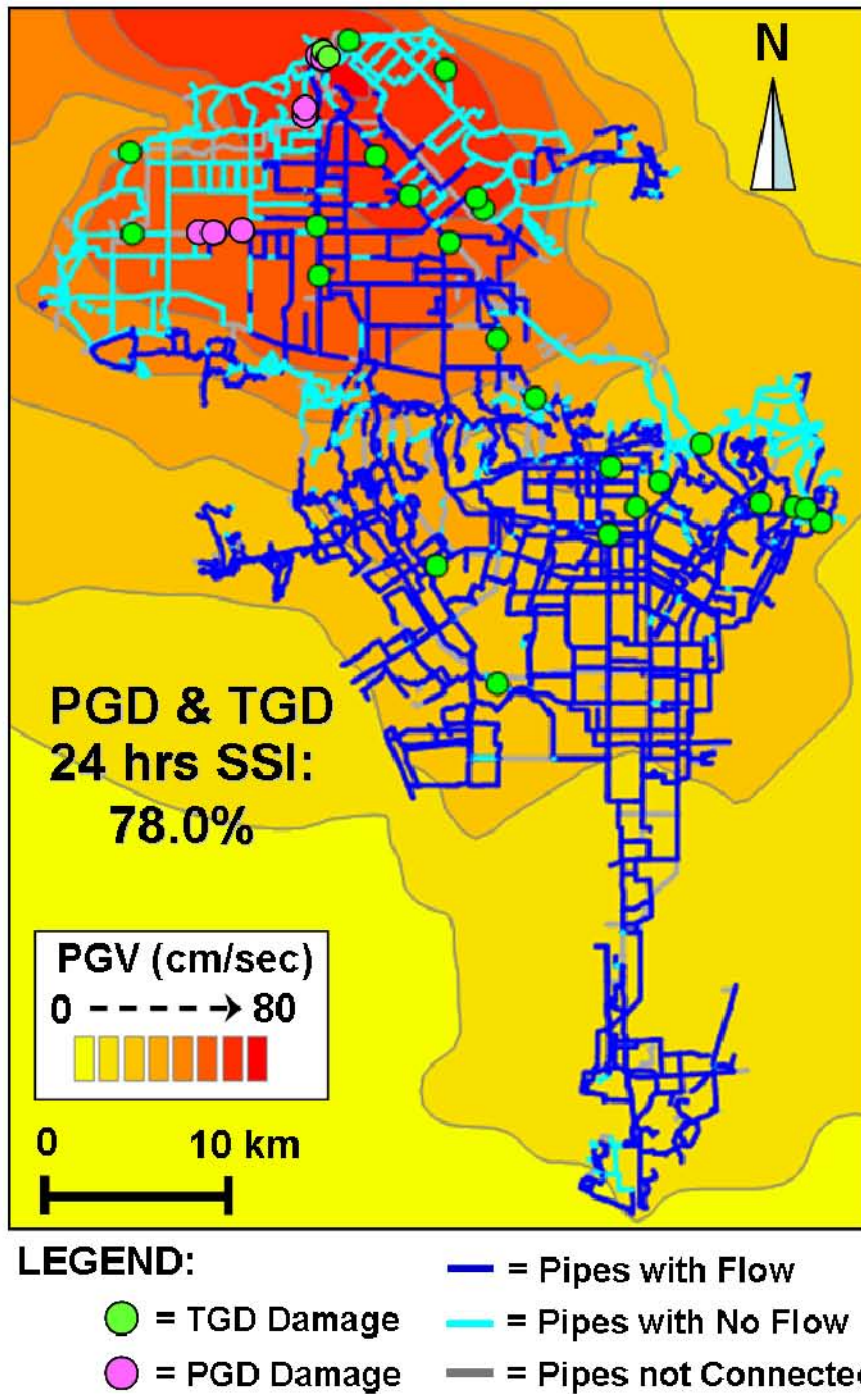


Figure 4.8 PGD and TGD Pipeline Damage Locations and Pipeline Flow at 24 Hours for the Combined PGD & TGD M_w 6.5 Repeat Northridge Earthquake Scenario

M_w6.5 Northridge Repeat Earthquake Scenario Results at 24 Hours

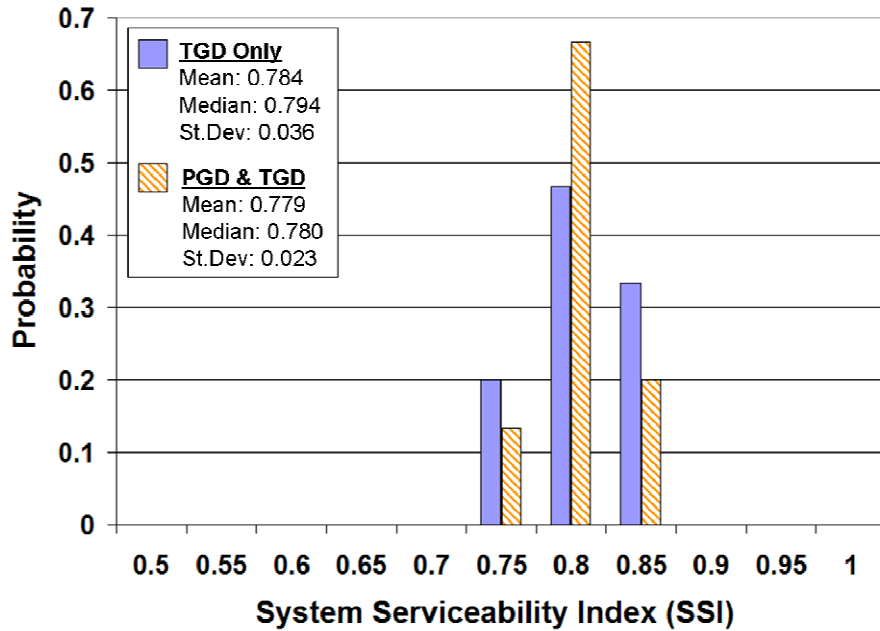


Figure 4.9 Histogram for TGD only and Combined PGD and TGD System Serviceability 24 Hours after a M_w6.5 Repeat Northridge Earthquake Scenario

4.3.3 M_w7.0 Scenario

The individual contribution of PGD- and TGD-induced damage to system performance was also explored for the LADWP hydraulic model when subject to a M_w7.0 repeat Northridge earthquake scenario. As with the M_w6.5 scenario described in the previous section, a winter demand was used in the Monte Carlo simulation. The additional nodal demands were applied in the local distribution networks affected by for the 4 zones of PGD. The results for the PGD only simulation are deterministic and the same as presented in Section 4.3.1.

The median case results 24 hours after the earthquake are presented in Figure 4.10. The TGD damage locations in pipes with diameters greater than 610 mm (24 in.) are shown as green dots. The PGV contours associated with the $M_w7.0$ repeat Northridge earthquake scenario are also shown. The median SSI immediately after the earthquake was 98.4%, and 24 hours later the median SSI was 71.7%. Figure 4.11 shows the median system performance for the combined PGD and TGD Monte Carlo simulation, where the PGD- and TGD-induced damage locations in pipelines with diameters larger than 610 mm (24 in.) are indicated. The median SSI immediately after the earthquake is 95.1%, and falls to 70.5% 24 hours later.

Figure 4.12 shows a histogram of the SSIs for the TGD only and combined PGD and TGD simulations. The Monte Carlo simulation convergence algorithm determined 15 simulations for the TGD only case, and 20 simulations for the combined PGD and TGD scenario. As explained in the previous section, the histogram uses an approximate probability index, normalizing the frequency of simulations for a particular SI with the total number of Monte Carlo simulations for that scenario, allowing comparison of performance outcomes for the TGD only and combined PGD and TGD scenarios. Again, there is only a very small difference in system serviceability 24 hours after the earthquake between the TGD only and combined PGD and TGD scenarios, indicating PGD-induced damage does not have as serious an affect on system performance as damage induced by TGD. Comparing Figures 4.9 and 4.12, the results for the $M_w7.0$ scenarios have a wider spread of SSIs than the $M_w6.5$ scenario results. Both the TGD only and combined PGD and TGD cases for the $M_w6.5$ produce SSIs within a range of 10%, between 75% and 85%. The

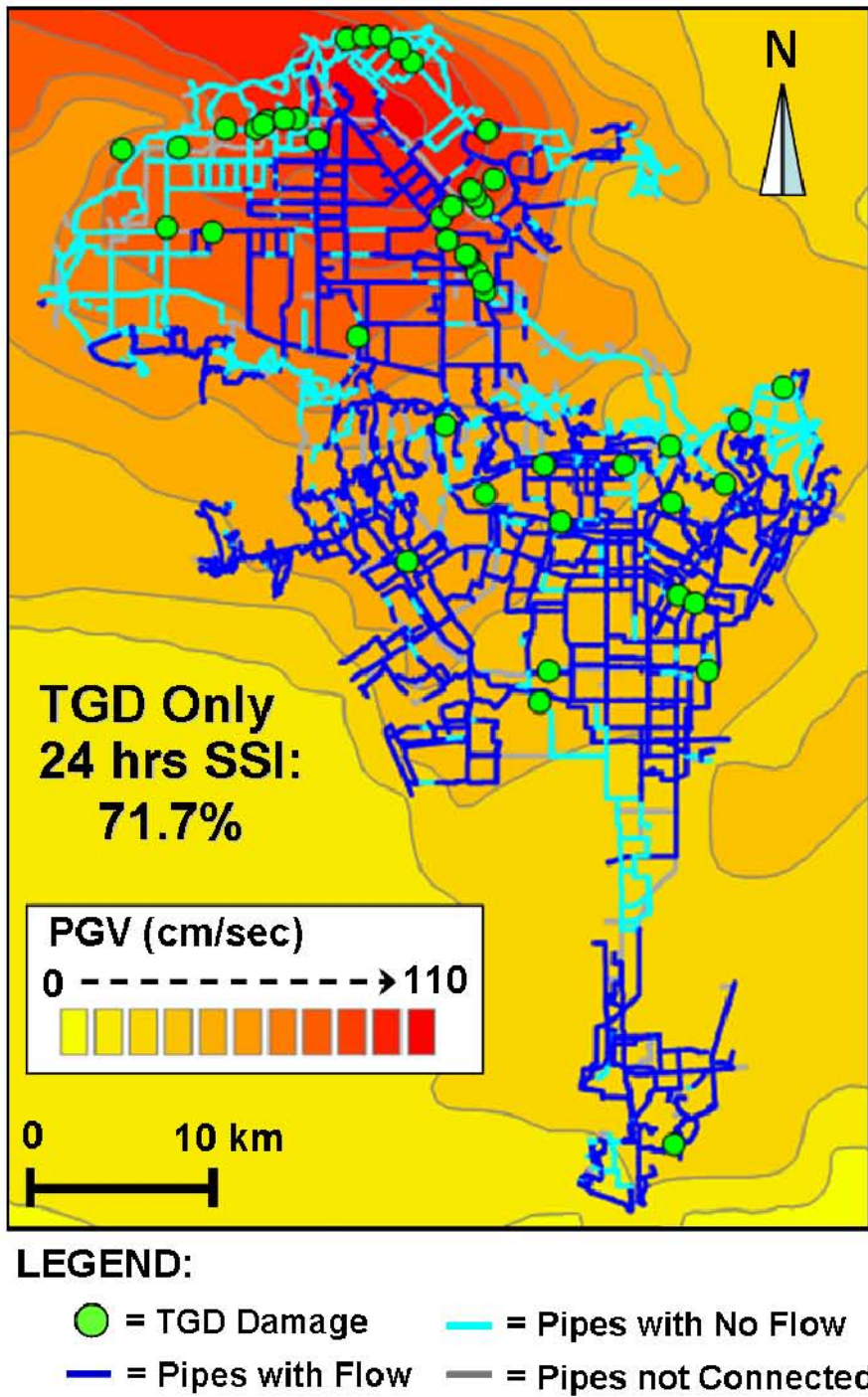
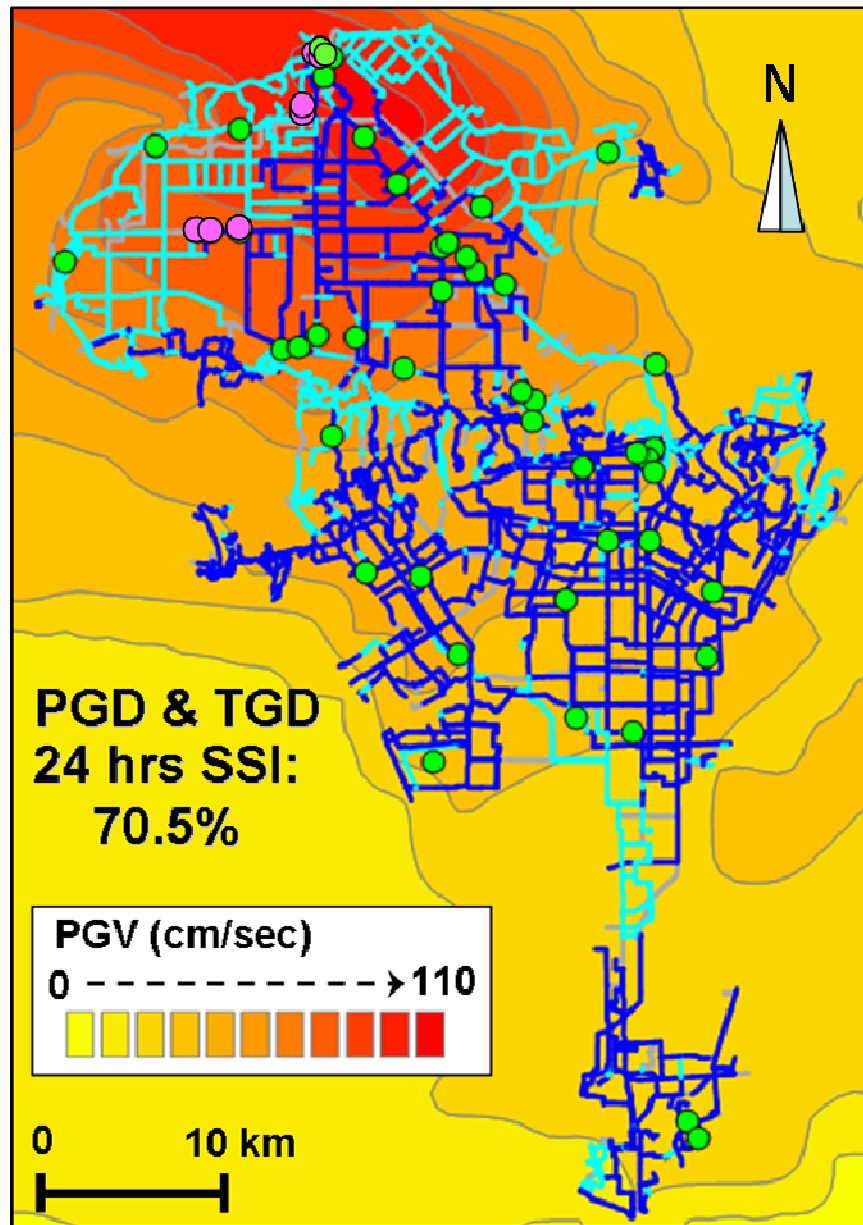


Figure 4.10 TGD Pipeline Damage Locations and Pipeline Flow at 24 Hours for the TGD Only M_w 7.0 Repeat Northridge Earthquake Scenario



LEGEND:

- = Pipes with Flow
- = Pipes with No Flow
- = Pipes not Connected
- = TGD Damage
- = PGD Damage

Figure 4.11 PGD and TGD Pipeline Damage Locations and Pipeline Flow at 24 Hours for the Combined PGD and TGD M_w 7.0 Repeat Northridge Earthquake Scenario

M_w7.0 Northridge Repeat Earthquake Scenario Results at 24 Hours

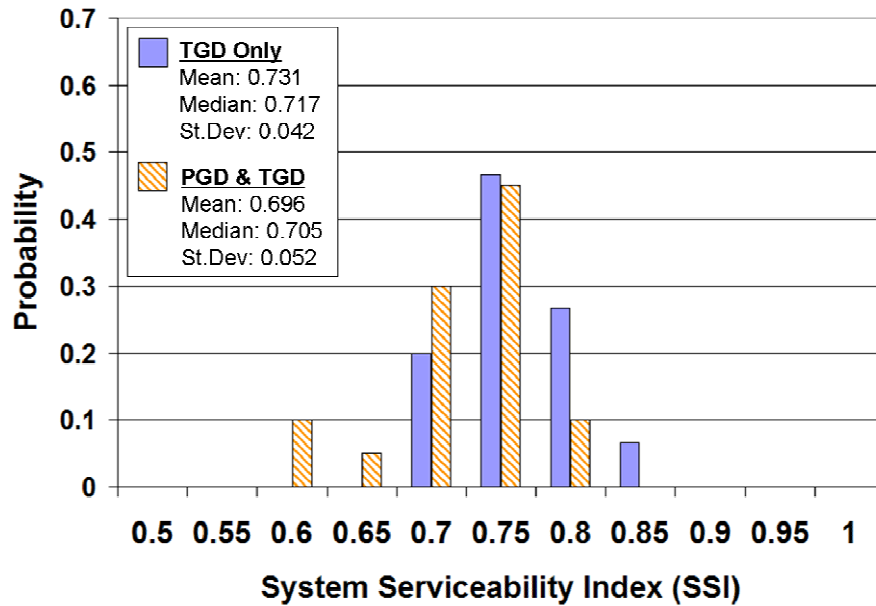


Figure 4.12 Histogram for TGD Only and Combined PGD and TGD System Serviceability 24 Hours after a M_w7.0 Repeat Northridge Earthquake Scenario

TGD only case for the M_w7.0 scenario yields SSIs between 70 and 85%, and the combined PGD and TGD M_w7.0 scenario can produce SSIs as low as 60% up through 80%.

4.4 Parametric Studies

In addition to PGD and TGD effects, there are several other factors that influence system behavior. These factors include: minimum negative pressure tolerance, the percentage of breaks and leaks for the damage generated by GIRAFFE, leakage rates, and leak type probabilities. The results of parametric studies for each are presented below. The simulations leading to these results were conducted using the 2002 LADWP system for winter demand, -0.034 MPa (-5 psi) tolerance, and a

damage partition of 5% breaks and 95% leaks, unless one of these parameters was varied as part of the studies, as described under the subheadings that follow.

4.4.1 Negative Pressure Tolerance

As described in Chapter 3, the hydraulic network model eliminates portions of the pipeline network that can no longer function reliably due to earthquake damage. This process transforms a damage state into an operational state by removing all pipelines that do not satisfy a minimal pressure tolerance. Normally, a water pipeline system can sustain some amount of vacuum or negative pressure. The amount of sustainable negative pressure is relatively low and determined by vacuum release valves and locations in the system where there is atmospheric leakage. When using GIRAFFE, one can specify a default pressure that determines the minimum sustainable pressure in the system. Because there is uncertainty regarding the appropriate level of minimum pressure, a sensitivity analysis was performed to evaluate system serviceability under different minimum pressure settings for damage caused by the Northridge earthquake.

Simulations were performed for minimum pressures of 0 MPa, -0.034 MPa (-5 psi), and -0.069 MPa (-10 psi) and the results are shown in Figure 4.13. At 24 hours after the earthquake, the median SSI for the 0 MPa, -0.034 MPa (-5 psi), and -0.069 MPa (-10 psi) simulations were 78.4%, 79.6% and 78.9%, respectively. The results are very similar, indicating that the selection of the minimum negative pressure tolerance for values between 0 and -0.069 MPa (-10 psi) does not have a large impact on system serviceability results (as long as the tolerance selected is within a realistic range).

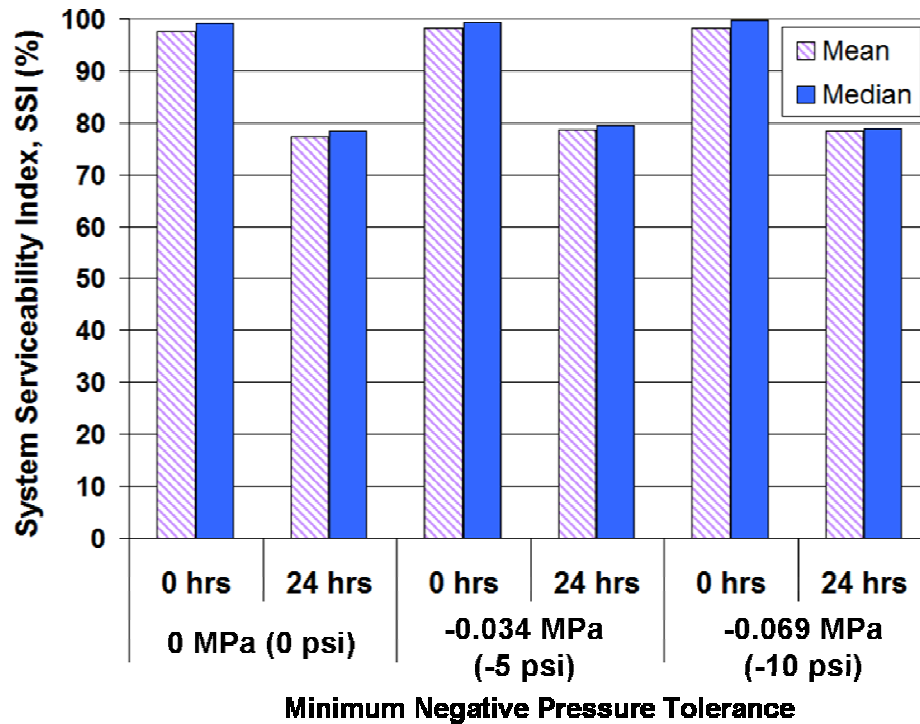


Figure 4.13 Mean and Median SSI values at 0 and 24 Hours for 0 MPa, -0.034 MPa (-5 psi), and -0.069 (-10 psi) Minimum Negative Pressure Tolerance

4.4.2 Percentage of Breaks vs. Leaks

Each earthquake damage location is classified as either a break or a leak, according to pipe damage probabilities set by the user. The GIRAFFE default probabilities are 5% for breaks and 95% for leaks, which is based on repair data from the 1994 Northridge earthquake. Simulations were also performed for the case of 20% breaks and 80% leaks which is consistent with HAZUS (NIBS, 1997) recommendations, and for 0% breaks and 100% leaks, which represents an upper bound condition for leakage.

The mean and median results for 0 and 24 hours following the earthquake are

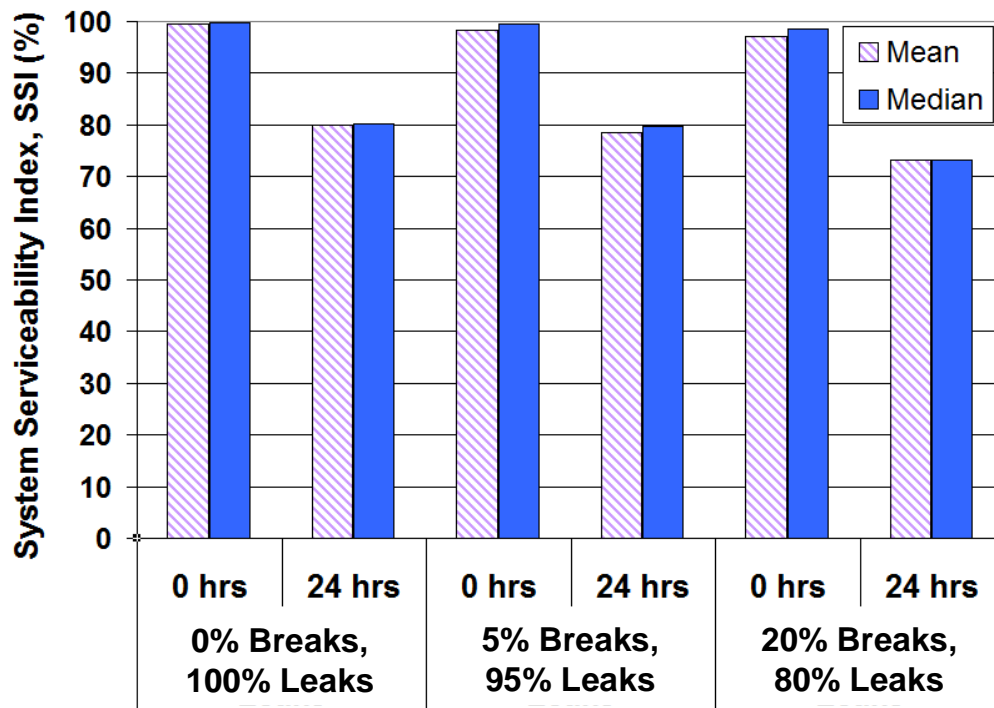


Figure 4.14 Mean and Median SSI values at 0 and 24 Hours after the Earthquake for Various Breaks/Leaks Scenarios

shown in Figure 4.14. The default case of 5% breaks and 95% leaks produces a median 24 hours SSI of 79.6%. The simulation with 20% breaks and 80% leaks yields a median 24 hours SSI of 73.2%. The 100% leaks simulation yields a median 24 hour SSI of 80.1%. A 15% increase in the proportion of breaks from 5 to 20% reduces system serviceability by about 6%.

4.4.3 Leakage Rate

The GIRAFFE program uses pipeline leakage rates based on curves developed by Shi (2006), shown in Figure 4.15, that relate leakage rate to pipe diameter for the types of leak associated with joint pullout, round crack, longitudinal crack, local loss

of pipe wall, and local tear of pipe wall. Figure 4.15 also indicates the pipe materials associated with each type of leak: cast iron (CI), ductile iron (DI), riveted steel (RS), welded steel (WS), and jointed concrete cylinder pipe (JCCP). These curves for leakage rates as a function of pipeline diameter were developed from well-known theoretical formulations for hydraulic head loss associated with leakage from an opening in the pipe wall (e.g., Jeppson, 1976) and validated with respect to flow measurements for orifice openings obtained from full-scale tests of sprinkler systems (Shi, 2006).

Although the leakage rate formulations were verified relative to actual test measurements and applied systematically to various leak scenarios for different types of pipeline, the leakage rate curves proposed by Shi (2006) are nevertheless based on limited test data and observed leakage conditions in the field. It is therefore desirable to evaluate the sensitivity of hydraulic network response to variations in the leakage rate curves to estimate how changes in flow rates related to uncertainty may affect system performance.

Simulations were performed in which flow rates associated with all types of leaks in Figure 4.15 were simultaneously increased and decreased by 50%. The baseline case using default leakage rates in Figure 4.15 results in a median SSI of 79.6% 24 hours after the earthquake. A 50% increase in leakage rates yields a 24 hours median SSI of 76.6%, and a 50% decrease in leakage rates produces a median SSI of 81.5%. The results shown in Figure 4.16 indicate that system performance is not significantly affected by a 50% fluctuation in leakage rates. The 50% fluctuations produce a change in SSI of 2-3% for the Northridge earthquake damage conditions.

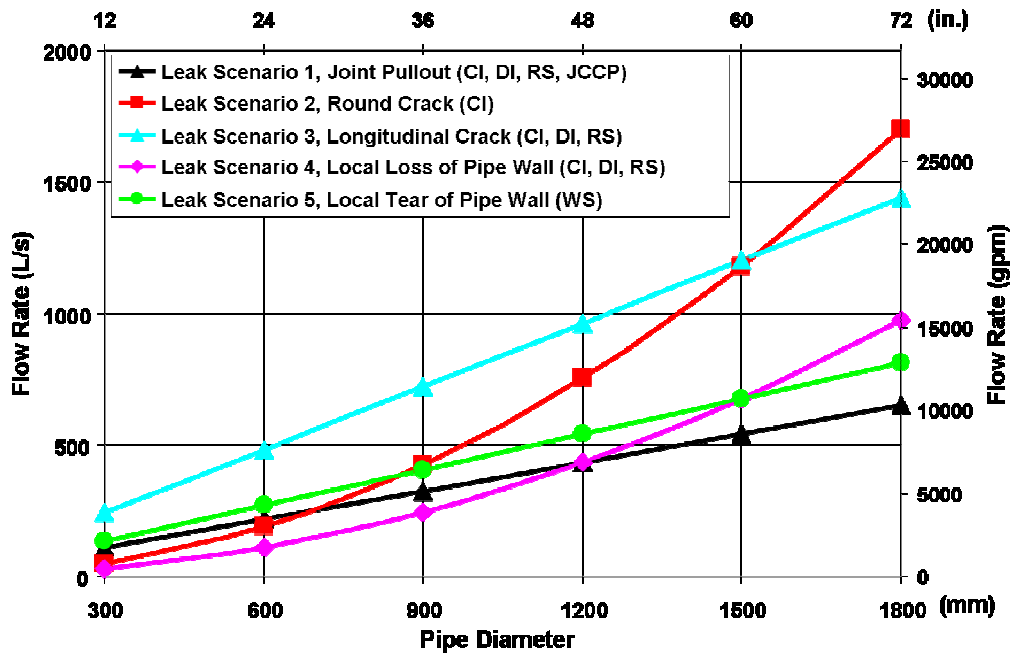


Figure 4.15 Leakage Rate Curves for the 5 Leak Types (Shi, 2006)

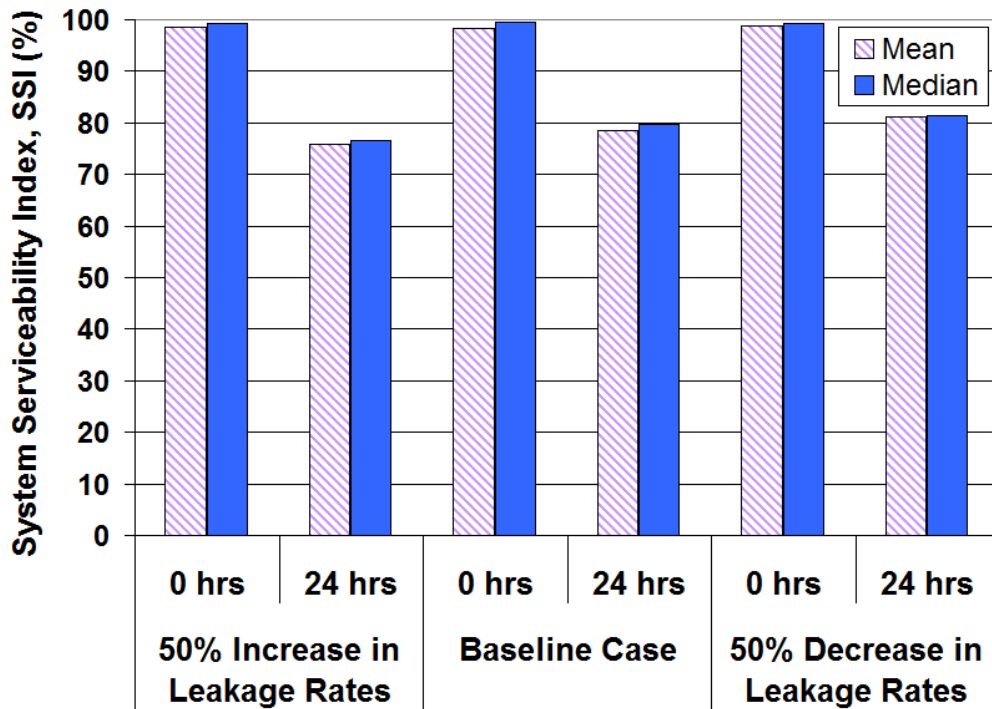


Figure 4.16 Mean and Median SSI values at 0 and 24 Hours after the Earthquake for 50% Increase and Decrease in Leakage Rate

4.4.4 Leak Type Probability

As explained in Chapter 3, weighted probabilities are assigned to the different types of leakage that may occur for a given type of pipe. For example, cast iron pipelines are assigned probabilities of 0.3, 0.5, 0.1, and 0.1 related to joint pullout, round crack, longitudinal crack, and local loss of pipe wall, respectively (see Table 3.1). The weighted probabilities were assigned on the basis of field observations and the expert opinion of engineering staff familiar with pipeline field repairs. It is desirable, therefore, to evaluate the sensitivity of hydraulic network simulation results to variation in the weighted probabilities to understand how uncertainties associated with this part of the leakage characterization can affect analytical outcomes.

To explore the sensitivity of system performance to leak type probabilities, two simulations were performed where “worst-case” leaks were given 100% probability of occurrence. The first simulation assumed a 100% probability for joint pullout and 0% probability for all other types of leaks for cast iron, ductile iron, riveted steel and jointed concrete pipes. The second simulation assumed a 100% probability for longitudinal cracks and 0% probability for all other types of leaks for cast iron, ductile iron, riveted steel and jointed concrete pipes. The default values for the welded steel pipes were not changed in either simulation, as local tear of pipe wall is the only crack likely to occur in these types of pipelines.

Figure 4.17 shows the results from the simulations as compared to a baseline simulation performed using the default probabilities. The median SSI 24 hours following the earthquake for 100% probability of joint pullout is 77.9%. For the case of 100% probability of longitudinal crack the median 24 hours SSI is 76.1%. The

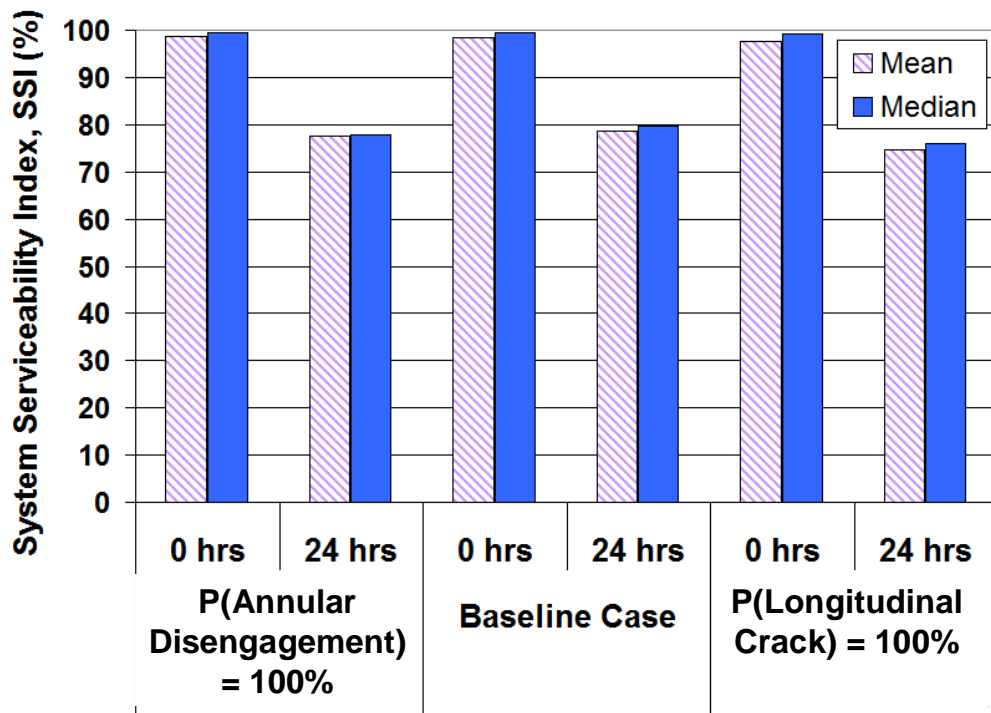


Figure 4.17 Mean and Median SSI values at 0 and 24 Hours after the Earthquake for Various Leak Type Probabilities

baseline case using the default leak probabilities yields a 24 hours SSI of 79.6%. These results indicate that system performance is not highly sensitive to a change in leak type probabilities.

4.5 Conclusions

Post-earthquake water supply performance is time-dependent because losses through leaking pipelines reduce tank and reservoir levels, thereby diminishing and in many instances cutting off pressure and flow in portions of the system. It is important therefore to account for time-dependent performance by modeling post-earthquake response incrementally according to time intervals. The minimum time step required

for modeling should be less than or equal to the smallest operational time increment needed for an accurate representation of system functionality, which will generally depend on the capacity of key storage facilities. For the LADWP system, a minimum time increment of 1 hour was needed for reliable time-dependent simulations. This interval is related to storage capacities of the Clearwell and several other tanks that have capacities that will run dry in less than 2 hours.

The most important factor affecting post-earthquake system performance is nodal demand. Water supply simulations based on the 1994 Northridge earthquake effects show a nonlinear decrease in system serviceability as the demand from the distribution system increases. The system serviceability 24 hours after the earthquake decreases from 71% for winter demand to 52% for summer demand, which is approximately 2.3 times higher than the winter demand. The simulation results show a 38% decrease in system serviceability after 24 hours for a fourfold increase in demand from winter demand conditions. The significant sensitivity of system performance to demand from the distribution system indicates that accounting for earthquake damage to distribution pipelines is important, especially when earthquake performance under elevated summer levels of demand is being evaluated.

Simulations were performed of post-earthquake water supply response after 24 hours for the actual damage associated with the 1994 Northridge earthquake and damage simulated for a M_w 6.5 and M_w 7.0 Northridge repeat earthquake scenarios. They show that TGD effects had the most important effects on water supply performance, with a substantially greater impact than PGD effects. TGD for the Northridge earthquake simulations was more pervasive than PGD damage, and affected major trunk lines important for substantial flows in the system.

The parametric study shows that system serviceability was not significantly influenced by moderate changes in negative pressure tolerance. Large changes in leakage rates, on the order of 100%, produced relatively small changes of 5% in system serviceability, whereas extreme changes in the weighted probabilities of leakage produced system serviceability changes of 3%. Changes in the percentages of breaks and leaks resulted in some of the largest changes in system serviceability, but even here the drop in serviceability going from 0% to 20% trunk line breaks was only 7%.

CHAPTER 5

DE-AGGREGATION OF EARTHQUAKE EFFECTS ON WATER SUPPLY PERFORMANCE

5.1 Introduction

As explained in previous chapters, the hydraulic network model embodied in the DSS for the LADWP water supply accounts comprehensively for various sources of earthquake damage and disruption. These sources include loss of the LAAs, damage to trunk and distribution pipelines from both PGD and TGD, loss of electric power affecting pump stations, and damage to facilities, such as tanks and reservoirs. Simulation of water supply response to the 1994 Northridge and Northridge repeat scenario earthquakes described in previous chapters account for the aggregate effects of all sources of seismic disruption.

Earthquake effects can also be de-aggregated, i.e. the water supply response can be simulated for one source of disruption at a time, or for any combination of sources. By de-aggregating the damage, the most important sources of disruption with respect to lost system service can be determined, thereby identifying system vulnerabilities and providing a rational basis for system improvements. De-aggregating the effects of different sources of earthquake damage also allows for the selective aggregation of damage effects so that the nonlinear characteristics of system performance can be quantified as the damage sources are re-combined.

Because the DSS is fully integrated with an advanced GIS, the damage in any part of the system can be evaluated, and the response of any part of the system to de-aggregated sources of damage can be determined. In this way, the geographical distribution of damage to multiple single or aggregated sources of damage can be assessed and visualized.

This chapter provides a description of the LADWP system model updated for 2007 conditions. The 15 different water service areas in the LADWP system are described, and used to show the geographic distribution of the water supply network behavior. Hydraulic network simulations were performed for the actual sources of earthquake damage, and disruption during the 1994 Northridge earthquake. The simulation results are summarized and discussed for de-aggregated source of damage associated with the loss of the LAAs, electric power outage, Northridge earthquake trunk line damage, and Northridge earthquake tank damage. Simulation results for the combined effects of these damage parameters are also presented, as well as simulation results including all sources of Northridge earthquake damage.

5.2 System Modeling

The hydraulic network simulations were performed for the actual 1994 Northridge earthquake damage and disruption of the water supply as described in Chapter 3 and Appendix B. The Northridge earthquake damage was characterized from a systematic assessment of pipeline repairs, fragility performance, and post-earthquake observations of system operability by Cornell researchers working in collaboration with LADWP personnel. The sources of system damage include the loss of the LAAs, electric power outage, trunk and distribution pipeline damage due to

PGD and TGD, and tank damage, from which individual sources of damage and select combinations of sources were used in the simulations as described in Section 5.3.

The 2002 LADWP hydraulic network model was updated to represent the configuration of the 2007 water system. Figure 5.1 highlights the major changes made to the model. Three major trunk lines were added: the Granada Trunk Line Relocation No. 2, the Sepulveda Feeder and the Magnolia-Burbank Trunk Line Extension. Since the Northridge earthquake, restrictions on open water reservoirs caused 4 major reservoirs to be removed from service: Encino Reservoir, Upper and Lower Hollywood Reservoir, and Lower Stone Canyon. This represents a loss of $3 \times 10^6 \text{ m}^3$ water storage capacity. The $37,850 \text{ m}^3$ (38×10^6 liter, 10 million gallon) Rowena Tank, at the base of the River Supply Conduit, has since been put in service. Working closely with LADWP engineers, some valve settings and pipe flow configurations were updated to represent current flow patterns.

The system response was evaluated for 15 water service areas, shown in Figure 5.2. Water service areas are geographic groupings of pipelines, pumps, valves, tanks, reservoirs, and demands that can be analyzed individually. From north to south the water service areas are: Granada Hills (GH), Foothills (FH), Sunland-Tujunga (ST), Valley Floor A, B and C (VF A, VF B, VF C), Encino Hills (EH), Santa Monica (SM), Hollywood Hills (HH), Mount Washington (MW), Highland Park (HP), Santa Ynez (SY), Westside (WS), Central City (CC), and Harbor (H). The Valley Floor, Central City, and Westside water service areas serve the highest demands in the system, delivering water to the most densely populated San Fernando Valley, downtown Los Angeles, and western Los Angeles communities. The remaining water

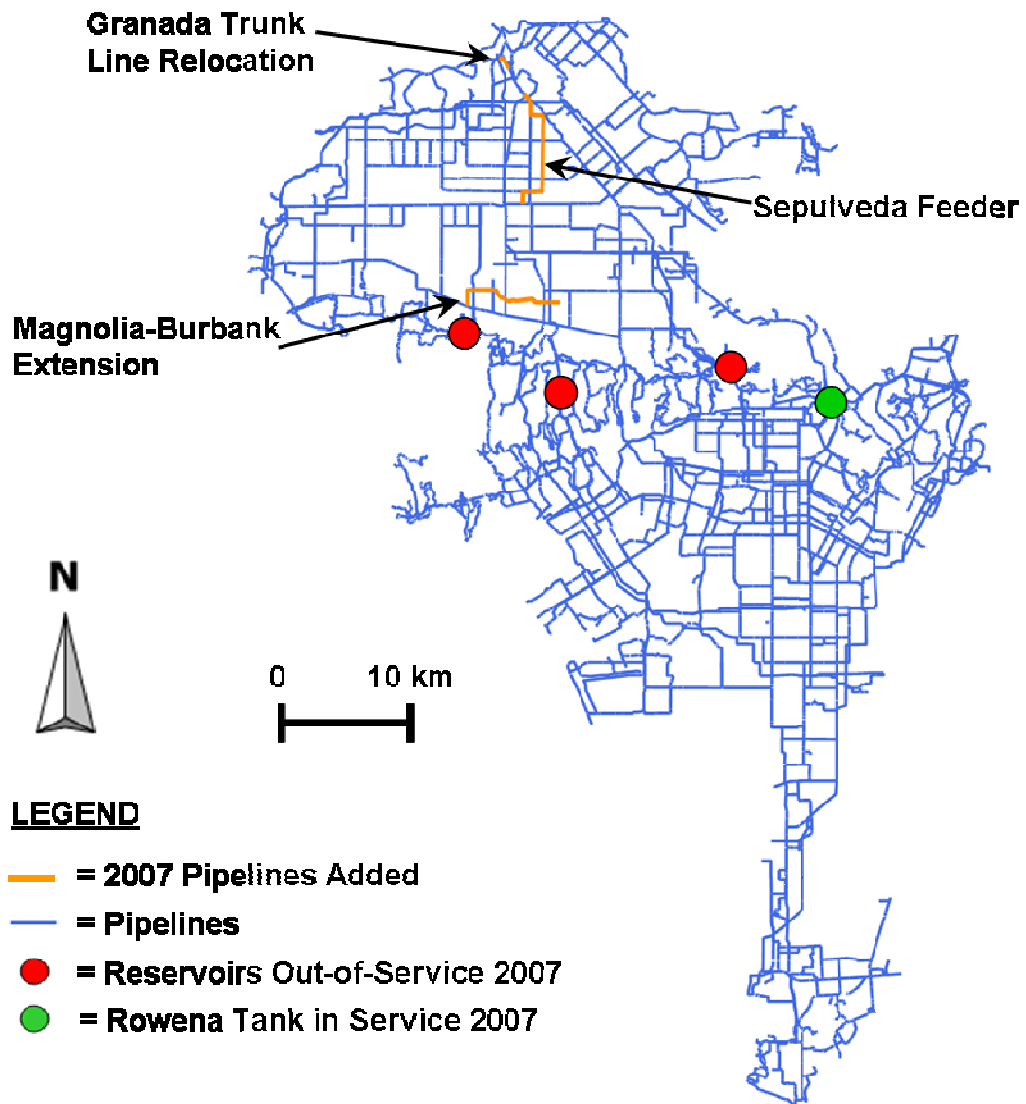


Figure 5.1 Modifications to 2002 LADWP Hydraulic Network to Produce 2007 Hydraulic Network

service areas are situated at higher elevations in the mountains surrounding Los Angeles, except for the lower elevation Harbor water service area. By showing the results for the 15 water service areas, one is able to understand the spatial variability of the system performance as expressed in terms of serviceability index (SI), which is the percentage of post-earthquake flows relative to pre-earthquake flows at all demand nodes within a water service area.

5.3 De-Aggregation of Earthquake Effects

In the following subsections, the de-aggregated water system performance effects are explored for three individual parameters: the loss of the LAAs, electric power outage, and Northridge earthquake trunk line damage. Simulation results for the combined effects of these parameters and distribution system damage are also presented.

5.3.1 System Performance Due to Los Angeles Aqueduct Outage

Nearly 50% of the LADWP water supply is provided by the First and Second Los Angeles Aqueducts (LAA1 and LAA2), which transport water from the Sierra Nevada Mountains in northern California to the City of Los Angeles (Wang, 2006). As a result of the Northridge earthquake, LAA1 was damaged but able to operate at very low flow for approximately 1 week after the earthquake to allow for repairs to be made to LAA2. Once repairs were made to LAA2, it was put back in service while LAA1 was repaired (Lund and Cooper, 1995). In addition, seismic damage in the Metropolitan Water District (MWD) Foothill Feeder curtailed the availability of water from that agency. Repairs made to LAA1 and LAA2 following Northridge were not

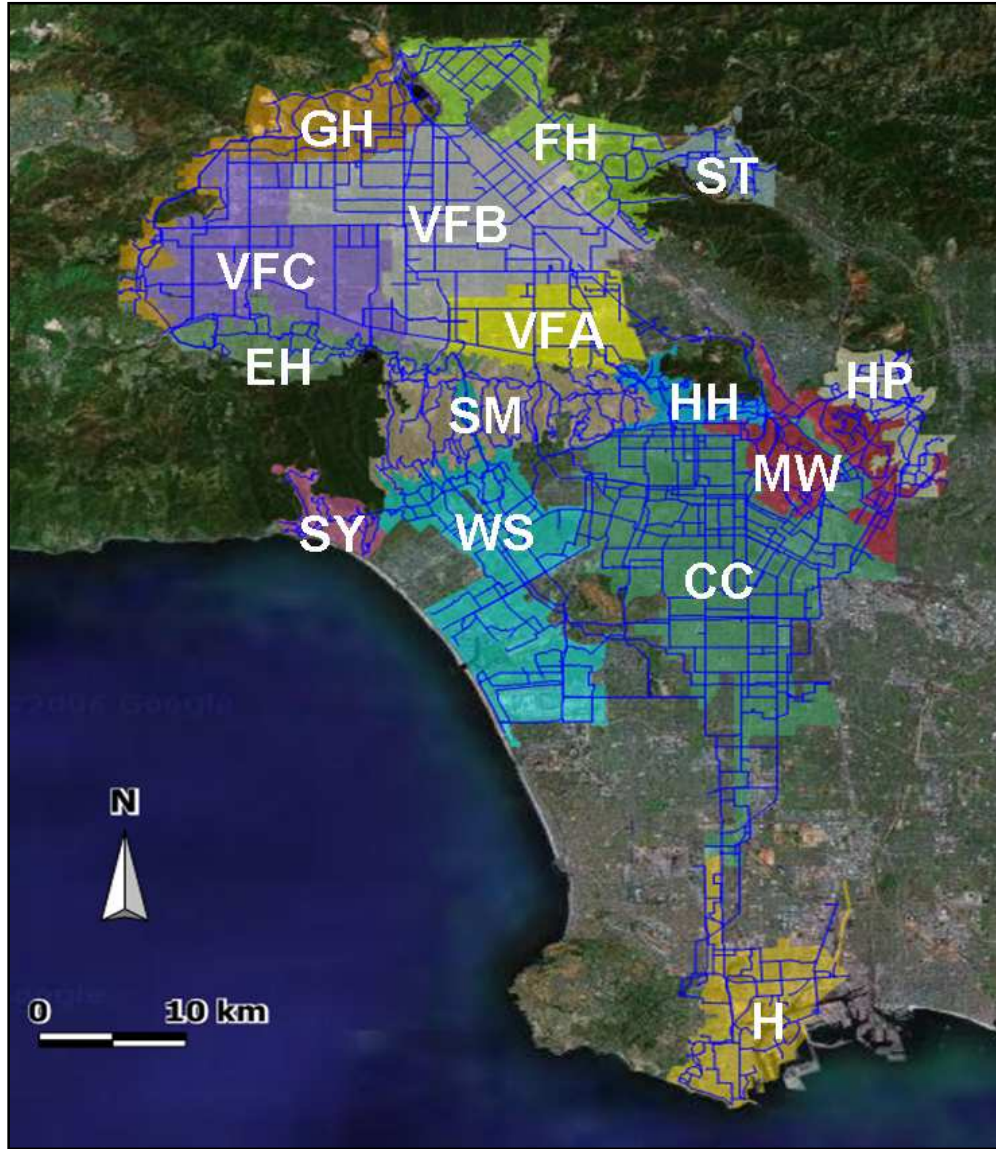


Figure 5.2 Water Service Areas in the LADWP System

sufficient to assure they would not be damaged in the event of a similar earthquake. Thus, in planning for a Northridge scenario earthquake, it is appropriate to assume disruption in LAA1 and LAA2 without inter-tie backup from MWD.

Figure 5.3 presents the SIs for the 15 water service areas after 24 hours with the LAAs not contributing to the LADWP water supply. The system SI after a 24 hour simulation with the aqueducts closed is 83%. Comparatively, an analysis performed with the LAAs open produces a 24 hour system SI of 100% for all water service areas. As shown in Figure 5.3, the water service areas most affected by the loss of the LAAs are the GH, FH and VF C areas in the upper San Fernando Valley. FH and VF C have SIs of 15% and 41%, respectively, while GH suffers a substantial decrease in SI to only 2%.

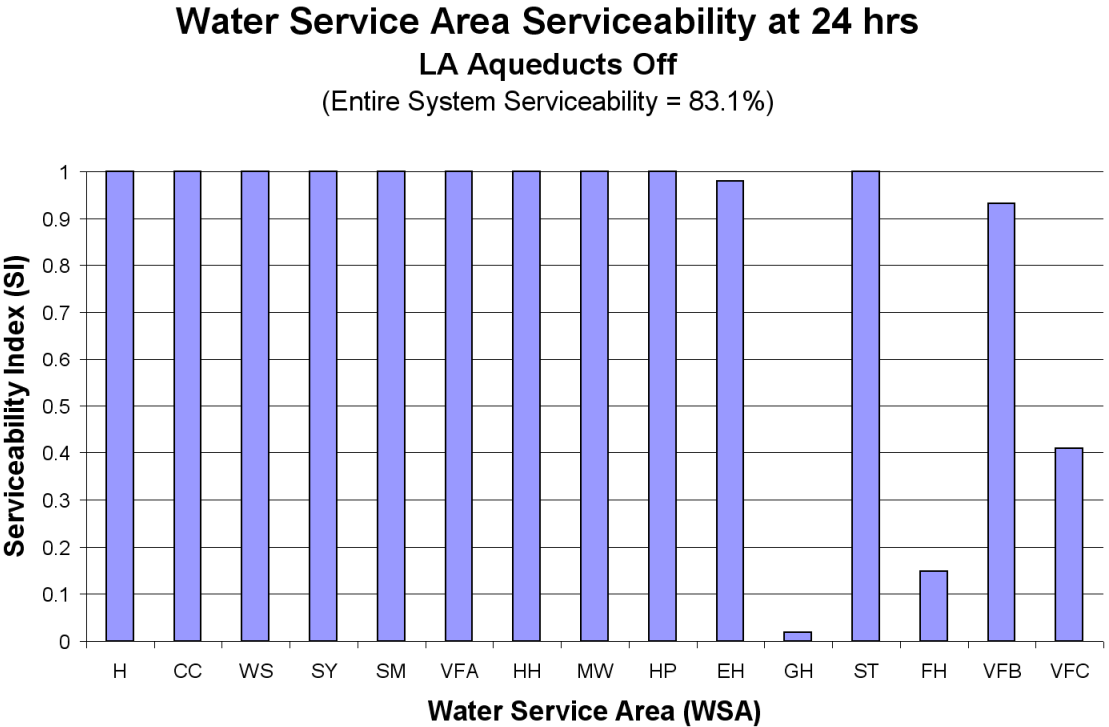


Figure 5.3 Serviceability Index after 24 Hours for 15 Water Service Areas with Loss of Los Angeles Aqueducts and No Other Damage

5.3.2 System Performance Due to Electric Power Outage

Figure 5.4 shows the de-aggregated results for the loss of electric power, which mainly affects the operation of pump stations. In the event of power loss, pump stations with secondary sources of power or back up generators will continue to operate with a modified number of pumps. Electric power outage data from the actual 1994 Northridge earthquake were used to simulate the configuration of pumps for various time increments following the earthquake event. It was found that using the configuration of pumps operating 2 hours following the earthquake for the entire 24 hour simulation produced nearly identical results (differed by less than 1%) to an analysis where power was incrementally restored to pump stations at 2, 6, 12, 18 and 24 hours. Thus, the 2 hour configuration of operational pumps was used as an equivalent power state for the 24 hour simulation. As shown in Figure 4, the system SI at 24 hours is nearly 93%. The GH, ST and FH water service areas have the lowest SIs of 51%, 54% and 54%, respectively.

The GH and FH water service areas are compromised in both this case and the parameter study with loss of the LAAs. In the electric power outage case, the Van Norman Pump Station 2 loses power and does not have a back-up power source. Although water is available, this station is not functioning and cannot pump water to the upper San Fernando Valley, and other pump station losses in ST affect serviceability in that region. When LAA1 and LAA2 are disrupted, water flow is curtailed to the upper San Fernando Valley. This lack of water primarily affects the GH and FH water service areas which are also largely affected in the electric power outage scenario where water is available, but the means to distribute it is compromised.

Water Service Area Serviceability at 24 hrs
LA Aqueducts On, Electric Power Loss
 (Entire System Serviceability = 92.7%)

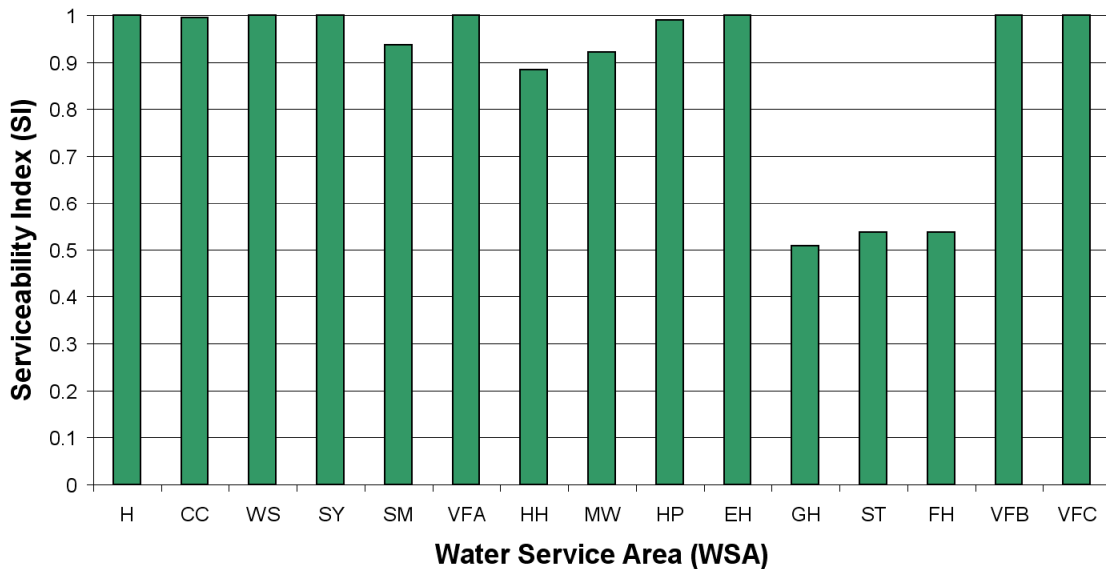


Figure 5.4 Serviceability Index after 24 Hours for 15 Water Service Areas with Electric Power Loss and No Other Damage

5.3.3 System Performance with Northridge Earthquake Trunk Line Damage

Working closely with LADWP engineers and their records from the Northridge earthquake, a database of 82 trunk line damage locations was compiled. Of the 82 locations, 68 were within the LADWP hydraulic network model and were explicitly applied to the system. Leaks that occurred in close proximity on the same trunk line were often modeled as one leak with an appropriately increased leak area. Leaks that occurred down stream of a break and thus had no effect on the system were not modeled. This reduced the number of damage locations to 27, as shown in Figure 5.5. Brown, et al. (1995) reported severe damage to 5 tanks in the LADWP system, 4

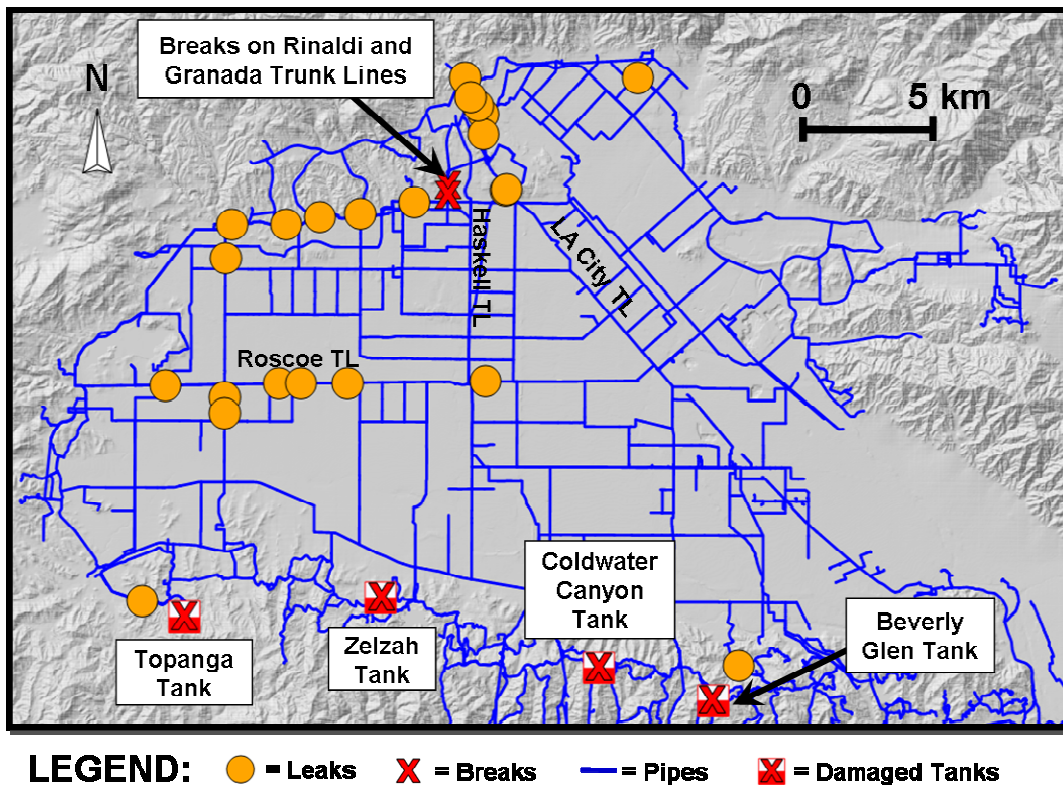


Figure 5.5 Northridge Trunk Line Damage

of which exist in the 2007 hydraulic model. This damage was included by disconnecting the inlet and outlet lines for the tanks.

Figure 5.6 represents the 24 hour de-aggregated results for Northridge earthquake trunk line damage. The water service areas most affected are GH, FH and VFC with SIs of 29%, 72% and 41%, respectively. Breaks in the Granada and Rinaldi Trunk Lines greatly reduced flow to the GH and VFC water service areas. Major leaks along the Roscoe Trunk Line further reduced serviceability in VFC. Leaks in the Van Norman Complex area and Van Norman Pump Station discharge line restricted flow to FH and GH.

The system performance for loss of the LAAs in Figure 5.3 shows similar loss of serviceability in the GH and VFC water service areas. Without the aqueducts, a significant amount of flow is lost for the GH and VFC areas. In this case, the main source of water is intact, but breaks on the Rinaldi and Granada Trunk Lines, and significant leaks on the Roscoe Trunk Line, produce a similar effect by limiting the movement of water.

Water Service Area Serviceability at 24 hrs
LA Aqueducts On, Northridge Trunk Line Damage
 (Entire System Serviceability = 86.5%)

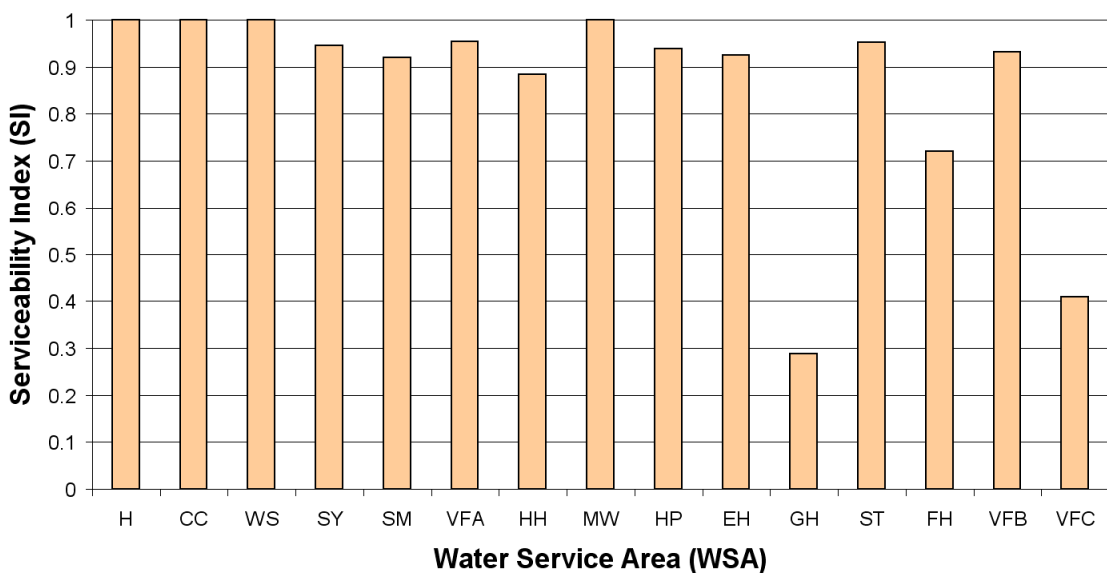


Figure 5.6 Serviceability Index after 24 Hours for 15 Water Service Areas with Northridge Trunk Line Damage and No Other Damage

5.3.4 System Performance Due to Tank Damage

Investigations of tank performance during the Northridge earthquake (Brown, et al., 1995) identified severe damage to 5 tanks in the LADWP system, 4 of which

exist in the 2007 hydraulic model: Zelzah, Topanga, Coldwater Canyon, and Beverly Glen Tanks (see Figure 5.6). This damage was included by disconnecting the inlet and outlet lines for the tanks.

A hydraulic network analysis performed for tank damage with the LAAs on showed that system wide serviceability was 100%, indicating that this scenario of tank damage has no effect on system serviceability with the LAAs in service. Results for a second 24-hour simulation with the tank damage and the LAAs out of service are shown in Figure 5.7. Comparison of these results with those of the LAAs off results (Figure 5.3) shows that the 4 damaged tanks have a minimal effect on system performance. The 24 hour SSI for the LAA off scenario was 83.1%, and drops slightly to 83.0% for the case with the LAAs off and the damaged tanks. The SY water service area is the most affected, dropping from 100% SI after 24 hours with no tank damage, to 94.5% when tank damage is included. As water is diverted in the system to cover the loss of tanks in the nearby service areas, the water supply to the SY service area is diminished.

Water Service Area Serviceability at 24 hrs LA Aqueducts Off, Northridge Tank Damage

(Entire System Serviceability = 83.0%)

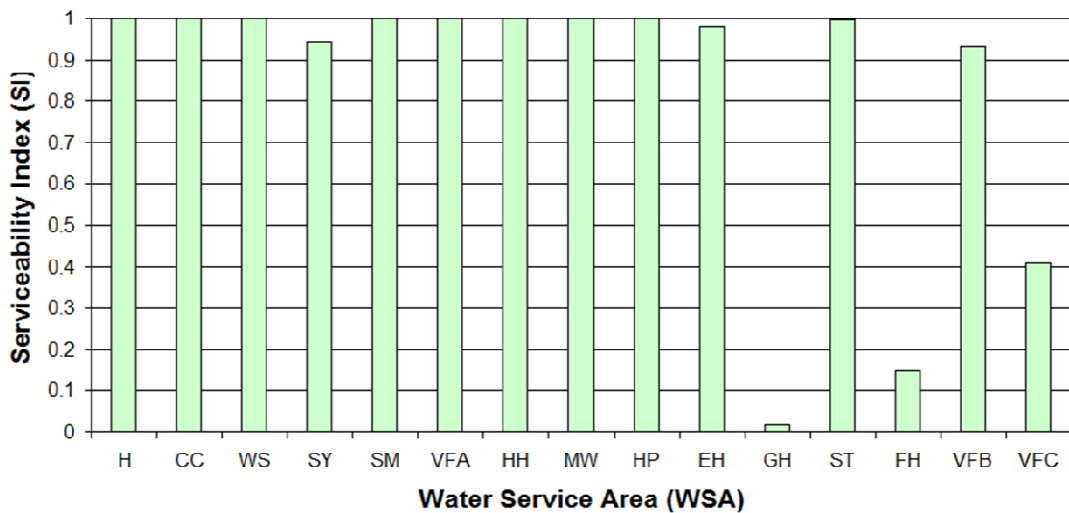


Figure 5.7 Serviceability Index after 24 Hours for 15 Water Service Areas with LAAs Off and Northridge Trunk Tank Damage

5.3.5 Combined Effects of Electric Power Loss and Northridge Trunk Line Damage on System Performance

Figure 5.8 shows the combined effects of electric power loss and Northridge trunk line damage to the system with the LAAs on. The entire system serviceability after 24 hours is approximately 83%, which is lower than the system serviceability results for loss of electric power and Northridge trunk line damage alone. The 54% and 52% SIs for the ST and FH regions are due to the loss of pumping capacity to distribute water in those service areas. The 41% SI in VFC is dominated by the Northridge trunk line damage, particularly the Granada and Rinaldi Trunk Line breaks, and leaks on the Roscoe Trunk Line. Serviceability in the GH water service

area drops to 2% due to the combined effect of electric power loss and trunk line damage.

Figure 5.9 shows the same study with loss of electric power and Northridge trunk line damage, but also includes the loss of the LAAs. These results emphasize the importance of the LAAs as a source of water because entire system serviceability drops to 69%. Water service areas in the central (EH, SM, HH, and MW) and northern (GH, FH, and ST) portions of the LADWP system are particularly affected due to loss of pump stations, and the reduced amount of water available for transmission.

Water Service Area Serviceability at 24 hrs
LA Aqueducts On, Northridge Trunk Line Damage
& Electric Power Loss
 (Entire System Serviceability = 82.6%)

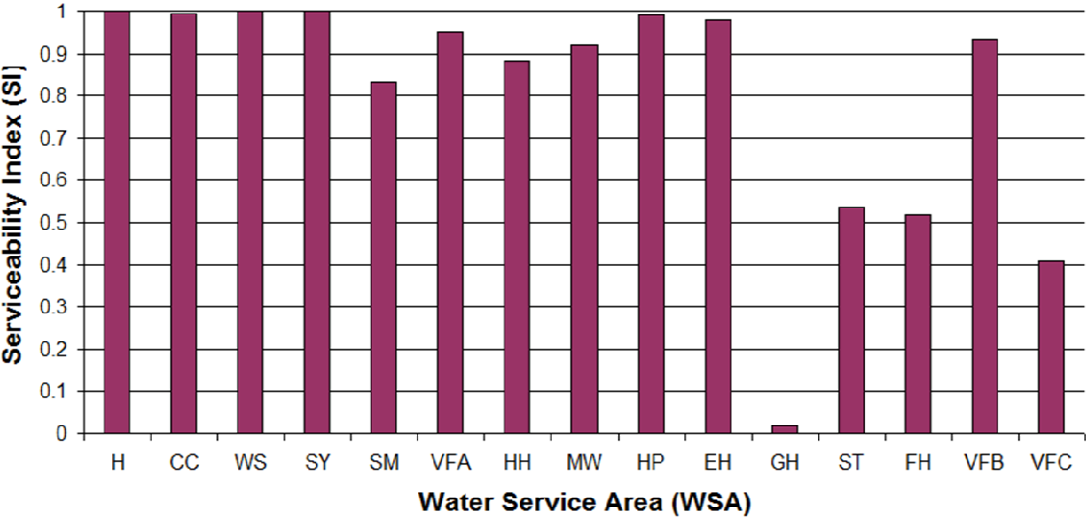


Figure 5.8 Serviceability Index after 24 Hours for 15 Water Service Areas with Northridge Trunk Line Damage and Electric Power Loss for Los Angeles Aqueducts

On

**Water Service Area Serviceability at 24 hrs
LA Aqueducts Off, Northridge Trunk Line Damage
& Electric Power Loss**

(Entire System Serviceability = 69.3%)

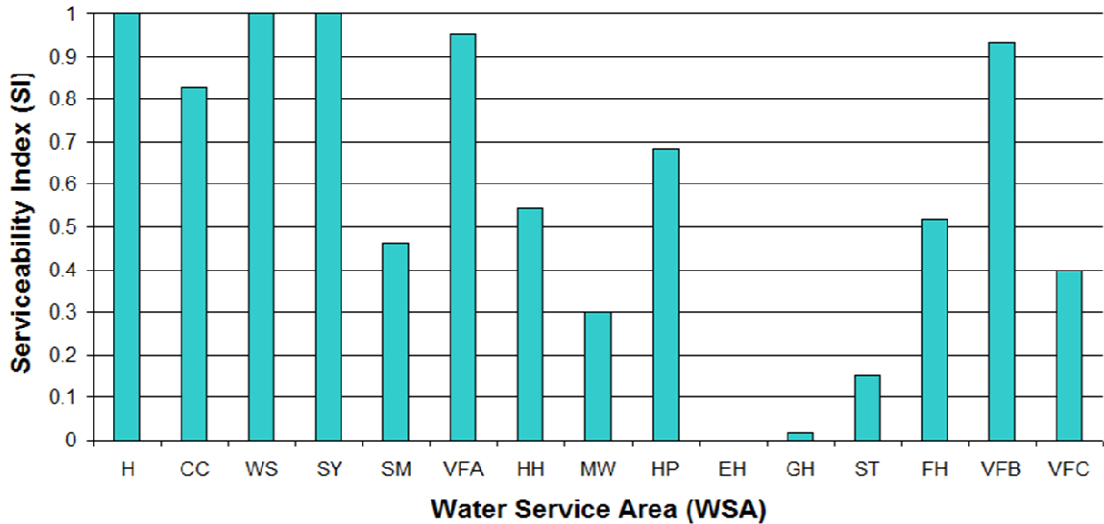


Figure 5.9 Serviceability Index after 24 Hours for 15 Water Service Areas with Northridge Trunk Line Damage, Electric Power Loss, and Los Angeles Aqueducts Off

5.3.6 Combined Effects of Los Angeles Aqueduct Outage, Electric Power Loss, Northridge Trunk Line Damage, and Distribution System Damage on System Performance

Figure 5.10 shows the results for a simulation with electric power loss, Northridge trunk line damage, and loss of the LAAs. In addition, distribution system damage is simulated by an increase in the nodal demands, as per fragility curves developed by Shi (2006). The entire system serviceability after 24 hours drops significantly to 39%. This study shows the importance of modeling damage to the distribution system, which was explored in the previous chapter. Sensitivity analyses from the previous chapter have demonstrated that demands imposed by the local

distribution system can have significant effects on serviceability. Comparison of Figures 5.8 and 5.9 shows the impact of distribution pipeline damage, which causes a drop in SSI from approximately 83% to 69%. The increase in demand from distribution system damage due to the earthquake affects the EH, HP, MW, and HH water service areas more severely than others. The impact of elevated distribution demands causes tanks within these water service areas to lose water more rapidly thereby cutting off flows and reducing local serviceability.

Water Service Area Serviceability at 24 hrs
LA Aqueducts Off, Northridge Trunk Line Damage, Electric
Power Loss & Distribution System Damage
 (Entire System Serviceability = 38.9%)

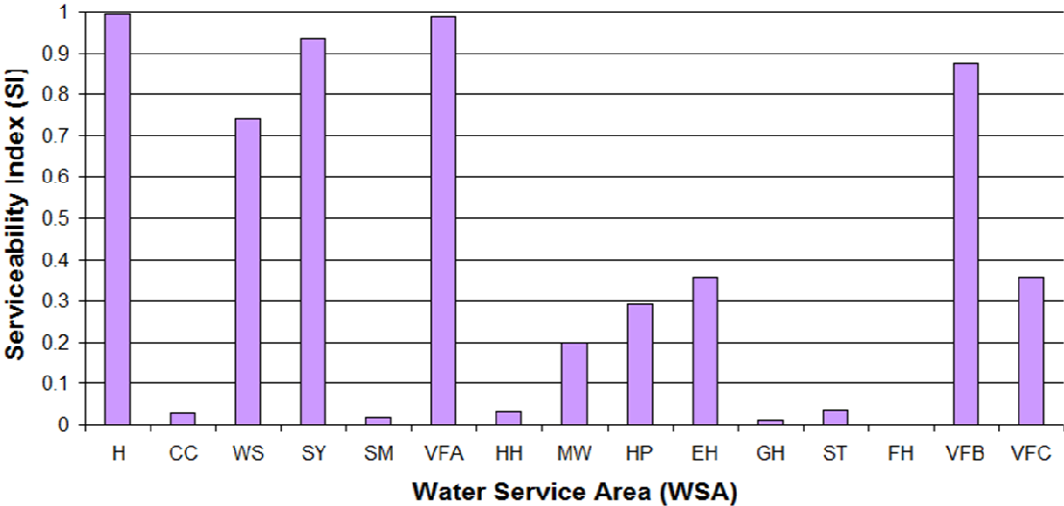


Figure 5.10 Serviceability Index after 24 Hours for 15 Water Service Areas with Northridge Trunk Line Damage, Electric Power Loss and Distribution System Damage for Los Angeles Aqueducts Off

5.4 Conclusions

The hydraulic network model embodied in the DSS for the LADWP water supply accounts comprehensively for combined sources of earthquake damage, including loss of the LAAs, damage from PGD and TGD to both trunk and distribution pipelines, loss of electric power, and damage to facilities. In the simulations, the individual sources of damage can be decoupled from their combined effects and studied one at a time. By de-aggregating the damage in this way, the most important sources of earthquake disruption can be determined. Moreover, the location and system conditions having the greatest influence on earthquake vulnerability can be identified and corrective measures taken to improve system-wide and local response.

De-aggregation studies performed for the actual 1994 Northridge earthquake damage and water supply disruptions were used to evaluate system performance to single and combined sources of damage. There was no significant impact on serviceability, either system-wide or locally, from tank damage. Loss of the LAAs, however, has a significant effect on water delivery. After 24 hours, there is a reduction of 17% in system serviceability, with severe loss of service in the northern foothills flanking the San Fernando Valley as well as in the western part of the valley.

Loss of electric power results in a reduction of approximately 7% in system serviceability with losses principally in service areas along the northern flank of San Fernando Valley. Loss of electricity removes Van Norman Pump Station No. 2 from the system, which pumps water to higher elevations surrounding the Van Norman Complex. As a result, flow is curtailed into the GH and FH water service areas.

Water losses from electric power outage affect many of the same localities most severely influenced by loss of the LAAs.

The LAAs provide water to 1) the Rinaldi Trunk Line which services the western San Fernando Valley, and 2) to Van Norman Pump Station No. 2 into trunk lines that service the western San Fernando Valley, and the water service area in the northwestern portion of the system. With the loss of the LAAs, water is not available to be pumped through Van Norman Pump Station No. 2, thereby curtailing flow to the western San Fernando Valley. Also, the loss of the LAAs restricts flow in the Rinaldi Trunk Line, further decreasing system serviceability in the western San Fernando Valley, particularly the VFC water service area.

In the case of electric power outage, the water is available from the LAAs, but the means to distribute it is compromised as Van Norman Pump Station No. 2 does not have a back-up power source. Without Van Norman Pump Station No. 2, flow in the Granada, Susana, and Foothill Trunk Lines is curtailed, and system serviceability is reduced in the western San Fernando Valley (particularly Granada Hills) and Foothill water service areas. These two cases have different causes for loss of water transmission, but produce similar patterns of lost system serviceability. In the case of the LAAs, the means to distribute water is intact (via Van Norman Pump Station No. 2) but a major source of water is lost. In the case of electric power outage, the major source of water (LAAs) is available, but the means to distribute it (Van Norman Pump Station No. 2) is not.

The reduction in system serviceability from only trunk line damage is 14.5%, and is concentrated locally in those service areas at higher elevations north of San

Fernando Valley as well as the western part of the valley. The locations of lost service from Northridge trunk line damage are geographically similar to those associated with disconnection of the LAAs and electric power outage because breaks on the Rinaldi and Granada Trunk Lines cut off flow to the western San Fernando Valley, and leaks in the Van Norman Complex and Van Norman Pump Station discharge line curtail flow to the FH and GH service areas in the north. The combined effects of Northridge trunk line damage and electric power loss contribute to a decline of approximately 17% in system serviceability similar to that associated with loss of the LAAs. The service areas most severely affected by LAA loss are the western San Fernando Valley and the Foothills area, which are also the areas most significantly compromised by the combined effects of trunk line damage and electric power outage.

In summary, the de-aggregation studies show that the LADWP distribution system is vulnerable to loss of the LAAs. These aqueducts provide flow to Van Norman Pump Station No. 2 and then to the Granada, Susana and Foothill Trunk Lines. The Granada and Susana trunk lines convey water to the western San Fernando Valley, and the Foothill Trunk Line conveys water to the Foothills service area. Water from the LAAs also feeds into the Rinaldi Trunk Line, another major source of water to the western San Fernando Valley. The lack of a back-up power source for Van Norman Pump Station No.2 is also a vulnerability. The loss of this pump station prevents the distribution of LAA water to the Granada, Susana, and Foothill Trunk Lines, which reduces serviceability in the western San Fernando Valley and Foothills regions.

CHAPTER 6

APPLICATION OF DECISION SUPPORT SYSTEM

6.1 Introduction

An unbounded problem is one that does not have a well-defined solution set and for which there may be many different outcomes. A DSS provides solutions for an unbounded problem in a way that allows managers to evaluate different potential outcomes and select the most appropriate measures to improve operability and performance. For problems that involve system response to extreme events, there are uncertainties associated with the demands, system capacity, models used for system simulation, and human error. System simulations for this class of problem must have strong stochastic attributes in demand and system capacity formulations. Running simulations for multiple scenarios provides a range of possible outcomes and a probabilistic basis for judging the most likely level of performance and its variability. Multiple simulations help to identify recurrent patterns of behavior and to plan for the many eventualities of an extreme event. Testing various plans and strategies by quantifying their effects improves the operators' ability to improvise and innovate during a real emergency.

This chapter applies the DSS to an unbounded problem of water supply management involving the removal of reservoirs from service because of water quality requirements and the impact of that process on water supply performance during a future earthquake. The reservoirs removed from service and their significance with respect to storage capacity are discussed. Water supply response for repeat Northridge

scenario earthquakes is analyzed, and the characteristics of the scenario earthquake simulations are described. Simulation results are presented for conditions in which the reservoirs removed from service are 1) disconnected from the system, and 2) reconnected on an emergency basis. The geographic distribution of system performance is assessed for the 15 water service areas of LADWP, and the results are summarized for service areas providing water to the most highly populated areas of Los Angeles. The implications of the simulations are discussed with respect to emergency planning, and conclusions are drawn regarding the operation of the system during a serious earthquake.

6.2 LADWP Reservoirs

The LADWP is presently undertaking an extensive capital improvement program to meet the requirements of the U.S. Environmental Protection Agency and California State Department of Health Services requirements with respect to surface water treatment and disinfection byproducts. Significant water system changes are necessary to meet the requirements. System changes include the removal of Encino, Hollywood, and Lower Stone Canyon Reservoirs from normal operating service, which places a much greater importance on the Los Angeles Reservoir and Van Norman Complex for reliable water distribution. Figure 6.1 shows the locations and approximate water storage capacities of the Los Angeles, Encino, Lower Stone Canyon, and Hollywood Reservoirs. The removal of these reservoirs represents a loss of about 34 million m³ of water from immediate use in the system.

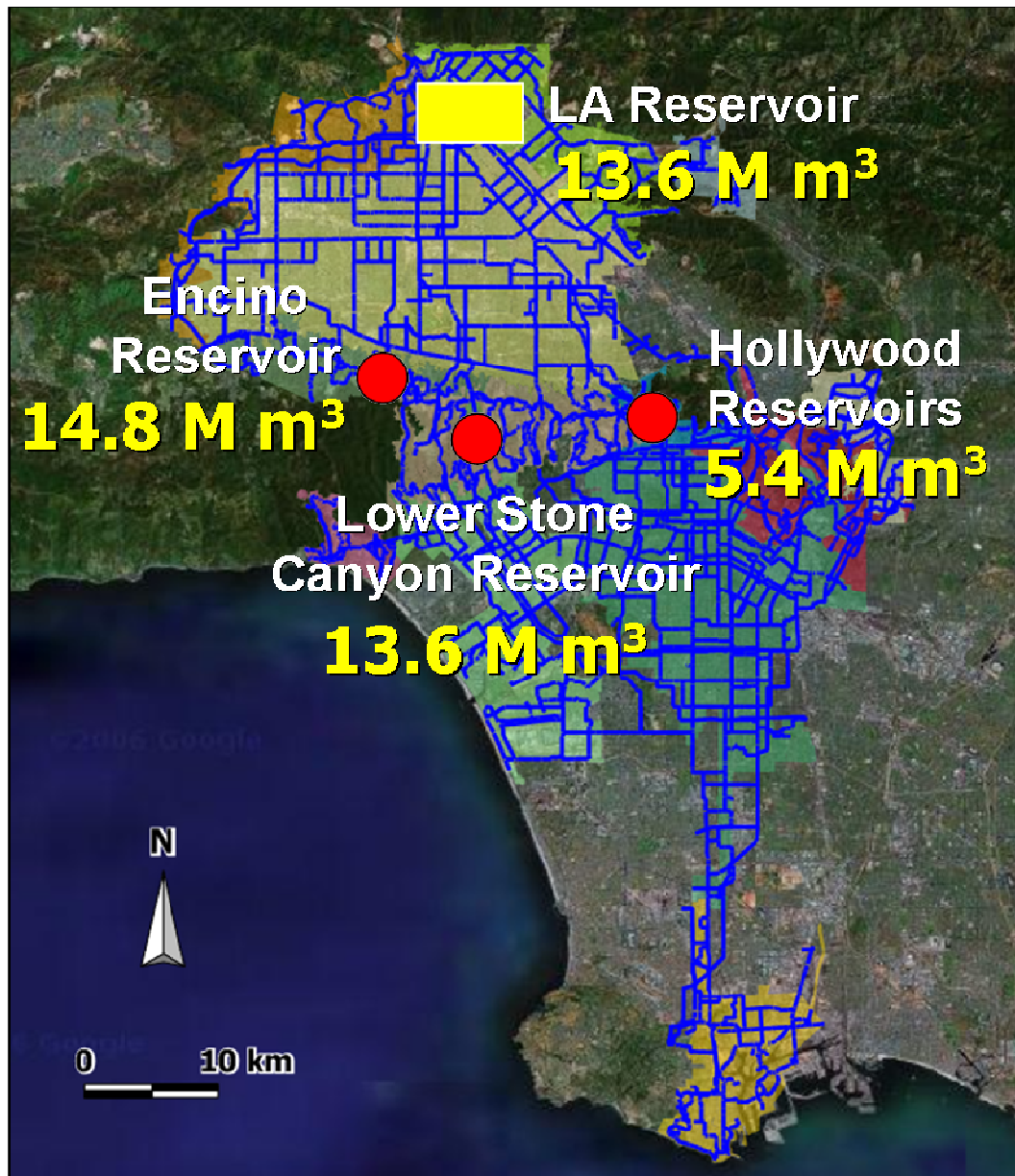


Figure 6.1 Locations and Storage Capacities of Los Angeles, Encino, Lower Stone Canyon, and Hollywood Reservoirs

6.3 Repeat M_w 7.0 Northridge Scenario Earthquake

A Northridge repeat earthquake scenario was selected to model system response with and without the removed reservoirs to evaluate their influence on the ability to supply water after an earthquake. The Northridge repeat earthquake scenario consists of a M_w 7.0 earthquake that is one of the 59 scenario earthquakes incorporated in the DSS to assess the aggregated seismic hazard for the LADWP system. This event is similar to the actual M_w 6.7 1994 Northridge earthquake and hence familiar and meaningful for operators and customers. The M_w 7.0 scenario earthquake is slightly stronger than its 1994 counterpart, but sufficiently similar to provide results that can be assessed relative to recent experience with system performance during the actual Northridge earthquake.

As pointed out by Davis, et al. (2007), system simulations for a repeat Northridge earthquake provide a credible basis for assessing how water quality improvements affect the seismic performance and recovery capability of the LADWP water supply. They can be used to evaluate seismic safety and to guide on-going capital improvement projects to ensure that seismic hazards are considered properly in relation to water quality and other hazard concerns (e.g., dam safety).

6.4 Simulation Results for M_w 7.0 Earthquake

This section presents the simulation results for a M_w 7.0 repeat Northridge earthquake scenario, including simulated trunk and distribution line damage, electric power outage, and tank fragility analysis for both winter and summer demand conditions. Pipeline flows as well as system-wide and local serviceability metrics are

presented and discussed. The geographic distribution of serviceability is assessed for the 15 water service areas of LADWP described in Chapter 5 (see Figure 5.2), and the results are summarized for service areas providing water to the most highly populated areas of Los Angeles.

6.4.1 System-wide Serviceability Results

Figure 6.2 shows the trunk line flow simulation results 24 hours after the earthquake, and corresponding median system serviceability indices (SSIs) for both summer and winter demand scenarios with the out-of-service reservoirs open and closed. As discussed in Chapter 3, Monte Carlo simulations are run according to an algorithm that uses a Poisson process to simulate the occurrence of pipeline damage based on seismic demands and pipe characteristics. Each simulation generates different damage scenarios, and the damaged system is reconfigured to remove portions of the system that have been physically disconnected, and rendered hydraulically unreliable by the presence of unsustainable negative pressures identified by the hydraulic network analyses. The user can specify the number of Monte Carlo simulations to be performed, or can allow the hydraulic network analysis program determine the number of simulations based on a self-termination algorithm that automatically stops when convergence criteria have been met. For the summer and winter demand scenarios, 15 simulations were run to meet the convergence requirements of the algorithm.

In Figure 6.2, the blue lines indicate trunk lines with flow that are still capable of providing water to demand nodes in the distribution system. The gray lines

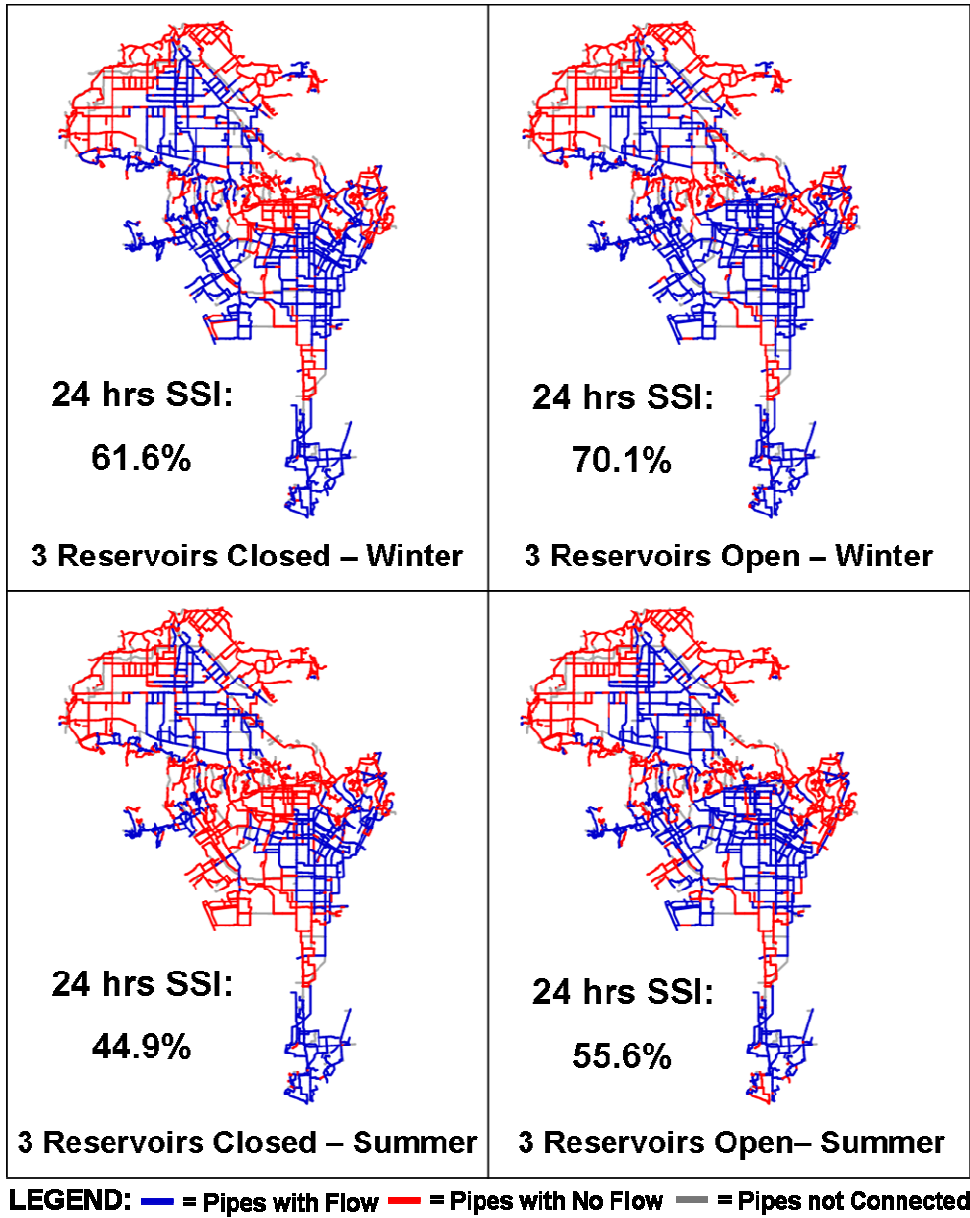


Figure 6.2 Median Trunk Line at 24 Hours for Summer and Winter Demands with Out-of-Service Reservoirs Open and Closed

**24hrs System SI Histogram Comparison of 2007 Winter System
Encino, Hollywood, LSC Reservoirs Open and Closed**

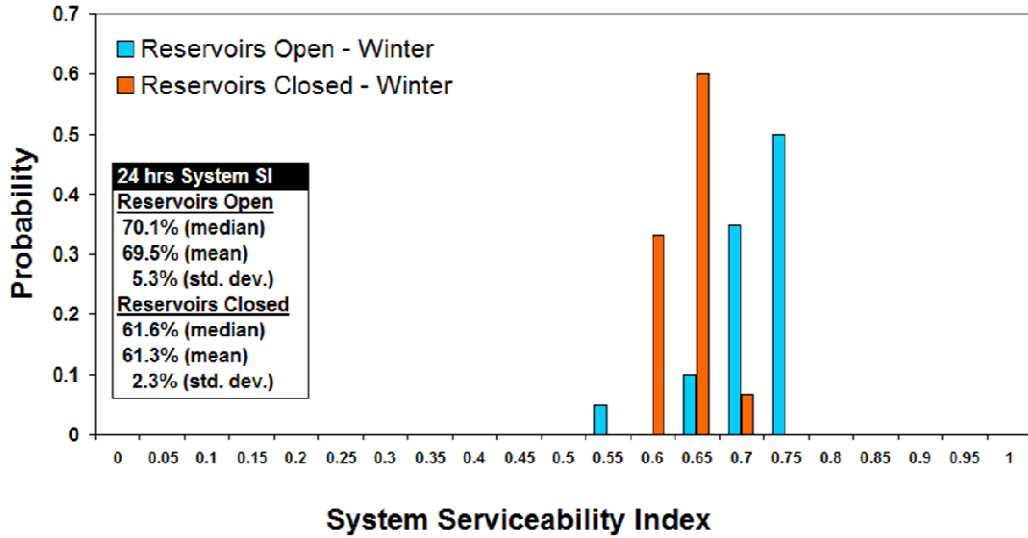


Figure 6.3 SSI at 24 Hours for Repeat Northridge Earthquake Scenario, Winter Demand with Out-of-Service Reservoirs Open and Closed

**24hrs System SI Histogram Comparison of 2007 Summer System
Encino, Hollywood, LSC Reservoirs Open and Closed**

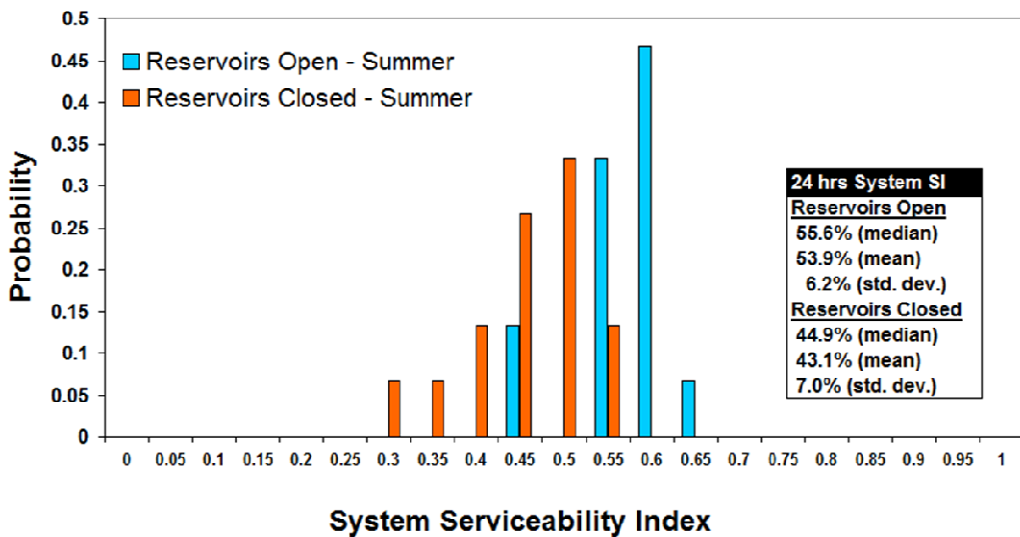


Figure 6.4 SSI at 24 Hours for Repeat Northridge Earthquake Scenario, Summer Demand, with Out-of-Service Reservoirs Open and Closed

represent Municipal Water District (MWD) trunk lines and well lines that are not connected to the LADWP network. Interties exist between these lines and the LADWP system that can be opened according to seasonal demand or in the event of an emergency. The red lines represent trunk lines that are not able to convey water with reliable levels of pressure and flow, and thus have been removed from the system.

As shown in Figure 6.2, the 24 hour, median SSI for winter demand with the reservoirs closed is 61.6%, and rises to 70.1% with the reservoirs open. Water flows associated with open reservoirs are improved primarily in the MW and HH water service areas located just north of the Los Angeles central business district. For a summer demand, the 24 hour, median SSI with the reservoirs closed is 44.9%, and increases to 55.6% with the reservoirs open. Consistent with the parametric studies described in Chapter 4, the SSI for summer demand is substantially lower than that for winter demand. Opening the reservoirs under summer demand has a greater effect on boosting SSI than the lower winter demand, with water flows improved primarily in the MW and HH water service areas, and the CC and WS water service areas that include downtown Los Angeles.

Each map in Figure 6.2 is for only one simulation corresponding to the median SSI. To obtain a better sense for the statistical variation in SSI outcomes, Figures 6.3 and 6.4 show 24 hour system-wide serviceability histograms for all 15 simulations with reservoirs open and closed, for winter and summer demand conditions, respectively. The SI statistics for 24 hours after the earthquake are summarized in these histograms by showing the number of Monte Carlo simulations resulting in a particular SI divided by the total number of simulations to provide an approximate

probability index. The histograms of “probability” allow comparison of performance outcomes when the Encino, Lower Stone Canyon, and Hollywood Hills Reservoirs are closed and open.

For the winter demand scenario, the SSIs for reservoirs open range from 55% to 75%. For the winter scenario with reservoirs closed, the range of SSIs is narrower, between 60% and 70%. Moreover, with reservoirs closed the probability of experiencing damage states towards the lower end of the range is significantly greater than when the reservoirs are open. In the summer demand scenario, the SSIs for reservoirs open range from 45% to 65%. With the reservoirs closed, the spread in SSIs becomes wider, ranging from 30% to 55%. These results indicate that post-earthquake system performance can degrade significantly with increased demand and that summer demand conditions contribute to lower bound seismic performance of the system. The spread in potential damage states, and thus the potential for very low levels of serviceability, increases with elevated demand.

6.4.2 Dense Population Area Serviceability Results

Figure 6.5 shows the water service areas superimposed on census block groups from 2000 TIGER/Line data. Each block group typically contains between 600 and 3000 people, with an optimum size of 1500. The WS, CC, HP and MW water service areas, highlighted in gold, represent some of the densest population areas in the LADWP system, including the Los Angeles central business district. Serviceability results can be compiled for any combination of water service areas. Using a GIS to identify the most populous water service areas helps to identify those portions of the city with densest housing and potentially highest vulnerability to fire spreading.

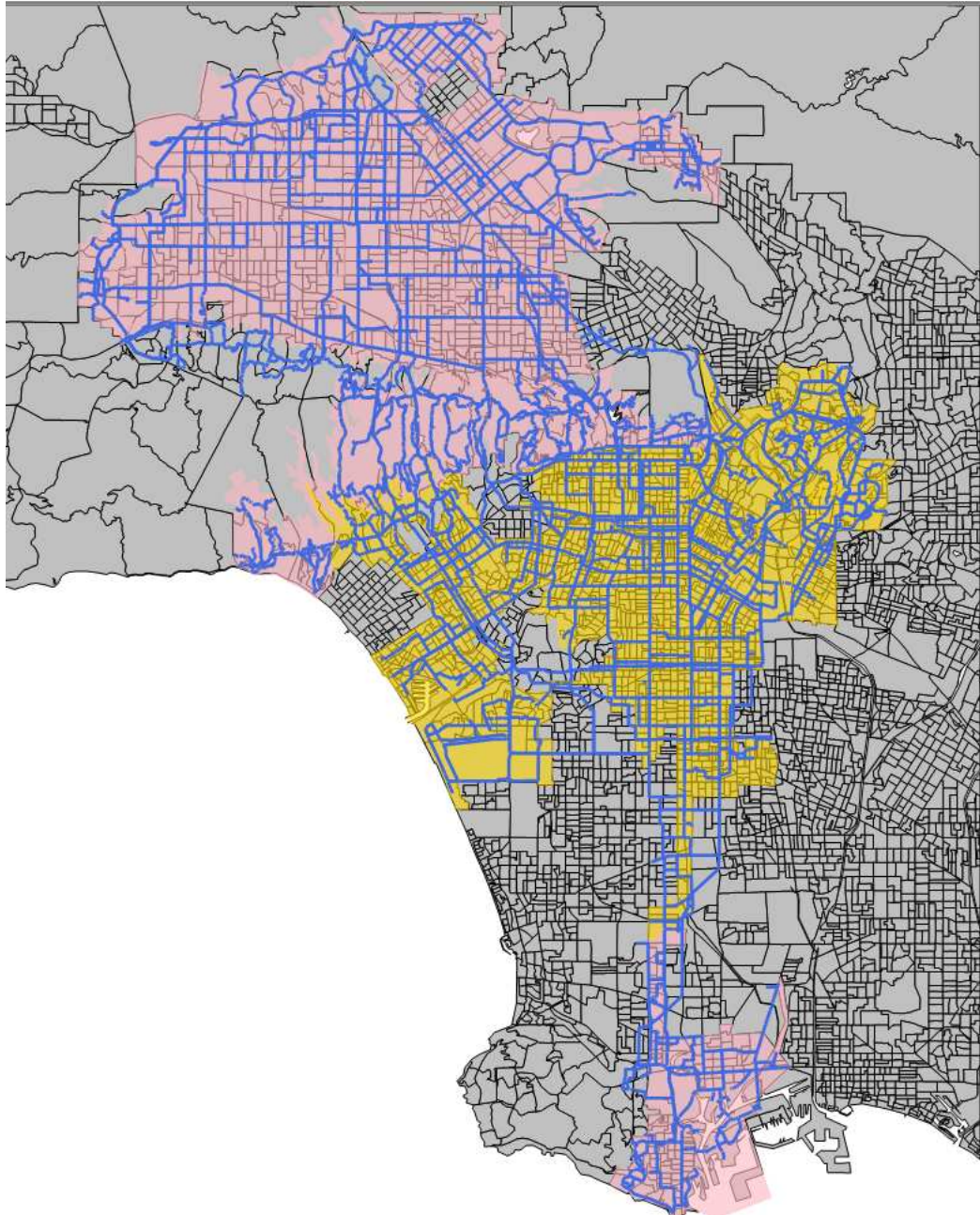


Figure 6.5 LADWP Pipelines and Water Service Areas Superimposed on 2000 Census Block Group Image

Figures 6.6 and 6.7 show the 24 hour serviceability results for the most densely populated service areas for both the winter and summer demand scenarios, respectively. For both demand conditions, the improvements in serviceability are more pronounced for the most densely populated water districts than for the entire system. The spread in potential outcomes is quite clear in Figure 6.6 for winter demand, with an increase in SI of more than 15% when the results for open reservoirs are compared to those for closed reservoirs. Similar to the results in Figures 6.3 and 6.4, the post-earthquake system performance degrades significantly with increased summer demand as shown by the histograms in Figure 6.7. There is a very substantial increase of approximately 23% in median SI for reservoirs open compared with reservoirs closed. Moreover, there is a notable shift to lower potential SIs for reservoirs closed, with some SIs as low as 15%. Hence, there is now the possibility of severe serviceability loss in those areas of Los Angeles with the highest populations.

Comparing Figures 6.3 and 6.4 with Figures 6.6 and 6.7 shows the value of evaluating serviceability for select geographic areas. Serviceability increases more markedly with reservoirs open for the most heavily populated areas of Los Angeles compared with system-wide serviceability for both winter and summer demands. The contrast is most pronounced for summer demand. Whereas the median serviceability throughout the entire system increases by about 11 % for reservoirs open, the median serviceability for the most populated areas increases by more than double this amount (23%) for reservoirs open.

The ability to obtain water system performance results for geographic subsets of the LADWP system can help system operators and planners. The knowledge that a repeat Northridge earthquake scenario under high summer demands may cause a

**24hrs System SI Histogram Comparison of 2007 Winter System
Encino, Hollywood, LSC Reservoirs Open and Closed
Dense Population Areas: WS, CC, HP & MW**

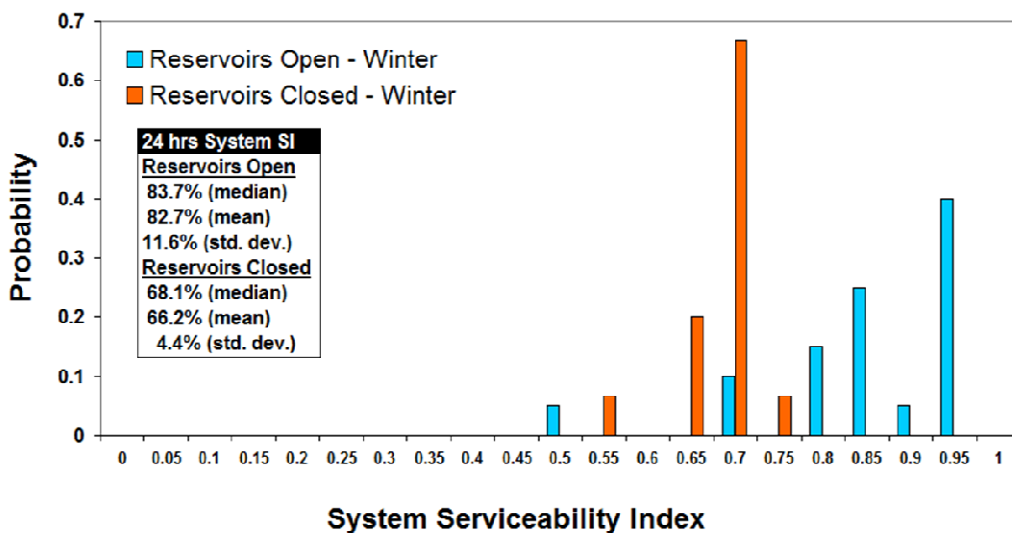


Figure 6.6 Dense Population Area SSI at 24 Hours for Repeat Northridge Earthquake Scenario, Winter Demand with Out-of-Service Reservoirs Open and Closed

**24hrs System SI Histogram Comparison of 2007 Summer System
Encino, Hollywood, LSC Reservoirs Open and Closed
Dense Population Areas: WS, CC, HP & MW**

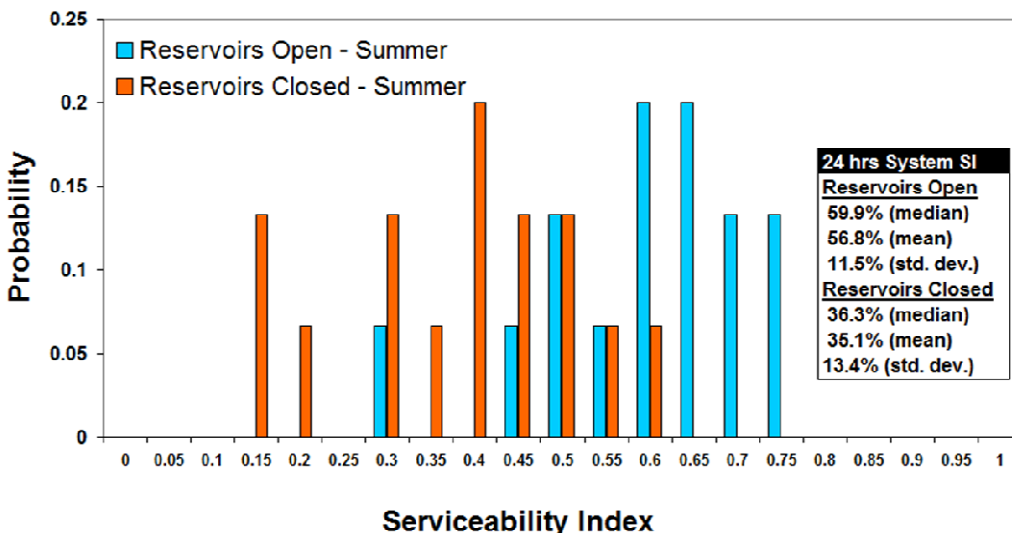


Figure 6.7 Dense Population Area SSI at 24 Hours for Repeat Northridge Earthquake Scenario, Summer Demand with Out-of-Service Reservoirs Open and Closed

concentrated loss of serviceability in the most densely populated areas aids in the development of mitigation strategies. Opening the out-of-service reservoirs on an emergency basis is most effective in the densely populated areas for increasing serviceability, which in turn reduces vulnerability to fire and fire spreading. The results show that opening the reservoirs immediately after a serious earthquake improves serviceability so significantly in densely populated areas that it is a plausible strategy for emergency response, even though such action will require water purification notices to be issued for the entire system.

6.4.3 Serviceability Results for the 15 Water Service Areas

To identify particular regions of the LADWP system that experience significant degradation in serviceability, results can be compiled according to the 15 water service areas (see Figure 5.2). Figure 6.8 compares the median serviceability results for a winter demand scenario at 24 hours after the earthquake for reservoirs open and closed. With reservoirs open, two of the 15 water service areas, FH and GH, have SIs below 25%. When the reservoirs are closed, only one additional water service area, HH, falls below 25% serviceability. Figure 6.9 shows the same comparison of median serviceability results for summer demand. With the reservoirs open, four of the 15 water service areas (SM, FH, GH, and ST) have SIs below 25%. When the reservoirs are closed, the HH, MW, and HP water service areas also drop below 25% serviceability.

Figure 6.10 presents the same results, but in a GIS format highlighting the location of the water service areas with SIs below 25%. The GH and FH water service areas are most susceptible to decreased water system performance, followed by the

Water Service Area Serviceability at 24 hrs
Repeat Northridge Earthquake Scenario - Winter Demand
Trunk Line & Distribution Line Damage, Electric Power Loss, Tank Fragility
Out-of-Service Reservoirs Open & Closed
 Entire System Serviceability = 70.1% (Reservoirs Open)
 61.6% (Reservoirs Closed)

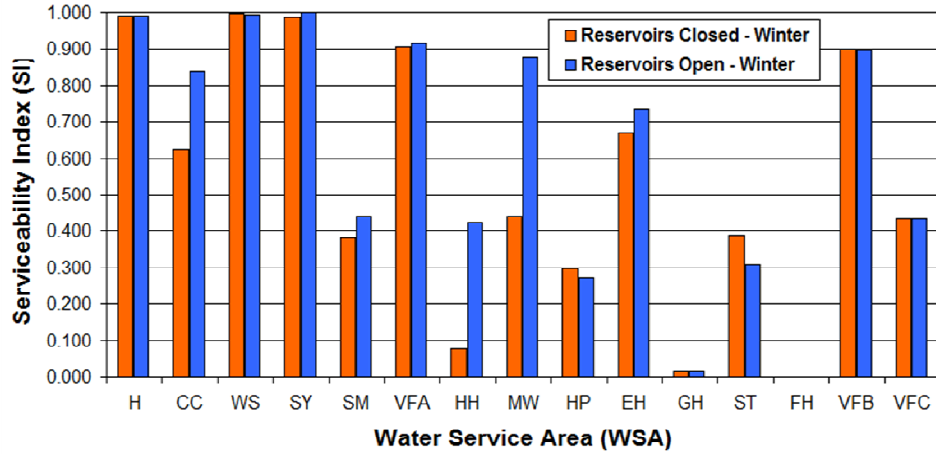


Figure 6.8 Serviceability Index at 24 Hours for 15 Water Service Areas for Winter Demand with Out-of-Service Reservoirs Open and Closed

Water Service Area Serviceability at 24 hrs
Repeat Northridge Earthquake Scenario - Summer Demand
Trunk Line & Distribution Line Damage, Electric Power Loss, Tank Fragility
Out-of-Service Reservoirs Open & Closed
 Entire System Serviceability = 55.6% (Reservoirs Open)
 44.9% (Reservoirs Closed)

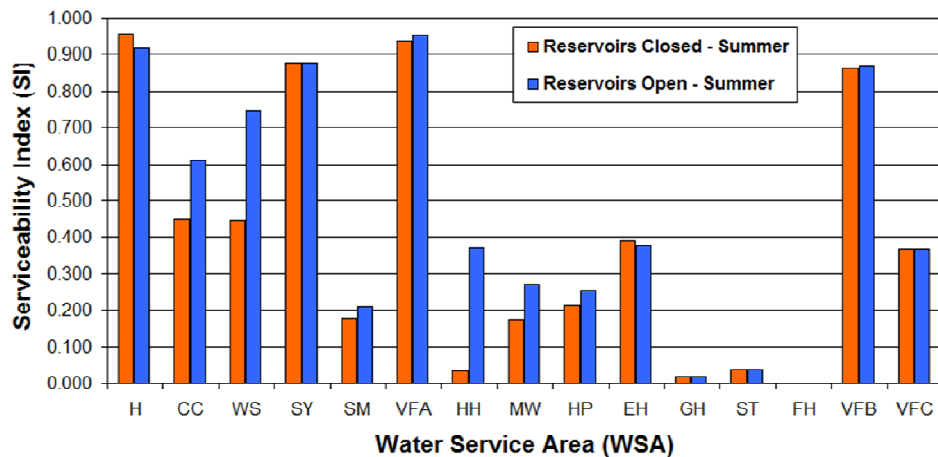


Figure 6.9 Serviceability Index at 24 Hours for 15 Water Service Areas for Summer Demand with Out-of-Service Reservoirs Open and Closed

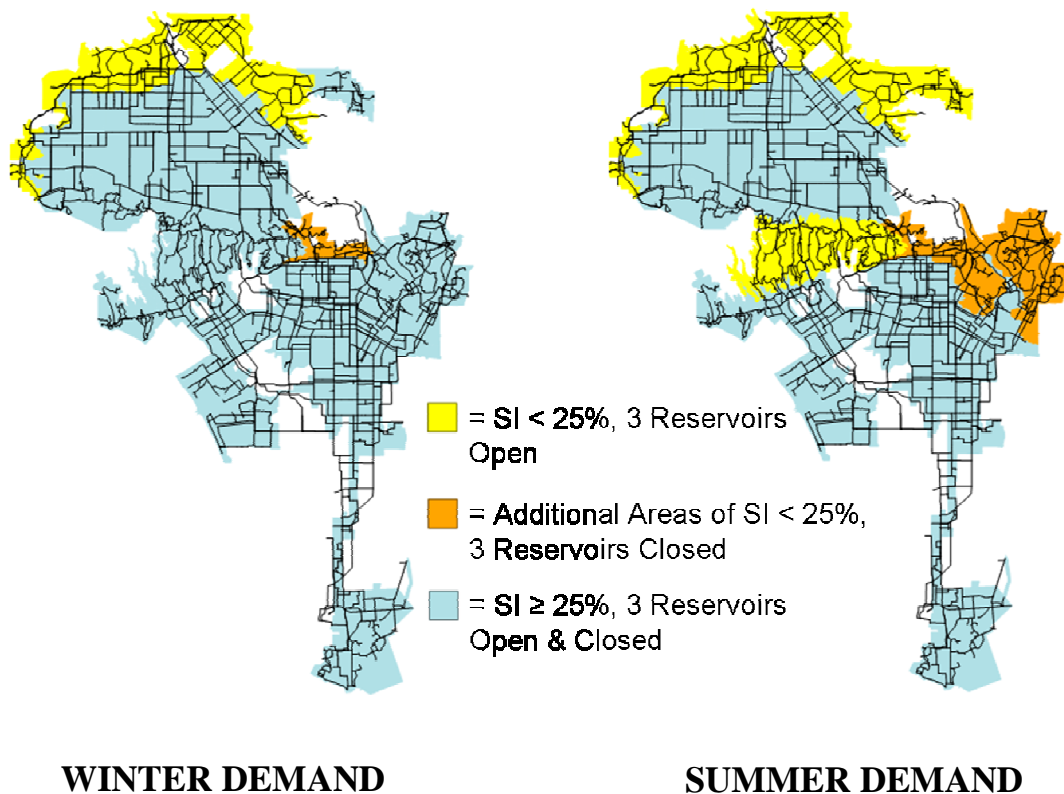


Figure 6.10 Comparison of 24 Hour SSI for the 15 Water Service Areas for a Repeat Northridge Earthquake Scenario, Out-of-Service Reservoirs Open and Closed for Winter and Summer Demand Scenarios

MW and HP service areas, indicating special consideration should be made as to how these areas are provided with water in the event of an earthquake.

The results of the de-aggregation analyses presented in Chapter 5 also show the GH and FH water service areas to be the most vulnerable to decreased water system performance. The analyses presented here and in Chapter 5 both illustrate the importance of the Los Angeles Aqueducts (LAAs) and Van Norman Pump Station No. 2. When the transmission of water from the LAAs is lost, the Granada, Rinaldi and

Susana Trunk Lines that feed the GH service area lose water. In addition, water to the FH service area via the Foothill Trunk Line is also restricted.

6.5 Conclusions

The LADWP system was modeled with and without several key reservoirs, which have been removed from service to meet water quality standards, to assess their influence on supplying water after an earthquake. These results indicate that post-earthquake system performance can degrade significantly with increased demand and that summer demand conditions contribute to lower bound seismic performance of the system. The spread in potential damage states, and thus the potential for very low levels of serviceability, increases with elevated demand.

The results also show that opening the disconnected reservoirs immediately after a serious earthquake improves serviceability, with the most substantial improvements experienced by water service areas with the highest population densities. Whereas the median serviceability for summer demand throughout the entire system increases by about 11% for reservoirs open, the median serviceability for the most populated areas increases by more than double this amount (23%) when the out-of-service reservoirs are opened. By increasing water supply serviceability, opening reservoirs also reduces vulnerability to fire and fire spreading. Opening the reservoirs immediately after a serious earthquake improves serviceability so significantly in densely populated areas that it is a plausible strategy for emergency response, even though such action will require water purification notices to be issued for the entire system.

The simulations performed for this study illustrate how complex system decisions involving long-term water quality standards and short-term emergency response measures can be supported by advanced systems modeling. Work, such as this, that links emergency response with public health decisions provides a good example of how system modeling provides the basis for decisions about earthquake effects on a regional scale and the complex performance of critical lifeline networks.

CHAPTER 7

SUMMARY AND CONCLUSIONS

7.1 Introduction

This report investigates water supply performance during earthquakes and extreme events. The effects of the WTC disaster on the NYC water supply is investigated in detail and hydraulic network analysis are performed for fireboat hose and pumper truck relays. Previous research by Shi (2006) and Wang (2006) is expanded to develop a functional DSS for the seismic and multihazard performance of water supplies, using the LADWP system as a test bed. Research on the seismic performance of water supplies involves the implementation of model improvements and upgrading the model developed by Shi (2006) and Wang (2006) to represent the LADWP system as of 2007, and these changes are described. This work also involves a parametric study of seismic water supply performance, de-aggregation of system simulation results according to individual sources of earthquake damage and geographic subsets of the LADWP system, and application of the methodology to an actual decision support problem faced by LADWP management.

This chapter provides a summary of major research findings associated with this report. The sections that follow summarize the research findings according to the five objectives of the research: 1) water supply performance during the WTC disaster; 2) model improvements and validation; 3) parametric study of seismic system performance; 4) de-aggregation of system simulation results; and 5) application of the

decision support system. The final section provides a discussion of research needs and future research directions.

7.2 Water Supply Performance During the WTC Disaster

In this study, the performance of the NYC water supply and fire protection systems during the WTC disaster is investigated in detail. The water losses sustained by distribution pipelines and their influence on fire fighting as well as telecommunication and transportation lifelines are evaluated. Hydraulic network analyses are performed to quantify the performance of hose and pumper truck relays from fireboats to the WTC site, and the performance of the fire protection system on NYC is compared with fire protection system performance during the 1989 Loma Prieta earthquake.

Water supply performance during the WTC disaster underscores the importance of water supply systems in crowded urban environments. Not only is the water distribution infrastructure critical for fire protection and the support of household and commercial activities, water main damage can rapidly cascade into damage of nearby gas, electric, telecommunications, and transportation facilities with substantial direct and indirect economic losses. Water from ruptured water mains during the WTC disaster flooded one of the commuter rail PATH tunnels, eventually threatening Exchange Place Station in New Jersey, and flooded a vault with telecommunication cables that carried financial data needed for securities trading on the New York Stock Exchange.

The analytical studies and results described in this chapter have important tactical ramifications for fire protection during extreme events. Fireboats are frequently equipped with high capacity pumps, well suited for spraying water on burning waterfront properties. When fireboats are used to pump water to shore, the principal bottleneck in the conveyance system is the hose size. Hydraulic network models by standard 89 mm (3.5 in.) hose lines and pumper trucks show that the maximum flow that can be delivered is only 10% of the pumping capacity of a large fireboat. The sensitivity analyses presented herein show considerable benefits from deploying 127 mm (5 in.) and 178 mm (7 in.) diameter hoses. Moreover, the analyses also show that two pumper trucks per relay, as opposed to three, is a better use of critical equipment when relay distances are in the range of 365 m (1,200 ft.) to 400 m (1,300 ft.).

From a strategic perspective, fireboat deployment during the WTC disaster and the Loma Prieta earthquake were essential for controlling fires. Estimated flows from fireboat pumping records and hydraulic network analyses indicate that water supplied from fireboats during the WTC disaster was approximately 150% of the water initially available in underground pipelines. Moreover, flow and pressure in underground pipelines declined steadily during 9/11 until all flow was shut off by isolating the area of suspected damage from the rest of the water distribution network. Similar disruption of the water supply was experienced after the Loma Prieta earthquake when seismic damage of underground pipelines deprived firefighters of water needed to extinguish the Marina fire. The loss of pipeline water was compensated by water pumped from the SFFD fireboat dispatched to the area of conflagration. Experience in the San Francisco after the Loma Prieta earthquake reinforces the WTC experience, and demonstrates that water can be conveyed rapidly from marine locations for

distances as great as 1 km (0.6 miles), provided that appropriate planning and equipment acquisition have been undertaken.

7.3 Model Improvements and Validation

A DSS has been developed for LADWP to plan operations, emergency response, and new system facilities and configurations to optimize water supply performance during and after earthquakes. The system is generic, and the architecture of its computer programs is adaptable to any water supply. The system works with a special program for damaged network flow modeling, known as Graphical Iterative Response Analysis for Flow Following Earthquakes (GIRAFFE). It simulates all 11,633 km (7,228 mi.) of water trunk and distribution pipelines and related facilities (e.g., tanks, reservoirs, pressure regulation stations, pump stations, etc.) in the LADWP system, and accounts for the aggregated seismic hazard in Los Angeles through an ensemble of 59 scenario earthquakes. The simulations are dynamic in time, and can account for loss of service as tanks and local reservoirs lose water over time through leaks and breaks in pipelines.

Specific model improvements were accomplished as part of this work. The model was upgraded to represent the LADWP system in 2007. The DSS now contains models for the LADWP system in 2002 and 2007. Modifications to the 2002 model can be implemented to represent system performance in 1994, thereby providing an appropriate basis for simulations of water supply response to the 1994 Northridge earthquake.

Additional model improvements include the ability to simulate the time dependent response of the system in a more robust manner by enabling the levels of tanks and reservoirs to vary. Critical system interactions between tanks and reservoirs can be lost if the simulation time increment does not reflect the smallest operational time increment for system functionality, which generally depends on the capacity of key storage facilities. For this reason, a one hour time increment is necessary for accurate simulation of the LADWP system. The model was also updated with the ability to include all sources of earthquake damage and disruption including the loss of the LAAs, loss of electric power, PGD and TGD effects in trunk and distribution pipelines, and fragility curves to probabilistically represent damage to facilities such as tanks, reservoirs, regulation stations, and pumps.

The hydraulic network model was validated through comparison of model results for the effects of the 1994 Northridge earthquake with the actual areas of lost water service and pre- and post-earthquake measurements of flow documented by LADWP. There is very good agreement between model results and LADWP records with respect to system-wide serviceability, geographic distribution of lost service, and pre- and post-earthquake flows over time at key locations. The median SSI 24 hours after the earthquake is 71.8%, which falls within LADWP estimates of 70-75% serviceability 24 hours after the actual Northridge earthquake (Adams, 2008). The simulated geographic distribution of lost service covers a larger area than that indicated by LADWP records, but these additional areas constitute less than 2% of total system demand. Hence, the model is biased to conservative results at high elevations that has only a small effect on system serviceability. Pre- and post-earthquake flows from the simulations were found to compare favorably with

Northridge flow records from 5 SCADA monitoring stations, indicating key areas of the system are being simulated accurately.

7.4 Parametric Study of Seismic System Performance

Post-earthquake water supply performance is time-dependent because losses through leaking pipelines reduce tank and reservoir levels, thereby diminishing, and in many instances cutting off, pressure and flow in portions of the system. It is important therefore to account for time-dependent performance by modeling post-earthquake response incrementally according to time intervals. The minimum time step required for modeling should be less than or equal to the smallest operational time increment needed for an accurate representation of system functionality, which will generally depend on the capacity of key storage facilities. For the LADWP system, a minimum time increment of 1 hour was needed for reliable time-dependent simulations. This interval is related to storage capacities of the Clearwell and several other tanks that have capacities that will run dry in less than 2 hours.

The most important factor affecting post-earthquake system performance is nodal demand. Water supply simulations based on the 1994 Northridge earthquake effects show a nonlinear decrease in system serviceability as the demand from the distribution system increases. The system serviceability 24 hours after the earthquake decreases from 71% for winter demand to 52% for summer demand, which represents a 19% decline. The simulation results show a 38% decrease in system serviceability after 24 hours for a fourfold increase in demand from winter demand conditions. The sensitivity of system performance to demand from the distribution system shows clearly that accounting for earthquake damage to distribution pipelines is important,

especially when earthquake performance under elevated summer levels of demand is being evaluated.

Simulations were performed of post-earthquake water supply response after 24 hours for the actual damage associated with the 1994 Northridge earthquake and damage simulated for a M_w 6.5 and M_w 7.0 Northridge repeat earthquake scenarios. They show that TGD effects had the most important effects on water supply performance, with a substantially greater impact than PGD effects. TGD for the Northridge earthquake simulations was more pervasive than PGD damage, and affected major trunk lines important for substantial flows in the system.

The parametric study shows that system serviceability was not significantly influenced by moderate changes in negative pressure tolerance. Large changes in leakage rates, on the order of 100%, produced relatively small changes of 5% in system serviceability, whereas extreme changes in the weighted probabilities of leakage produced system serviceability changes of 3%. Changes in the percentages of breaks and leaks resulted in some of the largest changes in system serviceability, but even here the drop in serviceability going from 0% to 20% trunk line breaks was only 7%.

7.5 De-Aggregation of System Simulation Results

The hydraulic network model embodied in the DSS for the LADWP water supply accounts comprehensively for combined sources of earthquake damage, including loss of the LAAs, damage from PGD and TGD to both trunk and distribution pipelines, loss of electric power, and damage to facilities. In the

simulations, the individual sources of damage can be decoupled from their combined effects and studied one at a time. By de-aggregating the damage in this way, the most important sources of earthquake disruption can be determined. Moreover, the location and system conditions having the greatest influence on earthquake vulnerability can be identified and corrective measures taken to improve system-wide and local response.

De-aggregation studies performed for the actual 1994 Northridge earthquake damage and water supply disruptions were used to evaluate system performance to single and combined sources of damage. There was no significant impact on serviceability, either system-wide or locally, from tank damage. Loss of the LAAs, however, has a significant effect on water delivery. After 24 hours, there is a reduction of 17% in system serviceability, with severe loss of service in the northern foothills flanking the San Fernando Valley as well as in the western part of the valley.

Loss of electric power results in a reduction of approximately 7% in system serviceability with losses principally in service areas along the northern flank of San Fernando Valley. Loss of electricity removes Van Norman Pump Station No. 2 from the system, which pumps water to higher elevations surrounding the Van Norman Complex. As a result, flow is curtailed in the GH, ST, and FH water service areas. Water losses from electric power outage affect many of the same localities.

The reduction in system serviceability from trunk line damage is 14.5% and is concentrated locally in those service areas at higher elevations north of San Fernando Valley as well as the western part of the valley, which are geographically similar to those affected by loss of the LAAs and by electric power outage. Breaks on the Rinaldi and Granada Trunk Lines cut off flow to the western portion of the San

Fernando Valley, and trunk line leaks in the Van Norman Complex reduce flow to the FH and GH service areas in the north.

The de-aggregation studies show that the LADWP distribution system is vulnerable to loss of the LAAs. These aqueducts provide flow to Van Norman Pump Station No. 2 and then to the Granada, Susana and Foothill Trunk Lines. The Granada and Susana trunk lines convey water to the western San Fernando Valley, and the Foothill Trunk Line conveys water to the Foothills service area. Water from the LAAs also feeds into the Rinaldi Trunk Line, another major source of water to the western San Fernando Valley.

The lack of a back-up power source for Van Norman Pump Station No.2 is also a vulnerability. The loss of this pump station prevents the distribution of LAA water to the Granada, Susana, and Foothill Trunk Lines, which reduces serviceability in the western San Fernando Valley and Foothills regions.

7.6 Application of Decision Support System

The LADWP system was modeled with and without several key reservoirs, which have been removed from service to meet water quality standards, to assess their influence on supplying water after an earthquake. These results indicate that post-earthquake system performance can degrade significantly with increased demand and that summer demand conditions contribute to lower bound seismic performance of the system. The spread in potential damage states, and thus the potential for very low levels of serviceability, increases with elevated demand.

The results also show that opening the disconnected reservoirs immediately after a serious earthquake improves serviceability, with the most substantial improvements experienced by water service areas with the highest population densities. Whereas the median serviceability for summer demand throughout the entire system increases by about 11% for reservoirs open, the median serviceability for the most populated areas increases by more than double this amount (23%) when the out-of-service reservoirs are opened. By increasing water supply serviceability, opening reservoirs also reduces vulnerability to fire and fire spreading. Opening the reservoirs immediately after a serious earthquake improves serviceability so significantly in densely populated areas that it is a plausible strategy for emergency response, even though such action will require water purification notices to be issued for the entire system.

The simulations performed for this study illustrate how complex system decisions involving long-term water quality standards and short-term emergency response measures can be supported by advanced systems modeling. Work, such as this, that links emergency response with public health decisions provides a good example of how system modeling provides the basis for decisions about earthquake effects on a regional scale and the complex performance of critical lifeline networks.

7.7 Future Research Directions

System simulations for multiple hydraulic network improvement strategies should be run in conjunction with optimization algorithms designed for evaluating factors such as cost and improved serviceability return so that the most cost-effective modifications of the system can be identified. For example, it would be useful to

explore strategies to increase post-earthquake serviceability performance in the vulnerable GH and FH water service areas. Results for such simulation and optimization runs would aid in system planning and funding allocation decisions. Exploring network improvement strategies for the aggregated LADWP seismic hazard will provide for a systematic optimization to address all major sources of earthquake activity.

As previously indicated, it is well recognized that PGD is one of the most pervasive causes of lifeline damage during earthquakes (O'Rourke, 1998). Although the severity of the lifeline damage caused by PGD is well documented and significant emphasis has been placed on it in guidelines for seismic design (e.g., ASCE, 1984; O'Rourke and Liu, 1999; Honegger and Nyman, 2004), there is no single method or approach that is currently adaptable for systematic application in the simulations for all 59 scenario earthquakes. Additional research is needed to develop a methodology for predicting PGD in a way suitable for reliable estimates of damage to underground pipelines and related water supply facilities.

This work shows that demand is the most important parameter affecting post-earthquake water system performance and operability on both a system-wide and local level. It was assumed for the actual Northridge earthquake and repeat Northridge earthquake scenarios that damage in the distribution networks adds to the pre-earthquake demand to generate post-earthquake flows. In other words, the pre-earthquake demand doesn't change. The favorable agreement between simulated system performance and the actual system performance after the Northridge earthquake implies that the demand conditions in the model are consistent with actual demands. It is important to recognize, however, that the actual demand after an

earthquake depends on water usage that may decline as people leave areas of heaviest damage. On the other hand, building and facility damage will often be accompanied by rupture or leakage in water service connections so that substantial water losses occur even if there is no intentional water usage in buildings abandoned or under-utilized after an earthquake. More research is needed to understand and quantify the actual post-earthquake demands in the local distribution systems as a function of changes in water usage and elevated levels of damage.

Currently, the GIRAFFE modeling approach transforms a damage state into an operational state by removing all pipelines that do not satisfy a minimum pressure tolerance, thus removing unreliable portions of the system to display the remaining part of the network that meets threshold serviceability requirements for minimum pressure tolerance. Within the first 24 hours after an earthquake, this provides a reasonable representation of system performance, and provides results that compare favorably with observed system response following the Northridge earthquake. For longer periods after the earthquake, portions of the system would be restored or re-configured. Work currently pursued by Çağnan and Davidson (2007) provides an avenue for improving the model and its application to restoration beginning 24 to 48 hours after an earthquake.

This research shows that water system performance, particularly as it relates to fire protection, is important for the operation of other infrastructure such as electric power, telecommunications, and transportation. Information regarding water supply disruption would be useful input into models being developed for the prediction of fire spread and impact. Further work focusing on the integration of the model for water supply with models for fire spread and impact would be valuable.

Limitations in current hydraulic network analysis software prevent the modeling of premise-logic-controls (PLCs) designed by LADWP to model the operational status of pumps. PLCs are a complex set of rules designed for many of the pump stations that relate pump operational status with water levels in associated tanks, pressures at nearby nodes, the operational status of other pumps, and flows in nearby system components. In this work, pumps that turn on and off based on a complex set of logic rules involving pressures, nearby tank levels and time of day, were configured to an equivalent state producing average system behavior for a 24 hour period. Further investigation into methods of incorporating PLCs is recommended.

CHAPTER 8

REFERENCES

- 9/11 Commission, (2005). *Final Report of the National Commission on Terrorist Attacks Upon the United States*.
<http://www.9-11commission.gov/report/911Report.pdf>
- Abrahamson, N.A. and Silva, W.J. (1997). "Empirical Response Spectral Attenuation Relations for Shallow Crustal Earthquakes." *Seismological Research Letters*, Vol. 68, No. 1, 94-127.
- Adams, M. (2008). Personal Communication.
- Armando, L. (1987). *Handbook of Hydraulic Engineering*. John Wiley & Sons, NY.
- ASCE (1984). "Guidelines for the Seismic Design of Oil and Gas Pipeline Systems." *ASCE TCLEE Committee on Gas and Liquid Fuel Lifelines*, ASCE, Reston, VA., 473 p.
- Ballantyne, D.B., Berg, E., Kennedy, J., Reneau, R., and Wu, D. (1990). "Earthquake Loss Estimation Modeling of the Seattle Water System." *Technical Report*. Kennedy/Jenks/Chilton, Federal Way, Wash, WA.
- Bardet, J.P., Mace, N., Tobita, T., and Hu, J. (1999a). "Large Scale Modeling of Liquefaction-Induced Ground Deformation Part I: A Four-Parameter MLR Model." *Proceedings of the 7th US-Japan Workshop on Earthquake Resistant Design of Lifeline Facilities and Countermeasures Against Soil Liquefaction*, MCEER-99-0019, Multidisciplinary Center for Earthquake Engineering Research, Buffalo, NY, 155-174.
- Bardet, J.P., Tobita, T., Mace, N., and Hu, J. (1999b). "Large Scale Modeling of Liquefaction-Induced Ground Deformation Part I: MLR Model Applications and Probabilistic Model." *Proceedings of the 7th US-Japan Workshop on Earthquake Resistant Design of Lifeline Facilities and Countermeasures Against Soil Liquefaction*, MCEER-99-0019, Multidisciplinary Center for Earthquake Engineering Research, Buffalo, NY, 175-190.
- Boore, D.M., Joyner, W.B., and Fumal, T.E. (1997). "Equations for Estimating Horizontal Response Spectra and Peak Acceleration from Western North American Earthquakes: A Summary of Recent Work." *Seismological Research Letters*, Vol. 68, No. 1, 128-153.

- Brown, K.J., Rugar, P.J., Davis, C.A., and Rulla, T.A. (1995). "Seismic Performance of Los Angeles Water Tanks." *Proceedings of the 4th U.S. Conference on Lifeline Earthquake Engineering*. ASCE, San Francisco, CA, 668-675.
- Bruneau, M., Chang, S.E., Eguchi, R.T., Lee, G.C., O'Rourke, T.D., Reinhorn, A.M., Shinozuka, M., Tierney, K., Wallace, W.A., and Winterfeldt, D. (2003). "A Framework to Quantitatively Assess and Enhance the Seismic Resilience of Communities." *Earthquake Spectra*, Vol. 19, No. 4, 733-752.
- Çağnan, Z. (2005). "Post-earthquake Restoration Modeling for Critical Lifeline Systems." *Ph.D. Dissertation*, School of Civil & Environmental Engineering, Cornell University, Ithaca, NY.
- Çağnan, Z., Davidson, R., and Guikema, S. (2006). "Post-earthquake Restoration Planning for Los Angeles Electric Power." *Earthquake Spectra*, Vol. 22, No. 3, 1-20.
- Çağnan, Z., and Davidson, R. (2007). "Discrete Event Simulation of the Post-earthquake Restoration Process for Electric Power Systems", *International Journal of Risk Assessment and Management*, Vol 7, No, 8, 1138-1156.
- Campbell, K.W., and Bozorgnia, Y. (2003). "Updated Near-Source Ground Motion (Attenuation) Relations for the Horizontal and Vertical Components of Peak Ground Acceleration and Acceleration Response Spectra." *Bulletin of the Seismological Society of America*, Vol. 93, No. 1, 314-331.
- Chang, S.E., Pasion, C., Tatebe, K., and Ahmad, R. (2008). "Linking Lifeline Infrastructure Performance and Community Disaster Resilience: Models and Multi-Stakeholder Processes." *Technical Report MCEER-08-0004*. Multidisciplinary Center for Earthquake Engineering Research, Buffalo, NY.
- Chang, S.E., Rose, A., Shinozuka, M., Svekla, W.D., and Tierney, K.J. (2000a). "Modeling Earthquake Impact on Urban Lifeline Systems: Advances and Integration." *Research Progress and Accomplishments: 1999-2000*, Multidisciplinary Center for Earthquake Engineering Research, Buffalo, NY.
- Chang, S.E., Seligson, H.A., and Eguchi, R.T. (1996). "Estimation of the Economic Impact of Multiple Lifeline Disruption: Memphis Light, Gas and Water Division Case Study." *Technical Report NCEER-96-0011*, National Center for Earthquake Engineering Research, Buffalo, NY.
- Chang, S.E., Shinozuka, M., and Moore II, J.E. (2000b). "Probabilistic Earthquake Scenarios: Extending Risk Analysis Methodologies to Spatially Distributed Systems." *Earthquake Spectra*, Vol. 16, No.3, 557-572.

- Chang, S.E., Svekla, W.D., and Shinozuka, M. (2002). "Linking Infrastructure and Urban Economy: Simulation of Water Disruption Impacts in Earthquakes." *Environment and Planning B*, Vol. 29, No. 2, 281-301.
- Chapin, D. (2001). Personal Communication.
- Davis, C.A. (2007). Personal Communication.
- Davis, C.A., Hu, J., O'Rourke, T.D., and Bonneau, A. (2007). "Seismic Performance Evaluation of LADWP Water System Using GIRAFFE." *Proceedings, 5th U.S.-Japan Workshop on Seismic Performance of Water Supplies*, Oakland, CA, Sponsored by American Water Works Association Research Foundation and Japan Water Works Association, 13p.
- Duke, C.M. and Moran, D.F. (1972). "Earthquakes and City Lifelines." *San Fernando Earthquake of February 9, 1971 and Public Policy*, Gate, G. O., ed., Joint Committee on Seismic Safety, California Legislature, San Jose, CA, 132p.
- Eguchi, R.T. (1982). "Earthquake Performance of Water Supply Components during the 1971 San Fernando Earthquake." *Technical Report 82-1396-2a*. J.H. Wiggins Company, Redondo Beach, CA.
- Eguchi, R.T. and Chung, R.M. (1995). "Performance of Lifelines during the January 17, 1994 Northridge Earthquake." *Lifeline Earthquake Engineering, TCLEE Monograph No. 6*. O'Rourke, M.J. ed., ASCE, Reston, VA, 120-127.
- Eguchi, R.T., Taylor, C.E., and Hasselman, T.K. (1983). "Earthquake Vulnerability Models for Water Supply Components." *Technical Report No. 83-1396-2c*. Prepared for the National Science Foundation, J.H. Wiggins Company, Redondo Beach, CA.
- Environmental Protection Agency, USA (EPA, 2007).
<http://www.epa.gov/nrmrl/wswrd/dw/epanet.html>
- Farrenkopf, P. (2005). Personal Communication.
- Federal Emergency Management Agency (FEMA, 1999). *HAZUS99 Technical Manual*. FEMA, Washington, D. C.
- Federal Emergency Management Agency (FEMA, 2006). *HAZUS-MH MR2 Technical Manual*. FEMA, Washington, D. C.
- Federal Emergency Management Agency (FEMA, 2002). "World Trade Center Building Performance Study: Data Collection, Preliminary Observations, and Recommendations." *FEMA 403*, FEMA, Washington, D. C.

- Federal Emergency Management Agency (FEMA, 2003). *FEMA-450: NEHRP Recommended Provisions for Seismic Regulations for New Buildings and Other Structures*. 2003 Edition, Washington, D. C., Developed by the Building Seismic Safety Council (BSSC) for FEMA.
- Fire Department of New York (FDNY, 2005).
<http://www.nyc.gov/html/fdny/html/home2.shtml>
- Hall, J.F. (1995). "Northridge Earthquake of January 17, 1994, Reconnaissance Report." *Earthquake Spectra*, EERI, Oakland, CA, April.
- Honegger, D. and Nyman, D.J. (2004) "Guidelines for the Seismic Design and Assessment of Natural Gas and Liquid Hydrocarbon Pipelines." *Pipeline Research Council International, Inc.*, Catalog No. L51927, Houston, TX.
- Hwang, H.H.M., Lin, H., and Shinozuka, M. (1998). "Seismic Performance Assessment of Water Delivery Systems." *Journal of Infrastructure Systems*, ASCE, Vol. 4, No. 3, 118-125.
- Jeon, S.-S. (2002). "Earthquake Performance of Pipelines and Residential Buildings and Rehabilitation with Cast-in-Place Pipe Lining Systems." *Ph.D. Dissertation*, School of Civil & Environmental Engineering, Cornell University, Ithaca, NY.
- Jeon, S.-S. and O'Rourke, T.D. (2005). "Northridge Earthquake Effects on Pipelines and Residential Buildings." *Bulletin of the Seismological Society of America*, Vol. 95, No.1, 294-318.
- Jeppson, R.W. (1976). *Analysis of Flow in Pipe Networks*. Ann Arbor Science Publisher, Ann Arbor, MI.
- Keen, Peter G.W. (1980). "Adaptive Design for Decision Support Systems." *ACM/Data Base*, Vol. 12, No. 1-2, 15-25.
- Khater, M.M. and Grigoriu, M.D. (1989). "Graphical Demonstration of Serviceability Analysis." *Proceedings of the 5th International Conference on Structural Safety and Reliability*, San Francisco, CA, August, 525-532.
- Khater, M.M. and Waisman, F. (1999). "Small Diameter Pipelines Sensitivity Analysis." *Internal Report from National Institute of Building Sciences*, Washington, D.C.

- Lawson, A. C. (1908). "The California Earthquake of April 18, 1906." *Report of the State Earthquake Investigation Commission*, Carnegie Institute of Washington, No. 87, Vol. I, 451p.
- Lee, J., Graf, W., Somerville, P., O'Rourke, T.D., and Shinozuka, M. (2005). "Development of Earthquake Scenarios for Use in Earthquake Risk Analysis for Lifeline Systems." *Report for the Los Angeles Department of Water and Power*, Los Angeles, CA, 34p.
- Lund, L. and Cooper, T. (1995). "Water System." *Northridge Earthquake: Lifeline Performance and Post-Earthquake Response, Technical Council on Lifeline Earthquake Engineering Monograph No. 8*, Schiff, A.J., ed., ASCE, New York, NY, 96-131.
- Lund, L., Davis, C. A., and Adams, M. L. (2005). "Water System Seismic Performance 1994 Northridge-1995 Kobe Earthquakes." *Proceedings of 4th Japan-US Workshop on Seismic Measures for Water Supply*. AWWARF/FWWA, Kobe, Japan, Jan. 26-28.
- Manson, M. (1908). *Reports on an Auxiliary Water Supply System for Fire Protection for San Francisco, California*. Board of Public Works, San Francisco, CA.
- Markov, I., Grigoriu, M.D., and O'Rourke, T.D. (1994). "An Evaluation of Seismic Serviceability Water Supply Networks with Application to the San Francisco Auxiliary Water Supply System." *Technical Report NCEER-94-0001*, National Center for Earthquake Engineering Research, Buffalo, NY.
- National Institute of Building Sciences (NIBS, 1997). *Earthquake Loss Estimation Methodology HAZUS 97: Technical Manual*. Prepared for Federal Emergency Management Agency, Washington, D.C.
- National Institute of Standards and Technology (NIST, 2005). *Final Report on the Collapse of the World Trade Center Towers*.
http://wtc.nist.gov/reports_october05.htm.
- New York City Department of Environmental Protection (NYC DEP, 2005).
<http://www.ci.nyc.ny.us/html/dep/home.html>
- O'Rourke, M.J. and Liu, X. (1999). "Response of Buried Pipelines Subject to Earthquake Effects." *Monograph No. 3*, Multidisciplinary Center for Earthquake Engineering Research, Buffalo, NY, 248 p.
- O'Rourke, M.J. and So, P. (2000). "Seismic Fragility Curves for On-Grade Steel Tanks." *Earthquake Spectra*, Vol. 16, No. 4, 801-815.

- O'Rourke, T.D. (1993). "Prospectus for Lifelines and Infrastructure Research." *The Art and Science of Structural Engineering*, N.K. Khachaturian, ed., Prentice-Hall, Inc., 37-58.
- O'Rourke, T.D. (1996). "Lifeline Engineering: State-of-the-Art." *Eleventh World Conference on Earthquake Engineering*, Paper No. 2172, ISBN No. 008-042822-3, Pergamon, Oxford, UK.
- O'Rourke, T.D. (1998). "An Overview of Geotechnical and Lifeline Earthquake Engineering." *Geotechnical Special Publication No. 75*, ASCE, Reston, VA.
- O'Rourke, T.D. (2007). "Critical Infrastructure, Interdependencies, and Resilience." *The Bridge*, National Academy of Engineering.
- O'Rourke, T.D., Bonneau, A., Pease, J., Shi, P., and Wang, Y. (2006). "Liquefaction Ground Failures in San Francisco." *Earthquake Spectra*, EERI, Oakland, CA, *Special 1906 San Francisco Earthquake* Vol. 22, No. 52, 691-6112.
- O'Rourke, T.D., Lembo, A.J., and Nozick, L.K. (2003). "Lessons Learned from the World Trade Center Disaster About Critical Utility Systems." *Beyond September 11th: an Account of Post Disaster Research*, Natural Hazards Research and Applications Information Center, Boulder, CO, 269-292.
- O'Rourke, T.D., Lembo, A.J., Nozick, L.K., and Bonneau, A.L. (2005a). "Resilient Infrastructure: Lessons from the WTC." *Crisis Response Journal*, Vol. 1, Issue 4, 40-42.
- O'Rourke, T.D., Lembo, A.J., Nozick, L.K., and Bonneau, A.L. (2005b). "Resilient Infrastructure: Lessons from the WTC." *Crisis Response Journal*, Vol. 2, Issue 1, 48-50.
- O'Rourke, T. D., Lembo, A.J., Nozick, L.K., and Bonneau, A.L. (2005c). "Resilient Infrastructure: Lessons from the WTC." *Crisis Response Journal*, Vol. 2, Issue 2, 44-47.
- O'Rourke, T.D. and Pease, J.W. (1992). "Large Ground Deformations and Their Effects on Lifeline Facilities: 1989 Loma Prieta Earthquake." *Case Studies of Liquefaction and Lifeline Performance During Past Earthquakes*, NCEER-92-0002, T.D. O'Rourke and M. Hamada, eds., National Center for Earthquake Engineering Research, Buffalo, NY, 5-1 - 5-85.
- O'Rourke, T.D., Stewart, H.E., and Jeon, S-S. (2001). "Geotechnical Aspects of Lifeline Engineering." *Geotechnical Engineering*, ICE, Vol. 149, No. 1, 13-26.

- O'Rourke, T.D., Wang, Y., and Shi, P. (2004). "Advances in Lifeline Earthquake Engineering." *Keynote Lecture of the 13th World Conference on Earthquake Engineering*, Paper No. 5003, Vancouver, B.C., Canada.
- Public Broadcasting Systems, (PBS, 2005).
<http://www.pbs.org/wnet/heroes/history2.html>
- Puchovsky, M.T. (1999). *Automatic Sprinkler Systems Handbooks*, National Fire Protection Association (NFPA).
- Ronald, E.W., Raymond, H.M., and Sharon, L.M. (1998). *Probability and Statistics for Engineering and Scientists*. 6th Edition, Prentice Hall/Upper Saddle River, NJ.
- Rose, A. (2006). "Innovation, Smart Growth, and Disaster-Resilient Communities." Paper presented at the Tinbergen Institute Symposium on Innovation, Smart Growth, Technology and Sustainable Development, Amsterdam, The Netherlands.
- Rose, A., Benavides, J., Chang, S., Szczesniak, P., and Lim, D. (1997). "The Regional Economic Impact of an Earthquake: Direct and Indirect Effects of Electricity Lifeline Disruptions." *Journal of Regional Science*, Vol. 37, Issue 3, 437-458.
- Rose, A. and Liao, S.-Y. (2003). "Understanding Sources of Economic Resiliency to Hazards: Modeling the Behavior of Lifeline Service Customers." *Research Progress and Accomplishments 2001-2003*, Multidisciplinary Center for Earthquake Engineering Research, Buffalo, NY, 149-160.
- Rose, A. and Liao, S.-Y. (2005). "Modeling Regional Economic Resilience to Disasters: A Computable General Equilibrium Analysis of Water Service Disruptions," *Journal of Regional Science* Vol. 45, Issue 1, 75-112.
- Sadigh, S., Chang, C.-Y., Egan, J.A., Makdisi, F., and Youngs, R.R. (1997). "Attenuation Relationships for Shallow Crustal Earthquakes Based on California Strong Motion Data." *Seismological Research Letters*, Vol. 68, No. 1, 180-189.
- Scawthorn, C., Porter, K., and Blackburn, F.T. (1992). "Performance of Emergency Services After the Earthquake." *The Loma Prieta Earthquake of October 17, 1989-Marina District, USGS Prof. Paper 1551-F*, T.D. O'Rourke and T. Holzer, eds., US Government Printing Office, Washington, DC.

- Scawthorn, C., O'Rourke, T.D., and Blackburn F.T. (2006). "The San Francisco Earthquake and Fire of 1906 - Enduring Lessons for Fire Protection and Water Supply." *Earthquake Spectra*, Vol. 22, The 1906 San Francisco Commemorative Issue.
- Schussler, H. (1906). *The Water Supply of San Francisco, California*. Martin B. Brown Press, New York, NY.
- Schwab, F. and Knoff, L. (1977). "Fast Surface Waves and Free Mode Computations." *Seismology: Surface Waves and Earth Oscillation Methods in Computation, Physics 11*, Academic Press, NY, 87-180.
- Sheldon, M.R. (2000). *Introduction to Probability and Statistics for Engineers and Scientists*. 2nd Edition, Harcourt and Technology Company, San Diego, CA.
- Shi, P. (2006). "Seismic Response Modeling of Water Supply Systems." *Ph.D. Dissertation*. Cornell University, Ithaca, NY.
- Shi, P., T.D. O'Rourke, and Wang, Y. (2006). "Simulation of Earthquake Water Supply Performance." *Proceedings of the 8th National Conference on Earthquake Engineering*, Paper No. 8NCEE-001295, EERI, Oakland, CA.
- Shinozuka, M., Feng, M., Dong, X., Chang, S. E., Cheng, T. -C., Jin, X., and Ala Saadeghvaziri, M. (2003). "Advances in Seismic Performance Evaluation of Power Systems." *MCEER Research Progress and Accomplishments 2001-2003, MCEER-03-SP01*, Multidisciplinary Center for Earthquake Engineering Research, Buffalo, NY, 1-15.
- Shinozuka, M., Hwang, H., and Murata, M. (1992). "Impacts on Water Supply of a Seismically Damaged Water Delivery System." *Lifeline Earthquake Engineering in the Central and Eastern US, Technical Council on Lifeline Earthquake Engineering Monograph No.5*. Ballantyne, D.B., ed., ASCE, Reston, VA, 43-57.
- Shinozuka, M., Rose, A., and Eguchi, R.T., eds. (1998). "Engineering and Socioeconomic Impacts of Earthquakes." *Multidisciplinary Center for Earthquake Engineering Research Monograph Series 2*. Multidisciplinary Center for Earthquake Engineering Research, Buffalo, NY.
- Shinozuka, M., Tan, R.Y., and Toike, T. (1981). "Serviceability of Water Transmission Systems under Seismic Risk." *Lifeline Earthquake Engineering, the Current State of Knowledge, 1981*, ASCE, New York, NY.
- Smith, D. (2002). *Report from Ground Zero: the Story of the Rescue Efforts at the World Trade Center*. Viking Press, New York, NY.

- Sprague Jr., R.H. and Watson, H., eds. (1989). *Decision Support Systems, Putting Theory into Practice, 2nd ed.* Prentice Hall, New Jersey.
- Steinbrugge, K.V., Schader, E.E., Bigglestone, H.C., and Weers, C.A. (1971). *San Fernando Earthquake, February, 9, 1971.* Pacific Fire Rating Bureau.
- Subcommittee on Water and Sewerage Systems (1973). "Earthquake Damage to Water and Sewerage Facilities, San Fernando, California Earthquake of February 9, 1971." *U.S. Department of Commerce, N.O.A.A., Washington, D.C., Vol. 2, 75-193.*
- Toprak, S. (1999). "Earthquake Effects on Buried Lifeline Systems." *Ph.D. Dissertation*, School of Civil & Environmental Engineering, Cornell University, Ithaca, NY.
- Turban, E. (1995). *Decision Support and Expert Systems, Management Support Systems, 4th ed.*, Prentice Hall, New Jersey.
- United States Geological Survey (USGS, 2005). <http://earthquake.usgs.gov/hazmaps/>
- Wang, Y. (2006). "Seismic Performance Evaluation of Water Supply Systems." *Ph.D. Dissertation*, School of Civil & Environmental Engineering, Cornell University, Ithaca, NY.
- Wang, Y. and O'Rourke, T.D. (2007). "Characterizations of Seismic Risk in Los Angeles Water Supply System." *Proceedings of the 5th China-Japan-US Trilateral Symposium on Lifeline Earthquake Engineering*, Haikou, China, Zhou X., Tanaka, Y., and Bardet, J. P., eds., 391-399.
- Wills, C. J., Petersen, M., Bryant, W. A., Reichle, M., Saucedo, G. J., Tan, S., Taylor, G., and Treiman, J. (2000). "A Site-Conditions Map for California Based on Geology and Shear Wave Velocity." *Bulletin of Seismological Society of America*, Vol. 90, No. 6B, S187-S208.
- Zimmerman, R. (2003). "Public Infrastructure Service Flexibility for Response and Recovery in the Attacks at the World Trade Center, September 11, 2001." *Beyond September 11th: An Account of Post-disaster Research, Program on Environment and Behavior Special Publication #39*, Natural Hazards Research and Information Center, University of Colorado, Boulder, CO, 241-268.

APPENDIX A

ADJUSTMENTS FOR VARIABLE DEMAND IN FRAGILITY RELATIONS FOR LOCAL WATER DISTRIBUTION NETWORKS

This appendix provides supplemental information associated with Chapter 3 that relates to nodal demand modeling.

Fragility curves for various portions of the water distribution system are defined on the basis of normalized demand, i.e., the water after an earthquake required at a demand node divided or normalized with respect to water required under normal operating conditions. The water required under normal conditions is referred to as the estimated demand. It varies throughout the day and throughout the year. The fragility curves are defined according to a reference estimated demand, taken as the average daily summer demand. The fragility curves are thus normalized according to this summer demand, and simulations for another demand need to 1) use fragility curves developed explicitly for that demand or, 2) adjust the fragility curves for summer demand with a conversion factor to produce the fragility curves for the desired demand.

To obtain a conversion factor, let D_S represent average daily summer demand, and ΔD_S represent change in summer demand due to earthquake damage. Normalized summer demand, ND_S , is calculated by:

$$ND_S = \frac{D_S + \Delta D_S}{D_S} \quad (1)$$

and modified normalized demand, MND , is given by:

$$MND = \left[\frac{D_s + \Delta D_s}{D_s} \right] \frac{D_s}{D_d} \quad (2)$$

in which D_d is the demand for a design state other than the average daily summer demand.

Rearranging the terms in Equation 2 yields,

$$\frac{\Delta D_s}{D_d} = MND - \frac{D_s}{D_d} \quad (3)$$

The normalized demand for the alternate design state, D_d , is

$$ND_d = \frac{D_d + \Delta D_d}{D_d} \quad (4)$$

We estimate $\Delta D_d = \alpha \Delta D_s$, where α is a scaling factor and function of the design state demand. Using this estimate with Equation 4, we get

$$ND_d = 1 + \alpha \frac{D_s}{D_d} \quad (5)$$

Combining Equations 2, 3 and 5 results in

$$ND_d = 1 + \alpha \frac{D_s}{D_d} (ND_s - 1) \quad (6)$$

which can be used to convert the normalized demand for summer to the normalized demand for a different design state, such as the average daily winter demand.

In this work, Equation 6 was used with $\alpha = 1$ to convert the fragility curves for summer demand to those for winter demand. Taking $\alpha = 1$ provides a simple and convenient conversion process and does not require the development of fragility curves for winter demand through multiple numerical simulations of various portions of the water distribution system. It assumes that changes in winter demand for various damage states are sufficiently close to changes in summer demand that parity in the demand changes can be assumed with acceptably low error.

To evaluate the validity of this assumption and to study the hydraulic network response of the distribution system under various damage states, numerical simulations were performed for average daily winter demand on a portion of the LADWP distribution system: Zone 1000, which is shown in Figure A.1. The distribution network model includes distribution pipelines and a portion of the trunk line system in the vicinity of the local distribution network. To illustrate better the locations of trunk and distribution pipelines, the relevant portion of the LADWP trunk line system model is superimposed on each distribution network.

The numerical simulation process and development of normalized demand curves for the winter demand were identical to those procedures followed by Shi (2006) in developing fragility curves for summer demands. Flows were monitored in representative trunk lines before and after earthquake damage to distribution networks. The flows after damage were normalized with respect to those before damage. Figure A.2 shows the results of the simulated (modeled) ND_w for the 4 trunk line measurement locations in local distribution system Zone 1000, versus the ND_w predicted by the linear approximation explained above. Lines for -15% and +35%

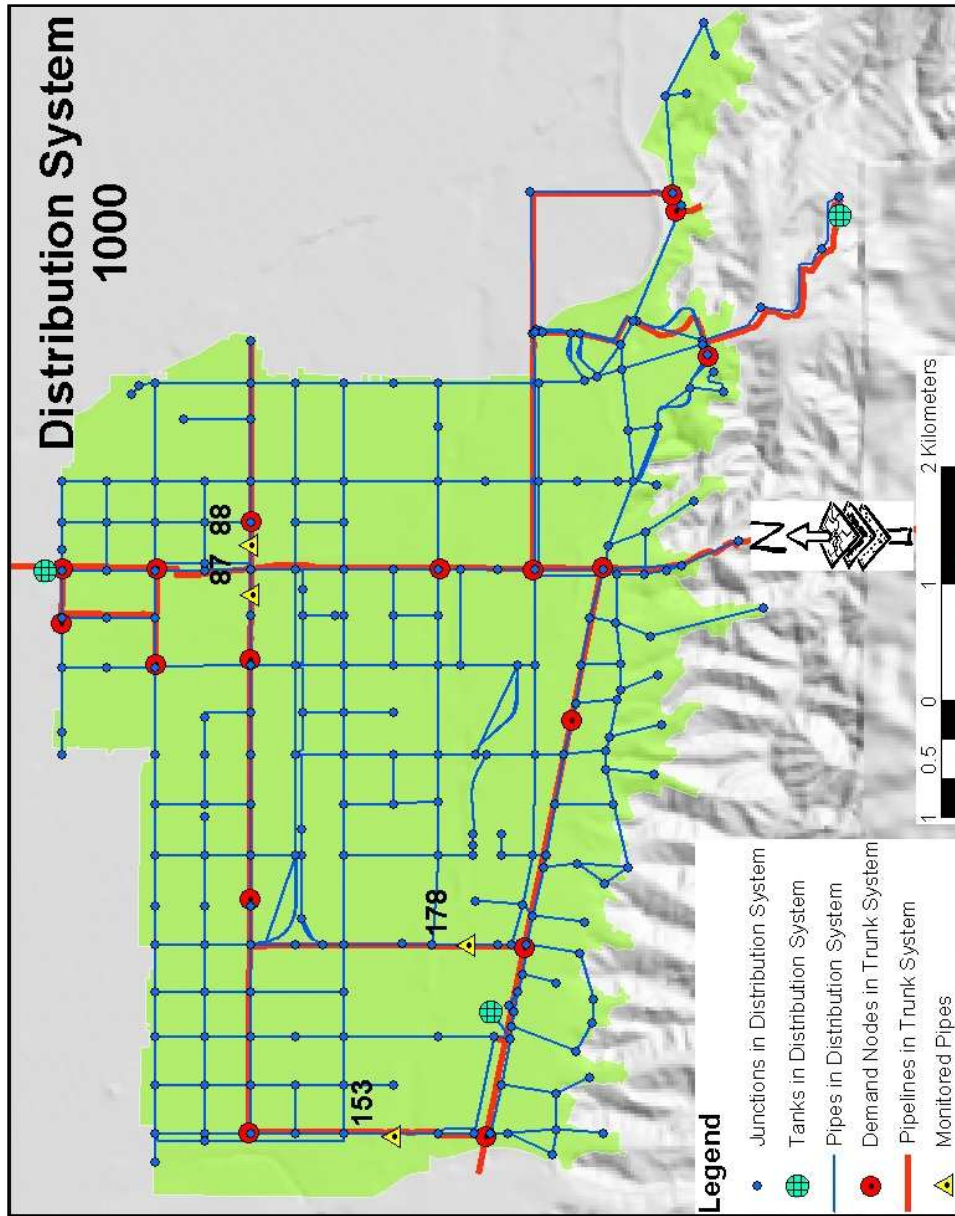


Figure A.1 Map Showing the Distribution System 1000 Hydraulic Network Model (Shi, 2006)

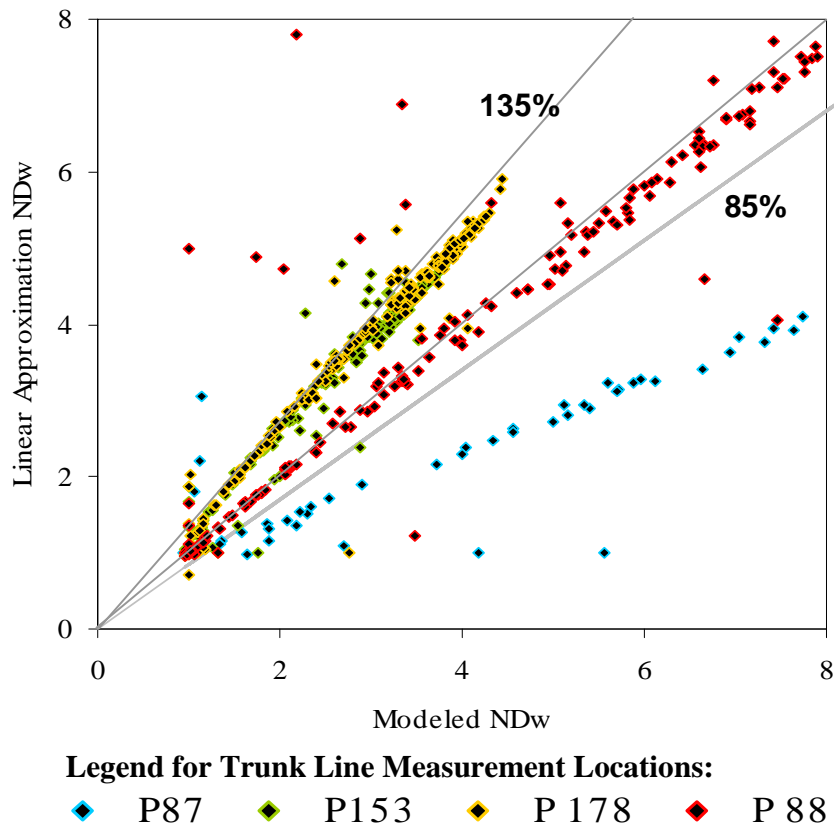


Figure A.2 Simulated vs. Linearly Approximated ND_w Values for Distribution Zone 1000

error are shown in the figure, and 70% of the data fall within these bounds. 72% of the data within these bounds falls between the 1:1 and 135% line, and 55% of all data plot above the 1:1 line.

It appears that the simulation model provides a reasonable estimation of normalized demand for most sampling locations, and overall a useful estimate of average normalized demand. It should be recognized that the simulated normalized demand has a high variability, so that simplified linear estimations may underestimate demands at some sampling locations by a relatively large margin.

APPENDIX B

LADWP TRUNK LINE DAMAGE FROM 1994 NORTHRIDGE EARTHQUAKE

This appendix updates the record of 67 locations of LADWP trunk line damage that occurred in the San Fernando Valley during the 1994 Northridge earthquake, as first compiled by Shi (2006). Closely working with LADWP engineers and their records from the Northridge earthquake, each damage location has been classified as PGD- or TGD-induced, with additional commentary when necessary. Complete descriptions of each damage location can be found in Shi (2006).

The Granada Trunk Line (GTL), Rinaldi Trunk Line (RTL), and Roscoe Trunk Line sustained severe damage during the earthquake. In total, 49 locations of damage occurred in these three trunk lines. Damage simulations of the three trunk lines are described under the first three subheadings that follow. Simulations of the other 18 locations of damage are described under the fourth subheading.

B.1 Granada Trunk Line

Figure B.1 shows the locations of Northridge earthquake damage in the GTL. Table B.1 gives detailed information for each damage location. Eight breaks and leaks in the vicinity of the Upper Debris Basin on the Van Norman Complex can be attributed to PGD effects. A break that caused approximately 508 mm (20in.) of separation at 11661 Balboa Blvd. and resulted in open channel flow, and compression failure just south of this break were both PGD-induced damage locations.

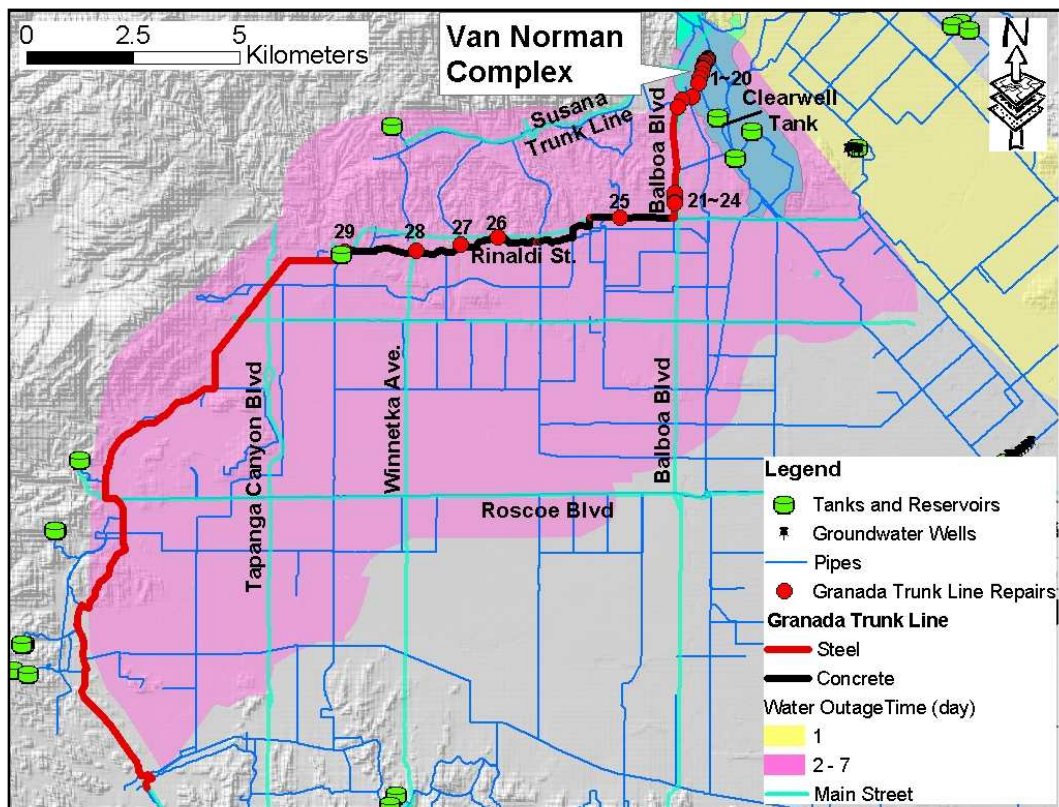


Figure B.1 Granada Trunk Line Repairs (Shi, 2006)

Table B.1 Granada Trunk Line Damage Information Summary

ID	Trunk Line	PGD or TGD	Location	Dia. (mm)	Pipe Material	Damage Descriptions	Hydraulic Modeling Assumptions	
							Leak/Break	Leak Dia. (mm)
1		PGD	Upper Debris Basin under Dike	1257	Steel	Crack at joint, approximate 300 mm long		
2		PGD	Upper Debris Basin under Dike	1257	Steel	Crack at joint, approximate 300 mm long Jagged tears, folded inward 76 mm, separated several tens mm, identified as major break by Davis (1999)		
3		PGD	Upper Debris Basin Sta. 3+68	1257	Steel	Jagged tears, folded inward 76 mm, separated several tens mm, identified as major break by Davis (1999)		
4		PGD	Upper Debris Basin Sta. 3+72	1257	Steel	Spigot flared inward 13 mm, compression		
5	Granada Trunk Line	PGD	Upper Debris Basin Sta. 6+21	1257	Steel	Folded inward and separated, identified as major break by Davis (1999) Jagged tears, folded inward 76 mm, separated several tens mm, identified as major break by Davis (1999)	Not modeled because Granada Trunk Line is completely disconnected downstream	N/A ¹
6		PGD	Upper Debris Basin Sta. 6+21	1257	Steel	Folded inward and separated 292 mm residual compressional displacement, coupling compressed 305 mm, slammed together, and separated 12 mm		
7		PGD	Upper Debris Basin Sta. 0+3.4 Relocated Line	1257	Steel	50 to 76 mm inside bulge, buckling at joint		
8		PGD	Upper Debris Basin Sta. 0+4.4 Relocated Line	1257	Steel	Crack at joint, approximate 300 mm long		
9		TGD	Utility Corridor, Sta 0+91.70	1257	Steel	Crack at joint, approximate 300 mm long		
10		TGD	Utility Corridor, Sta. 3+39 to 3+48	1257	Steel	Jagged tears, folded inward 76 mm, separated several tens mm, identified as major break by Davis (1999)		

Table B.1 (Continued)

ID	Trunk Line	PGD or TGD	Location	Dia. (mm)	Pipe Material	Damage Descriptions	Hydraulic Modeling Assumptions	
							Leak/Break	Leak Dia. (mm)
11		TGD	Utility Corridor, Sta. 3+60	1257	Steel	50 mm compressional displacement		
12		TGD	Utility Corridor, Sta. 5+40	1257	Steel	Cement mortar failure		
13		TGD	Utility Corridor, Sta. 6+98.4	1257	Steel	76 mm extensional displacement		
14		TGD	Utility Corridor, Sta. 9+68.4	1257	Steel	76 mm extensional displacement		
15	Granada Trunk Line	TGD	Utility Corridor, Sta. 13+28.5	1257	Steel	102 mm extensional displacement	Not modeled because Granada Trunk Line is completely disconnected down stream	N/A ¹
16		TGD	Utility Corridor, Sta. 16+49.9	1257	Steel	50 mm extensional displacement		
17		TGD	Utility Corridor, Sta. 17+40	1257	Steel	Cement mortar failure		
18		TGD	Utility Corridor, Sta. 26+89.18	1257	Steel	76 mm extensional displacement		
19		TGD	Utility Corridor, Sta. 39+60	1257	Steel	30 mm extensional displacement		
20		TGD	Barboa Blvd at Valve between Woodley and Colvin	1257	Steel	Damaged and leaking, extensional movement		

Table B.1 (Continued)

ID	Trunk Line	PGD or TGD	Location	Dia. (mm)	Pipe Material	Damage Descriptions	Hydraulic Modeling Assumptions	
							Leak/Break	Leak Dia. (mm)
21	Granada Trunk Line	TGD	17200 Balboa Blvd at Lonillard	1257	Steel	Joint fracture, extensional movement	Break	N/A ¹
22		TGD	Balboa Blvd. Sta. 115+80	1257	Steel	Separated joint, tension		
23		PGD	11661 Balboa Blvd.	1257	Steel	Pulled apart 508 mm, extensional movement		
24		PGD	Balboa Blvd. Sta. 129+56	1257	Steel	Pipe telescoped inside itself, compression		
25		TGD	East of Shoshone	1220	Concrete	Unknown	Leak	122 (Scenario 1)
26		TGD	Wilbur	1220	Concrete	Unknown	Leak	122 (Scenario 1)
27		TGD	Tampa Ave. at 118 Fwy	1220	Concrete	Joint fracture, joint fractured along side existing weld	Leak	122 (Scenario 1)
28		TGD	Between Melvin & Wurmetka	1220	Concrete	Unknown	Leak	122 (Scenario 1)
29		TGD	Desoto Reservoir, North side	1220	Concrete	Joint fracture, joint fractured along side existing weld	Leak	122 (Scenario 1)

1: Not Applicable

B.2 Rinaldi Trunk Line

Figure B.2 shows the locations of Northridge earthquake damage in the RTL. Table B.2 gives detailed information for each damage location. Six separation and compression failures occurred in the RTL along Balboa Blvd., in locations parallel to the breaks in the GTL. Each of these damage locations can be attributed to PGD effects.

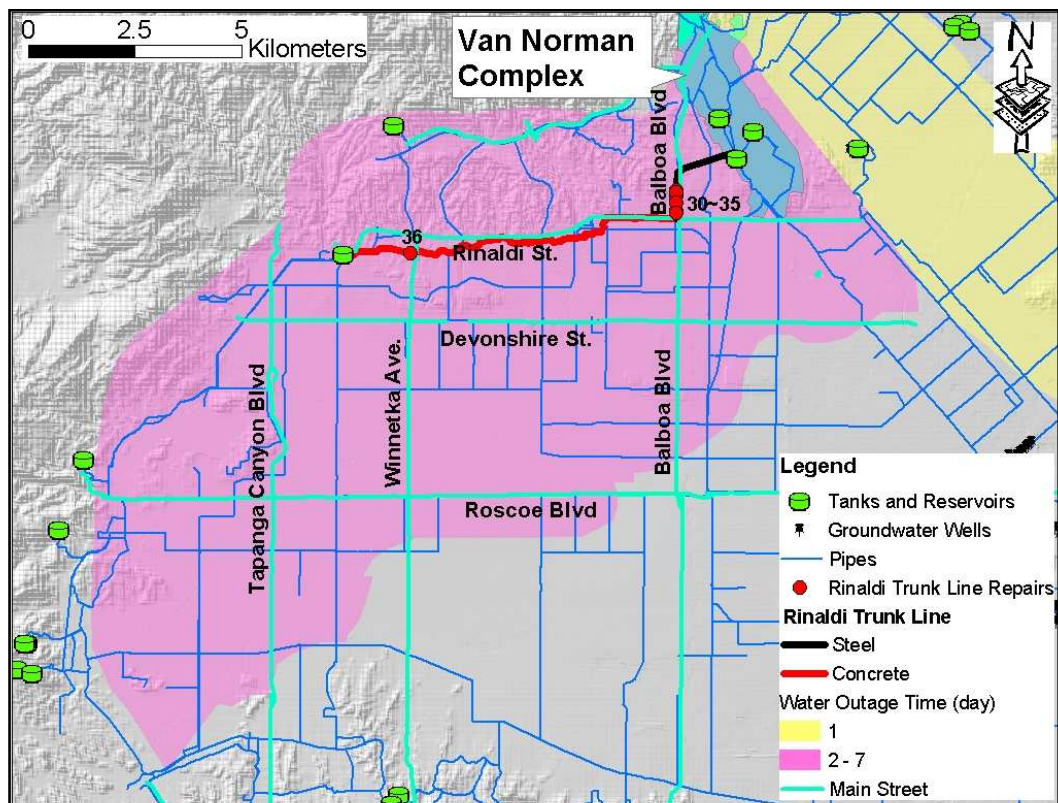


Figure B.2 Rinaldi Trunk Line Repairs (Shi, 2006)

Table B.2 Rinaldi Trunk Line Damage Information Summary

ID	Trunk Line	PGD or TGD	Location	Dia. (mm)	Pipe Material	Damage Descriptions	Hydraulic Modeling Assumptions	
							Leak/Break	Leak Dia. (mm)
30	Rinaldi Trunk Line	PGD	Balboa Blvd. 91 m North of above	1727	Steel	Extensional movement	Break	N/A ¹
31		PGD	11700 Balboa Blvd.	1727	Steel	Pulled apart 508 mm, extensional movement		
32		PGD	Balboa Blvd. Sta. 62+12	1727	Steel	13 mm separation, extensional movement		
33		PGD	Balboa Blvd. Sta. 63+72	1753	Steel	102 mm separation, extensional movement		
34		PGD	Balboa Blvd. Sta. 65+87	1727	Steel	Cement mortar failure		
35		PGD	11539 Balboa Blvd.	1727	Steel	Compression		
36		TGD	West of Winnetka St. Sta. 1219+10 (west of Melvin)	1372	Concrete	Multiple cracks in 4.9-m section of pipe, cracked at a cut-off wall		

1: Not Applicable

B.3 Roscoe Trunk Line

Figure B.3 shows the locations of Northridge earthquake damage in the Roscoe Trunk Line. Table B.3 gives detailed information for each damage location. Thirteen breaks and leaks occurred along the Roscoe Trunk Line, and while the cause of all damages is not confirmed, USGS documented PGD in the general region. Chapter 4 of this report presents the locations of four zones of PGD from Northridge earthquake PGD based on previous work conducted by Jeon (2002) and USGS. It was decided that the Roscoe Trunk Line repairs that fell within the zone of PGD in that area would be modeled as PGD-induced damage. Hence, repair locations numbered 40-46 in Figure B.3 and Table B.4 are attributed to PGD effects.

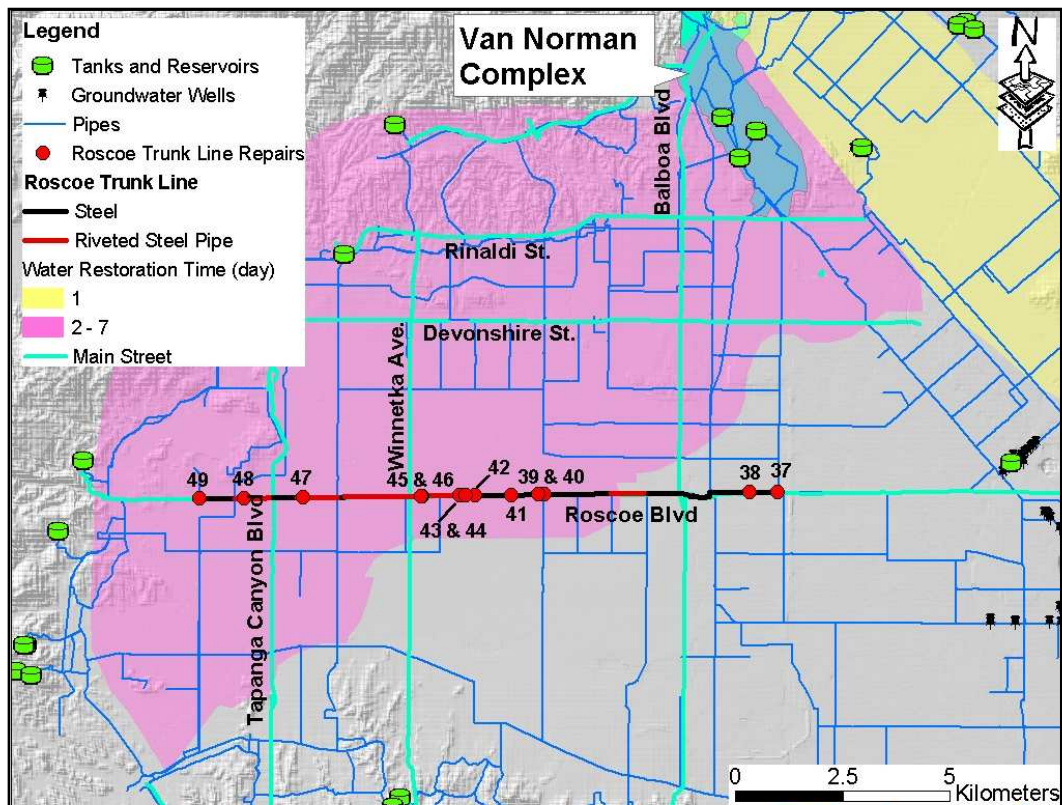


Figure B.3 Roscoe Trunk Line Repairs (Shi, 2006)

Table B.3 Roscoe Trunk Line Damage Information Summary

ID	Trunk Line	PGD or TGD	Location	Dia. (mm)	Pipe Material	Damage Descriptions	Hydraulic Modeling Assumptions	
							Leak/Break	Leak Dia. (mm)
37	Roscoe Trunk Line	TGD	Haskel Ave	1524	Steel	Unknown	Leak	147 (Scenario 5)
38		TGD	Woodley Ave	1321	Steel	Unknown		
39		TGD	Reseda Blvd.	1016	Steel	No observable pipe movement		
40		PGD	Reseda Blvd., 140 m West, 18546 Roscoe Blvd	1016	Steel	No observable pipe movement		125 (Scenario 5)
41		PGD	Wilbur Ave. 53 m East 18844 Roscoe Blvd.	1016	Steel	No observable pipe movement		
42		PGD	Tampa	1016	Steel	No observable pipe movement		
43		PGD	Calvin	1016	Riveted Steel	No observable pipe movement		251 (WA ¹)
44		PGD	Shirley Ave. 46 m East	991	Riveted Steel	No observable pipe movement		
45		PGD	Oakdale, 18 m West	1067	Riveted Steel	No observable pipe movement		254 (WA ¹)
46		PGD	Oakdale, 58 m West	1067	Riveted Steel	Unknown		
47		TGD	Canoga Ave	1295	Riveted Steel	Unknown		147 (WA ¹)
48		TGD	Faralone Ave. 171 m West 22259 Roscoe Blvd.	1372	Riveted Steel	Unknown		150 (WA ¹)
49		TGD	Fallbrook Ave. West Side	914	Riveted Steel	No observable pipe movement		100 (WA ¹)

1: Weighted Average of Orifice Dia. from All Possible Leak Scenarios according to the Probability of Each Leak Scenario

B.4 Other Trunk Lines

Figures B.4 and B.5 show the locations of 18 additional trunk line repairs that occurred in other trunk lines in the LADWP system. Tables B.4 and B.5 give detailed information for each damage location. One location in Figure B.4 and Table B.4 can be attributed to PGD effects: slip joint wrinkling that occurred on the Van Norman Pumps Station Discharge Line, just north of the Olden St. Trunk Line connection (next to the Bypass Channel). Conversations with Davis (2007) at LADWP revealed that this damage occurred as a result of the “Juvenile Hall Slide”, and was similar to a tear. Conversations with LADWP personnel also lead to the decision that the Los Angeles City Trunk Line was a leak (not a break), and was not likely caused by PGD. A riveted steel section of the City Trunk Line was severely damaged at the toe of the lower San Fernando Dam as the pipe exits the ground to pier supports. The unique conditions of pipeline transition from underground to above-ground, and deterioration from age and corrosion were most likely the main reasons for vulnerability to seismic damage. Upon post-earthquake inspection, no evidence of PGD was found in the vicinity of the City Trunk Line leak, but Davis (2007) notes that evidence could have been obscured by ground erosion from the pipe leak. The City Trunk Line leak was modeled as a 1, 451 l/s (23,000 gpm) leak, and attributed to TGD effects.

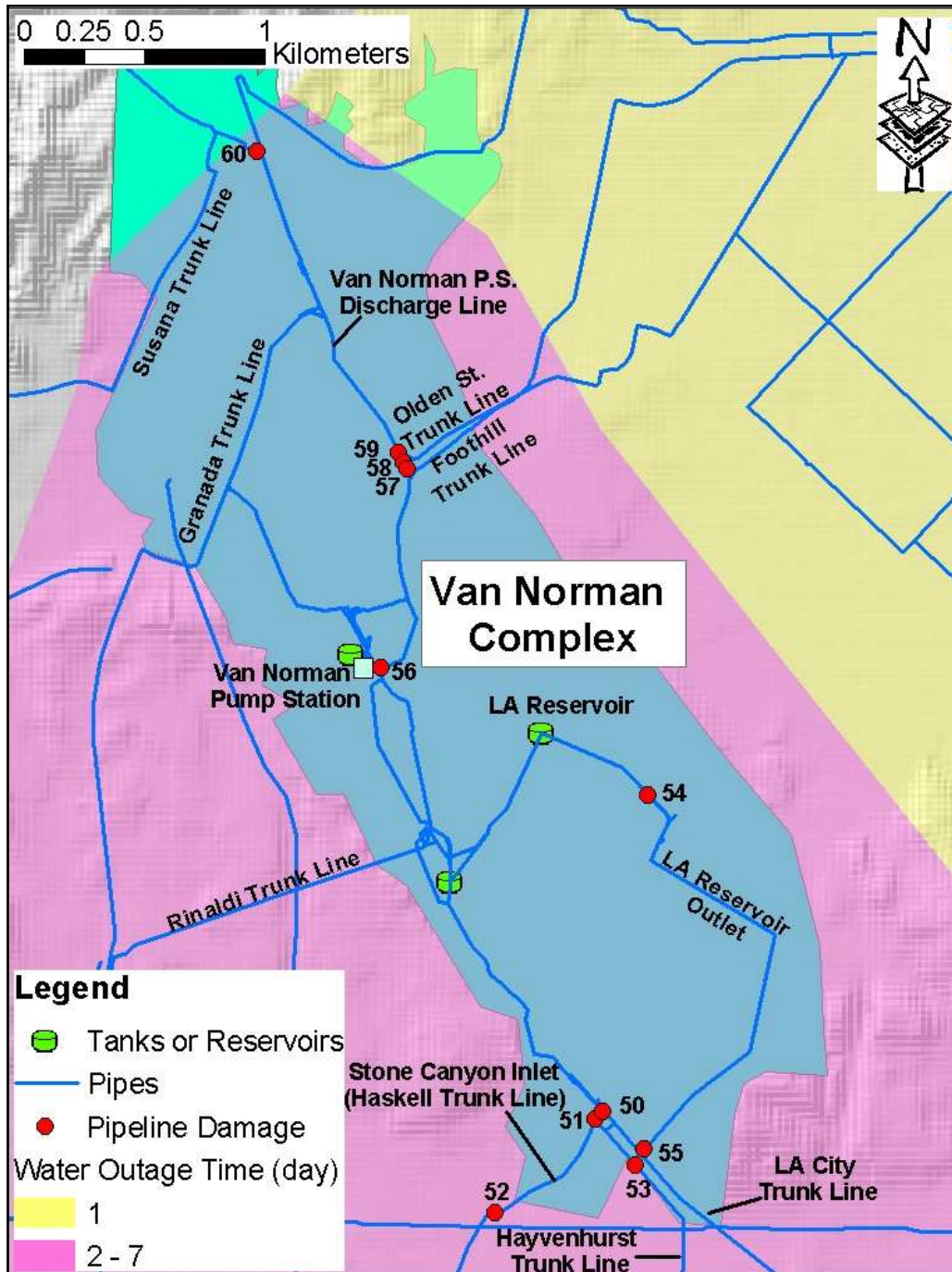


Figure B.4 Other Trunk Line Damage Locations (Shi, 2006)

Table B.4 Other Trunk Line Damage Information Summary 1

Repair ID	Trunk Line	PGD or TGD	Location	Dia. (mm)	Pipe Material	Damage Descriptions	Leak/Break	Leak Dia. (mm)
50	City Trunk Line	TGD	Lower San Fernando Dam	1829	Riveted Steel	Tear at longitudinal seam	Leak	N/A
51	Stone Canyon Inlet	TGD	762-mm main at Hayvenhurst Trunk Line	1524	Steel	Leak at coupling, ruptured gasket	Leak	137 (Scenario 1)
52	Stone Canyon Inlet	TGD	1219-mm butterfly valve at LAR outlet	1524	Steel	Leak at coupling, ruptured gasket	Leak	137 (Scenario 1)
53	Hayvenhurst Trunk Line	TGD	Rinaldi & Woodley NE corner	1372	Riveted Steel	Sheared rivets, up to 25 mm compressional movement	Leak	130 (Scenario 1)
54	LA Reservoir Outlet	TGD	Butterfly valve at vault below dam	3048	Steel	Leak at coupling	Leak	193 (Scenario 1)
55	LA Reservoir Outlet	TGD	At City Trunk Line	3048	Steel	Leak at coupling, tear in gasket	Leak	193 (Scenario 1)
56	Van Norman P.S. Discharge Line	TGD	Pier supports	1372	Steel	Ring girder collapse, displaced pier supports, no damage to pipe connections, only pipe damage came from pipe falling on concrete pier after girder collapse	No leak/No break	N/A
57	Van Norman P.S. Discharge Line	PGD	Between Foothill and Olden St. Trunk Line's	1372	Steel	Compression, bow, wrinkle and rip in gasket, pipe shell bowed	Leak	130 (Scenario 1)
58	Van Norman P.S. Discharge Line	TGD	Between Foothill and Olden St. Trunk Line's	305	Steel	Compression, shear	No leak/No break	N/A
59	Van Norman P.S. Discharge Line	TGD	North of Olden St. Trunk Line	1372	Steel	Compression buckle, 30 mm lateral offset	No leak/No break	N/A
60	Susana Trunk Line	TGD	Penstock Pump Station	1372	Steel	102 mm flange gasket tapped off	Leak	109 (Scenario 1)

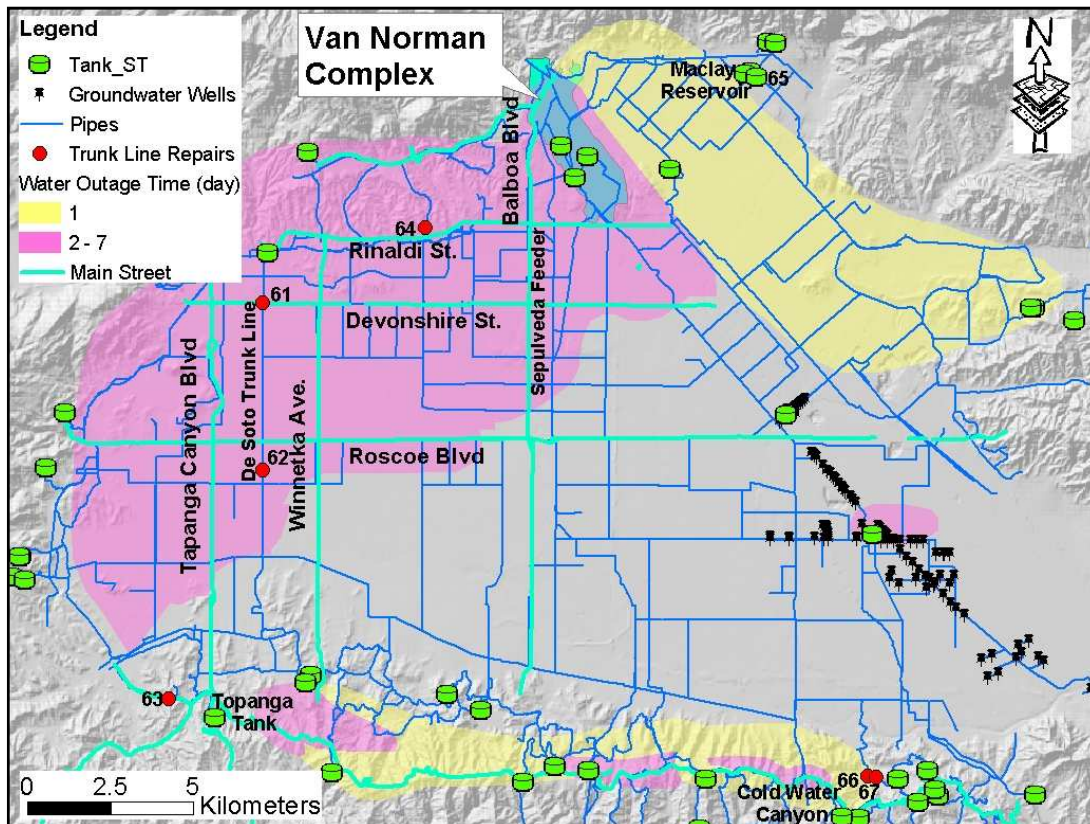


Figure B.5 Other Trunk Line Repairs outside Van Norman Complex

Table B.5 Other Trunk Line Damage Information Summary 2

ID	Trunk Line	PGD or TGD	Location	Dia. (mm)	Pipe Material	Damage Description	Hydraulic Modeling Assumptions	
							Leak/Break	Leak Dia. (mm)
61	Desoto Trunk Line	TGD	Ingomar	1067	Steel	Unknown	Leak	127 (WA ¹)
62	Desoto Trunk Line	TGD	Devonshire	1372	Steel	Unknown	Leak	145 (WA ¹)
63		TGD	Near Topanga Tank	914	Steel	Unknown	Leak	117 (WA ¹)
64	Reseda Trunk Line	TGD	Asuncion St. (1.5 blocks North of Rinaldi)	762	Steel	Unknown	Leak	107 (WA ¹)
65		TGD	Near Maclay Reservoir	914	Ductile Iron?	Unknown	Leak	109 (WA ¹)
66		TGD	Near Cold Water Canyon Tank	610	Ductile Iron?	Unknown		
67		TGD	Near Cold Water Canyon Tank	610	Ductile Iron?	Unknown	Leak	175 (WA ¹)

1: Weighted Average of Orifice Dia. from All Possible Leak Scenarios according to the Probability of Each Leak Scenario

APPENDIX C

MODELING PROCEDURES FOR PUMPS AND TANKS AT HIGH ELEVATIONS

The hydraulic network used in this study is based on the actual network used by LADWP for in-house analysis of their system. At LADWP, the system is divided into several major regions for which simulations are run to analyze flows locally. Experts run and maintain the hydraulic network model for each region. Experts can fine tune the smaller regions to model accurately the system configuration and operational characteristics. The remaining portions of the system, outside the region being modeled, are represented by a system of virtual demands and virtual tanks that mimic the inflow and outflow (supply and demand) from the remainder of the system.

For the purposes of this study, it was necessary to create a hydraulic network model that accurately represents the full LADWP system to evaluate entire system performance. Many challenges were associated with trying to model accurately individual system components while maintaining realistic overall system performance. For example, fine tuning valve settings in one trunk line can yield precise local flows for a typical winter day, but flows in a nearby interconnected pipe line can then show unrealistic flows and, in turn, cause unrealistic behavior in other parts of the system. When working with smaller subsets of the system, as is done at LADWP, it is easier to fine-tune the hydraulic network model without causing adverse reactions elsewhere in the system. The larger the system, the larger the potential for adverse/unrealistic effects due to a system change, and more effort is thus required to verify that the

remaining portion of the network is still functioning properly (i.e. more system to check).

Many pump stations alter operational status based on associated system performance characteristics. Limitations in current hydraulic network analysis software prevent the modeling of premise-logic-controls (PLCs) designed by LADWP to model the operational status of pumps. PLCs are a complex set of rules designed for many of the pump stations that relate pump operational status with water levels in associated tanks, pressures at nearby nodes, the operational status of other pumps, and flows in nearby system components.

Pump station configurations were set such that they produced average flows for a 24 hour period. A study was conducted for the Mount Washington Pump Station, located in the central, eastern portion of the LADWP system. A simulation was performed for a system where a simplified set of PLCs were manually added for the pump station, and compared with a simulation where the pump station had no logic rules associated with it. (Note: EPANET can handle a few simple logic rules, but cannot run with logic rules for more than several pump stations at a time).

Figure C.1 shows the results of two simulations 24 hours after a repeat Northridge earthquake scenario. In one simulation, PLCs are included as a collection of simple logic rules for the Mount Washington Pump Station (i.e. PLCs are “on”), and in the second simulation PLCs are not included, (i.e. PLCs are “off”). The simulation with logic rules shows that the Mount Washington pump station keeps pipelines in the area in service, whereas without the logic rules, the pump station does not perform at the necessary level to keep the area in service. This study reveals that a

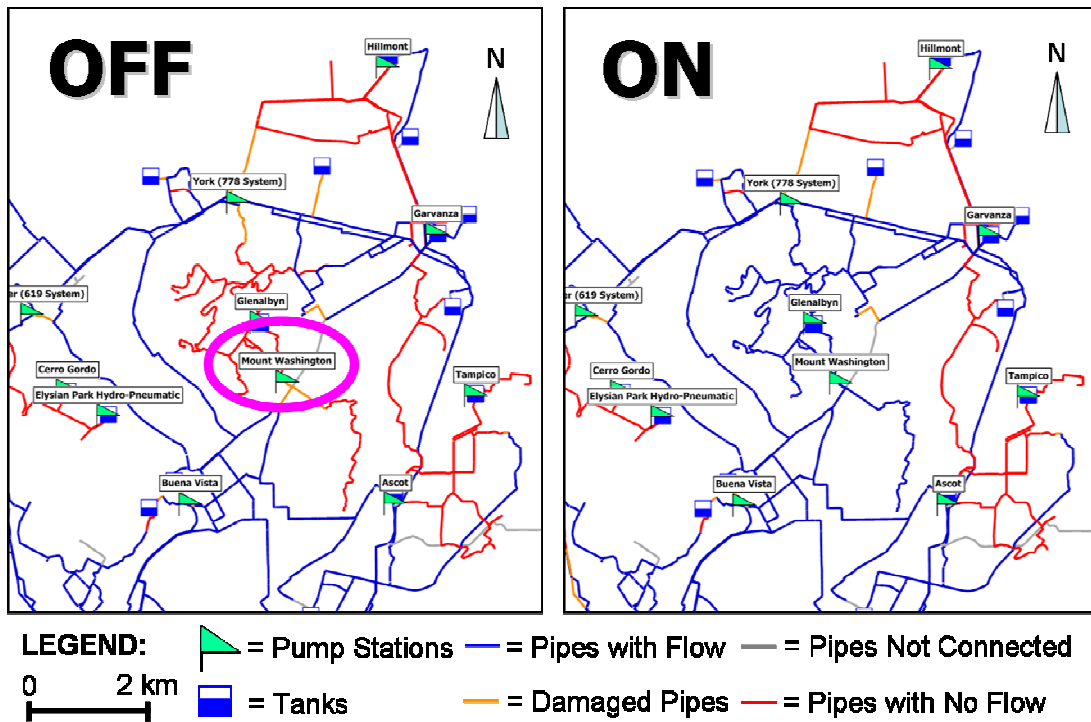


Figure C.1 Simulation Results for Mount Washington Pump Premise Logic Controls
Off and On

more accurate modeling of pump stations can be achieved with the inclusion of PLC-type rules to control the operational status of pumps. Incorporation of specialized logic controls for more accurate pump station simulation is recommended in the concluding chapter of this work.

APPENDIX D

SIZE DISTRIBUTION OF PIPELINES IN LOS ANGELES AND NEW YORK CITY WATER SUPPLIES

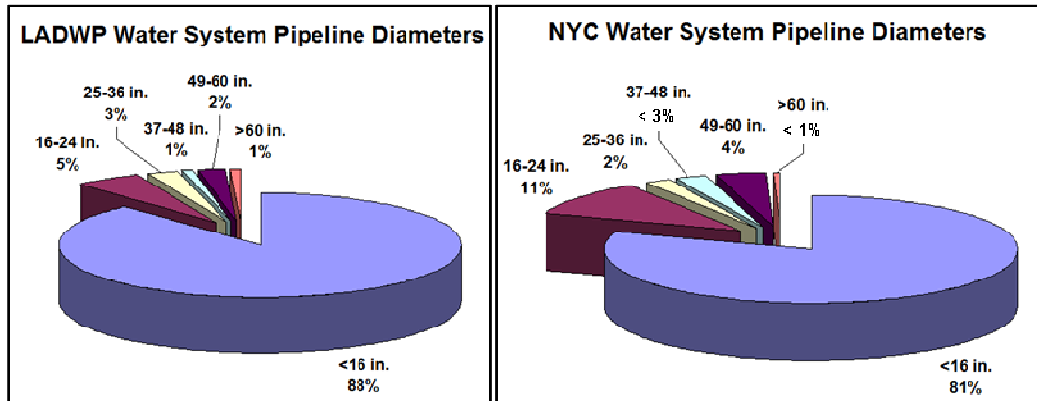


Figure D.1 Pipeline Diameters in the NYC and LADWP Water Systems

Statistics from 2002 were compiled for the composition of pipeline diameters in the LADWP (Jeon, 2002) and NYC (Chapin, 2001) water systems. The LADWP and NYC water systems contain approximately 11,633 km (7,228 mi.) and 6.134 km (9,872 mi.) of pipeline, respectively. As shown in Figure D.1, the majority of pipelines in both systems are distribution pipelines, with diameters less than 400 mm (16 in.). 88% of the pipelines in the LADWP water supply system (Jeon, 2002) and 82% of pipelines in the NYC water system (Chapin, 2001) have diameters less than 400 mm (16 in.). Only 12-20% of all pipelines for both systems have diameters greater than 610 mm (24 in.), indicating they are part of the trunk line system.

As discussed in Chapter 4, expertly modeling pipelines with diameters less than 400 mm (16 in.), which populate the distribution systems, would involve the

construction of hydraulic network models for 82-88% of the pipelines, or on average 8,000 km (4,971 mi.) of pipelines for each of the Los Angeles and NYC systems.

MCEER Technical Reports

MCEER publishes technical reports on a variety of subjects written by authors funded through MCEER. These reports are available from both MCEER Publications and the National Technical Information Service (NTIS). Requests for reports should be directed to MCEER Publications, MCEER, University at Buffalo, State University of New York, Red Jacket Quadrangle, Buffalo, New York 14261. Reports can also be requested through NTIS, 5285 Port Royal Road, Springfield, Virginia 22161. NTIS accession numbers are shown in parenthesis, if available.

- NCEER-87-0001 "First-Year Program in Research, Education and Technology Transfer," 3/5/87, (PB88-134275, A04, MF-A01).
- NCEER-87-0002 "Experimental Evaluation of Instantaneous Optimal Algorithms for Structural Control," by R.C. Lin, T.T. Soong and A.M. Reinhorn, 4/20/87, (PB88-134341, A04, MF-A01).
- NCEER-87-0003 "Experimentation Using the Earthquake Simulation Facilities at University at Buffalo," by A.M. Reinhorn and R.L. Ketter, to be published.
- NCEER-87-0004 "The System Characteristics and Performance of a Shaking Table," by J.S. Hwang, K.C. Chang and G.C. Lee, 6/1/87, (PB88-134259, A03, MF-A01). This report is available only through NTIS (see address given above).
- NCEER-87-0005 "A Finite Element Formulation for Nonlinear Viscoplastic Material Using a Q Model," by O. Gyebi and G. Dasgupta, 11/2/87, (PB88-213764, A08, MF-A01).
- NCEER-87-0006 "Symbolic Manipulation Program (SMP) - Algebraic Codes for Two and Three Dimensional Finite Element Formulations," by X. Lee and G. Dasgupta, 11/9/87, (PB88-218522, A05, MF-A01).
- NCEER-87-0007 "Instantaneous Optimal Control Laws for Tall Buildings Under Seismic Excitations," by J.N. Yang, A. Akbarpour and P. Ghaemmaghami, 6/10/87, (PB88-134333, A06, MF-A01). This report is only available through NTIS (see address given above).
- NCEER-87-0008 "IDARC: Inelastic Damage Analysis of Reinforced Concrete Frame - Shear-Wall Structures," by Y.J. Park, A.M. Reinhorn and S.K. Kunnath, 7/20/87, (PB88-134325, A09, MF-A01). This report is only available through NTIS (see address given above).
- NCEER-87-0009 "Liquefaction Potential for New York State: A Preliminary Report on Sites in Manhattan and Buffalo," by M. Budhu, V. Vijayakumar, R.F. Giese and L. Baumgras, 8/31/87, (PB88-163704, A03, MF-A01). This report is available only through NTIS (see address given above).
- NCEER-87-0010 "Vertical and Torsional Vibration of Foundations in Inhomogeneous Media," by A.S. Veletsos and K.W. Dotson, 6/1/87, (PB88-134291, A03, MF-A01). This report is only available through NTIS (see address given above).
- NCEER-87-0011 "Seismic Probabilistic Risk Assessment and Seismic Margins Studies for Nuclear Power Plants," by Howard H.M. Hwang, 6/15/87, (PB88-134267, A03, MF-A01). This report is only available through NTIS (see address given above).
- NCEER-87-0012 "Parametric Studies of Frequency Response of Secondary Systems Under Ground-Acceleration Excitations," by Y. Yong and Y.K. Lin, 6/10/87, (PB88-134309, A03, MF-A01). This report is only available through NTIS (see address given above).
- NCEER-87-0013 "Frequency Response of Secondary Systems Under Seismic Excitation," by J.A. HoLung, J. Cai and Y.K. Lin, 7/31/87, (PB88-134317, A05, MF-A01). This report is only available through NTIS (see address given above).
- NCEER-87-0014 "Modelling Earthquake Ground Motions in Seismically Active Regions Using Parametric Time Series Methods," by G.W. Ellis and A.S. Cakmak, 8/25/87, (PB88-134283, A08, MF-A01). This report is only available through NTIS (see address given above).
- NCEER-87-0015 "Detection and Assessment of Seismic Structural Damage," by E. DiPasquale and A.S. Cakmak, 8/25/87, (PB88-163712, A05, MF-A01). This report is only available through NTIS (see address given above).

- NCEER-87-0016 "Pipeline Experiment at Parkfield, California," by J. Isenberg and E. Richardson, 9/15/87, (PB88-163720, A03, MF-A01). This report is available only through NTIS (see address given above).
- NCEER-87-0017 "Digital Simulation of Seismic Ground Motion," by M. Shinozuka, G. Deodatis and T. Harada, 8/31/87, (PB88-155197, A04, MF-A01). This report is available only through NTIS (see address given above).
- NCEER-87-0018 "Practical Considerations for Structural Control: System Uncertainty, System Time Delay and Truncation of Small Control Forces," J.N. Yang and A. Akbarpour, 8/10/87, (PB88-163738, A08, MF-A01). This report is only available through NTIS (see address given above).
- NCEER-87-0019 "Modal Analysis of Nonclassically Damped Structural Systems Using Canonical Transformation," by J.N. Yang, S. Sarkani and F.X. Long, 9/27/87, (PB88-187851, A04, MF-A01).
- NCEER-87-0020 "A Nonstationary Solution in Random Vibration Theory," by J.R. Red-Horse and P.D. Spanos, 11/3/87, (PB88-163746, A03, MF-A01).
- NCEER-87-0021 "Horizontal Impedances for Radially Inhomogeneous Viscoelastic Soil Layers," by A.S. Veletsos and K.W. Dotson, 10/15/87, (PB88-150859, A04, MF-A01).
- NCEER-87-0022 "Seismic Damage Assessment of Reinforced Concrete Members," by Y.S. Chung, C. Meyer and M. Shinozuka, 10/9/87, (PB88-150867, A05, MF-A01). This report is available only through NTIS (see address given above).
- NCEER-87-0023 "Active Structural Control in Civil Engineering," by T.T. Soong, 11/11/87, (PB88-187778, A03, MF-A01).
- NCEER-87-0024 "Vertical and Torsional Impedances for Radially Inhomogeneous Viscoelastic Soil Layers," by K.W. Dotson and A.S. Veletsos, 12/87, (PB88-187786, A03, MF-A01).
- NCEER-87-0025 "Proceedings from the Symposium on Seismic Hazards, Ground Motions, Soil-Liquefaction and Engineering Practice in Eastern North America," October 20-22, 1987, edited by K.H. Jacob, 12/87, (PB88-188115, A23, MF-A01). This report is available only through NTIS (see address given above).
- NCEER-87-0026 "Report on the Whittier-Narrows, California, Earthquake of October 1, 1987," by J. Pantelic and A. Reinhorn, 11/87, (PB88-187752, A03, MF-A01). This report is available only through NTIS (see address given above).
- NCEER-87-0027 "Design of a Modular Program for Transient Nonlinear Analysis of Large 3-D Building Structures," by S. Srivastav and J.F. Abel, 12/30/87, (PB88-187950, A05, MF-A01). This report is only available through NTIS (see address given above).
- NCEER-87-0028 "Second-Year Program in Research, Education and Technology Transfer," 3/8/88, (PB88-219480, A04, MF-A01).
- NCEER-88-0001 "Workshop on Seismic Computer Analysis and Design of Buildings With Interactive Graphics," by W. McGuire, J.F. Abel and C.H. Conley, 1/18/88, (PB88-187760, A03, MF-A01). This report is only available through NTIS (see address given above).
- NCEER-88-0002 "Optimal Control of Nonlinear Flexible Structures," by J.N. Yang, F.X. Long and D. Wong, 1/22/88, (PB88-213772, A06, MF-A01).
- NCEER-88-0003 "Substructuring Techniques in the Time Domain for Primary-Secondary Structural Systems," by G.D. Manolis and G. Juhn, 2/10/88, (PB88-213780, A04, MF-A01).
- NCEER-88-0004 "Iterative Seismic Analysis of Primary-Secondary Systems," by A. Singhal, L.D. Lutes and P.D. Spanos, 2/23/88, (PB88-213798, A04, MF-A01).
- NCEER-88-0005 "Stochastic Finite Element Expansion for Random Media," by P.D. Spanos and R. Ghanem, 3/14/88, (PB88-213806, A03, MF-A01).

- NCEER-88-0006 "Combining Structural Optimization and Structural Control," by F.Y. Cheng and C.P. Pantelides, 1/10/88, (PB88-213814, A05, MF-A01).
- NCEER-88-0007 "Seismic Performance Assessment of Code-Designed Structures," by H.H-M. Hwang, J-W. Jaw and H-J. Shau, 3/20/88, (PB88-219423, A04, MF-A01). This report is only available through NTIS (see address given above).
- NCEER-88-0008 "Reliability Analysis of Code-Designed Structures Under Natural Hazards," by H.H-M. Hwang, H. Ushiba and M. Shinozuka, 2/29/88, (PB88-229471, A07, MF-A01). This report is only available through NTIS (see address given above).
- NCEER-88-0009 "Seismic Fragility Analysis of Shear Wall Structures," by J-W Jaw and H.H-M. Hwang, 4/30/88, (PB89-102867, A04, MF-A01).
- NCEER-88-0010 "Base Isolation of a Multi-Story Building Under a Harmonic Ground Motion - A Comparison of Performances of Various Systems," by F-G Fan, G. Ahmadi and I.G. Tadjbakhsh, 5/18/88, (PB89-122238, A06, MF-A01). This report is only available through NTIS (see address given above).
- NCEER-88-0011 "Seismic Floor Response Spectra for a Combined System by Green's Functions," by F.M. Lavelle, L.A. Bergman and P.D. Spanos, 5/1/88, (PB89-102875, A03, MF-A01).
- NCEER-88-0012 "A New Solution Technique for Randomly Excited Hysteretic Structures," by G.Q. Cai and Y.K. Lin, 5/16/88, (PB89-102883, A03, MF-A01).
- NCEER-88-0013 "A Study of Radiation Damping and Soil-Structure Interaction Effects in the Centrifuge," by K. Weissman, supervised by J.H. Prevost, 5/24/88, (PB89-144703, A06, MF-A01).
- NCEER-88-0014 "Parameter Identification and Implementation of a Kinematic Plasticity Model for Frictional Soils," by J.H. Prevost and D.V. Griffiths, to be published.
- NCEER-88-0015 "Two- and Three- Dimensional Dynamic Finite Element Analyses of the Long Valley Dam," by D.V. Griffiths and J.H. Prevost, 6/17/88, (PB89-144711, A04, MF-A01).
- NCEER-88-0016 "Damage Assessment of Reinforced Concrete Structures in Eastern United States," by A.M. Reinhorn, M.J. Seidel, S.K. Kunnath and Y.J. Park, 6/15/88, (PB89-122220, A04, MF-A01). This report is only available through NTIS (see address given above).
- NCEER-88-0017 "Dynamic Compliance of Vertically Loaded Strip Foundations in Multilayered Viscoelastic Soils," by S. Ahmad and A.S.M. Israil, 6/17/88, (PB89-102891, A04, MF-A01).
- NCEER-88-0018 "An Experimental Study of Seismic Structural Response With Added Viscoelastic Dampers," by R.C. Lin, Z. Liang, T.T. Soong and R.H. Zhang, 6/30/88, (PB89-122212, A05, MF-A01). This report is available only through NTIS (see address given above).
- NCEER-88-0019 "Experimental Investigation of Primary - Secondary System Interaction," by G.D. Manolis, G. Juhn and A.M. Reinhorn, 5/27/88, (PB89-122204, A04, MF-A01).
- NCEER-88-0020 "A Response Spectrum Approach For Analysis of Nonclassically Damped Structures," by J.N. Yang, S. Sarkani and F.X. Long, 4/22/88, (PB89-102909, A04, MF-A01).
- NCEER-88-0021 "Seismic Interaction of Structures and Soils: Stochastic Approach," by A.S. Veletsos and A.M. Prasad, 7/21/88, (PB89-122196, A04, MF-A01). This report is only available through NTIS (see address given above).
- NCEER-88-0022 "Identification of the Serviceability Limit State and Detection of Seismic Structural Damage," by E. DiPasquale and A.S. Cakmak, 6/15/88, (PB89-122188, A05, MF-A01). This report is available only through NTIS (see address given above).
- NCEER-88-0023 "Multi-Hazard Risk Analysis: Case of a Simple Offshore Structure," by B.K. Bhartia and E.H. Vanmarcke, 7/21/88, (PB89-145213, A05, MF-A01).

- NCEER-88-0024 "Automated Seismic Design of Reinforced Concrete Buildings," by Y.S. Chung, C. Meyer and M. Shinozuka, 7/5/88, (PB89-122170, A06, MF-A01). This report is available only through NTIS (see address given above).
- NCEER-88-0025 "Experimental Study of Active Control of MDOF Structures Under Seismic Excitations," by L.L. Chung, R.C. Lin, T.T. Soong and A.M. Reinhorn, 7/10/88, (PB89-122600, A04, MF-A01).
- NCEER-88-0026 "Earthquake Simulation Tests of a Low-Rise Metal Structure," by J.S. Hwang, K.C. Chang, G.C. Lee and R.L. Ketter, 8/1/88, (PB89-102917, A04, MF-A01).
- NCEER-88-0027 "Systems Study of Urban Response and Reconstruction Due to Catastrophic Earthquakes," by F. Kozin and H.K. Zhou, 9/22/88, (PB90-162348, A04, MF-A01).
- NCEER-88-0028 "Seismic Fragility Analysis of Plane Frame Structures," by H.H-M. Hwang and Y.K. Low, 7/31/88, (PB89-131445, A06, MF-A01).
- NCEER-88-0029 "Response Analysis of Stochastic Structures," by A. Kardara, C. Bucher and M. Shinozuka, 9/22/88, (PB89-174429, A04, MF-A01).
- NCEER-88-0030 "Nonnormal Accelerations Due to Yielding in a Primary Structure," by D.C.K. Chen and L.D. Lutes, 9/19/88, (PB89-131437, A04, MF-A01).
- NCEER-88-0031 "Design Approaches for Soil-Structure Interaction," by A.S. Veletsos, A.M. Prasad and Y. Tang, 12/30/88, (PB89-174437, A03, MF-A01). This report is available only through NTIS (see address given above).
- NCEER-88-0032 "A Re-evaluation of Design Spectra for Seismic Damage Control," by C.J. Turkstra and A.G. Tallin, 11/7/88, (PB89-145221, A05, MF-A01).
- NCEER-88-0033 "The Behavior and Design of Noncontact Lap Splices Subjected to Repeated Inelastic Tensile Loading," by V.E. Sagan, P. Gergely and R.N. White, 12/8/88, (PB89-163737, A08, MF-A01).
- NCEER-88-0034 "Seismic Response of Pile Foundations," by S.M. Mamoon, P.K. Banerjee and S. Ahmad, 11/1/88, (PB89-145239, A04, MF-A01).
- NCEER-88-0035 "Modeling of R/C Building Structures With Flexible Floor Diaphragms (IDARC2)," by A.M. Reinhorn, S.K. Kunnath and N. Panahshahi, 9/7/88, (PB89-207153, A07, MF-A01).
- NCEER-88-0036 "Solution of the Dam-Reservoir Interaction Problem Using a Combination of FEM, BEM with Particular Integrals, Modal Analysis, and Substructuring," by C-S. Tsai, G.C. Lee and R.L. Ketter, 12/31/88, (PB89-207146, A04, MF-A01).
- NCEER-88-0037 "Optimal Placement of Actuators for Structural Control," by F.Y. Cheng and C.P. Pantelides, 8/15/88, (PB89-162846, A05, MF-A01).
- NCEER-88-0038 "Teflon Bearings in Aseismic Base Isolation: Experimental Studies and Mathematical Modeling," by A. Mokha, M.C. Constantinou and A.M. Reinhorn, 12/5/88, (PB89-218457, A10, MF-A01). This report is available only through NTIS (see address given above).
- NCEER-88-0039 "Seismic Behavior of Flat Slab High-Rise Buildings in the New York City Area," by P. Weidlinger and M. Ettouney, 10/15/88, (PB90-145681, A04, MF-A01).
- NCEER-88-0040 "Evaluation of the Earthquake Resistance of Existing Buildings in New York City," by P. Weidlinger and M. Ettouney, 10/15/88, to be published.
- NCEER-88-0041 "Small-Scale Modeling Techniques for Reinforced Concrete Structures Subjected to Seismic Loads," by W. Kim, A. El-Attar and R.N. White, 11/22/88, (PB89-189625, A05, MF-A01).
- NCEER-88-0042 "Modeling Strong Ground Motion from Multiple Event Earthquakes," by G.W. Ellis and A.S. Cakmak, 10/15/88, (PB89-174445, A03, MF-A01).

- NCEER-88-0043 "Nonstationary Models of Seismic Ground Acceleration," by M. Grigoriu, S.E. Ruiz and E. Rosenblueth, 7/15/88, (PB89-189617, A04, MF-A01).
- NCEER-88-0044 "SARCF User's Guide: Seismic Analysis of Reinforced Concrete Frames," by Y.S. Chung, C. Meyer and M. Shinozuka, 11/9/88, (PB89-174452, A08, MF-A01).
- NCEER-88-0045 "First Expert Panel Meeting on Disaster Research and Planning," edited by J. Pantelic and J. Stoyke, 9/15/88, (PB89-174460, A05, MF-A01).
- NCEER-88-0046 "Preliminary Studies of the Effect of Degrading Infill Walls on the Nonlinear Seismic Response of Steel Frames," by C.Z. Chrysostomou, P. Gergely and J.F. Abel, 12/19/88, (PB89-208383, A05, MF-A01).
- NCEER-88-0047 "Reinforced Concrete Frame Component Testing Facility - Design, Construction, Instrumentation and Operation," by S.P. Pessiki, C. Conley, T. Bond, P. Gergely and R.N. White, 12/16/88, (PB89-174478, A04, MF-A01).
- NCEER-89-0001 "Effects of Protective Cushion and Soil Compliancy on the Response of Equipment Within a Seismically Excited Building," by J.A. HoLung, 2/16/89, (PB89-207179, A04, MF-A01).
- NCEER-89-0002 "Statistical Evaluation of Response Modification Factors for Reinforced Concrete Structures," by H.H-M. Hwang and J-W. Jaw, 2/17/89, (PB89-207187, A05, MF-A01).
- NCEER-89-0003 "Hysteretic Columns Under Random Excitation," by G-Q. Cai and Y.K. Lin, 1/9/89, (PB89-196513, A03, MF-A01).
- NCEER-89-0004 "Experimental Study of 'Elephant Foot Bulge' Instability of Thin-Walled Metal Tanks," by Z-H. Jia and R.L. Ketter, 2/22/89, (PB89-207195, A03, MF-A01).
- NCEER-89-0005 "Experiment on Performance of Buried Pipelines Across San Andreas Fault," by J. Isenberg, E. Richardson and T.D. O'Rourke, 3/10/89, (PB89-218440, A04, MF-A01). This report is available only through NTIS (see address given above).
- NCEER-89-0006 "A Knowledge-Based Approach to Structural Design of Earthquake-Resistant Buildings," by M. Subramani, P. Gergely, C.H. Conley, J.F. Abel and A.H. Zaghaw, 1/15/89, (PB89-218465, A06, MF-A01).
- NCEER-89-0007 "Liquefaction Hazards and Their Effects on Buried Pipelines," by T.D. O'Rourke and P.A. Lane, 2/1/89, (PB89-218481, A09, MF-A01).
- NCEER-89-0008 "Fundamentals of System Identification in Structural Dynamics," by H. Imai, C-B. Yun, O. Maruyama and M. Shinozuka, 1/26/89, (PB89-207211, A04, MF-A01).
- NCEER-89-0009 "Effects of the 1985 Michoacan Earthquake on Water Systems and Other Buried Lifelines in Mexico," by A.G. Ayala and M.J. O'Rourke, 3/8/89, (PB89-207229, A06, MF-A01).
- NCEER-89-R010 "NCEER Bibliography of Earthquake Education Materials," by K.E.K. Ross, Second Revision, 9/1/89, (PB90-125352, A05, MF-A01). This report is replaced by NCEER-92-0018.
- NCEER-89-0011 "Inelastic Three-Dimensional Response Analysis of Reinforced Concrete Building Structures (IDARC-3D), Part I - Modeling," by S.K. Kunnath and A.M. Reinhorn, 4/17/89, (PB90-114612, A07, MF-A01). This report is available only through NTIS (see address given above).
- NCEER-89-0012 "Recommended Modifications to ATC-14," by C.D. Poland and J.O. Malley, 4/12/89, (PB90-108648, A15, MF-A01).
- NCEER-89-0013 "Repair and Strengthening of Beam-to-Column Connections Subjected to Earthquake Loading," by M. Corazao and A.J. Durrani, 2/28/89, (PB90-109885, A06, MF-A01).
- NCEER-89-0014 "Program EXKAL2 for Identification of Structural Dynamic Systems," by O. Maruyama, C-B. Yun, M. Hoshiya and M. Shinozuka, 5/19/89, (PB90-109877, A09, MF-A01).

- NCEER-89-0015 "Response of Frames With Bolted Semi-Rigid Connections, Part I - Experimental Study and Analytical Predictions," by P.J. DiCorso, A.M. Reinhorn, J.R. Dickerson, J.B. Radzinski and W.L. Harper, 6/1/89, to be published.
- NCEER-89-0016 "ARMA Monte Carlo Simulation in Probabilistic Structural Analysis," by P.D. Spanos and M.P. Mignolet, 7/10/89, (PB90-109893, A03, MF-A01).
- NCEER-89-P017 "Preliminary Proceedings from the Conference on Disaster Preparedness - The Place of Earthquake Education in Our Schools," Edited by K.E.K. Ross, 6/23/89, (PB90-108606, A03, MF-A01).
- NCEER-89-0017 "Proceedings from the Conference on Disaster Preparedness - The Place of Earthquake Education in Our Schools," Edited by K.E.K. Ross, 12/31/89, (PB90-207895, A012, MF-A02). This report is available only through NTIS (see address given above).
- NCEER-89-0018 "Multidimensional Models of Hysteretic Material Behavior for Vibration Analysis of Shape Memory Energy Absorbing Devices, by E.J. Graesser and F.A. Cozzarelli, 6/7/89, (PB90-164146, A04, MF-A01).
- NCEER-89-0019 "Nonlinear Dynamic Analysis of Three-Dimensional Base Isolated Structures (3D-BASIS)," by S. Nagarajaiah, A.M. Reinhorn and M.C. Constantinou, 8/3/89, (PB90-161936, A06, MF-A01). This report has been replaced by NCEER-93-0011.
- NCEER-89-0020 "Structural Control Considering Time-Rate of Control Forces and Control Rate Constraints," by F.Y. Cheng and C.P. Pantelides, 8/3/89, (PB90-120445, A04, MF-A01).
- NCEER-89-0021 "Subsurface Conditions of Memphis and Shelby County," by K.W. Ng, T-S. Chang and H-H.M. Hwang, 7/26/89, (PB90-120437, A03, MF-A01).
- NCEER-89-0022 "Seismic Wave Propagation Effects on Straight Jointed Buried Pipelines," by K. Elhadi and M.J. O'Rourke, 8/24/89, (PB90-162322, A10, MF-A02).
- NCEER-89-0023 "Workshop on Serviceability Analysis of Water Delivery Systems," edited by M. Grigoriu, 3/6/89, (PB90-127424, A03, MF-A01).
- NCEER-89-0024 "Shaking Table Study of a 1/5 Scale Steel Frame Composed of Tapered Members," by K.C. Chang, J.S. Hwang and G.C. Lee, 9/18/89, (PB90-160169, A04, MF-A01).
- NCEER-89-0025 "DYNA1D: A Computer Program for Nonlinear Seismic Site Response Analysis - Technical Documentation," by Jean H. Prevost, 9/14/89, (PB90-161944, A07, MF-A01). This report is available only through NTIS (see address given above).
- NCEER-89-0026 "1:4 Scale Model Studies of Active Tendon Systems and Active Mass Dampers for Aseismic Protection," by A.M. Reinhorn, T.T. Soong, R.C. Lin, Y.P. Yang, Y. Fukao, H. Abe and M. Nakai, 9/15/89, (PB90-173246, A10, MF-A02). This report is available only through NTIS (see address given above).
- NCEER-89-0027 "Scattering of Waves by Inclusions in a Nonhomogeneous Elastic Half Space Solved by Boundary Element Methods," by P.K. Hadley, A. Askar and A.S. Cakmak, 6/15/89, (PB90-145699, A07, MF-A01).
- NCEER-89-0028 "Statistical Evaluation of Deflection Amplification Factors for Reinforced Concrete Structures," by H.H.M. Hwang, J-W. Jaw and A.L. Ch'ng, 8/31/89, (PB90-164633, A05, MF-A01).
- NCEER-89-0029 "Bedrock Accelerations in Memphis Area Due to Large New Madrid Earthquakes," by H.H.M. Hwang, C.H.S. Chen and G. Yu, 11/7/89, (PB90-162330, A04, MF-A01).
- NCEER-89-0030 "Seismic Behavior and Response Sensitivity of Secondary Structural Systems," by Y.Q. Chen and T.T. Soong, 10/23/89, (PB90-164658, A08, MF-A01).
- NCEER-89-0031 "Random Vibration and Reliability Analysis of Primary-Secondary Structural Systems," by Y. Ibrahim, M. Grigoriu and T.T. Soong, 11/10/89, (PB90-161951, A04, MF-A01).

- NCEER-89-0032 "Proceedings from the Second U.S. - Japan Workshop on Liquefaction, Large Ground Deformation and Their Effects on Lifelines, September 26-29, 1989," Edited by T.D. O'Rourke and M. Hamada, 12/1/89, (PB90-209388, A22, MF-A03).
- NCEER-89-0033 "Deterministic Model for Seismic Damage Evaluation of Reinforced Concrete Structures," by J.M. Bracci, A.M. Reinhorn, J.B. Mander and S.K. Kunnath, 9/27/89, (PB91-108803, A06, MF-A01).
- NCEER-89-0034 "On the Relation Between Local and Global Damage Indices," by E. DiPasquale and A.S. Cakmak, 8/15/89, (PB90-173865, A05, MF-A01).
- NCEER-89-0035 "Cyclic Undrained Behavior of Nonplastic and Low Plasticity Silts," by A.J. Walker and H.E. Stewart, 7/26/89, (PB90-183518, A10, MF-A01).
- NCEER-89-0036 "Liquefaction Potential of Surficial Deposits in the City of Buffalo, New York," by M. Budhu, R. Giese and L. Baumgrass, 1/17/89, (PB90-208455, A04, MF-A01).
- NCEER-89-0037 "A Deterministic Assessment of Effects of Ground Motion Incoherence," by A.S. Veletsos and Y. Tang, 7/15/89, (PB90-164294, A03, MF-A01).
- NCEER-89-0038 "Workshop on Ground Motion Parameters for Seismic Hazard Mapping," July 17-18, 1989, edited by R.V. Whitman, 12/1/89, (PB90-173923, A04, MF-A01).
- NCEER-89-0039 "Seismic Effects on Elevated Transit Lines of the New York City Transit Authority," by C.J. Costantino, C.A. Miller and E. Heymsfield, 12/26/89, (PB90-207887, A06, MF-A01).
- NCEER-89-0040 "Centrifugal Modeling of Dynamic Soil-Structure Interaction," by K. Weissman, Supervised by J.H. Prevost, 5/10/89, (PB90-207879, A07, MF-A01).
- NCEER-89-0041 "Linearized Identification of Buildings With Cores for Seismic Vulnerability Assessment," by I-K. Ho and A.E. Aktan, 11/1/89, (PB90-251943, A07, MF-A01).
- NCEER-90-0001 "Geotechnical and Lifeline Aspects of the October 17, 1989 Loma Prieta Earthquake in San Francisco," by T.D. O'Rourke, H.E. Stewart, F.T. Blackburn and T.S. Dickerman, 1/90, (PB90-208596, A05, MF-A01).
- NCEER-90-0002 "Nonnormal Secondary Response Due to Yielding in a Primary Structure," by D.C.K. Chen and L.D. Lutes, 2/28/90, (PB90-251976, A07, MF-A01).
- NCEER-90-0003 "Earthquake Education Materials for Grades K-12," by K.E.K. Ross, 4/16/90, (PB91-251984, A05, MF-A05). This report has been replaced by NCEER-92-0018.
- NCEER-90-0004 "Catalog of Strong Motion Stations in Eastern North America," by R.W. Busby, 4/3/90, (PB90-251984, A05, MF-A01).
- NCEER-90-0005 "NCEER Strong-Motion Data Base: A User Manual for the GeoBase Release (Version 1.0 for the Sun3)," by P. Friberg and K. Jacob, 3/31/90 (PB90-258062, A04, MF-A01).
- NCEER-90-0006 "Seismic Hazard Along a Crude Oil Pipeline in the Event of an 1811-1812 Type New Madrid Earthquake," by H.H.M. Hwang and C-H.S. Chen, 4/16/90, (PB90-258054, A04, MF-A01).
- NCEER-90-0007 "Site-Specific Response Spectra for Memphis Sheahan Pumping Station," by H.H.M. Hwang and C.S. Lee, 5/15/90, (PB91-108811, A05, MF-A01).
- NCEER-90-0008 "Pilot Study on Seismic Vulnerability of Crude Oil Transmission Systems," by T. Ariman, R. Dobry, M. Grigoriu, F. Kozin, M. O'Rourke, T. O'Rourke and M. Shinozuka, 5/25/90, (PB91-108837, A06, MF-A01).
- NCEER-90-0009 "A Program to Generate Site Dependent Time Histories: EQGEN," by G.W. Ellis, M. Srinivasan and A.S. Cakmak, 1/30/90, (PB91-108829, A04, MF-A01).
- NCEER-90-0010 "Active Isolation for Seismic Protection of Operating Rooms," by M.E. Talbott, Supervised by M. Shinozuka, 6/8/9, (PB91-110205, A05, MF-A01).

- NCEER-90-0011 "Program LINEARID for Identification of Linear Structural Dynamic Systems," by C-B. Yun and M. Shinozuka, 6/25/90, (PB91-110312, A08, MF-A01).
- NCEER-90-0012 "Two-Dimensional Two-Phase Elasto-Plastic Seismic Response of Earth Dams," by A.N. Yiagos, Supervised by J.H. Prevost, 6/20/90, (PB91-110197, A13, MF-A02).
- NCEER-90-0013 "Secondary Systems in Base-Isolated Structures: Experimental Investigation, Stochastic Response and Stochastic Sensitivity," by G.D. Manolis, G. Juhn, M.C. Constantinou and A.M. Reinhorn, 7/1/90, (PB91-110320, A08, MF-A01).
- NCEER-90-0014 "Seismic Behavior of Lightly-Reinforced Concrete Column and Beam-Column Joint Details," by S.P. Pessiki, C.H. Conley, P. Gergely and R.N. White, 8/22/90, (PB91-108795, A11, MF-A02).
- NCEER-90-0015 "Two Hybrid Control Systems for Building Structures Under Strong Earthquakes," by J.N. Yang and A. Daniellians, 6/29/90, (PB91-125393, A04, MF-A01).
- NCEER-90-0016 "Instantaneous Optimal Control with Acceleration and Velocity Feedback," by J.N. Yang and Z. Li, 6/29/90, (PB91-125401, A03, MF-A01).
- NCEER-90-0017 "Reconnaissance Report on the Northern Iran Earthquake of June 21, 1990," by M. Mehrain, 10/4/90, (PB91-125377, A03, MF-A01).
- NCEER-90-0018 "Evaluation of Liquefaction Potential in Memphis and Shelby County," by T.S. Chang, P.S. Tang, C.S. Lee and H. Hwang, 8/10/90, (PB91-125427, A09, MF-A01).
- NCEER-90-0019 "Experimental and Analytical Study of a Combined Sliding Disc Bearing and Helical Steel Spring Isolation System," by M.C. Constantinou, A.S. Mokha and A.M. Reinhorn, 10/4/90, (PB91-125385, A06, MF-A01). This report is available only through NTIS (see address given above).
- NCEER-90-0020 "Experimental Study and Analytical Prediction of Earthquake Response of a Sliding Isolation System with a Spherical Surface," by A.S. Mokha, M.C. Constantinou and A.M. Reinhorn, 10/11/90, (PB91-125419, A05, MF-A01).
- NCEER-90-0021 "Dynamic Interaction Factors for Floating Pile Groups," by G. Gazetas, K. Fan, A. Kaynia and E. Kausel, 9/10/90, (PB91-170381, A05, MF-A01).
- NCEER-90-0022 "Evaluation of Seismic Damage Indices for Reinforced Concrete Structures," by S. Rodriguez-Gomez and A.S. Cakmak, 9/30/90, PB91-171322, A06, MF-A01).
- NCEER-90-0023 "Study of Site Response at a Selected Memphis Site," by H. Desai, S. Ahmad, E.S. Gazetas and M.R. Oh, 10/11/90, (PB91-196857, A03, MF-A01).
- NCEER-90-0024 "A User's Guide to Strongmo: Version 1.0 of NCEER's Strong-Motion Data Access Tool for PCs and Terminals," by P.A. Friberg and C.A.T. Susch, 11/15/90, (PB91-171272, A03, MF-A01).
- NCEER-90-0025 "A Three-Dimensional Analytical Study of Spatial Variability of Seismic Ground Motions," by L-L. Hong and A.H.-S. Ang, 10/30/90, (PB91-170399, A09, MF-A01).
- NCEER-90-0026 "MUMOID User's Guide - A Program for the Identification of Modal Parameters," by S. Rodriguez-Gomez and E. DiPasquale, 9/30/90, (PB91-171298, A04, MF-A01).
- NCEER-90-0027 "SARCF-II User's Guide - Seismic Analysis of Reinforced Concrete Frames," by S. Rodriguez-Gomez, Y.S. Chung and C. Meyer, 9/30/90, (PB91-171280, A05, MF-A01).
- NCEER-90-0028 "Viscous Dampers: Testing, Modeling and Application in Vibration and Seismic Isolation," by N. Makris and M.C. Constantinou, 12/20/90 (PB91-190561, A06, MF-A01).
- NCEER-90-0029 "Soil Effects on Earthquake Ground Motions in the Memphis Area," by H. Hwang, C.S. Lee, K.W. Ng and T.S. Chang, 8/2/90, (PB91-190751, A05, MF-A01).

- NCEER-91-0001 "Proceedings from the Third Japan-U.S. Workshop on Earthquake Resistant Design of Lifeline Facilities and Countermeasures for Soil Liquefaction, December 17-19, 1990," edited by T.D. O'Rourke and M. Hamada, 2/1/91, (PB91-179259, A99, MF-A04).
- NCEER-91-0002 "Physical Space Solutions of Non-Proportionally Damped Systems," by M. Tong, Z. Liang and G.C. Lee, 1/15/91, (PB91-179242, A04, MF-A01).
- NCEER-91-0003 "Seismic Response of Single Piles and Pile Groups," by K. Fan and G. Gazetas, 1/10/91, (PB92-174994, A04, MF-A01).
- NCEER-91-0004 "Damping of Structures: Part 1 - Theory of Complex Damping," by Z. Liang and G. Lee, 10/10/91, (PB92-197235, A12, MF-A03).
- NCEER-91-0005 "3D-BASIS - Nonlinear Dynamic Analysis of Three Dimensional Base Isolated Structures: Part II," by S. Nagarajaiah, A.M. Reinhorn and M.C. Constantinou, 2/28/91, (PB91-190553, A07, MF-A01). This report has been replaced by NCEER-93-0011.
- NCEER-91-0006 "A Multidimensional Hysteretic Model for Plasticity Deforming Metals in Energy Absorbing Devices," by E.J. Graesser and F.A. Cozzarelli, 4/9/91, (PB92-108364, A04, MF-A01).
- NCEER-91-0007 "A Framework for Customizable Knowledge-Based Expert Systems with an Application to a KBES for Evaluating the Seismic Resistance of Existing Buildings," by E.G. Ibarra-Anaya and S.J. Fennes, 4/9/91, (PB91-210930, A08, MF-A01).
- NCEER-91-0008 "Nonlinear Analysis of Steel Frames with Semi-Rigid Connections Using the Capacity Spectrum Method," by G.G. Deierlein, S-H. Hsieh, Y-J. Shen and J.F. Abel, 7/2/91, (PB92-113828, A05, MF-A01).
- NCEER-91-0009 "Earthquake Education Materials for Grades K-12," by K.E.K. Ross, 4/30/91, (PB91-212142, A06, MF-A01). This report has been replaced by NCEER-92-0018.
- NCEER-91-0010 "Phase Wave Velocities and Displacement Phase Differences in a Harmonically Oscillating Pile," by N. Makris and G. Gazetas, 7/8/91, (PB92-108356, A04, MF-A01).
- NCEER-91-0011 "Dynamic Characteristics of a Full-Size Five-Story Steel Structure and a 2/5 Scale Model," by K.C. Chang, G.C. Yao, G.C. Lee, D.S. Hao and Y.C. Yeh," 7/2/91, (PB93-116648, A06, MF-A02).
- NCEER-91-0012 "Seismic Response of a 2/5 Scale Steel Structure with Added Viscoelastic Dampers," by K.C. Chang, T.T. Soong, S-T. Oh and M.L. Lai, 5/17/91, (PB92-110816, A05, MF-A01).
- NCEER-91-0013 "Earthquake Response of Retaining Walls; Full-Scale Testing and Computational Modeling," by S. Alampalli and A-W.M. Elgamal, 6/20/91, to be published.
- NCEER-91-0014 "3D-BASIS-M: Nonlinear Dynamic Analysis of Multiple Building Base Isolated Structures," by P.C. Tsopelas, S. Nagarajaiah, M.C. Constantinou and A.M. Reinhorn, 5/28/91, (PB92-113885, A09, MF-A02).
- NCEER-91-0015 "Evaluation of SEAOC Design Requirements for Sliding Isolated Structures," by D. Theodossiou and M.C. Constantinou, 6/10/91, (PB92-114602, A11, MF-A03).
- NCEER-91-0016 "Closed-Loop Modal Testing of a 27-Story Reinforced Concrete Flat Plate-Core Building," by H.R. Somaprasad, T. Toksoy, H. Yoshiyuki and A.E. Aktan, 7/15/91, (PB92-129980, A07, MF-A02).
- NCEER-91-0017 "Shake Table Test of a 1/6 Scale Two-Story Lightly Reinforced Concrete Building," by A.G. El-Attar, R.N. White and P. Gergely, 2/28/91, (PB92-222447, A06, MF-A02).
- NCEER-91-0018 "Shake Table Test of a 1/8 Scale Three-Story Lightly Reinforced Concrete Building," by A.G. El-Attar, R.N. White and P. Gergely, 2/28/91, (PB93-116630, A08, MF-A02).
- NCEER-91-0019 "Transfer Functions for Rigid Rectangular Foundations," by A.S. Veletsos, A.M. Prasad and W.H. Wu, 7/31/91, to be published.

- NCEER-91-0020 "Hybrid Control of Seismic-Excited Nonlinear and Inelastic Structural Systems," by J.N. Yang, Z. Li and A. Daniellians, 8/1/91, (PB92-143171, A06, MF-A02).
- NCEER-91-0021 "The NCEER-91 Earthquake Catalog: Improved Intensity-Based Magnitudes and Recurrence Relations for U.S. Earthquakes East of New Madrid," by L. Seeber and J.G. Armbruster, 8/28/91, (PB92-176742, A06, MF-A02).
- NCEER-91-0022 "Proceedings from the Implementation of Earthquake Planning and Education in Schools: The Need for Change - The Roles of the Changemakers," by K.E.K. Ross and F. Winslow, 7/23/91, (PB92-129998, A12, MF-A03).
- NCEER-91-0023 "A Study of Reliability-Based Criteria for Seismic Design of Reinforced Concrete Frame Buildings," by H.H.M. Hwang and H-M. Hsu, 8/10/91, (PB92-140235, A09, MF-A02).
- NCEER-91-0024 "Experimental Verification of a Number of Structural System Identification Algorithms," by R.G. Ghanem, H. Gavin and M. Shinozuka, 9/18/91, (PB92-176577, A18, MF-A04).
- NCEER-91-0025 "Probabilistic Evaluation of Liquefaction Potential," by H.H.M. Hwang and C.S. Lee," 11/25/91, (PB92-143429, A05, MF-A01).
- NCEER-91-0026 "Instantaneous Optimal Control for Linear, Nonlinear and Hysteretic Structures - Stable Controllers," by J.N. Yang and Z. Li, 11/15/91, (PB92-163807, A04, MF-A01).
- NCEER-91-0027 "Experimental and Theoretical Study of a Sliding Isolation System for Bridges," by M.C. Constantinou, A. Kartoum, A.M. Reinhorn and P. Bradford, 11/15/91, (PB92-176973, A10, MF-A03).
- NCEER-92-0001 "Case Studies of Liquefaction and Lifeline Performance During Past Earthquakes, Volume 1: Japanese Case Studies," Edited by M. Hamada and T. O'Rourke, 2/17/92, (PB92-197243, A18, MF-A04).
- NCEER-92-0002 "Case Studies of Liquefaction and Lifeline Performance During Past Earthquakes, Volume 2: United States Case Studies," Edited by T. O'Rourke and M. Hamada, 2/17/92, (PB92-197250, A20, MF-A04).
- NCEER-92-0003 "Issues in Earthquake Education," Edited by K. Ross, 2/3/92, (PB92-222389, A07, MF-A02).
- NCEER-92-0004 "Proceedings from the First U.S. - Japan Workshop on Earthquake Protective Systems for Bridges," Edited by I.G. Buckle, 2/4/92, (PB94-142239, A99, MF-A06).
- NCEER-92-0005 "Seismic Ground Motion from a Haskell-Type Source in a Multiple-Layered Half-Space," A.P. Theoharis, G. Deodatis and M. Shinozuka, 1/2/92, to be published.
- NCEER-92-0006 "Proceedings from the Site Effects Workshop," Edited by R. Whitman, 2/29/92, (PB92-197201, A04, MF-A01).
- NCEER-92-0007 "Engineering Evaluation of Permanent Ground Deformations Due to Seismically-Induced Liquefaction," by M.H. Baziar, R. Dobry and A-W.M. Elgamal, 3/24/92, (PB92-222421, A13, MF-A03).
- NCEER-92-0008 "A Procedure for the Seismic Evaluation of Buildings in the Central and Eastern United States," by C.D. Poland and J.O. Malley, 4/2/92, (PB92-222439, A20, MF-A04).
- NCEER-92-0009 "Experimental and Analytical Study of a Hybrid Isolation System Using Friction Controllable Sliding Bearings," by M.Q. Feng, S. Fujii and M. Shinozuka, 5/15/92, (PB93-150282, A06, MF-A02).
- NCEER-92-0010 "Seismic Resistance of Slab-Column Connections in Existing Non-Ductile Flat-Plate Buildings," by A.J. Durrani and Y. Du, 5/18/92, (PB93-116812, A06, MF-A02).
- NCEER-92-0011 "The Hysteretic and Dynamic Behavior of Brick Masonry Walls Upgraded by Ferrocement Coatings Under Cyclic Loading and Strong Simulated Ground Motion," by H. Lee and S.P. Prawl, 5/11/92, to be published.
- NCEER-92-0012 "Study of Wire Rope Systems for Seismic Protection of Equipment in Buildings," by G.F. Demetriades, M.C. Constantinou and A.M. Reinhorn, 5/20/92, (PB93-116655, A08, MF-A02).

- NCEER-92-0013 "Shape Memory Structural Dampers: Material Properties, Design and Seismic Testing," by P.R. Witting and F.A. Cozzarelli, 5/26/92, (PB93-116663, A05, MF-A01).
- NCEER-92-0014 "Longitudinal Permanent Ground Deformation Effects on Buried Continuous Pipelines," by M.J. O'Rourke, and C. Nordberg, 6/15/92, (PB93-116671, A08, MF-A02).
- NCEER-92-0015 "A Simulation Method for Stationary Gaussian Random Functions Based on the Sampling Theorem," by M. Grigoriu and S. Balopoulou, 6/11/92, (PB93-127496, A05, MF-A01).
- NCEER-92-0016 "Gravity-Load-Designed Reinforced Concrete Buildings: Seismic Evaluation of Existing Construction and Detailing Strategies for Improved Seismic Resistance," by G.W. Hoffmann, S.K. Kunnath, A.M. Reinhorn and J.B. Mander, 7/15/92, (PB94-142007, A08, MF-A02).
- NCEER-92-0017 "Observations on Water System and Pipeline Performance in the Limón Area of Costa Rica Due to the April 22, 1991 Earthquake," by M. O'Rourke and D. Ballantyne, 6/30/92, (PB93-126811, A06, MF-A02).
- NCEER-92-0018 "Fourth Edition of Earthquake Education Materials for Grades K-12," Edited by K.E.K. Ross, 8/10/92, (PB93-114023, A07, MF-A02).
- NCEER-92-0019 "Proceedings from the Fourth Japan-U.S. Workshop on Earthquake Resistant Design of Lifeline Facilities and Countermeasures for Soil Liquefaction," Edited by M. Hamada and T.D. O'Rourke, 8/12/92, (PB93-163939, A99, MF-E11).
- NCEER-92-0020 "Active Bracing System: A Full Scale Implementation of Active Control," by A.M. Reinhorn, T.T. Soong, R.C. Lin, M.A. Riley, Y.P. Wang, S. Aizawa and M. Higashino, 8/14/92, (PB93-127512, A06, MF-A02).
- NCEER-92-0021 "Empirical Analysis of Horizontal Ground Displacement Generated by Liquefaction-Induced Lateral Spreads," by S.F. Bartlett and T.L. Youd, 8/17/92, (PB93-188241, A06, MF-A02).
- NCEER-92-0022 "IDARC Version 3.0: Inelastic Damage Analysis of Reinforced Concrete Structures," by S.K. Kunnath, A.M. Reinhorn and R.F. Lobo, 8/31/92, (PB93-227502, A07, MF-A02).
- NCEER-92-0023 "A Semi-Empirical Analysis of Strong-Motion Peaks in Terms of Seismic Source, Propagation Path and Local Site Conditions, by M. Kamiyama, M.J. O'Rourke and R. Flores-Berrones, 9/9/92, (PB93-150266, A08, MF-A02).
- NCEER-92-0024 "Seismic Behavior of Reinforced Concrete Frame Structures with Nonductile Details, Part I: Summary of Experimental Findings of Full Scale Beam-Column Joint Tests," by A. Beres, R.N. White and P. Gergely, 9/30/92, (PB93-227783, A05, MF-A01).
- NCEER-92-0025 "Experimental Results of Repaired and Retrofitted Beam-Column Joint Tests in Lightly Reinforced Concrete Frame Buildings," by A. Beres, S. El-Borgi, R.N. White and P. Gergely, 10/29/92, (PB93-227791, A05, MF-A01).
- NCEER-92-0026 "A Generalization of Optimal Control Theory: Linear and Nonlinear Structures," by J.N. Yang, Z. Li and S. Vongchavalitkul, 11/2/92, (PB93-188621, A05, MF-A01).
- NCEER-92-0027 "Seismic Resistance of Reinforced Concrete Frame Structures Designed Only for Gravity Loads: Part I - Design and Properties of a One-Third Scale Model Structure," by J.M. Bracci, A.M. Reinhorn and J.B. Mander, 12/1/92, (PB94-104502, A08, MF-A02).
- NCEER-92-0028 "Seismic Resistance of Reinforced Concrete Frame Structures Designed Only for Gravity Loads: Part II - Experimental Performance of Subassemblages," by L.E. Aycaardi, J.B. Mander and A.M. Reinhorn, 12/1/92, (PB94-104510, A08, MF-A02).
- NCEER-92-0029 "Seismic Resistance of Reinforced Concrete Frame Structures Designed Only for Gravity Loads: Part III - Experimental Performance and Analytical Study of a Structural Model," by J.M. Bracci, A.M. Reinhorn and J.B. Mander, 12/1/92, (PB93-227528, A09, MF-A01).

- NCEER-92-0030 "Evaluation of Seismic Retrofit of Reinforced Concrete Frame Structures: Part I - Experimental Performance of Retrofitted Subassemblages," by D. Choudhuri, J.B. Mander and A.M. Reinhorn, 12/8/92, (PB93-198307, A07, MF-A02).
- NCEER-92-0031 "Evaluation of Seismic Retrofit of Reinforced Concrete Frame Structures: Part II - Experimental Performance and Analytical Study of a Retrofitted Structural Model," by J.M. Bracci, A.M. Reinhorn and J.B. Mander, 12/8/92, (PB93-198315, A09, MF-A03).
- NCEER-92-0032 "Experimental and Analytical Investigation of Seismic Response of Structures with Supplemental Fluid Viscous Dampers," by M.C. Constantinou and M.D. Symans, 12/21/92, (PB93-191435, A10, MF-A03). This report is available only through NTIS (see address given above).
- NCEER-92-0033 "Reconnaissance Report on the Cairo, Egypt Earthquake of October 12, 1992," by M. Khater, 12/23/92, (PB93-188621, A03, MF-A01).
- NCEER-92-0034 "Low-Level Dynamic Characteristics of Four Tall Flat-Plate Buildings in New York City," by H. Gavin, S. Yuan, J. Grossman, E. Pekelis and K. Jacob, 12/28/92, (PB93-188217, A07, MF-A02).
- NCEER-93-0001 "An Experimental Study on the Seismic Performance of Brick-Infilled Steel Frames With and Without Retrofit," by J.B. Mander, B. Nair, K. Wojtkowski and J. Ma, 1/29/93, (PB93-227510, A07, MF-A02).
- NCEER-93-0002 "Social Accounting for Disaster Preparedness and Recovery Planning," by S. Cole, E. Pantoja and V. Razak, 2/22/93, (PB94-142114, A12, MF-A03).
- NCEER-93-0003 "Assessment of 1991 NEHRP Provisions for Nonstructural Components and Recommended Revisions," by T.T. Soong, G. Chen, Z. Wu, R-H. Zhang and M. Grigoriu, 3/1/93, (PB93-188639, A06, MF-A02).
- NCEER-93-0004 "Evaluation of Static and Response Spectrum Analysis Procedures of SEAOC/UBC for Seismic Isolated Structures," by C.W. Winters and M.C. Constantinou, 3/23/93, (PB93-198299, A10, MF-A03).
- NCEER-93-0005 "Earthquakes in the Northeast - Are We Ignoring the Hazard? A Workshop on Earthquake Science and Safety for Educators," edited by K.E.K. Ross, 4/2/93, (PB94-103066, A09, MF-A02).
- NCEER-93-0006 "Inelastic Response of Reinforced Concrete Structures with Viscoelastic Braces," by R.F. Lobo, J.M. Bracci, K.L. Shen, A.M. Reinhorn and T.T. Soong, 4/5/93, (PB93-227486, A05, MF-A02).
- NCEER-93-0007 "Seismic Testing of Installation Methods for Computers and Data Processing Equipment," by K. Kosar, T.T. Soong, K.L. Shen, J.A. HoLung and Y.K. Lin, 4/12/93, (PB93-198299, A07, MF-A02).
- NCEER-93-0008 "Retrofit of Reinforced Concrete Frames Using Added Dampers," by A. Reinhorn, M. Constantinou and C. Li, to be published.
- NCEER-93-0009 "Seismic Behavior and Design Guidelines for Steel Frame Structures with Added Viscoelastic Dampers," by K.C. Chang, M.L. Lai, T.T. Soong, D.S. Hao and Y.C. Yeh, 5/1/93, (PB94-141959, A07, MF-A02).
- NCEER-93-0010 "Seismic Performance of Shear-Critical Reinforced Concrete Bridge Piers," by J.B. Mander, S.M. Waheed, M.T.A. Chaudhary and S.S. Chen, 5/12/93, (PB93-227494, A08, MF-A02).
- NCEER-93-0011 "3D-BASIS-TABS: Computer Program for Nonlinear Dynamic Analysis of Three Dimensional Base Isolated Structures," by S. Nagarajaiah, C. Li, A.M. Reinhorn and M.C. Constantinou, 8/2/93, (PB94-141819, A09, MF-A02).
- NCEER-93-0012 "Effects of Hydrocarbon Spills from an Oil Pipeline Break on Ground Water," by O.J. Helweg and H.H.M. Hwang, 8/3/93, (PB94-141942, A06, MF-A02).
- NCEER-93-0013 "Simplified Procedures for Seismic Design of Nonstructural Components and Assessment of Current Code Provisions," by M.P. Singh, L.E. Suarez, E.E. Matheu and G.O. Maldonado, 8/4/93, (PB94-141827, A09, MF-A02).
- NCEER-93-0014 "An Energy Approach to Seismic Analysis and Design of Secondary Systems," by G. Chen and T.T. Soong, 8/6/93, (PB94-142767, A11, MF-A03).

- NCEER-93-0015 "Proceedings from School Sites: Becoming Prepared for Earthquakes - Commemorating the Third Anniversary of the Loma Prieta Earthquake," Edited by F.E. Winslow and K.E.K. Ross, 8/16/93, (PB94-154275, A16, MF-A02).
- NCEER-93-0016 "Reconnaissance Report of Damage to Historic Monuments in Cairo, Egypt Following the October 12, 1992 Dahshur Earthquake," by D. Sykora, D. Look, G. Croci, E. Karaesmen and E. Karaesmen, 8/19/93, (PB94-142221, A08, MF-A02).
- NCEER-93-0017 "The Island of Guam Earthquake of August 8, 1993," by S.W. Swan and S.K. Harris, 9/30/93, (PB94-141843, A04, MF-A01).
- NCEER-93-0018 "Engineering Aspects of the October 12, 1992 Egyptian Earthquake," by A.W. Elgamal, M. Amer, K. Adalier and A. Abul-Fadl, 10/7/93, (PB94-141983, A05, MF-A01).
- NCEER-93-0019 "Development of an Earthquake Motion Simulator and its Application in Dynamic Centrifuge Testing," by I. Krstelj, Supervised by J.H. Prevost, 10/23/93, (PB94-181773, A-10, MF-A03).
- NCEER-93-0020 "NCEER-Taisei Corporation Research Program on Sliding Seismic Isolation Systems for Bridges: Experimental and Analytical Study of a Friction Pendulum System (FPS)," by M.C. Constantinou, P. Tsopelas, Y-S. Kim and S. Okamoto, 11/1/93, (PB94-142775, A08, MF-A02).
- NCEER-93-0021 "Finite Element Modeling of Elastomeric Seismic Isolation Bearings," by L.J. Billings, Supervised by R. Shepherd, 11/8/93, to be published.
- NCEER-93-0022 "Seismic Vulnerability of Equipment in Critical Facilities: Life-Safety and Operational Consequences," by K. Porter, G.S. Johnson, M.M. Zadeh, C. Scawthorn and S. Eder, 11/24/93, (PB94-181765, A16, MF-A03).
- NCEER-93-0023 "Hokkaido Nansei-oki, Japan Earthquake of July 12, 1993, by P.I. Yanev and C.R. Scawthorn, 12/23/93, (PB94-181500, A07, MF-A01).
- NCEER-94-0001 "An Evaluation of Seismic Serviceability of Water Supply Networks with Application to the San Francisco Auxiliary Water Supply System," by I. Markov, Supervised by M. Grigoriu and T. O'Rourke, 1/21/94, (PB94-204013, A07, MF-A02).
- NCEER-94-0002 "NCEER-Taisei Corporation Research Program on Sliding Seismic Isolation Systems for Bridges: Experimental and Analytical Study of Systems Consisting of Sliding Bearings, Rubber Restoring Force Devices and Fluid Dampers," Volumes I and II, by P. Tsopelas, S. Okamoto, M.C. Constantinou, D. Ozaki and S. Fujii, 2/4/94, (PB94-181740, A09, MF-A02 and PB94-181757, A12, MF-A03).
- NCEER-94-0003 "A Markov Model for Local and Global Damage Indices in Seismic Analysis," by S. Rahman and M. Grigoriu, 2/18/94, (PB94-206000, A12, MF-A03).
- NCEER-94-0004 "Proceedings from the NCEER Workshop on Seismic Response of Masonry Infills," edited by D.P. Abrams, 3/1/94, (PB94-180783, A07, MF-A02).
- NCEER-94-0005 "The Northridge, California Earthquake of January 17, 1994: General Reconnaissance Report," edited by J.D. Goltz, 3/11/94, (PB94-193943, A10, MF-A03).
- NCEER-94-0006 "Seismic Energy Based Fatigue Damage Analysis of Bridge Columns: Part I - Evaluation of Seismic Capacity," by G.A. Chang and J.B. Mander, 3/14/94, (PB94-219185, A11, MF-A03).
- NCEER-94-0007 "Seismic Isolation of Multi-Story Frame Structures Using Spherical Sliding Isolation Systems," by T.M. Al-Hussaini, V.A. Zayas and M.C. Constantinou, 3/17/94, (PB94-193745, A09, MF-A02).
- NCEER-94-0008 "The Northridge, California Earthquake of January 17, 1994: Performance of Highway Bridges," edited by I.G. Buckle, 3/24/94, (PB94-193851, A06, MF-A02).
- NCEER-94-0009 "Proceedings of the Third U.S.-Japan Workshop on Earthquake Protective Systems for Bridges," edited by I.G. Buckle and I. Friedland, 3/31/94, (PB94-195815, A99, MF-A06).

- NCEER-94-0010 "3D-BASIS-ME: Computer Program for Nonlinear Dynamic Analysis of Seismically Isolated Single and Multiple Structures and Liquid Storage Tanks," by P.C. Tsopelas, M.C. Constantinou and A.M. Reinhorn, 4/12/94, (PB94-204922, A09, MF-A02).
- NCEER-94-0011 "The Northridge, California Earthquake of January 17, 1994: Performance of Gas Transmission Pipelines," by T.D. O'Rourke and M.C. Palmer, 5/16/94, (PB94-204989, A05, MF-A01).
- NCEER-94-0012 "Feasibility Study of Replacement Procedures and Earthquake Performance Related to Gas Transmission Pipelines," by T.D. O'Rourke and M.C. Palmer, 5/25/94, (PB94-206638, A09, MF-A02).
- NCEER-94-0013 "Seismic Energy Based Fatigue Damage Analysis of Bridge Columns: Part II - Evaluation of Seismic Demand," by G.A. Chang and J.B. Mander, 6/1/94, (PB95-18106, A08, MF-A02).
- NCEER-94-0014 "NCEER-Taisei Corporation Research Program on Sliding Seismic Isolation Systems for Bridges: Experimental and Analytical Study of a System Consisting of Sliding Bearings and Fluid Restoring Force/Damping Devices," by P. Tsopelas and M.C. Constantinou, 6/13/94, (PB94-219144, A10, MF-A03).
- NCEER-94-0015 "Generation of Hazard-Consistent Fragility Curves for Seismic Loss Estimation Studies," by H. Hwang and J-R. Huo, 6/14/94, (PB95-181996, A09, MF-A02).
- NCEER-94-0016 "Seismic Study of Building Frames with Added Energy-Absorbing Devices," by W.S. Pong, C.S. Tsai and G.C. Lee, 6/20/94, (PB94-219136, A10, A03).
- NCEER-94-0017 "Sliding Mode Control for Seismic-Excited Linear and Nonlinear Civil Engineering Structures," by J. Yang, J. Wu, A. Agrawal and Z. Li, 6/21/94, (PB95-138483, A06, MF-A02).
- NCEER-94-0018 "3D-BASIS-TABS Version 2.0: Computer Program for Nonlinear Dynamic Analysis of Three Dimensional Base Isolated Structures," by A.M. Reinhorn, S. Nagarajaiah, M.C. Constantinou, P. Tsopelas and R. Li, 6/22/94, (PB95-182176, A08, MF-A02).
- NCEER-94-0019 "Proceedings of the International Workshop on Civil Infrastructure Systems: Application of Intelligent Systems and Advanced Materials on Bridge Systems," Edited by G.C. Lee and K.C. Chang, 7/18/94, (PB95-252474, A20, MF-A04).
- NCEER-94-0020 "Study of Seismic Isolation Systems for Computer Floors," by V. Lambrou and M.C. Constantinou, 7/19/94, (PB95-138533, A10, MF-A03).
- NCEER-94-0021 "Proceedings of the U.S.-Italian Workshop on Guidelines for Seismic Evaluation and Rehabilitation of Unreinforced Masonry Buildings," Edited by D.P. Abrams and G.M. Calvi, 7/20/94, (PB95-138749, A13, MF-A03).
- NCEER-94-0022 "NCEER-Taisei Corporation Research Program on Sliding Seismic Isolation Systems for Bridges: Experimental and Analytical Study of a System Consisting of Lubricated PTFE Sliding Bearings and Mild Steel Dampers," by P. Tsopelas and M.C. Constantinou, 7/22/94, (PB95-182184, A08, MF-A02).
- NCEER-94-0023 "Development of Reliability-Based Design Criteria for Buildings Under Seismic Load," by Y.K. Wen, H. Hwang and M. Shinozuka, 8/1/94, (PB95-211934, A08, MF-A02).
- NCEER-94-0024 "Experimental Verification of Acceleration Feedback Control Strategies for an Active Tendon System," by S.J. Dyke, B.F. Spencer, Jr., P. Quast, M.K. Sain, D.C. Kaspari, Jr. and T.T. Soong, 8/29/94, (PB95-212320, A05, MF-A01).
- NCEER-94-0025 "Seismic Retrofitting Manual for Highway Bridges," Edited by I.G. Buckle and I.F. Friedland, published by the Federal Highway Administration (PB95-212676, A15, MF-A03).
- NCEER-94-0026 "Proceedings from the Fifth U.S.-Japan Workshop on Earthquake Resistant Design of Lifeline Facilities and Countermeasures Against Soil Liquefaction," Edited by T.D. O'Rourke and M. Hamada, 11/7/94, (PB95-220802, A99, MF-E08).

- NCEER-95-0001 “Experimental and Analytical Investigation of Seismic Retrofit of Structures with Supplemental Damping: Part 1 - Fluid Viscous Damping Devices,” by A.M. Reinhorn, C. Li and M.C. Constantinou, 1/3/95, (PB95-266599, A09, MF-A02).
- NCEER-95-0002 “Experimental and Analytical Study of Low-Cycle Fatigue Behavior of Semi-Rigid Top-And-Seat Angle Connections,” by G. Pekcan, J.B. Mander and S.S. Chen, 1/5/95, (PB95-220042, A07, MF-A02).
- NCEER-95-0003 “NCEER-ATC Joint Study on Fragility of Buildings,” by T. Anagnos, C. Rojahn and A.S. Kiremidjian, 1/20/95, (PB95-220026, A06, MF-A02).
- NCEER-95-0004 “Nonlinear Control Algorithms for Peak Response Reduction,” by Z. Wu, T.T. Soong, V. Gattulli and R.C. Lin, 2/16/95, (PB95-220349, A05, MF-A01).
- NCEER-95-0005 “Pipeline Replacement Feasibility Study: A Methodology for Minimizing Seismic and Corrosion Risks to Underground Natural Gas Pipelines,” by R.T. Eguchi, H.A. Seligson and D.G. Honegger, 3/2/95, (PB95-252326, A06, MF-A02).
- NCEER-95-0006 “Evaluation of Seismic Performance of an 11-Story Frame Building During the 1994 Northridge Earthquake,” by F. Naeim, R. DiSulio, K. Benuska, A. Reinhorn and C. Li, to be published.
- NCEER-95-0007 “Prioritization of Bridges for Seismic Retrofitting,” by N. Basöz and A.S. Kiremidjian, 4/24/95, (PB95-252300, A08, MF-A02).
- NCEER-95-0008 “Method for Developing Motion Damage Relationships for Reinforced Concrete Frames,” by A. Singhal and A.S. Kiremidjian, 5/11/95, (PB95-266607, A06, MF-A02).
- NCEER-95-0009 “Experimental and Analytical Investigation of Seismic Retrofit of Structures with Supplemental Damping: Part II - Friction Devices,” by C. Li and A.M. Reinhorn, 7/6/95, (PB96-128087, A11, MF-A03).
- NCEER-95-0010 “Experimental Performance and Analytical Study of a Non-Ductile Reinforced Concrete Frame Structure Retrofitted with Elastomeric Spring Dampers,” by G. Pekcan, J.B. Mander and S.S. Chen, 7/14/95, (PB96-137161, A08, MF-A02).
- NCEER-95-0011 “Development and Experimental Study of Semi-Active Fluid Damping Devices for Seismic Protection of Structures,” by M.D. Symans and M.C. Constantinou, 8/3/95, (PB96-136940, A23, MF-A04).
- NCEER-95-0012 “Real-Time Structural Parameter Modification (RSPM): Development of Innervated Structures,” by Z. Liang, M. Tong and G.C. Lee, 4/11/95, (PB96-137153, A06, MF-A01).
- NCEER-95-0013 “Experimental and Analytical Investigation of Seismic Retrofit of Structures with Supplemental Damping: Part III - Viscous Damping Walls,” by A.M. Reinhorn and C. Li, 10/1/95, (PB96-176409, A11, MF-A03).
- NCEER-95-0014 “Seismic Fragility Analysis of Equipment and Structures in a Memphis Electric Substation,” by J-R. Huo and H.H.M. Hwang, 8/10/95, (PB96-128087, A09, MF-A02).
- NCEER-95-0015 “The Hanshin-Awaji Earthquake of January 17, 1995: Performance of Lifelines,” Edited by M. Shinozuka, 11/3/95, (PB96-176383, A15, MF-A03).
- NCEER-95-0016 “Highway Culvert Performance During Earthquakes,” by T.L. Youd and C.J. Beckman, available as NCEER-96-0015.
- NCEER-95-0017 “The Hanshin-Awaji Earthquake of January 17, 1995: Performance of Highway Bridges,” Edited by I.G. Buckle, 12/1/95, to be published.
- NCEER-95-0018 “Modeling of Masonry Infill Panels for Structural Analysis,” by A.M. Reinhorn, A. Madan, R.E. Valles, Y. Reichmann and J.B. Mander, 12/8/95, (PB97-110886, MF-A01, A06).
- NCEER-95-0019 “Optimal Polynomial Control for Linear and Nonlinear Structures,” by A.K. Agrawal and J.N. Yang, 12/11/95, (PB96-168737, A07, MF-A02).

- NCEER-95-0020 "Retrofit of Non-Ductile Reinforced Concrete Frames Using Friction Dampers," by R.S. Rao, P. Gergely and R.N. White, 12/22/95, (PB97-133508, A10, MF-A02).
- NCEER-95-0021 "Parametric Results for Seismic Response of Pile-Supported Bridge Bents," by G. Mylonakis, A. Nikolaou and G. Gazetas, 12/22/95, (PB97-100242, A12, MF-A03).
- NCEER-95-0022 "Kinematic Bending Moments in Seismically Stressed Piles," by A. Nikolaou, G. Mylonakis and G. Gazetas, 12/23/95, (PB97-113914, MF-A03, A13).
- NCEER-96-0001 "Dynamic Response of Unreinforced Masonry Buildings with Flexible Diaphragms," by A.C. Costley and D.P. Abrams, 10/10/96, (PB97-133573, MF-A03, A15).
- NCEER-96-0002 "State of the Art Review: Foundations and Retaining Structures," by I. Po Lam, to be published.
- NCEER-96-0003 "Ductility of Rectangular Reinforced Concrete Bridge Columns with Moderate Confinement," by N. Wehbe, M. Saiidi, D. Sanders and B. Douglas, 11/7/96, (PB97-133557, A06, MF-A02).
- NCEER-96-0004 "Proceedings of the Long-Span Bridge Seismic Research Workshop," edited by I.G. Buckle and I.M. Friedland, to be published.
- NCEER-96-0005 "Establish Representative Pier Types for Comprehensive Study: Eastern United States," by J. Kulicki and Z. Prucz, 5/28/96, (PB98-119217, A07, MF-A02).
- NCEER-96-0006 "Establish Representative Pier Types for Comprehensive Study: Western United States," by R. Imbsen, R.A. Schamber and T.A. Osterkamp, 5/28/96, (PB98-118607, A07, MF-A02).
- NCEER-96-0007 "Nonlinear Control Techniques for Dynamical Systems with Uncertain Parameters," by R.G. Ghanem and M.I. Bujakov, 5/27/96, (PB97-100259, A17, MF-A03).
- NCEER-96-0008 "Seismic Evaluation of a 30-Year Old Non-Ductile Highway Bridge Pier and Its Retrofit," by J.B. Mander, B. Mahmoodzadegan, S. Bhadra and S.S. Chen, 5/31/96, (PB97-110902, MF-A03, A10).
- NCEER-96-0009 "Seismic Performance of a Model Reinforced Concrete Bridge Pier Before and After Retrofit," by J.B. Mander, J.H. Kim and C.A. Ligozio, 5/31/96, (PB97-110910, MF-A02, A10).
- NCEER-96-0010 "IDARC2D Version 4.0: A Computer Program for the Inelastic Damage Analysis of Buildings," by R.E. Valles, A.M. Reinhorn, S.K. Kunnath, C. Li and A. Madan, 6/3/96, (PB97-100234, A17, MF-A03).
- NCEER-96-0011 "Estimation of the Economic Impact of Multiple Lifeline Disruption: Memphis Light, Gas and Water Division Case Study," by S.E. Chang, H.A. Seligson and R.T. Eguchi, 8/16/96, (PB97-133490, A11, MF-A03).
- NCEER-96-0012 "Proceedings from the Sixth Japan-U.S. Workshop on Earthquake Resistant Design of Lifeline Facilities and Countermeasures Against Soil Liquefaction, Edited by M. Hamada and T. O'Rourke, 9/11/96, (PB97-133581, A99, MF-A06).
- NCEER-96-0013 "Chemical Hazards, Mitigation and Preparedness in Areas of High Seismic Risk: A Methodology for Estimating the Risk of Post-Earthquake Hazardous Materials Release," by H.A. Seligson, R.T. Eguchi, K.J. Tierney and K. Richmond, 11/7/96, (PB97-133565, MF-A02, A08).
- NCEER-96-0014 "Response of Steel Bridge Bearings to Reversed Cyclic Loading," by J.B. Mander, D-K. Kim, S.S. Chen and G.J. Premus, 11/13/96, (PB97-140735, A12, MF-A03).
- NCEER-96-0015 "Highway Culvert Performance During Past Earthquakes," by T.L. Youd and C.J. Beckman, 11/25/96, (PB97-133532, A06, MF-A01).
- NCEER-97-0001 "Evaluation, Prevention and Mitigation of Pounding Effects in Building Structures," by R.E. Valles and A.M. Reinhorn, 2/20/97, (PB97-159552, A14, MF-A03).
- NCEER-97-0002 "Seismic Design Criteria for Bridges and Other Highway Structures," by C. Rojahn, R. Mayes, D.G. Anderson, J. Clark, J.H. Hom, R.V. Nutt and M.J. O'Rourke, 4/30/97, (PB97-194658, A06, MF-A03).

- NCEER-97-0003 "Proceedings of the U.S.-Italian Workshop on Seismic Evaluation and Retrofit," Edited by D.P. Abrams and G.M. Calvi, 3/19/97, (PB97-194666, A13, MF-A03).
- NCEER-97-0004 "Investigation of Seismic Response of Buildings with Linear and Nonlinear Fluid Viscous Dampers," by A.A. Seleemah and M.C. Constantinou, 5/21/97, (PB98-109002, A15, MF-A03).
- NCEER-97-0005 "Proceedings of the Workshop on Earthquake Engineering Frontiers in Transportation Facilities," edited by G.C. Lee and I.M. Friedland, 8/29/97, (PB98-128911, A25, MR-A04).
- NCEER-97-0006 "Cumulative Seismic Damage of Reinforced Concrete Bridge Piers," by S.K. Kunnath, A. El-Bahy, A. Taylor and W. Stone, 9/2/97, (PB98-108814, A11, MF-A03).
- NCEER-97-0007 "Structural Details to Accommodate Seismic Movements of Highway Bridges and Retaining Walls," by R.A. Imbsen, R.A. Schamber, E. Thorkildsen, A. Kartoum, B.T. Martin, T.N. Rosser and J.M. Kulicki, 9/3/97, (PB98-108996, A09, MF-A02).
- NCEER-97-0008 "A Method for Earthquake Motion-Damage Relationships with Application to Reinforced Concrete Frames," by A. Singhal and A.S. Kiremidjian, 9/10/97, (PB98-108988, A13, MF-A03).
- NCEER-97-0009 "Seismic Analysis and Design of Bridge Abutments Considering Sliding and Rotation," by K. Fishman and R. Richards, Jr., 9/15/97, (PB98-108897, A06, MF-A02).
- NCEER-97-0010 "Proceedings of the FHWA/NCEER Workshop on the National Representation of Seismic Ground Motion for New and Existing Highway Facilities," edited by I.M. Friedland, M.S. Power and R.L. Mayes, 9/22/97, (PB98-128903, A21, MF-A04).
- NCEER-97-0011 "Seismic Analysis for Design or Retrofit of Gravity Bridge Abutments," by K.L. Fishman, R. Richards, Jr. and R.C. Divito, 10/2/97, (PB98-128937, A08, MF-A02).
- NCEER-97-0012 "Evaluation of Simplified Methods of Analysis for Yielding Structures," by P. Tsopelas, M.C. Constantinou, C.A. Kircher and A.S. Whittaker, 10/31/97, (PB98-128929, A10, MF-A03).
- NCEER-97-0013 "Seismic Design of Bridge Columns Based on Control and Repairability of Damage," by C-T. Cheng and J.B. Mander, 12/8/97, (PB98-144249, A11, MF-A03).
- NCEER-97-0014 "Seismic Resistance of Bridge Piers Based on Damage Avoidance Design," by J.B. Mander and C-T. Cheng, 12/10/97, (PB98-144223, A09, MF-A02).
- NCEER-97-0015 "Seismic Response of Nominally Symmetric Systems with Strength Uncertainty," by S. Balopoulou and M. Grigoriu, 12/23/97, (PB98-153422, A11, MF-A03).
- NCEER-97-0016 "Evaluation of Seismic Retrofit Methods for Reinforced Concrete Bridge Columns," by T.J. Wipf, F.W. Klaiber and F.M. Russo, 12/28/97, (PB98-144215, A12, MF-A03).
- NCEER-97-0017 "Seismic Fragility of Existing Conventional Reinforced Concrete Highway Bridges," by C.L. Mullen and A.S. Cakmak, 12/30/97, (PB98-153406, A08, MF-A02).
- NCEER-97-0018 "Loss Assessment of Memphis Buildings," edited by D.P. Abrams and M. Shinozuka, 12/31/97, (PB98-144231, A13, MF-A03).
- NCEER-97-0019 "Seismic Evaluation of Frames with Infill Walls Using Quasi-static Experiments," by K.M. Mosalam, R.N. White and P. Gergely, 12/31/97, (PB98-153455, A07, MF-A02).
- NCEER-97-0020 "Seismic Evaluation of Frames with Infill Walls Using Pseudo-dynamic Experiments," by K.M. Mosalam, R.N. White and P. Gergely, 12/31/97, (PB98-153430, A07, MF-A02).
- NCEER-97-0021 "Computational Strategies for Frames with Infill Walls: Discrete and Smeared Crack Analyses and Seismic Fragility," by K.M. Mosalam, R.N. White and P. Gergely, 12/31/97, (PB98-153414, A10, MF-A02).

- NCEER-97-0022 "Proceedings of the NCEER Workshop on Evaluation of Liquefaction Resistance of Soils," edited by T.L. Youd and I.M. Idriss, 12/31/97, (PB98-155617, A15, MF-A03).
- MCEER-98-0001 "Extraction of Nonlinear Hysteretic Properties of Seismically Isolated Bridges from Quick-Release Field Tests," by Q. Chen, B.M. Douglas, E.M. Maragakis and I.G. Buckle, 5/26/98, (PB99-118838, A06, MF-A01).
- MCEER-98-0002 "Methodologies for Evaluating the Importance of Highway Bridges," by A. Thomas, S. Eshenaur and J. Kulicki, 5/29/98, (PB99-118846, A10, MF-A02).
- MCEER-98-0003 "Capacity Design of Bridge Piers and the Analysis of Overstrength," by J.B. Mander, A. Dutta and P. Goel, 6/1/98, (PB99-118853, A09, MF-A02).
- MCEER-98-0004 "Evaluation of Bridge Damage Data from the Loma Prieta and Northridge, California Earthquakes," by N. Basoz and A. Kiremidjian, 6/2/98, (PB99-118861, A15, MF-A03).
- MCEER-98-0005 "Screening Guide for Rapid Assessment of Liquefaction Hazard at Highway Bridge Sites," by T. L. Youd, 6/16/98, (PB99-118879, A06, not available on microfiche).
- MCEER-98-0006 "Structural Steel and Steel/Concrete Interface Details for Bridges," by P. Ritchie, N. Kaulh and J. Kulicki, 7/13/98, (PB99-118945, A06, MF-A01).
- MCEER-98-0007 "Capacity Design and Fatigue Analysis of Confined Concrete Columns," by A. Dutta and J.B. Mander, 7/14/98, (PB99-118960, A14, MF-A03).
- MCEER-98-0008 "Proceedings of the Workshop on Performance Criteria for Telecommunication Services Under Earthquake Conditions," edited by A.J. Schiff, 7/15/98, (PB99-118952, A08, MF-A02).
- MCEER-98-0009 "Fatigue Analysis of Unconfined Concrete Columns," by J.B. Mander, A. Dutta and J.H. Kim, 9/12/98, (PB99-123655, A10, MF-A02).
- MCEER-98-0010 "Centrifuge Modeling of Cyclic Lateral Response of Pile-Cap Systems and Seat-Type Abutments in Dry Sands," by A.D. Gadre and R. Dobry, 10/2/98, (PB99-123606, A13, MF-A03).
- MCEER-98-0011 "IDARC-BRIDGE: A Computational Platform for Seismic Damage Assessment of Bridge Structures," by A.M. Reinhorn, V. Simeonov, G. Mylonakis and Y. Reichman, 10/2/98, (PB99-162919, A15, MF-A03).
- MCEER-98-0012 "Experimental Investigation of the Dynamic Response of Two Bridges Before and After Retrofitting with Elastomeric Bearings," by D.A. Wendichansky, S.S. Chen and J.B. Mander, 10/2/98, (PB99-162927, A15, MF-A03).
- MCEER-98-0013 "Design Procedures for Hinge Restrainers and Hinge Sear Width for Multiple-Frame Bridges," by R. Des Roches and G.L. Fenves, 11/3/98, (PB99-140477, A13, MF-A03).
- MCEER-98-0014 "Response Modification Factors for Seismically Isolated Bridges," by M.C. Constantinou and J.K. Quarshie, 11/3/98, (PB99-140485, A14, MF-A03).
- MCEER-98-0015 "Proceedings of the U.S.-Italy Workshop on Seismic Protective Systems for Bridges," edited by I.M. Friedland and M.C. Constantinou, 11/3/98, (PB2000-101711, A22, MF-A04).
- MCEER-98-0016 "Appropriate Seismic Reliability for Critical Equipment Systems: Recommendations Based on Regional Analysis of Financial and Life Loss," by K. Porter, C. Scawthorn, C. Taylor and N. Blais, 11/10/98, (PB99-157265, A08, MF-A02).
- MCEER-98-0017 "Proceedings of the U.S. Japan Joint Seminar on Civil Infrastructure Systems Research," edited by M. Shinozuka and A. Rose, 11/12/98, (PB99-156713, A16, MF-A03).
- MCEER-98-0018 "Modeling of Pile Footings and Drilled Shafts for Seismic Design," by I. PoLam, M. Kapuskar and D. Chaudhuri, 12/21/98, (PB99-157257, A09, MF-A02).

- MCEER-99-0001 "Seismic Evaluation of a Masonry Infilled Reinforced Concrete Frame by Pseudodynamic Testing," by S.G. Buonopane and R.N. White, 2/16/99, (PB99-162851, A09, MF-A02).
- MCEER-99-0002 "Response History Analysis of Structures with Seismic Isolation and Energy Dissipation Systems: Verification Examples for Program SAP2000," by J. Scheller and M.C. Constantinou, 2/22/99, (PB99-162869, A08, MF-A02).
- MCEER-99-0003 "Experimental Study on the Seismic Design and Retrofit of Bridge Columns Including Axial Load Effects," by A. Dutta, T. Kokorina and J.B. Mander, 2/22/99, (PB99-162877, A09, MF-A02).
- MCEER-99-0004 "Experimental Study of Bridge Elastomeric and Other Isolation and Energy Dissipation Systems with Emphasis on Uplift Prevention and High Velocity Near-source Seismic Excitation," by A. Kasalanati and M. C. Constantinou, 2/26/99, (PB99-162885, A12, MF-A03).
- MCEER-99-0005 "Truss Modeling of Reinforced Concrete Shear-flexure Behavior," by J.H. Kim and J.B. Mander, 3/8/99, (PB99-163693, A12, MF-A03).
- MCEER-99-0006 "Experimental Investigation and Computational Modeling of Seismic Response of a 1:4 Scale Model Steel Structure with a Load Balancing Supplemental Damping System," by G. Pekcan, J.B. Mander and S.S. Chen, 4/2/99, (PB99-162893, A11, MF-A03).
- MCEER-99-0007 "Effect of Vertical Ground Motions on the Structural Response of Highway Bridges," by M.R. Button, C.J. Cronin and R.L. Mayes, 4/10/99, (PB2000-101411, A10, MF-A03).
- MCEER-99-0008 "Seismic Reliability Assessment of Critical Facilities: A Handbook, Supporting Documentation, and Model Code Provisions," by G.S. Johnson, R.E. Sheppard, M.D. Quilici, S.J. Eder and C.R. Scawthorn, 4/12/99, (PB2000-101701, A18, MF-A04).
- MCEER-99-0009 "Impact Assessment of Selected MCEER Highway Project Research on the Seismic Design of Highway Structures," by C. Rojahn, R. Mayes, D.G. Anderson, J.H. Clark, D'Appolonia Engineering, S. Gloyd and R.V. Nutt, 4/14/99, (PB99-162901, A10, MF-A02).
- MCEER-99-0010 "Site Factors and Site Categories in Seismic Codes," by R. Dobry, R. Ramos and M.S. Power, 7/19/99, (PB2000-101705, A08, MF-A02).
- MCEER-99-0011 "Restraint Design Procedures for Multi-Span Simply-Supported Bridges," by M.J. Randall, M. Saiidi, E. Maragakis and T. Isakovic, 7/20/99, (PB2000-101702, A10, MF-A02).
- MCEER-99-0012 "Property Modification Factors for Seismic Isolation Bearings," by M.C. Constantinou, P. Tsopelas, A. Kasalanati and E. Wolff, 7/20/99, (PB2000-103387, A11, MF-A03).
- MCEER-99-0013 "Critical Seismic Issues for Existing Steel Bridges," by P. Ritchie, N. Kauh and J. Kulicki, 7/20/99, (PB2000-101697, A09, MF-A02).
- MCEER-99-0014 "Nonstructural Damage Database," by A. Kao, T.T. Soong and A. Vender, 7/24/99, (PB2000-101407, A06, MF-A01).
- MCEER-99-0015 "Guide to Remedial Measures for Liquefaction Mitigation at Existing Highway Bridge Sites," by H.G. Cooke and J. K. Mitchell, 7/26/99, (PB2000-101703, A11, MF-A03).
- MCEER-99-0016 "Proceedings of the MCEER Workshop on Ground Motion Methodologies for the Eastern United States," edited by N. Abrahamson and A. Becker, 8/11/99, (PB2000-103385, A07, MF-A02).
- MCEER-99-0017 "Quindío, Colombia Earthquake of January 25, 1999: Reconnaissance Report," by A.P. Asfura and P.J. Flores, 10/4/99, (PB2000-106893, A06, MF-A01).
- MCEER-99-0018 "Hysteretic Models for Cyclic Behavior of Deteriorating Inelastic Structures," by M.V. Sivaselvan and A.M. Reinhorn, 11/5/99, (PB2000-103386, A08, MF-A02).

- MCEER-99-0019 "Proceedings of the 7th U.S.- Japan Workshop on Earthquake Resistant Design of Lifeline Facilities and Countermeasures Against Soil Liquefaction," edited by T.D. O'Rourke, J.P. Bardet and M. Hamada, 11/19/99, (PB2000-103354, A99, MF-A06).
- MCEER-99-0020 "Development of Measurement Capability for Micro-Vibration Evaluations with Application to Chip Fabrication Facilities," by G.C. Lee, Z. Liang, J.W. Song, J.D. Shen and W.C. Liu, 12/1/99, (PB2000-105993, A08, MF-A02).
- MCEER-99-0021 "Design and Retrofit Methodology for Building Structures with Supplemental Energy Dissipating Systems," by G. Pekcan, J.B. Mander and S.S. Chen, 12/31/99, (PB2000-105994, A11, MF-A03).
- MCEER-00-0001 "The Marmara, Turkey Earthquake of August 17, 1999: Reconnaissance Report," edited by C. Scawthorn; with major contributions by M. Bruneau, R. Eguchi, T. Holzer, G. Johnson, J. Mander, J. Mitchell, W. Mitchell, A. Papageorgiou, C. Scaethorn, and G. Webb, 3/23/00, (PB2000-106200, A11, MF-A03).
- MCEER-00-0002 "Proceedings of the MCEER Workshop for Seismic Hazard Mitigation of Health Care Facilities," edited by G.C. Lee, M. Ettouney, M. Grigoriu, J. Hauer and J. Nigg, 3/29/00, (PB2000-106892, A08, MF-A02).
- MCEER-00-0003 "The Chi-Chi, Taiwan Earthquake of September 21, 1999: Reconnaissance Report," edited by G.C. Lee and C.H. Loh, with major contributions by G.C. Lee, M. Bruneau, I.G. Buckle, S.E. Chang, P.J. Flores, T.D. O'Rourke, M. Shinozuka, T.T. Soong, C-H. Loh, K-C. Chang, Z-J. Chen, J-S. Hwang, M-L. Lin, G-Y. Liu, K-C. Tsai, G.C. Yao and C-L. Yen, 4/30/00, (PB2001-100980, A10, MF-A02).
- MCEER-00-0004 "Seismic Retrofit of End-Sway Frames of Steel Deck-Truss Bridges with a Supplemental Tendon System: Experimental and Analytical Investigation," by G. Pekcan, J.B. Mander and S.S. Chen, 7/1/00, (PB2001-100982, A10, MF-A02).
- MCEER-00-0005 "Sliding Fragility of Unrestrained Equipment in Critical Facilities," by W.H. Chong and T.T. Soong, 7/5/00, (PB2001-100983, A08, MF-A02).
- MCEER-00-0006 "Seismic Response of Reinforced Concrete Bridge Pier Walls in the Weak Direction," by N. Abo-Shadi, M. Saiidi and D. Sanders, 7/17/00, (PB2001-100981, A17, MF-A03).
- MCEER-00-0007 "Low-Cycle Fatigue Behavior of Longitudinal Reinforcement in Reinforced Concrete Bridge Columns," by J. Brown and S.K. Kunnath, 7/23/00, (PB2001-104392, A08, MF-A02).
- MCEER-00-0008 "Soil Structure Interaction of Bridges for Seismic Analysis," I. PoLam and H. Law, 9/25/00, (PB2001-105397, A08, MF-A02).
- MCEER-00-0009 "Proceedings of the First MCEER Workshop on Mitigation of Earthquake Disaster by Advanced Technologies (MEDAT-1), edited by M. Shinozuka, D.J. Inman and T.D. O'Rourke, 11/10/00, (PB2001-105399, A14, MF-A03).
- MCEER-00-0010 "Development and Evaluation of Simplified Procedures for Analysis and Design of Buildings with Passive Energy Dissipation Systems, Revision 01," by O.M. Ramirez, M.C. Constantinou, C.A. Kircher, A.S. Whittaker, M.W. Johnson, J.D. Gomez and C. Chrysostomou, 11/16/01, (PB2001-105523, A23, MF-A04).
- MCEER-00-0011 "Dynamic Soil-Foundation-Structure Interaction Analyses of Large Caissons," by C-Y. Chang, C-M. Mok, Z-L. Wang, R. Settgast, F. Waggoner, M.A. Ketchum, H.M. Gonnermann and C-C. Chin, 12/30/00, (PB2001-104373, A07, MF-A02).
- MCEER-00-0012 "Experimental Evaluation of Seismic Performance of Bridge Restrainers," by A.G. Vlassis, E.M. Maragakis and M. Saiid Saiidi, 12/30/00, (PB2001-104354, A09, MF-A02).
- MCEER-00-0013 "Effect of Spatial Variation of Ground Motion on Highway Structures," by M. Shinozuka, V. Saxena and G. Deodatis, 12/31/00, (PB2001-108755, A13, MF-A03).
- MCEER-00-0014 "A Risk-Based Methodology for Assessing the Seismic Performance of Highway Systems," by S.D. Werner, C.E. Taylor, J.E. Moore, II, J.S. Walton and S. Cho, 12/31/00, (PB2001-108756, A14, MF-A03).

- MCEER-01-0001 “Experimental Investigation of P-Delta Effects to Collapse During Earthquakes,” by D. Vian and M. Bruneau, 6/25/01, (PB2002-100534, A17, MF-A03).
- MCEER-01-0002 “Proceedings of the Second MCEER Workshop on Mitigation of Earthquake Disaster by Advanced Technologies (MEDAT-2),” edited by M. Bruneau and D.J. Inman, 7/23/01, (PB2002-100434, A16, MF-A03).
- MCEER-01-0003 “Sensitivity Analysis of Dynamic Systems Subjected to Seismic Loads,” by C. Roth and M. Grigoriu, 9/18/01, (PB2003-100884, A12, MF-A03).
- MCEER-01-0004 “Overcoming Obstacles to Implementing Earthquake Hazard Mitigation Policies: Stage 1 Report,” by D.J. Alesch and W.J. Petak, 12/17/01, (PB2002-107949, A07, MF-A02).
- MCEER-01-0005 “Updating Real-Time Earthquake Loss Estimates: Methods, Problems and Insights,” by C.E. Taylor, S.E. Chang and R.T. Eguchi, 12/17/01, (PB2002-107948, A05, MF-A01).
- MCEER-01-0006 “Experimental Investigation and Retrofit of Steel Pile Foundations and Pile Bents Under Cyclic Lateral Loadings,” by A. Shama, J. Mander, B. Blabac and S. Chen, 12/31/01, (PB2002-107950, A13, MF-A03).
- MCEER-02-0001 “Assessment of Performance of Bolu Viaduct in the 1999 Duzce Earthquake in Turkey” by P.C. Roussis, M.C. Constantinou, M. Erdik, E. Durukal and M. Dicleli, 5/8/02, (PB2003-100883, A08, MF-A02).
- MCEER-02-0002 “Seismic Behavior of Rail Counterweight Systems of Elevators in Buildings,” by M.P. Singh, Rildova and L.E. Suarez, 5/27/02. (PB2003-100882, A11, MF-A03).
- MCEER-02-0003 “Development of Analysis and Design Procedures for Spread Footings,” by G. Mylonakis, G. Gazetas, S. Nikolaou and A. Chauncey, 10/02/02, (PB2004-101636, A13, MF-A03, CD-A13).
- MCEER-02-0004 “Bare-Earth Algorithms for Use with SAR and LIDAR Digital Elevation Models,” by C.K. Huyck, R.T. Eguchi and B. Houshmand, 10/16/02, (PB2004-101637, A07, CD-A07).
- MCEER-02-0005 “Review of Energy Dissipation of Compression Members in Concentrically Braced Frames,” by K.Lee and M. Bruneau, 10/18/02, (PB2004-101638, A10, CD-A10).
- MCEER-03-0001 “Experimental Investigation of Light-Gauge Steel Plate Shear Walls for the Seismic Retrofit of Buildings” by J. Berman and M. Bruneau, 5/2/03, (PB2004-101622, A10, MF-A03, CD-A10).
- MCEER-03-0002 “Statistical Analysis of Fragility Curves,” by M. Shinozuka, M.Q. Feng, H. Kim, T. Uzawa and T. Ueda, 6/16/03, (PB2004-101849, A09, CD-A09).
- MCEER-03-0003 “Proceedings of the Eighth U.S.-Japan Workshop on Earthquake Resistant Design of Lifeline Facilities and Countermeasures Against Liquefaction,” edited by M. Hamada, J.P. Bardet and T.D. O’Rourke, 6/30/03, (PB2004-104386, A99, CD-A99).
- MCEER-03-0004 “Proceedings of the PRC-US Workshop on Seismic Analysis and Design of Special Bridges,” edited by L.C. Fan and G.C. Lee, 7/15/03, (PB2004-104387, A14, CD-A14).
- MCEER-03-0005 “Urban Disaster Recovery: A Framework and Simulation Model,” by S.B. Miles and S.E. Chang, 7/25/03, (PB2004-104388, A07, CD-A07).
- MCEER-03-0006 “Behavior of Underground Piping Joints Due to Static and Dynamic Loading,” by R.D. Meis, M. Maragakis and R. Siddharthan, 11/17/03, (PB2005-102194, A13, MF-A03, CD-A00).
- MCEER-04-0001 “Experimental Study of Seismic Isolation Systems with Emphasis on Secondary System Response and Verification of Accuracy of Dynamic Response History Analysis Methods,” by E. Wolff and M. Constantinou, 1/16/04 (PB2005-102195, A99, MF-E08, CD-A00).
- MCEER-04-0002 “Tension, Compression and Cyclic Testing of Engineered Cementitious Composite Materials,” by K. Kesner and S.L. Billington, 3/1/04, (PB2005-102196, A08, CD-A08).


- MCEER-04-0003 “Cyclic Testing of Braces Laterally Restrained by Steel Studs to Enhance Performance During Earthquakes,” by O.C. Celik, J.W. Berman and M. Bruneau, 3/16/04, (PB2005-102197, A13, MF-A03, CD-A00).
- MCEER-04-0004 “Methodologies for Post Earthquake Building Damage Detection Using SAR and Optical Remote Sensing: Application to the August 17, 1999 Marmara, Turkey Earthquake,” by C.K. Huyck, B.J. Adams, S. Cho, R.T. Eguchi, B. Mansouri and B. Houshmand, 6/15/04, (PB2005-104888, A10, CD-A00).
- MCEER-04-0005 “Nonlinear Structural Analysis Towards Collapse Simulation: A Dynamical Systems Approach,” by M.V. Sivaselvan and A.M. Reinhorn, 6/16/04, (PB2005-104889, A11, MF-A03, CD-A00).
- MCEER-04-0006 “Proceedings of the Second PRC-US Workshop on Seismic Analysis and Design of Special Bridges,” edited by G.C. Lee and L.C. Fan, 6/25/04, (PB2005-104890, A16, CD-A00).
- MCEER-04-0007 “Seismic Vulnerability Evaluation of Axially Loaded Steel Built-up Laced Members,” by K. Lee and M. Bruneau, 6/30/04, (PB2005-104891, A16, CD-A00).
- MCEER-04-0008 “Evaluation of Accuracy of Simplified Methods of Analysis and Design of Buildings with Damping Systems for Near-Fault and for Soft-Soil Seismic Motions,” by E.A. Pavlou and M.C. Constantinou, 8/16/04, (PB2005-104892, A08, MF-A02, CD-A00).
- MCEER-04-0009 “Assessment of Geotechnical Issues in Acute Care Facilities in California,” by M. Lew, T.D. O’Rourke, R. Dobry and M. Koch, 9/15/04, (PB2005-104893, A08, CD-A00).
- MCEER-04-0010 “Scissor-Jack-Damper Energy Dissipation System,” by A.N. Sigaher-Boyle and M.C. Constantinou, 12/1/04 (PB2005-108221).
- MCEER-04-0011 “Seismic Retrofit of Bridge Steel Truss Piers Using a Controlled Rocking Approach,” by M. Pollino and M. Bruneau, 12/20/04 (PB2006-105795).
- MCEER-05-0001 “Experimental and Analytical Studies of Structures Seismically Isolated with an Uplift-Restraint Isolation System,” by P.C. Roussis and M.C. Constantinou, 1/10/05 (PB2005-108222).
- MCEER-05-0002 “A Versatile Experimentation Model for Study of Structures Near Collapse Applied to Seismic Evaluation of Irregular Structures,” by D. Kusumastuti, A.M. Reinhorn and A. Rutenberg, 3/31/05 (PB2006-101523).
- MCEER-05-0003 “Proceedings of the Third PRC-US Workshop on Seismic Analysis and Design of Special Bridges,” edited by L.C. Fan and G.C. Lee, 4/20/05, (PB2006-105796).
- MCEER-05-0004 “Approaches for the Seismic Retrofit of Braced Steel Bridge Piers and Proof-of-Concept Testing of an Eccentrically Braced Frame with Tubular Link,” by J.W. Berman and M. Bruneau, 4/21/05 (PB2006-101524).
- MCEER-05-0005 “Simulation of Strong Ground Motions for Seismic Fragility Evaluation of Nonstructural Components in Hospitals,” by A. Wanitkorkul and A. Filiatrault, 5/26/05 (PB2006-500027).
- MCEER-05-0006 “Seismic Safety in California Hospitals: Assessing an Attempt to Accelerate the Replacement or Seismic Retrofit of Older Hospital Facilities,” by D.J. Alesch, L.A. Arendt and W.J. Petak, 6/6/05 (PB2006-105794).
- MCEER-05-0007 “Development of Seismic Strengthening and Retrofit Strategies for Critical Facilities Using Engineered Cementitious Composite Materials,” by K. Kesner and S.L. Billington, 8/29/05 (PB2006-111701).
- MCEER-05-0008 “Experimental and Analytical Studies of Base Isolation Systems for Seismic Protection of Power Transformers,” by N. Murota, M.Q. Feng and G-Y. Liu, 9/30/05 (PB2006-111702).
- MCEER-05-0009 “3D-BASIS-ME-MB: Computer Program for Nonlinear Dynamic Analysis of Seismically Isolated Structures,” by P.C. Tsopelas, P.C. Roussis, M.C. Constantinou, R. Buchanan and A.M. Reinhorn, 10/3/05 (PB2006-111703).
- MCEER-05-0010 “Steel Plate Shear Walls for Seismic Design and Retrofit of Building Structures,” by D. Vian and M. Bruneau, 12/15/05 (PB2006-111704).

- MCEER-05-0011 "The Performance-Based Design Paradigm," by M.J. Astrella and A. Whittaker, 12/15/05 (PB2006-111705).
- MCEER-06-0001 "Seismic Fragility of Suspended Ceiling Systems," H. Badillo-Almaraz, A.S. Whittaker, A.M. Reinhorn and G.P. Cimellaro, 2/4/06 (PB2006-111706).
- MCEER-06-0002 "Multi-Dimensional Fragility of Structures," by G.P. Cimellaro, A.M. Reinhorn and M. Bruneau, 3/1/06 (PB2007-106974, A09, MF-A02, CD A00).
- MCEER-06-0003 "Built-Up Shear Links as Energy Dissipators for Seismic Protection of Bridges," by P. Dusicka, A.M. Itani and I.G. Buckle, 3/15/06 (PB2006-111708).
- MCEER-06-0004 "Analytical Investigation of the Structural Fuse Concept," by R.E. Vargas and M. Bruneau, 3/16/06 (PB2006-111709).
- MCEER-06-0005 "Experimental Investigation of the Structural Fuse Concept," by R.E. Vargas and M. Bruneau, 3/17/06 (PB2006-111710).
- MCEER-06-0006 "Further Development of Tubular Eccentrically Braced Frame Links for the Seismic Retrofit of Braced Steel Truss Bridge Piers," by J.W. Berman and M. Bruneau, 3/27/06 (PB2007-105147).
- MCEER-06-0007 "REDARS Validation Report," by S. Cho, C.K. Huyck, S. Ghosh and R.T. Eguchi, 8/8/06 (PB2007-106983).
- MCEER-06-0008 "Review of Current NDE Technologies for Post-Earthquake Assessment of Retrofitted Bridge Columns," by J.W. Song, Z. Liang and G.C. Lee, 8/21/06 (PB2007-106984).
- MCEER-06-0009 "Liquefaction Remediation in Silty Soils Using Dynamic Compaction and Stone Columns," by S. Thevanayagam, G.R. Martin, R. Nashed, T. Shenthan, T. Kanagalingam and N. Ecemis, 8/28/06 (PB2007-106985).
- MCEER-06-0010 "Conceptual Design and Experimental Investigation of Polymer Matrix Composite Infill Panels for Seismic Retrofitting," by W. Jung, M. Chiewanichakorn and A.J. Aref, 9/21/06 (PB2007-106986).
- MCEER-06-0011 "A Study of the Coupled Horizontal-Vertical Behavior of Elastomeric and Lead-Rubber Seismic Isolation Bearings," by G.P. Warn and A.S. Whittaker, 9/22/06 (PB2007-108679).
- MCEER-06-0012 "Proceedings of the Fourth PRC-US Workshop on Seismic Analysis and Design of Special Bridges: Advancing Bridge Technologies in Research, Design, Construction and Preservation," Edited by L.C. Fan, G.C. Lee and L. Ziang, 10/12/06 (PB2007-109042).
- MCEER-06-0013 "Cyclic Response and Low Cycle Fatigue Characteristics of Plate Steels," by P. Dusicka, A.M. Itani and I.G. Buckle, 11/1/06 (PB2007-106987).
- MCEER-06-0014 "Proceedings of the Second US-Taiwan Bridge Engineering Workshop," edited by W.P. Yen, J. Shen, J-Y. Chen and M. Wang, 11/15/06 (PB2008-500041).
- MCEER-06-0015 "User Manual and Technical Documentation for the REDARSTM Import Wizard," by S. Cho, S. Ghosh, C.K. Huyck and S.D. Werner, 11/30/06 (PB2007-114766).
- MCEER-06-0016 "Hazard Mitigation Strategy and Monitoring Technologies for Urban and Infrastructure Public Buildings: Proceedings of the China-US Workshops," edited by X.Y. Zhou, A.L. Zhang, G.C. Lee and M. Tong, 12/12/06 (PB2008-500018).
- MCEER-07-0001 "Static and Kinetic Coefficients of Friction for Rigid Blocks," by C. Kafali, S. Fathali, M. Grigoriu and A.S. Whittaker, 3/20/07 (PB2007-114767).
- MCEER-07-0002 "Hazard Mitigation Investment Decision Making: Organizational Response to Legislative Mandate," by L.A. Arendt, D.J. Alesch and W.J. Petak, 4/9/07 (PB2007-114768).
- MCEER-07-0003 "Seismic Behavior of Bidirectional-Resistant Ductile End Diaphragms with Unbonded Braces in Straight or Skewed Steel Bridges," by O. Celik and M. Bruneau, 4/11/07 (PB2008-105141).

- MCEER-07-0004 “Modeling Pile Behavior in Large Pile Groups Under Lateral Loading,” by A.M. Dodds and G.R. Martin, 4/16/07(PB2008-105142).
- MCEER-07-0005 “Experimental Investigation of Blast Performance of Seismically Resistant Concrete-Filled Steel Tube Bridge Piers,” by S. Fujikura, M. Bruneau and D. Lopez-Garcia, 4/20/07 (PB2008-105143).
- MCEER-07-0006 “Seismic Analysis of Conventional and Isolated Liquefied Natural Gas Tanks Using Mechanical Analogs,” by I.P. Christovasilis and A.S. Whittaker, 5/1/07.
- MCEER-07-0007 “Experimental Seismic Performance Evaluation of Isolation/Restraint Systems for Mechanical Equipment – Part 1: Heavy Equipment Study,” by S. Fathali and A. Filiatrault, 6/6/07 (PB2008-105144).
- MCEER-07-0008 “Seismic Vulnerability of Timber Bridges and Timber Substructures,” by A.A. Sharma, J.B. Mander, I.M. Friedland and D.R. Allicock, 6/7/07 (PB2008-105145).
- MCEER-07-0009 “Experimental and Analytical Study of the XY-Friction Pendulum (XY-FP) Bearing for Bridge Applications,” by C.C. Marin-Artieda, A.S. Whittaker and M.C. Constantinou, 6/7/07 (PB2008-105191).
- MCEER-07-0010 “Proceedings of the PRC-US Earthquake Engineering Forum for Young Researchers,” Edited by G.C. Lee and X.Z. Qi, 6/8/07 (PB2008-500058).
- MCEER-07-0011 “Design Recommendations for Perforated Steel Plate Shear Walls,” by R. Purba and M. Bruneau, 6/18/07, (PB2008-105192).
- MCEER-07-0012 “Performance of Seismic Isolation Hardware Under Service and Seismic Loading,” by M.C. Constantinou, A.S. Whittaker, Y. Kalpakidis, D.M. Fenz and G.P. Warn, 8/27/07, (PB2008-105193).
- MCEER-07-0013 “Experimental Evaluation of the Seismic Performance of Hospital Piping Subassemblies,” by E.R. Goodwin, E. Maragakis and A.M. Itani, 9/4/07, (PB2008-105194).
- MCEER-07-0014 “A Simulation Model of Urban Disaster Recovery and Resilience: Implementation for the 1994 Northridge Earthquake,” by S. Miles and S.E. Chang, 9/7/07, (PB2008-106426).
- MCEER-07-0015 “Statistical and Mechanistic Fragility Analysis of Concrete Bridges,” by M. Shinozuka, S. Banerjee and S-H. Kim, 9/10/07, (PB2008-106427).
- MCEER-07-0016 “Three-Dimensional Modeling of Inelastic Buckling in Frame Structures,” by M. Schachter and AM. Reinhorn, 9/13/07, (PB2008-108125).
- MCEER-07-0017 “Modeling of Seismic Wave Scattering on Pile Groups and Caissons,” by I. Po Lam, H. Law and C.T. Yang, 9/17/07 (PB2008-108150).
- MCEER-07-0018 “Bridge Foundations: Modeling Large Pile Groups and Caissons for Seismic Design,” by I. Po Lam, H. Law and G.R. Martin (Coordinating Author), 12/1/07 (PB2008-111190).
- MCEER-07-0019 “Principles and Performance of Roller Seismic Isolation Bearings for Highway Bridges,” by G.C. Lee, Y.C. Ou, Z. Liang, T.C. Niu and J. Song, 12/10/07 (PB2009-110466).
- MCEER-07-0020 “Centrifuge Modeling of Permeability and Pinning Reinforcement Effects on Pile Response to Lateral Spreading,” by L.L. Gonzalez-Lagos, T. Abdoun and R. Dobry, 12/10/07 (PB2008-111191).
- MCEER-07-0021 “Damage to the Highway System from the Pisco, Perú Earthquake of August 15, 2007,” by J.S. O’Connor, L. Mesa and M. Nykamp, 12/10/07, (PB2008-108126).
- MCEER-07-0022 “Experimental Seismic Performance Evaluation of Isolation/Restraint Systems for Mechanical Equipment – Part 2: Light Equipment Study,” by S. Fathali and A. Filiatrault, 12/13/07 (PB2008-111192).
- MCEER-07-0023 “Fragility Considerations in Highway Bridge Design,” by M. Shinozuka, S. Banerjee and S.H. Kim, 12/14/07 (PB2008-111193).


- MCEER-07-0024 “Performance Estimates for Seismically Isolated Bridges,” by G.P. Warn and A.S. Whittaker, 12/30/07 (PB2008-112230).
- MCEER-08-0001 “Seismic Performance of Steel Girder Bridge Superstructures with Conventional Cross Frames,” by L.P. Carden, A.M. Itani and I.G. Buckle, 1/7/08, (PB2008-112231).
- MCEER-08-0002 “Seismic Performance of Steel Girder Bridge Superstructures with Ductile End Cross Frames with Seismic Isolators,” by L.P. Carden, A.M. Itani and I.G. Buckle, 1/7/08 (PB2008-112232).
- MCEER-08-0003 “Analytical and Experimental Investigation of a Controlled Rocking Approach for Seismic Protection of Bridge Steel Truss Piers,” by M. Pollino and M. Bruneau, 1/21/08 (PB2008-112233).
- MCEER-08-0004 “Linking Lifeline Infrastructure Performance and Community Disaster Resilience: Models and Multi-Stakeholder Processes,” by S.E. Chang, C. Pasion, K. Tatebe and R. Ahmad, 3/3/08 (PB2008-112234).
- MCEER-08-0005 “Modal Analysis of Generally Damped Linear Structures Subjected to Seismic Excitations,” by J. Song, Y-L. Chu, Z. Liang and G.C. Lee, 3/4/08 (PB2009-102311).
- MCEER-08-0006 “System Performance Under Multi-Hazard Environments,” by C. Kafali and M. Grigoriu, 3/4/08 (PB2008-112235).
- MCEER-08-0007 “Mechanical Behavior of Multi-Spherical Sliding Bearings,” by D.M. Fenz and M.C. Constantinou, 3/6/08 (PB2008-112236).
- MCEER-08-0008 “Post-Earthquake Restoration of the Los Angeles Water Supply System,” by T.H.P. Tabucchi and R.A. Davidson, 3/7/08 (PB2008-112237).
- MCEER-08-0009 “Fragility Analysis of Water Supply Systems,” by A. Jacobson and M. Grigoriu, 3/10/08 (PB2009-105545).
- MCEER-08-0010 “Experimental Investigation of Full-Scale Two-Story Steel Plate Shear Walls with Reduced Beam Section Connections,” by B. Qu, M. Bruneau, C-H. Lin and K-C. Tsai, 3/17/08 (PB2009-106368).
- MCEER-08-0011 “Seismic Evaluation and Rehabilitation of Critical Components of Electrical Power Systems,” S. Ersoy, B. Feizi, A. Ashrafi and M. Ala Saadeghvaziri, 3/17/08 (PB2009-105546).
- MCEER-08-0012 “Seismic Behavior and Design of Boundary Frame Members of Steel Plate Shear Walls,” by B. Qu and M. Bruneau, 4/26/08 . (PB2009-106744).
- MCEER-08-0013 “Development and Appraisal of a Numerical Cyclic Loading Protocol for Quantifying Building System Performance,” by A. Filiatrault, A. Wanitkorkul and M. Constantinou, 4/27/08 (PB2009-107906).
- MCEER-08-0014 “Structural and Nonstructural Earthquake Design: The Challenge of Integrating Specialty Areas in Designing Complex, Critical Facilities,” by W.J. Petak and D.J. Alesch, 4/30/08 (PB2009-107907).
- MCEER-08-0015 “Seismic Performance Evaluation of Water Systems,” by Y. Wang and T.D. O’Rourke, 5/5/08 (PB2009-107908).
- MCEER-08-0016 “Seismic Response Modeling of Water Supply Systems,” by P. Shi and T.D. O’Rourke, 5/5/08 (PB2009-107910).
- MCEER-08-0017 “Numerical and Experimental Studies of Self-Centering Post-Tensioned Steel Frames,” by D. Wang and A. Filiatrault, 5/12/08 (PB2009-110479).
- MCEER-08-0018 “Development, Implementation and Verification of Dynamic Analysis Models for Multi-Spherical Sliding Bearings,” by D.M. Fenz and M.C. Constantinou, 8/15/08 (PB2009-107911).
- MCEER-08-0019 “Performance Assessment of Conventional and Base Isolated Nuclear Power Plants for Earthquake Blast Loadings,” by Y.N. Huang, A.S. Whittaker and N. Luco, 10/28/08 (PB2009-107912).
- MCEER-08-0020 “Remote Sensing for Resilient Multi-Hazard Disaster Response – Volume I: Introduction to Damage Assessment Methodologies,” by B.J. Adams and R.T. Eguchi, 11/17/08.

- MCEER-08-0021 “Remote Sensing for Resilient Multi-Hazard Disaster Response – Volume II: Counting the Number of Collapsed Buildings Using an Object-Oriented Analysis: Case Study of the 2003 Bam Earthquake,” by L. Gusella, C.K. Huyck and B.J. Adams, 11/17/08.
- MCEER-08-0022 “Remote Sensing for Resilient Multi-Hazard Disaster Response – Volume III: Multi-Sensor Image Fusion Techniques for Robust Neighborhood-Scale Urban Damage Assessment,” by B.J. Adams and A. McMillan, 11/17/08.
- MCEER-08-0023 “Remote Sensing for Resilient Multi-Hazard Disaster Response – Volume IV: A Study of Multi-Temporal and Multi-Resolution SAR Imagery for Post-Katrina Flood Monitoring in New Orleans,” by A. McMillan, J.G. Morley, B.J. Adams and S. Chesworth, 11/17/08.
- MCEER-08-0024 “Remote Sensing for Resilient Multi-Hazard Disaster Response – Volume V: Integration of Remote Sensing Imagery and VIEWS™ Field Data for Post-Hurricane Charley Building Damage Assessment,” by J.A. Womble, K. Mehta and B.J. Adams, 11/17/08.
- MCEER-08-0025 “Building Inventory Compilation for Disaster Management: Application of Remote Sensing and Statistical Modeling,” by P. Sarabandi, A.S. Kiremidjian, R.T. Eguchi and B. J. Adams, 11/20/08 (PB2009-110484).
- MCEER-08-0026 “New Experimental Capabilities and Loading Protocols for Seismic Qualification and Fragility Assessment of Nonstructural Systems,” by R. Retamales, G. Mosqueda, A. Filiatrault and A. Reinhorn, 11/24/08 (PB2009-110485).
- MCEER-08-0027 “Effects of Heating and Load History on the Behavior of Lead-Rubber Bearings,” by I.V. Kalpakidis and M.C. Constantinou, 12/1/08.
- MCEER-08-0028 “Experimental and Analytical Investigation of Blast Performance of Seismically Resistant Bridge Piers,” by S.Fujikura and M. Bruneau, 12/8/08.
- MCEER-08-0029 “Evolutionary Methodology for Aseismic Decision Support,” by Y. Hu and G. Dargush, 12/15/08.
- MCEER-08-0030 “Development of a Steel Plate Shear Wall Bridge Pier System Conceived from a Multi-Hazard Perspective,” by D. Keller and M. Bruneau, 12/19/08.
- MCEER-09-0001 “Modal Analysis of Arbitrarily Damped Three-Dimensional Linear Structures Subjected to Seismic Excitations,” by Y.L. Chu, J. Song and G.C. Lee, 1/31/09.
- MCEER-09-0002 “Air-Blast Effects on Structural Shapes,” by G. Ballantyne and A.S. Whittaker, 2/12/09.
- MCEER-09-0003 “Water Supply Performance During Earthquakes and Extreme Events,” by A.L. Bonneau and T.D. O’Rourke, 2/16/09.



EARTHQUAKE ENGINEERING TO EXTREME EVENTS

University at Buffalo, The State University of New York
Red Jacket Quadrangle ■ Buffalo, New York 14261
Phone: (716) 645-3391 ■ Fax: (716) 645-3399
E-mail: mceer@buffalo.edu ■ WWW Site <http://mceer.buffalo.edu>



University at Buffalo *The State University of New York*

ISSN 1520-295X